MULTI-TARGETED STRATEGIES FOR MODULATING RECEPTOR AND NON-RECEPTOR TYROSINE KINASES INVOLVED IN ADVERSE SIGNALING IN SOLID TUMOURS

Suman Rao

Division of Experimental Medicine

Faculty of Medicine

McGill University

Montreal, Canada

July 2015

A thesis submitted to McGill University in partial fulfillment of the requirements of the degree of Doctor of Philosophy

ABSTRACT

Targeted therapy is designed to block specific oncogenic products involved in disordered signaling, with the purpose of inducing selective therapy. However the activation of compensatory and alternate signaling pathways to bypass the inhibitory effects of targeted therapies has led to both intrinsic and acquired resistance. Here, in order to abrogate these adverse signaling nodes, we investigated two major approaches: (a) the design of single agents termed "combi-molecules" targeted to key players of multiple signaling pathways and (b) the determination of Achilles' heels in this complex network of signaling pathways to be targeted for effective therapy. This thesis focuses on the targeting of EGFR, c-Src and c-Met, three tyrosine kinases that are involved in adverse signaling in solid tumours. Our results showed that: (a) programming AL622, a single molecule targeted to EGFR and c-Src, to further release two intact kinase inhibitors, AL621 (EGFR inhibitory arm) and PP2 (c-Src inhibitory arm) did not suffice to induce sustained and balanced EGFR-c-Src targeting, (b) substituting the PP2 moiety for a thiazolylaminopyrimidine scaffold, led to AL776, a balanced EGFR-c-Src targeting combi-molecule, which permitted the validation of a new targeting model termed "type III combi-targeting". Further investigation on the mode of targeting of multiple signaling pathways led to the molecular analysis of concomitant administration of 2-4 clinical kinase inhibitors to induce tandem blockade of EGFR, c-Met, c-Src and STAT3. We discovered that despite the complex signaling evoked by these three tyrosine kinases, targeting only two kinases, which we refer to as the Achilles' heels of the signaling network was sufficient to induce potent growth inhibition. Furthermore, we developed parameters to evaluate the efficacy of single multi-targeted molecules (e.g. combi-

molecules) in comparison with equimolar 2-drug combinations. This has led to the definition of the principle of "balanced targeting" according to which an equimolar combination is said to be "balanced" when the IC50 values of growth inhibition for the two drugs in combination is less than that of each individual drug. Using data generated from a large number of experiments, we found that balanced targeting could be observed when the fold-difference between the IC50 values of two individual drugs was less than or equal to 6 and established a new parameter **ε** termed "potency index" that can be used to assess balanced targeting. We discovered a significantly linear correlation (R^2=0.95) between **ε** and the fold-differences between the IC50 values of the two individual drugs. Combi-molecules being theoretically designed to generate effects corresponding to equimolar combinations, we established that they should be compared with the latter only when they are balanced. Thus, a new parameter **Ω** defined as the IC50 value for growth inhibition over that of a "balanced targeted" equimolar combination was proposed for measuring the potency of combi-molecules. Based upon our data, a given equimolar combination can be used as a reference for determining the potency of a combi-molecule, only when its **ε** value is less than 5 and the latter agent can be considered for further development only when **Ω** is less than or equal to 1.

Our results *in toto* suggest that multi-targeted approaches to block adverse effects of key oncogenic kinases is a promising strategy for the abrogation of complex signaling pathways in refractory tumours.

RESUME

Les thérapies ciblées ont été conçues dans le but de bloquer des cibles oncogéniques spécifiques dans des voies de signalisation dérégulées, afin d'induire une thérapie sélective. Cependant, l'activation de voies de signalisation compensatoires et alternatives permettant d'outrepasser les effets inhibiteurs des thérapies ciblées a entraîné l'apparition de résistances intrinsèques et acquises. Ici, dans le but de supprimer ces nœuds de signalisation défavorables, nous avons étudié deux approches majeures : (a) la conception de molécules uniques appelées « combi-molécules » ciblant des acteurs clés de nombreuses voies de signalisation cellulaire et (b) la mise en évidence du talon d'Achille de ces réseaux complexes de signalisation dont le ciblage permettrait d'accroitre l'efficacité thérapeutique. Cette thèse se focalise sur le ciblage d'EGFR, c-Src and c-Met, trois tyrosines kinases induisant des effets pro-tumoraux dans les tumeurs solides. Nos résultats montrent que : (a) programmer AL622, une molécule ciblant EGFR et c-Src, à libérer deux inhibiteurs de kinases intactes, AL621 (bras inhibiteur d'EGFR) et PP2 (bras inhibiteur de c-Src) ne permet pas un ciblage stable et, équilibré de la signalisation EGFR-c-Src (b) substituer la fraction PP2 par une moitié thiazolylaminopyrimidine a mené au développement de l'AL776, une combi-molécule ciblant de façon équilibrée EGFR-c-Src, permettant ainsi la validation d'un nouveau mode de ciblage nommé combi-ciblage de type III. Des études plus approfondies sur le mode de ciblage de plusieurs voies de signalisation cellulaire ont entraîné l'analyse moléculaire d'une administration concomitante de 2-4 inhibiteurs de kinases cliniques afin d'induire le blocage en tandem d'EGFR, c-Met, c-Src et STAT3. Nous avons découvert que malgré les signalisations complexes évoquées par ces trois tyrosines kinases EGFR, c-Met et c-Src, cibler

seulement deux kinases, que nous désignons comme le talon d'Achille du réseau, était suffisant pour induire une forte inhibition de la croissance cellulaire. Par ailleurs, nous avons développé des paramètres permettant d'évaluer l'efficacité de molécules uniques multi-cibles (telles que les combi-molécules) en comparaison avec une combinaison équimolaire de deux molécules. Ceci a permis la définition du principe de « ciblage équilibré » selon lequel une combinaison équimolaire est dite « équilibrée » quand sa valeur d'IC50 est inférieure à celle de chacune des molécules seules. Par l'utilisation de données générées à partir de nombreuses expériences, nous avons mis en évidence qu'un ciblage équilibré pourrait être observé quand la différence entre les IC50 des deux molécules seules était inférieure ou égale à 6, et nous avons établi un nouveau paramètre **ε** nommé « indice de potentialité » pouvant être utilisé pour évaluer un ciblage équilibré. Nous avons trouvé une corrélation linéaire significative (R^2=0,95) entre **ε** et la différence entre les IC50 des deux molécules. Les combi-molécules étant théoriquement conçues pour générer des effets similaires à une combinaison équimolaire, nous avons établi qu'elles devaient être comparées à cette dernière seulement quand elles sont équilibrées. Ainsi, un nouveau paramètre **Ω**, établi comme l'IC50 de l'inhibition de croissance divisée par celle d'une combinaison équimolaire équilibrée, a été défini afin de mesurer l'efficacité des combi-molécules. Selon nos données, une combinaison équimolaire donnée peut servir de référence afin de déterminer l'efficacité d'une combi-molécule, seulement quand sa valeur **ε** est inférieure à 5 et cette molécule ne peut être considérée digne d'un développement approfondi que quand **Ω** est inférieur à 1. Nos résultats *in toto* suggèrent que les approches multi-ciblées visant à bloquer les effets négatifs et

compensatoires de kinases oncogéniques clés est une stratégie prometteuse permettant d'abroger les signalisations complexes dans les tumeurs réfractaires.

ACKNOWLEDGEMENT

It might be the end of one journey, but it certainly feels like the beginning of many more to come. And no matter where the road takes me, I shall forever remember where it all started.

While the last five years have been incredibly enriching in every aspect, it would not have been possible without the help and support of several people that I would like to take a moment to thank.

I will begin by expressing my gratitude towards my supervisor, Dr. Jean-Claude, who gave me the opportunity to pursue my PhD in his lab, and has always encouraged and guided me in the right direction. Through all our meetings and discussion, he has always challenged me to think bigger and deeper, which has allowed me to broaden my scientific knowledge and hone my skills as a budding researcher. I have always appreciated the freedom that he has given me to explore various possibilities with my research, which has made this journey all the more exciting and fulfilling. Finally, I would like to thank him for believing in me and pushing me towards seeing optimism, even in situations with dwindling hope, which is a quality that I hope to never let go and always embrace as I move forward.

Of course, no lab is complete without its lab members and everything that they have to offer! I must take this opportunity to thank all my current and past members of this lab, who have been such an integral part of this journey. From the people who have been directly involved in my research to the ones who have trained and helped me, have been instrumental in guiding my work forward and I will forever be thankful for their valuable inputs and time.

Finally, I cannot end without thanking my family and friends, who have stood by me through this entire journey and have always supported and encouraged me to work hard and achieve my goals.

Today, I have reached the end, but it would not have been possible without the presence of all of you in my life and your kind words of love and support. For that and for always being there, I would like to express my heartfelt appreciation and gratitude.

Thank you!

CONTRIBUTIONS OF AUTHORS

This manuscript-based thesis is composed of four manuscripts and the contributions of each author are stated below.

CHAPTER 2: Biological effects of AL622, a molecule rationally designed to release an EGFR and a c-Src kinase inhibitor.

This paper was published in Chemical Biology and Drug Design in December 2012 (80 (6), p981-91). Dr. Anne-Laure Larroque Lombard synthesized the combi-molecule, AL622, performed its degradation and fluorescence analysis in cells and wrote the chemistry section of the manuscript. Dr. Na Ning carried out part of the biological work including invasion, wound-healing and cell proliferation assays. I carried out several biological assays and this has marked my first steps into the field of kinase targeting. I also helped with the preparation of the manuscript. Dr. Sylvia Lauwagie and Dr. Laëtitia Coudray contributed towards the synthesis of molecules. Ruba Halaoui carried out part of the *in vitro* kinase enzyme assay. Dr. Ying Huang trained and assisted Dr. Na Ning. Dr. Bertrand Jean-Claude revised the manuscript and made the necessary changes.

CHAPTER 3: Target modulation by a kinase inhibitor engineered to induce a tandem blockade of the epidermal growth factor receptor (EGFR) and c-Src: the concept of type III combi-targeting

This paper was published in the Journal PLOS ONE in February 2015 (10(2): e0117215).

I have participated in the design, execution and the interpretation of the experiments in this paper. I have significantly contributed to the writing of the manuscript and handled

all referee-requested revisions. Other contributions to this paper to be acknowledged are those of Dr. Anne-Laure Larroque-Lombard, Dr. Lisa Peyrard, Dr. Zakaria Rachid and Cedric Thauvin who contributed to the chemical synthesis of the molecules. I am also grateful to Dr. Christopher Williams who helped with the molecular modeling. Dr. Bertrand Jean-Claude overlooked the proceedings of the experimental work and revised the manuscript.

CHAPTER 4: Pharmacological probing of signaling redundancy mediated by receptor and non-receptor tyrosine kinases revealed Achilles' heels in castrate resistant prostate cancer

This manuscript was submitted to Molecular Cancer Therapeutics (July 2015) and is currently under revision.

I contributed to the design of all the experiments performed in this chapter and was actively involved in the discussions that led to the analysis of signaling pathways studied therein. I have also contributed to the decision process towards the direction that needed to be taken towards the advancement of this work. For the *in vivo* work, I was sent to Toulouse, France in the context of the “64e session de la Commission permanente de coopération franco-québécoise (CPCFQ)", to perform studies on a xenograft model under the supervision of Dr. Ben Allal. I am also very grateful to Dr. Jean-Pierre Delord, Dr. Etienne Chatelut and Dr. Anne-Laure Larroque-Lombard for organizing my trip to Toulouse. The latter trip has given me the opportunity to be initiated to *in vivo* xenograft models. Dr. Bertrand Jean-Claude made all the necessary comments and revised the manuscript.

CHAPTER 5: Quantitative analysis of the potency of equimolar two-drug combinations and combi-molecules involving kinase inhibitors against human tumour cells: the concept of "balanced targeting".

This manuscript was submitted to Molecular Cancer Therapeutics (July 2015) and is currently under revision.

The original idea of this work came from my own observations of the trends in the data acquired in the course of my experiments on kinase-kinase targeting studies. Although similar observations were made previously, my contribution has been to drive the pool of data towards notions that could be parameterized. Discussions with Dr. Benoît Thibault and Dr. Bertrand Jean-Claude led to the final parameterization of the potency index. Dr. Benoît Thibault and Martin Rupp provided data obtained from their own experiments that helped validate the theory. Combi-molecules analyzed in this chapter were synthesized by Dr. Anne-Laure Larroque-Lombard, Dr. Lisa Peyrard and Dr. Cedric Thauvin. Dr. Bertrand Jean-Claude helped with the design, conception and preparation of the manuscript.

TABLE OF CONTENTS

LIST OF ABBREVIATIONS

ABVD - Adriamycin, Bleomycin, Vinblastine and Dacarbazine

AEV – Avian Erythroblastosis Virus

AMP – Adenosine Monophosphate

ATP – Adenosine Triphosphate

BCR – Breakpoint Cluster Region

CHOP - Cyclophosphamide, Adriamycin or Hydroxy doxorubicin, Vincristine or Oncovin and Prednisone

CML – Chronic Myelogenous Leukemia

CREB – cAMP Response Element Binding

CHK – CSK Homology Kinase

CSK – C-terminal Src Kinase

COX – Cyclooxygenase

DNA – Deoxyribonucleic Acid

EGF – Epidermal Growth Factor

EGFR – Epidermal Growth Factor Receptor

EMT – Epithelial to Mesenchymal Transition

ERK – Extracellular signal-Regulated Kinase

FAK – Focal Adhesion Kinase

FGFR – Fibroblast Growth Factor Receptor

GAB-1 - Grb2-associated binding protein-1

GPCR – G-Protein Coupled Receptor

GRIM-19 - Genes Associated with Retinoid IFN Induced Mortality (GRIM)-19

GTP – Guanosine Triphosphate

HB-EGF - Heparin Binding Epidermal Growth Factor

HER2 – Human Epidermal Growth Factor Receptor-2

HGF – Hepatocyte Growth Factor

HGFR – Hepatocyte Growth Factor Receptor (commonly referred to as c-Met)

IGF1-R – Insulin-like Growth Factor-1 Receptor

IL - Interleukins

JAK – Janus Kinase

MAPK – Mitogen Activated Protein Kinase

MEK - MAPK/Extracellular signal-regulated Kinase

MGMT – O6-Methylguanine DNA Methyltransferase

MMPs – Matrix Metalloproteases

mTOR – Mammalian Target of Rapamycin

NFκ-B – Nuclear Factor Kappa B

NSCLC – Non-Small Cell Lung Cancer

PDGF – Platelet Derived Growth Factor

PDGFR – Platelet Derived Growth Factor Receptor

PDK1 - 3'-Phosphoinositide-Dependent Kinase-1

PH – Pleckstrin Homology

PKA – Protein Kinase A

PKB – Protein Kinase B (commonly referred to as Akt)

PI3K – Phosphotidylinositol-3-Kinase

PIAS3 - Protein Inhibitors of STAT3 (PIAS3)

PIK3CA - Phosphatidylinositol 3-Kinase Catalytic Alpha

PIP2 – Phosphotidylinositol-4,5-bisphosphate

PIP3 – Phosphotidylinositol-3,4,5-triphosphate

PTB – Phosphotyrosine Binding

PTEN – Phosphatase and Tensin Homolog

PTP – Protein Tyrosine Phosphatase

PTK – Protein Tyrosine Kinase

RNA – Ribonucleic Acid

RTK – Receptor Tyrosine Kinases

RSV – Rous Sarcoma Virus

SCLC – Small Cell Lung Cancer

SH1/2/3/4 – Src Homology

SHC – Src Homology Containing

SHP - The Src Homology 2 domain tyrosine Phosphatases

SOCS - Suppressors of Cytokine Signaling

SOS – Son of Sevenless

STAT – Signal Transducers and Activators of Transcription

TEM - Temozolomide

TGF-α - Transforming Growth Factor - alpha

TKI – Tyrosine Kinase Inhibitors

TNBC – Triple Negative Breast Cancer

VEGF – Vascular Endothelial Growth Factor

VEGFR – Vascular Endothelial Growth Factor Receptor

CHAPTER 1

INTRODUCTION

1.1 PREFACE

A recent report showed that the clinical attrition rate for oncology was almost four-fold higher compared with other diseases, highlighting the debilitating challenge associated with cancer drug discovery (1). The inability of many cytotoxic agents to specifically target cancer cells has contributed to their lack of selectivity and thus enhanced toxicity in the clinic. However, the past few years have seen a significant shift in the approach towards the treatment of cancer, with the development of more selective molecules designed to inhibit specific oncogenes. This has led to the era of targeted therapies. A major discovery that paved the way for a promising new targeting approach was that of Gleevec (imatinib), the first tyrosine kinase inhibitor (TKI) approved for the treatment of Chronic Myelogenous Leukemia (CML). Gleevec was designed to specifically inhibit the oncogenic product of the Philadelphia chromosome encoding a fusion protein termed Bcr-Abl (2). Since then, several key findings on molecular mechanisms driving cancer progression have shed light on the major deregulated oncogenic signaling pathways in different cancers. Following the approval of imatinib, several small molecule inhibitors have been approved for the treatment of various cancers driven by different oncogenic protein kinases. These include gefitinib and erlotinib for epidermal growth factor receptor (EGFR), bevacizumab for vascular endothelial growth factor receptor (VEGFR), crizotinib for ALK and hepatocyte growth factor receptor (c-Met), vemurafenib for BRAF, etc. (3). Despite an improvement in target selectivity, the clinical efficacy of these inhibitors has been significantly mitigated by the onset of resistance mechanisms. A complex network of signaling nodes originating from different kinases engaging in signaling crosstalk, and activation of compensatory signaling pathways are known to

significantly contribute to tumour heterogeneity, thereby decreasing sensitivity to kinase inhibitors.

Together, these properties of cancer cells have challenged the "one-drug-one-disease" paradigm. Cancer cells are known to evade cytotoxic lesions by activating multiple signaling pathways. Unfortunately, a similar type of response has been reported for kinase inhibitors, which despite their ability to block a given pathway leading to growth and proliferation, results in the activation of an alternative signaling event that reverts the initial growth inhibitory effect. The blockade of multiple signaling pathways seems to be a sine-qua-non for sustained growth inhibition. Consequently, there is an urgent need for the development of multi-targeted drugs directed at key signaling proteins involved in these adverse signaling pathways. Within this context, our laboratory has designed and synthesized a novel class of compounds termed "combi-molecules" that are capable of blocking two or more divergent targets (e.g. EGFR and DNA) either as an intact structure, or upon undergoing hydrolysis to release their two inhibitory arms (4, 5). In contrast to our previous generation of combi-targeting drugs, which were primarily directed at EGFR and DNA, the current thesis is exclusively focused on the targeting of multiple kinases without intervention of any cytotoxic lesion or DNA interactive agents. We sought to determine and study mechanisms of cell response when two or more kinases are targeted by small molecules using both a single multi-targeted molecule approach and combinations of multiple tyrosine kinase inhibitors. While the common trend for enhancing the potency of tyrosine kinase inhibitors is to design combinations with non-kinase cytotoxic agents such as DNA damaging agents and radiation, this thesis

works with the hypothesis that sustained potency can be driven by targeting key kinases in the complex network, which we name the Achilles' heels of the network.

1.2. PROTEIN TYROSINE KINASES

It is now known that a complex and tightly regulated network of signal transduction pathways controls growth, proliferation, cell-cell communication, differentiation, metabolism and cell death. Together, these processes are known to maintain tissue homeostasis. An intricate framework of signaling proteins including cell surface receptors, cytoplasmic, ribosomal, cytoskeletal, nuclear proteins and transcription factors forms this complex array of signaling pathways. Communication between these signaling proteins spanning the length of the extracellular milieu all the way down to the genomic DNA is controlled by specific and precise events that are tightly regulated. One such signaling event, that is considered to be a major mechanism driving these signaling pathways is the reversible phosphorylation and dephosphorylation of the hydroxyl-group of key amino acid residues including serine, threonine and tyrosine on these signaling proteins, which is carried out by a specialized class of enzymes termed protein kinases (6). These belong to the large family of phosphotransferases that possess intrinsic enzymatic properties owing to a catalytic domain that can transfer the γ-phosphate from an ATP molecule to a hydroxylamine residue on the substrate protein (7, 8). Based on the amino acid residue that is phosphorylated, protein kinases are further classified as serine/threonine or tyrosine kinases, although they are structurally related with a high level of sequence homology. While protein tyrosine kinase (PTK) activity is now considered a fundamental molecular mechanism regulating cellular functions, very little

was known about signal transduction pathways until 50-60 years ago. The next section briefly summarizes the major breakthroughs that enhanced our understanding of the molecular basis of cell signaling.

1.2.1 Historical timeline of the discovery of protein tyrosine kinases

Several landmark discoveries spanning the length of the previous century have brought us to our current state of understanding and appreciation of the importance of cellular signaling. Although, the first phosphate group on a protein was identified in 1906 it was not until much later that the role of kinases was elucidated (9). The next few insightful clues demonstrating the role of phosphorylation in regulating cellular functions came from studies focusing on the biochemical pathways of cellular metabolism. The late 1930s saw the discovery of glycogen phosphorylase, which was followed by the discovery of phosphorylase kinase, an enzyme capable of converting the former from its inactive form to active form in the presence of ATP (10). Between 1950 to the late 60s was an interesting period that led to the discovery of the second messenger cyclic AMP triggered by a hormone, and was shown to activate another kinase termed cyclic-AMP-dependent protein kinase, later known as protein kinase A (PKA). This in turn was found to play a crucial role in the activation of phosphorylase kinase that is required for the activation of glycogen phosphorylase (10, 11). These discoveries made in the 50s, unmasked for the first time a true "signaling cascade" where transfer of a phosphate group from one substrate to the other controlled cellular functions. However, it was not until 20 years later that other signaling cascades began to be identified. Like PKA,

several other serine/threonine kinases with intrinsic kinase activity were identified by the 70s (10).

However, in 1979, a breakthrough discovery demonstrated for the first time, a tyrosine kinase activity in a protein called *v-Src*, which is encoded by the transforming oncogene of the Rous Sarcoma Virus (RSV), which is the truncated form of its cellular counterpart, c-Src (12). Sequence analysis revealed that *v-Src* showed homology with the catalytic domain of PKA, a serine kinase and was later shown to phosphorylate tyrosine residues on other proteins, suggesting that it possessed intrinsic kinase activity (6).

In the 1980s, the discovery of tyrosine kinase activity associated with EGFR upon stimulation with its ligand, the epidermal growth factor or EGF linked cellular function to tyrosine kinase activity (13-15). Subsequent studies revealed that EGFR could not only phosphorylate exogenous substrates but also "self" phosphorylate specific tyrosine residues leading to the activation of signal transduction pathways (16-19). Around this time, another receptor, c-Met with intrinsic tyrosine kinase activity was discovered as the product of the Tpr-Met oncogene, which resulted from chromosomal rearrangement of the TPR and MET genes in osteosarcoma cells treated with a chemical carcinogen (20-23). Soon after these discoveries, receptors for platelet derived growth factor (PDGF), insulin and insulin-like growth factor 1 (IGF-1) were shown to possess intrinsic tyrosine kinase activity upon binding to their cognate ligands (7, 24). These were key findings that established a link between tyrosine phosphorylation mediated by growth factor receptors and their regulation of cell growth and proliferation.

Subsequent work in the late 1980s and the 1990s continued to explore the mechanistic role of PTKs and other serine/threonine kinases, which led to the discovery of signaling

cascades. Some of the major pathways identified were the JAK-STAT pathway, the classical MAPK and the PI3K pathways, which regulate growth, proliferation, differentiation, invasion and survival in cells (10). These were significant discoveries that underlined the true nature of signal transduction that transmit growth, proliferation, survival and cell death signaling.

Overall, these insightful findings contributed to enhancing our knowledge of the molecular mechanisms controlling the cell and established PTKs as important regulators of cell signaling. Figure 1.1 summarizes the timeline of these invaluable discoveries over the last century.

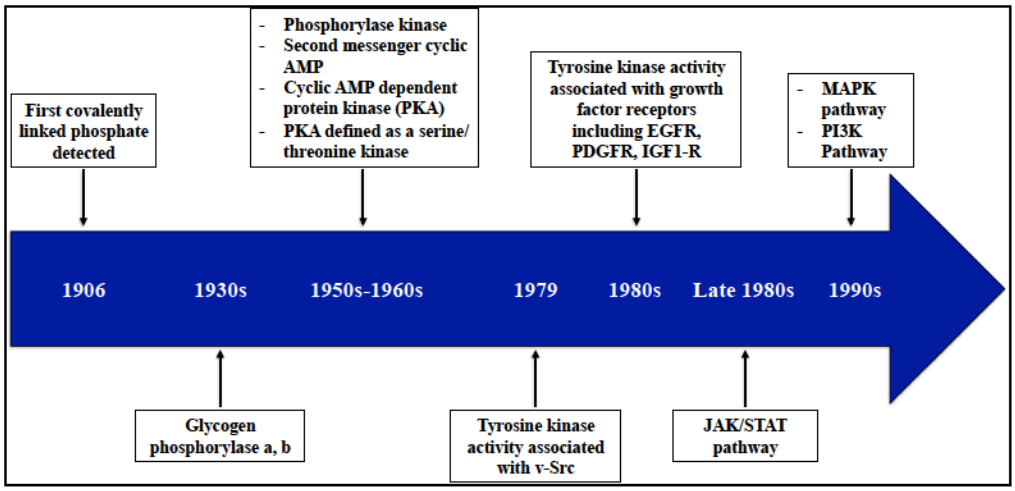

Figure 1.1: Historical overview. Key findings leading up to the discovery of protein tyrosine kinases (PTKs) and their role in cellular signaling

1.3. CLASSIFICATION OF PTKS AS RECEPTOR AND NON-RECEPTOR TYROSINE KINASES

With the sequencing of the human genome in 2000, it has been shown that 2% of the human genome accounts for protein kinases (520 known protein kinases), of which >90

account for protein tyrosine kinases (PTKs) (25, 26). These are further classified as receptor tyrosine kinases (RTKs) and non-receptor tyrosine kinases (non-RTKs) based on their overall structure, function and cellular localization. RTKs are glycosylated transmembrane proteins consisting of an extracellular domain for ligand binding, a transmembrane helix domain and a cytoplasmic region that possesses intrinsic enzymatic property (kinase domain) and binding sites for protein substrates mediating downstream signaling (7, 27).

The large family of RTKs includes the EGFR family (EGFR or Her1 or ErbB1, Her2 or ErbB2, Her3 or ErbB3 and Her4 or ErbB4), PDGFR, insulin-like growth factor-1 receptor (IGF1-R), c-Met and VEGFR. RTKs are activated upon binding exogenous growth factors (e.g. EGFR, PDGF, VEGF, etc.) that lead to cell growth, proliferation, differentiation, migration, invasion, embryogenesis, wound-healing, angiogenesis and survival through activation of signal transduction pathways (19). These growth factor receptors or RTKs, thus play a crucial role during early developmental stages but maintain tissue homeostasis by balancing cell growth, differentiation and programmed cell death (8, 28).

Non-RTKs are cytoplasmic kinases of modular structure that are activated downstream of growth factor receptors or RTKs (e.g. EGFR, PDGFR, c-Met, VEGFR), cytokine receptors and other transmembrane receptors such as integrins and G-protein coupled receptors (GPCRs), leading to the activation of signaling cascades that control important cellular functions such as growth, proliferation, migration, invasion, angiogenesis and apoptosis (29). Non-RTKs are classified into different families based on their structural and functional properties. Commonly expressed non-RTKs include the Src Family

Kinases (c-Src, Fyn, Lyn, Lck, Fgr, Yes, Yrk, Blk and Hck), Abl family (c-Abl, Arg), Janus Kinases or JAK family (JAK1, JAK2, JAK3 and TYK2), the Focal Adhesion Kinase family (FAK, Pyk2), etc. (29-36). In case of cytokine receptors that lack intrinsic enzymatic activity, non-RTKs serve as catalytic subunits that play a key role in transducing signals through phosphorylation events (e.g. IL6 binding to gp130 receptor subunits activates JAKs downstream, that lead to signal transduction) (37). However, in case of RTKs that possess intrinsic kinase activity, non-RTKs serve as signaling subunits by associating with different receptors, thereby leading to diversity in cell signaling and signaling crosstalks (29). Non-RTKs such as c-Abl, besides serving as signaling subunits also regulate transcriptional activity in the nucleus (35). Therefore, a tightly regulated network of RTKs and non-RTKs form an integral part of the signaling cascades controlling key cellular functions.

Since the primary focus of this thesis is on the tumorigenic properties of EGFR, c-Met, c-Src and the complex signaling crosstalk between them, the next few sections are dedicated to the structure, function and physiological properties of these kinases prior to discussing their role in cancers.

1.3.1. EGFR structure and activation

A. Structure

EGFR is a transmembrane receptor that consists of an extracellular region, a transmembrane helix that continues into the juxtamembrane domain and an intracellular cytoplasmic region. As seen in figure 1.2A, the extracellular region of EGFR consists of four domains termed domain I (or L1 where L stands for large), domain II (or CR-1 for

cysteine rich), domain III (L2) and domain IV (CR-2). While domains I and III interact with the ligand, domains II and IV are essential for receptor dimerization (38-40). EGFR can form homo- or heterodimers with other members of its family (e.g. EGFR-Her2, EGFR-Her3). The transmembrane domain is mainly α-helical, which is followed by the juxtamembrane domain that possesses regulatory functions, such as receptor downregulation and ligand-dependent internalization. This is followed by the kinase domain, which consists of an ATP-binding site between the N-terminal and C-terminal lobes. Detailed explanation of the structure, function and regulation of the kinase domain is given in the next section. Finally, the kinase domain is followed by the carboxy-terminal tail, which consists of tyrosine residues that undergo phosphorylation and create docking sites for various signaling proteins, thereby modulating receptor-mediated signaling (8, 40).

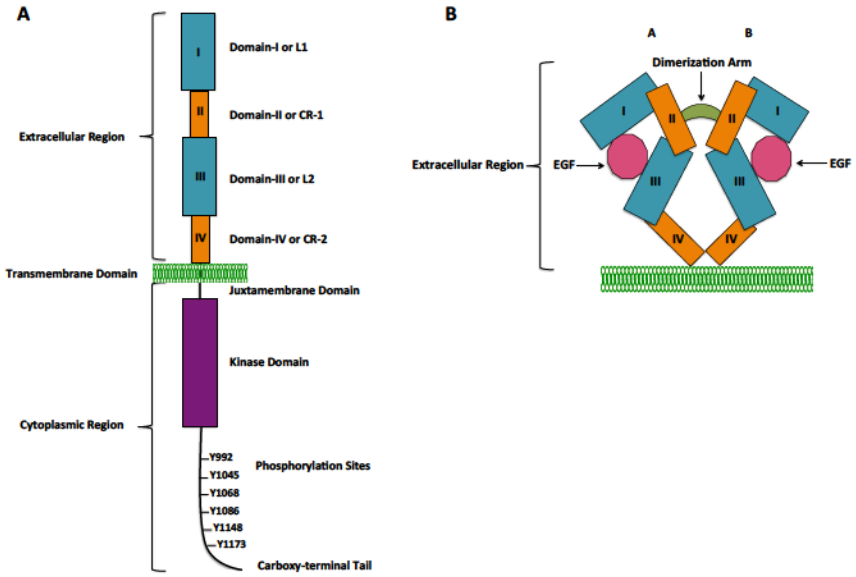

Figure 1.2: EGFR Structure and ligand binding. (A) The EGFR structure is primarily divided into an extracellular region, a single-pass alpha-helical transmembrane domain and a cytoplasmic region. The extracellular region facilitates ligand binding (domains I

and III) and receptor dimerization (domains II and IV). The cytoplasmic region consists of the kinase domain as well as the C-terminal region with specific tyrosine residues, which upon undergoing phosphorylation serve as docking sites for the binding of key signaling proteins. **(B)** Ligand binding is mediated by domains I and III, which in turn leads to conformational changes that expose the dimerization arm facilitating interactions between the two monomeric units.

B. Activation

EGFR is known to have seven ligands, including the epidermal growth factor (EGF), transforming growth factor (TGF)-α, heparin binding epidermal growth factor (HB-EGF), amphiregulin, betacellulin, epiregulin and epigen (41-45). As seen in figure 1.2B, each monomeric receptor (depicted as A and B) binds one ligand through interactions with domains I and III of the receptor (46-48). Ligand binding leads to conformational changes in the extracellular region that expose the domain II loop (or dimerization arm) into the interface, allowing the two ligand-bound monomeric receptors to interact with each other (Fig. 1.2B). Interactions between domains II and IV of each receptor bring the two monomers together, resulting in receptor dimerization, and subsequent activation of the kinase domain (40).

The kinase domain of all PTKs shares homology with the serine/threonine kinases and is about 300 amino acids long with a two-domain architecture consisting of a smaller N-lobe and a larger C-lobe. The N-lobe is made up of a five-strand β-sheet and a single α-helix, while the C-lobe is largely made of α-helices. Upon activation, ATP binds in the cleft between the two lobes, while protein substrates interact with the C-lobe (Fig. 2C).

Several polypeptide segments including the α-helix C in the N-lobe and the activation loop (A-loop) in the C-lobe contribute towards regulation of the kinase domain (49). In general, the A-loop maintains the receptor in an inactive state by occluding the active site and posing steric hindrance to the binding of ATP or protein substrate. The A-loop consists of conserved tyrosine residues (Tyr845 in EGFR, Tyr1234, 1235 in c-Met and Tyr419 in c-Src) that requires phosphorylation for receptor activation (except in the case of EGFR), and as a result, remains deeply buried and unexposed when the receptor is inactivated (50, 51). Ligand binding and receptor dimerization lead to conformational changes within the kinase domain and subsequent activation (27, 49, 52, 53). A ribbon-structure of a prototypical protein kinase domain has been shown in figure 1.3, which is based on the structure of the insulin receptor kinase bound to an ATP analog and a substrate (downloaded from Protein Data Bank, PDB code: 1IR3) (54). The N-lobe is represented in blue and the C-lobe in green. ATP binds in the cleft between the two lobes, while the peptide substrate binds in the active site, which is no longer inhibited by the A-loop (blue, labeled in the C-lobe). The receptor is inactive when the A-loop occludes the active site and causes steric hindrance to the binding of ATP or substrate.

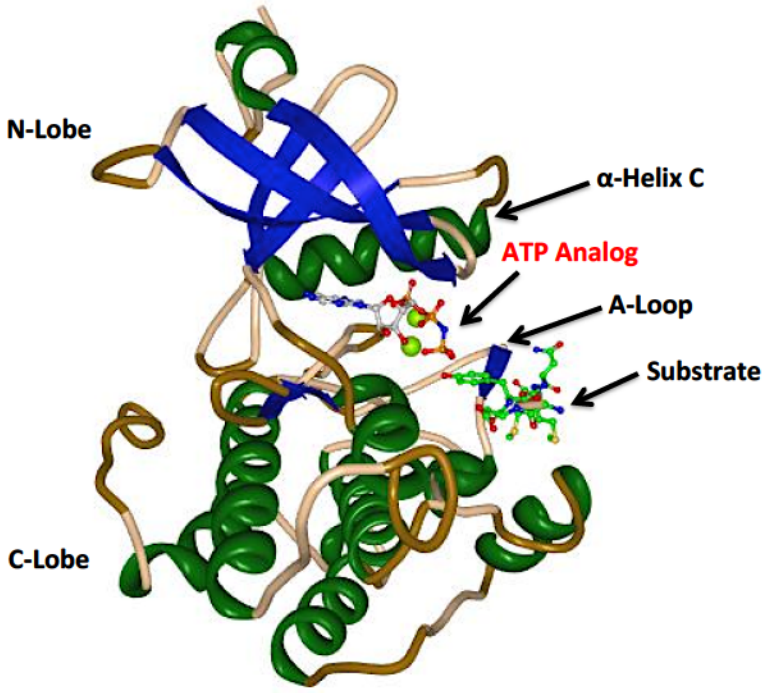

Figure 1.3: Ribbon structure of the prototypical kinase domain based on the structure of insulin receptor kinase. N-lobe is in blue, C-lobe in green and the a-helix C loop in the N-lobe (green), activation loop or A-loop in the C-lobe (blue), ATP analog as well as the peptide substrate are labeled accordingly. Downloaded from Protein Data Bank (PDB code: 1IR3, phosphorylated insulin receptor tyrosine kinase in complex with peptide substrate and ATP analog) (54).

Studies involving the substitution of the conserved tyrosine (Y) residue in the activation loop with a phenylalanine (F) residue to suppress phosphorylation activity, led to compromised kinase activity in most RTKs and non-RTKs (50, 51). However, mutations involving Y845F in EGFR did not affect its kinase activity, suggesting that EGFR activation was not dependent on phosphorylation of Y845 (55). Zhang *et al.* (56) showed using crystal lattices of activated and inactivated EGFR that ligand binding and receptor

dimerization lead to the formation of asymmetric dimers where the N-lobe of one kinase domain is juxtaposed with the C-lobe of the other kinase domain. This in turn leads to allosteric interactions that removes the autoinhibition caused by the activation loop and activates the kinase domain (56). An activated kinase can then phosphorylate tyrosine residues including Y992, Y1045, Y1068, Y1086, Y1148 and Y1173 in the C-terminal tail of EGFR that serve as docking site for proteins that activate signaling cascades downstream (Fig. 1.2B) (57).

1.3.2. c-Met structure and activation

A. Structure

Like EGFR, c-Met is a transmembrane receptor, the extracellular region of which consists of three domains including the Sema domain comprising an α-subunit that forms disulfide bridges with the β-subunit (Fig. 1.4). The Sema domain bears sequence homology to domains found in plexins and semaphorins that are large transmembrane receptors with cysteine-rich extracellular domains and secreted membrane-linked molecules with an extracellular domain, respectively (58, 59). The Sema domain in c-Met is followed by a PSI domain [found in plexins, semaphorins and integrins (60)] and an IPT domain [immunoglobulin-plexin-transcription, which are related to immunoglobulin-like domains found in integrins, plexins and transcription factors (61)] that is linked to the transmembrane domain. This is followed by an intracellular cytoplasmic region, which consists of a juxtamembrane domain, kinase domain and a regulatory C-terminal tail (62). The only known ligand for c-Met is the hepatocyte growth factor (HGF) or scatter factor (SF), which is secreted as pro-HGF that is cleaved by extracellular

proteases to generate mature HGF consisting of α- and β-chains linked by disulfide bridges (63, 64). This bivalent ligand binds c-Met by forming high-affinity interactions with the PSI domain via its α-chain (required for receptor binding) and forms low-affinity interactions with the Sema domain via its β-chain (required for c-Met activation) (65-67). Binding of HGF to each monomeric receptor leads to receptor dimerization followed by activation of the kinase domain (65, 66).

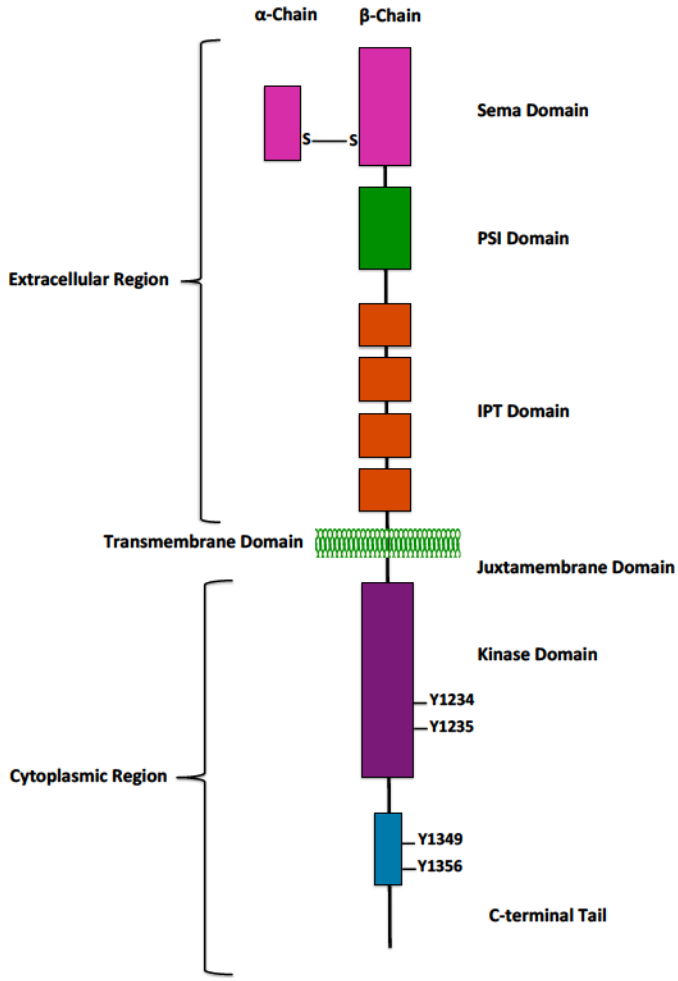

Figure 1.4: Structure of c-Met and its functional domains. The c-Met receptor consists of an extracellular region, a single pass alpha-helical transmembrane domain and a cytoplasmic region. The extracellular region consists of specific domains that facilitate the binding of HGF, leading to receptor dimerization. The cytoplasmic region includes

the kinase domain and the C-terminal regulatory tail, which consists of key tyrosine residues that serve as docking sites for the binding of signaling proteins upon undergoing phosphorylation.

B. Activation

The kinase domain is maintained in an inactive state by the activation loop blocking access to ATP or substrate to the catalytic domain. Phosphorylation of the two regulatory tyrosine residues, Y1234 and Y1235, on the activation loop is required for c-Met activation (50). Upon ligand binding and receptor dimerization, conformational changes bring the kinase domains of the two monomers in close proximity facilitating the *trans*-phosphorylation of the tyrosine residues. Y1235, which is more solvent-exposed and thus easily accessible within the activation loop, is phosphorylated first. However, complete removal of autoinhibition and thus, receptor activation only occurs following phosphorylation of the second tyrosine residue, Y1234. This indicates a "dual-switch" mechanism that tightly regulates the c-Met kinase domain, where phosphorylation of both residues is required for complete activation of the receptor (68). This in turn leads to the phosphorylation of tyrosine residues 1349 and 1356 in the C-terminal tail of the receptor that act as docking sites for proteins, leading to the activation of signaling cascades downstream (Fig. 1.4) (69, 70).

1.3.3. c-Src structure and activation

A. Structure

Unlike EGFR and c-Met, c-Src is a cytoplasmic protein of modular structure where different domains are joined together by linkers. As depicted in figure 1.5A, the c-Src protein structure can be divided into six regions: (a) Src homology-4 or SH4 domain, (b) a Unique domain, (c) an SH3 domain, (d) an SH2 domain, (e) a catalytic domain and (f) a negative regulatory tail (71). The SH4 domain is in the N-terminus region of the protein and contains special sites for lipid modifications. For instance, the N-terminal glycine is important for the addition of a myristol-group that helps anchor c-Src to the plasma membrane (72). Following the SH4 domain is a "Unique" domain that is particular to different members of the Src Family Kinases (SFKs) and participates in receptor and protein interactions. In case of c-Src, serine and threonine residues have been identified in this region that undergo phosphorylation, mediate protein-protein interactions and regulation of catalytic activity (30). The Unique domain is followed by three modular domains (SH3, SH2 and catalytic domain), which are found in several different proteins including non-RTKs, lipid kinases, receptors, transcription factors, etc. (73). The SH3 domain of c-Src participates in intra- and intermolecular interactions that regulate its kinase activity, its localization and substrate binding. This particular domain is important for protein-protein interactions, which is mediated by its ability to specifically recognize proline-rich sequences with the conserved P-X-X-P sequence (P = proline and X = amino acid) that are known to form polyproline type II (PPII) helices (74). Following the SH3 domain in the structure is the SH2, which binds short amino acid sequences containing a phosphotyrosine residue with preference for leucine. The SH2 domain regulates kinase activity as well as protein-protein interactions. The SH2 domain of c-Src is followed by a negative regulatory C-terminal tail. (Fig. 1.5) (30, 73, 75).

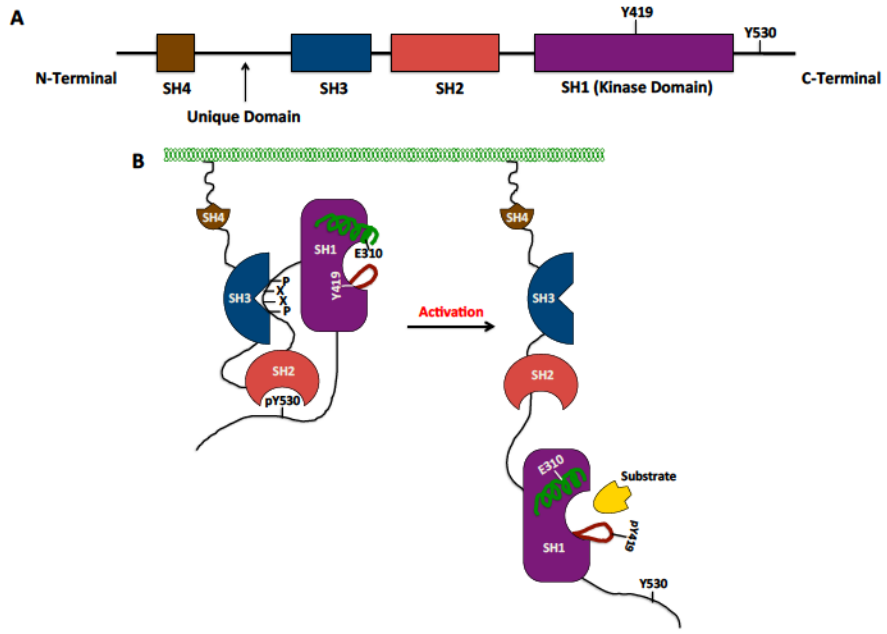

Figure 1.5: Structure and activation of c-Src. (A) c-Src consists of several modular domains termed the Src homology (SH) domains, each with a specific function. The N-terminal region consists of the SH4 and unique domains that facilitate anchoring to the plasma membrane. The SH3 domain mediates intra or inter-molecular protein-protein interactions through the recognition of proline-rich sequences. The SH2 domain plays a key role in recognizing phosphorylated tyrosine residues, and together the SH3 and SH2 domains play a key role in substrate recognition and binding. The SH1 domain is the kinase domain that has intrinsic catalytic activity. Finally, the C-terminal region of c-Src consists of the negative regulatory tyrosine residue, Y530, which undergoes phosphorylation and allows the protein to adopt a closed and inactive conformation. **(B)** c-Src activation is triggered by switching from a "closed" to a more "open" conformation, which is facilitated by dephosphorylation of the tyrosine 530 residue by phosphatases or through competitive binding of the SH2 domain to other phosphorylated

tyrosine residues. This in turn leads to conformational changes that activate the kinase domain and the c-Src protein.

Unlike RTKs, c-Src is maintained in a "closed" conformation through intramolecular interactions between its different domains (Fig. 1.5B). This is primarily aided by the interaction between the SH2 domain and the phosphorylated tyrosine residue Y530 in the C-terminal tail (76-78). Two known kinases, C-terminal c-Src kinase (CSK) (79) or CSK homologous kinase (CHK) are responsible for phosphorylating Y530, which acts as a negative regulator of c-Src (80). In addition, interactions between the SH3 domain and the linker that joins the SH2 and catalytic domains further stabilize the inactive conformation of c-Src (81). Overall, the c-Src inactive conformation is maintained by the intramolecular interactions between the SH2 domain and the C-terminal tyrosine residue along with those between the SH3 domain and the linker region between the SH2 and the catalytic domains.

The SH2 and SH3 domains do not occlude the catalytic domain but maintain the inactive conformation through distortions of the regulatory α-helix C loop (glutamic acid, E310). The activation loop causes steric hindrance to substrate binding and keeps Y419 inaccessible to phosphorylation (Fig. 1.5B) (82, 83). Note that the phosphorylation residues are often represented in the literature as Y416 (instead of Y419) and Y527 (instead of Y530), which are the corresponding tyrosine residues of c-Src in chicken, where c-Src was originally discovered as the viral oncogene *v-Src* (84). However in this work, the residues will be referred to as Y419 and Y530.

B. Activation

c-Src undergoes activation ("open" conformation) in one or more of the following ways: (a) dephosphorylation of Y530 by phosphatases, including protein tyrosine phosphatase (PTP)-α, PTP-γ, SHP-1 or SHP-2 or, (b) binding of the SH2 domain to phosphorylated tyrosine residues on other protein substrates that competitively disrupts the relatively weaker interaction between SH2 and the phosphorylated Y530 in the C-terminal region (30, 84). This in turn results in the activation of the c-Src intrinsic kinase activity and promotes relocalization of c-Src at different sites where it exerts its cellular functions (Fig. 1.5B) (84).

1.4. SIGNAL TRANSDUCTION PATHWAYS ACTIVATED DOWNSTREAM OF EGFR, C-MET AND C-SRC

Soon after the discovery of the c-Src structure, the Src homology domains (i.e., SH2 and SH3) were identified in several other proteins associated with signal transduction pathways. These signaling proteins of modular structure are classified as adaptors based on their ability to bind phosphorylated tyrosine residues on RTKs including EGFR and c-Met and participate in signaling cascades through their protein-protein interacting domains. Adaptor proteins generally lack enzymatic activity and possess one or more of the following domains: SH2 domain, the phosphotyrosine binding or PTB domain, SH3 domain and the pleckstrin homology or PH domain (85). Among these, adaptors containing the SH2, PTB or SH3 domain are involved in protein-protein interactions, while those containing the PH domain are involved in protein-lipid interactions. While SH2 and SH3 domains bind phosphorylated tyrosine residues, the latter domain binds

proline rich sequences (85). Adaptors commonly known to participate in signaling cascades originating from RTKs are the Src homology containing or Shc protein (86) (SH2 and PTB domains), the growth factor binding protein-2 or Grb2 (87) (SH2 and SH3 domains), PLC-gamma (16), Grb2-associated binding protein-1 or Gab-1 protein (88) (PH domain, proline rich sequences and a specific Met binding domain or MBD that is specific to c-Met binding) (73, 89). Consequently, other signaling proteins such as STATs (90) and the p85 regulatory subunit of PI3K (91) were also discovered to contain one or more of these modular domains that facilitate their protein binding and ligand-specific interactions leading to activation of signaling pathways downstream of receptors.

As previously mentioned, non-RTKs including c-Src are activated following protein-protein interactions facilitated by their modular structure, which leads to conformational changes and subsequent activation of their catalytic domain. c-Src is activated downstream of several membrane receptors including RTKs, integrins, G-protein coupled receptors (GPCRs) and cytokine receptors, functioning as an important signaling subunit downstream of receptors, regulating key cellular functions (30).

The next section describes canonical pathways activated by EGFR and c-Met, as well as highlights the role of c-Src as a key player in regulating different cellular functions through its involvement in various signaling pathways.

1.4.1. Activation of the Mitogen Activated Protein Kinase (MAPK) pathway

The Ras-Raf-MEK-ERK1/2 cascade belongs to the family of MAPK pathways classified on the basis of the type of MAPK activated by the signaling cascade. The MAPK pathways are evolutionarily conserved and are involved in cellular growth, proliferation,

differentiation, migration and apoptosis. To date, there are six groups of known MAPKs and these include extracellular signal-related kinases (ERK) 1/2, 3/4, 5, 7/8, JNK1/2/3 and p38 isoforms, among which, the ERK pathway is one of the best studied and found to be commonly deregulated in cancers (92, 93). The MAPK pathway can be defined as a three-tier kinase module wherein the MAPK is phosphorylated and activated by a MAPK-kinase (MAPKK), which in turn is phosphorylated and activated by a MAPKK-kinase (MAPKKK) that is activated by upstream proteins in response to extracellular signals (92).

Upon binding its ligand (e.g. EGF) and undergoing receptor dimerization and activation, EGFR autophosphorylates tyrosine residues on its C-terminal tail. Grb2, an adaptor protein, which is associated with son of sevenless (SOS), a guanine exchange factor, either directly binds phosphorylated Y1068 or Y1086 via its SH2 domain or indirectly by associating with the SH2 domain of Shc, which binds EGFR via its PTB domain at phosphorylated Y1148 or Y1173 (Fig. 1.6) (48, 94-96).

As for the receptor c-Met, following activation, Grb2-SOS may associate directly with it through its Y1356 or indirectly by binding Shc at Y1349, which in turn binds c-Met via its PTB domain (Fig. 1.6) (62, 97, 98).

The binding of Grb2-SOS to the receptor, brings SOS in close proximity with the membrane-bound Ras-GDP, a small molecule GTPase serving as a regulatory switch of the MAPK pathway, which is quickly exchanged for a GTP moiety. Ras-GTP subsequently recruits Raf-1 to the plasma membrane, which contains several regulatory phosphorylation sites, of which some are phosphorylated in their inactive state while others are phosphorylated by membrane-associated kinases to generate active Raf-1 (99,

100). Two such sites are Y340 and Y341 that are phosphorylated by c-Src and result in the activation of Raf-1 (101-103). The role of c-Src is not only implicated in the phosphorylation and activation of Raf-1 (and its close family member Raf-A), but it is also known to activate the Ras-Raf-MEK-ERK1/2 pathway by phosphorylating Shc, which then recruits the Grb2-SOS complex leading to the activation of Ras (104, 105). Once activated, Raf-1, a MAPKKK, leads to the phosphorylation and activation of MEK1/2, a MAPKK. MEK1/2 then phosphorylates and activates the last "tier" of this kinase module, ERK1/2, two MAPKs, which then translocate to the nucleus and activate transcription factors including c-Myc, c-Fos, c-Jun, CREB, Ap-1, Ets, etc., that control cell cycle progression, growth, proliferation and survival (Figure 1.6) (105).

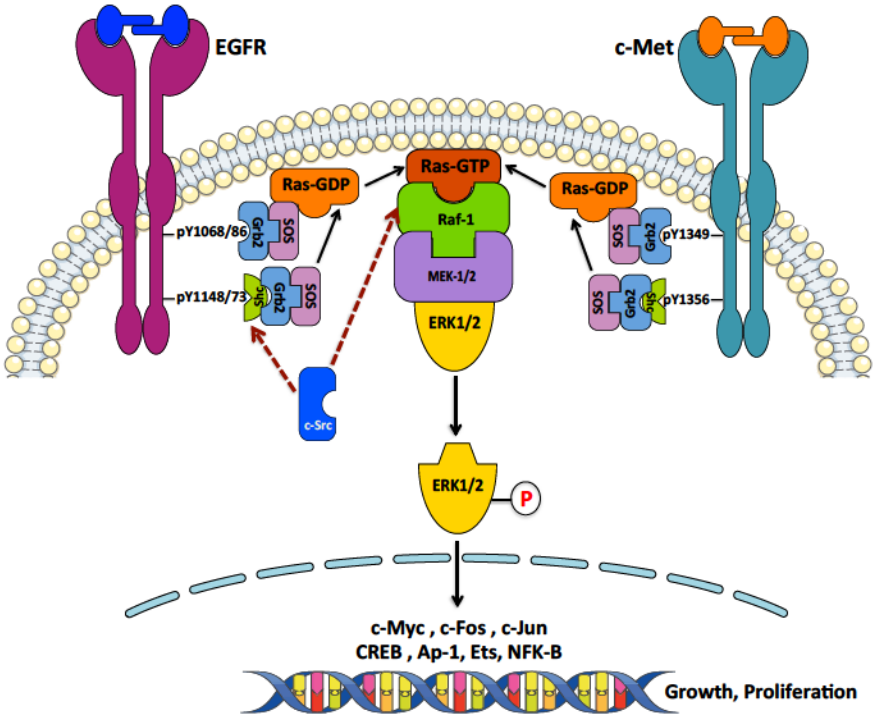

Figure 1.6: Activation of the MAPK pathway by EGFR, c-Met and c-Src. Receptor activation leads to the binding of the Grb2/SOS complex to phosphorylated tyrosine residues either directly or via Shc leading to the activation of the Ras protein. Once

activated, Ras activates Raf-1 via inducing conformational changes, which is further activated upon being phosphorylated on specific tyrosine residues by proteins such as c-Src. Activated Raf-1, a serine/threonine kinase phosphorylates MEK1/2, a dual-specificity kinase that further activate ERK1/2 by phosphorylating them on tyrosine and threonine residues. Activated ERK1/2 translocate to the nucleus and activate specific transcription factors regulating cell growth, proliferation and survival.

1.4.2. Activation of the Phosphotidylinositol-3-Kinase (PI3K) pathway

The phosphatidylinositol-3-kinase (PI3K) pathway is another major pathway activated downstream of receptor and non-receptor kinases that regulates growth, proliferation, survival, apoptosis, motility and metabolism (106). PI3Ks belong to the large family of lipid kinases that phosphorylate the 3'-OH of phosphatidylinositols at the plasma membrane. The family of PI3Ks is further classified into class I, class II and class III on the basis of substrate specificity, structure, function and mechanisms of activation. RTKs, GPCRs and Ras activate class I PI3Ks. Class II PI3Ks are activated by receptors and GPCRs activated by growth factors, hormones and cytokines and lead to vascular trafficking. Vacuolar protein sorting 34 (Vps34), the unique member of class III PI3Ks is involved in membrane trafficking (107).

Class I PI3Ks are the best characterized and are implicated in cancer progression (108, 109). These exist as heterodimers that consist of a regulatory subunit and a catalytic subunit (p110). The mammalian genome encodes four different isoforms of p110 (α, β, γ and δ) and several different regulatory units. The p110α is known to heterodimerize with p85, which serves as the regulatory subunit that binds receptors and non-receptors

through its SH2 domain (110). The p85 regulatory subunit of PI3K does not have a direct binding site on the C-terminal tail of EGFR and is thus activated by: (a) binding HER3 as part of the EGFR-HER3 heterodimer, (b) binding Gab-1 that is coupled with EGFR or (c) binding Y920 residue that is phosphorylated by c-Src (111-114). Unlike EGFR, c-Met has a direct binding site for p85, which can also bind the receptor indirectly via Gab-1 (62). The p85 subunit also binds the SH3 domain of c-Src via recognition of proline-rich sequences, leading to the activation of the PI3K pathway, in a c-Src-dependent manner (115).

Binding of the p85 regulatory subunit to an activated receptor or non-receptor thus results in the activation of the p110α catalytic subunit, which phosphorylates phosphatidylinositol-4,5-phosphate (PIP2) to phosphatidylinositol-3,4,5-phosphate (PIP3), the latter serving as a second messenger of the class I PI3K pathway. The phosphatase and tensin homolog (PTEN) is an important negative regulator of the PI3K pathway, which is known to dephosphorylate PIP3 to generate PIP2, leading to deactivation of downstream signaling. Both PIP2 and PIP3 act as docking sites for proteins containing the pleckstrin homology (PH) domain, including PDK-1 and protein kinase B/AKT (PKB/Akt). PI3K activation leads to translocation of Akt to the plasma membrane via its PH-domain, which is further activated by PDK-1 that phosphorylates threonine 308 on its activation loop (107). Phosphorylation of a second site, serine 473, is required for complete activation of Akt, which is carried out by the mammalian target of rapamycin (mTOR) complex protein, mTORC2 (116). Activated Akt is an important effector of the PI3K pathway that phosphorylates several substrates downstream affecting cellular growth, proliferation, metabolism, survival and apoptosis (107, 117). Table 1.1

below summarizes a list of substrates that are phosphorylated by Akt, and their respective functions.

Table 1.1: Akt substrates and the corresponding effect induced by Akt phosphorylation[106, 117]

Substrate	Physiological Function	Akt-mediated Effect
Bad	Pro-apoptotic	Inhibition
Procaspase-9	Pro-apoptotic	Inhibition
FOXO	Pro-apoptotic	Inhibition
CREB	Survival	Activation
IKK	NFK-B activation, survival	Activation
mTORC1	Protein synthesis, translation	Activation
GSK-3	Metabolism, growth	Inhibition
p21	Growth, proliferation	Inhibition
p27	Growth, proliferation	Inhibition
Mdm2	Inhibition of p53	Activation

1.4.3. Activation of the Signal Transducers and Activators of Transcription (STAT-3) pathway

The signal transducers and activators of transcription (STAT) proteins are transcription factors playing a key role in regulating cell cycle progression, differentiation and survival in cells (118). The STAT family consists of seven members including STAT1, STAT2, STAT3, STAT4, STAT5a, STAT5b and STAT6, of which STAT1, STAT3 and STAT5 are known to be overexpressed in cancers and play a role in carcinogenesis (119). STAT proteins consist of an oligomerization domain, a DNA binding domain and an SH2 domain that is required for their activation. While STAT3 and STAT5 are known to promote growth, proliferation and survival, STAT1 behaves as a tumour suppressor by

causing cell cycle arrest and inducing apoptosis (120). STAT2, 4 and 6 are primarily activated downstream of cytokine receptors and do not play a role in carcinogenesis (121).

In the canonical JAK-STAT pathway, ligand binding to the receptor (i.e., cytokine IL6 binding to glycoprotein130 or gp130 receptor subunits) leads to the binding and activation of the catalytic domain of the non-RTK, JAK (JAK family members, JAK1, 2, 3 or Tyk2). JAKs, unlike other non-RTKs lack an SH2 or SH3 domain and bind receptors via their JAK homology or JH domains that recognize proline rich sequences on the receptor, which activates their catalytic domain leading to the phosphorylation of tyrosine residues on the cytokine receptor. These phosphorylated tyrosine residues recruit STAT proteins that bind the receptor via their SH2 domain, followed by phosphorylation of key tyrosine residues on their SH2 domain by JAKs (Y701 on STAT1 (122), Y705 on STAT3 (123) and Y694 on STAT5 (124)). Each phosphorylated STAT protein then homo- or heterodimerizes with another activated STAT protein and translocates to the nucleus to mediate transcriptional changes by binding specific regions on the DNA (Fig. 1.7) (35, 121, 125).

Unlike cytokine receptors that lack intrinsic kinase activity and require the catalytic function of JAKs to activate STATs, growth factor receptors and non-receptor tyrosine kinases including EGFR, c-Met and c-Src are known to directly activate STATs through their intrinsic catalytic properties (Fig. 1.7) (126). Indeed, ligand-dependent activation of EGFR leads to STAT3 phosphorylation, in a JAK-independent manner, despite JAK1 being phosphorylated in response to EGF stimulation (35, 127, 128). Furthermore, STAT3 does not bind to phosphotyrosine residues on the C-terminal tail of EGFR, but

remains constitutively associated with the receptor. However, their activation is strictly dependent on the tyrosine kinase activity of EGFR. Another proposed mechanism for STAT3 activation by the receptor is via c-Src, which is activated in response to EGF stimulation (48). Early evidence that there is a close association between c-Src and STAT3 came from studies demonstrating that STAT3 was constitutively phosphorylated in cells transformed by the viral oncogene, *v-Src* (129, 130). Furthermore, c-Src being activated downstream of several receptors including cytokine receptors (e.g. IL3 receptor) resulted in the activation of STAT3 in a JAK-independent manner (131). Together, these suggest a role for c-Src mediated activation of STAT3 upon ligand binding to growth factor receptors (e.g. EGFR, PDGFR) as well as cytokine receptors (e.g. IL3) (132, 133).

In case of c-Met, STAT3 is activated in response to stimulation with HGF, by directly associating with phosphorylated tyrosine residues on the C-terminal tail of the receptor or indirectly by binding the adaptor protein, Gab-1 (134).

Following activation, STAT3 can also be phosphorylated on its C-terminal tail on Serine727, which is required for its enhanced transcriptional activity. The wide range of STAT3 target genes controlling key cellular functions include Cyclin D1, Cyclin D3, c-Myc, p21 and p27 (regulators of cell cycle progression), VEGF, HGF, FGF (regulators of angiogenesis), MMPs, vimentin, (regulators of invasion and migration) and finally, Bcl-2, Bcl-xl, Survivin and Mcl-1 (regulators of survival) (Fig. 1.7) (135).

Members of the Suppressors of Cytokine Signaling (SOCS) family, SOCS1 and SOCS3, Protein Inhibitors of STAT3 (PIAS3) and Genes Associated with Retinoid IFN Induced Mortality (GRIM) GRIM-19 negatively regulate STAT3. SOCS-1 and SOCS-3 possess

an SH2 domain through which they bind and inhibit JAKs, which in turn inhibits STAT3 activation (121).

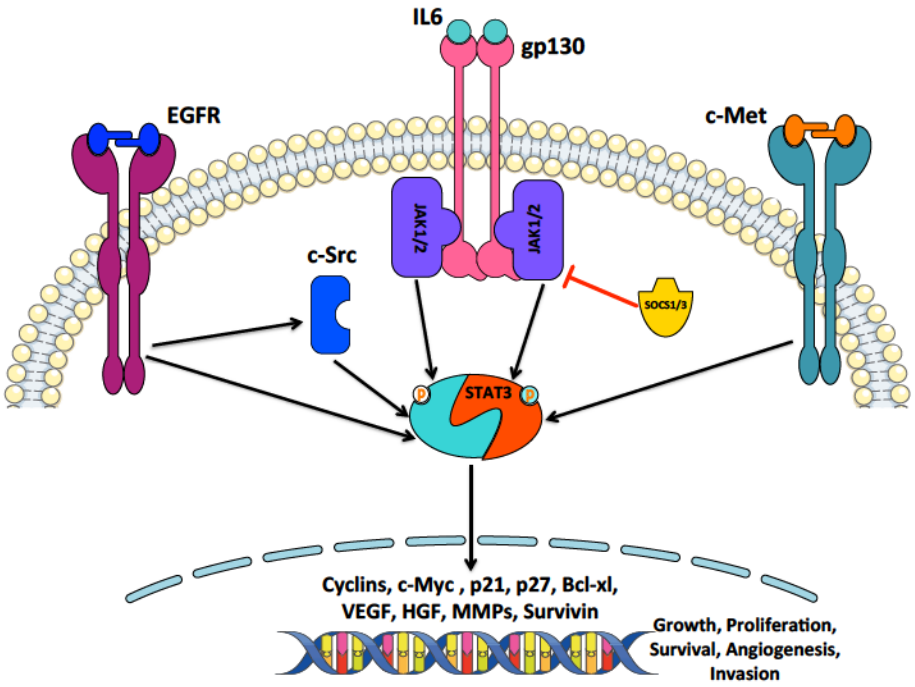

Figure 1.7: Activation of the JAK1/2-STAT3 pathway by gp130, EGFR, c-Met and c-Src. IL6 binding to its receptor, gp130 leads to activation of JAK1/2, which in turn phosphorylates STAT3 (on tyrosine 705 residue) resulting in its dimerization, nuclear localization and activation of specific genes. EGFR, c-Met and c-Src are also known to activate STAT3 by directly phosphorylating it in a JAK-independent manner.

1.4.4. Activation of c-Src downstream of EGFR and c-Met

The association between EGFR and c-Src is very well known and documented. In the late 1980s, the group of Sarah J Parsons demonstrated using transfected C3H10T1/2 mouse fibroblasts (normal cell behavior and morphology) that overexpression of wild type c-Src showed 200-500% increase in EGF-induced DNA synthesis (measured using [^{3}H] thymidine incorporation) compared with untransfected cells, suggesting a role for c-Src

in EGFR-mediated mitogenesis. In this context, there is a need for functional integrity of c-Src domains mediating membrane attachment, protein-protein interactions and kinase activity (136, 137). Further work involving C3H10T1/2 fibroblasts doubly overexpressing EGFR and c-Src demonstrated higher levels of EGF-induced DNA synthesis, heterocomplex formation between EGFR and c-Src, phosphorylation of novel tyrosine residues (Y845 and Y1101) on EGFR by c-Src and enhanced phosphorylation of Shc and PLC-gamma, compared with cells overexpressing either EGFR or c-Src alone. These studies indicated strong synergistic interactions between EGFR and c-Src upon ligand-mediated stimulation and activation of the receptor. Furthermore, studies using fibroblasts transfected with kinase dead c-Src or Y845F mutant EGFR showed decreased mitogenic potential compared with cells transfected with wild type c-Src or Y845 EGFR, indicating that c-Src was necessary to potentiate the mitogenic effects of EGFR. Importantly, these synergistic interactions appeared to be independent of the MAPK pathway since ERK2 signaling remained activated under Y845F or wild type conditions (138, 139). Later on, it was demonstrated that c-Src mediated phosphorylation of EGFR on Y845 leads to activation of the STAT5b pathway, which is responsible for enhanced EGF-induced c-Src dependent mitogenesis in cells expressing both kinases (140). Activation of c-Src downstream of EGFR leads to phosphorylation of different substrates with EGFR being one of them, as previously mentioned. Phosphorylation of Y845 not only activates the STAT5b pathway that promotes mitogenesis, but also other targets such as cyclooxygenase-II or COX-II, which promotes survival. Y845 is located in the activation loop of the EGFR kinase domain and despite being homologous to the autophosphorylation site required for activation of the catalytic domain of all protein

tyrosine kinases, its phosphorylation is independent of ligand-induced EGFR kinase activation. Consequently, since phosphorylation of Y845 depends on the catalytic activity of c-Src and not EGFR, it has been noted that c-Src, upon undergoing activation downstream of other receptors can phosphorylate Y845 and activate signaling pathways downstream, in an EGF-independent manner (141). In fact, c-Src has been implicated in the transactivation of EGFR by integrins and GPCRs, leading to Y845 phosphorylation and activation of signaling pathways (142-144). Besides activating STAT5b and COX-II pathways, phosphorylation of Y845 by c-Src is also required for Zn2+ induced Ras activation (145). As previously mentioned, c-Src affects EGFR-mediated survival by phosphorylating Y920 on the receptor creating a binding site for p85 (PI3K regulatory subunit) and activation of the PI3K pathway (113). It is also known to phosphorylate Shc, which is required for Grb2-SOS binding and activation of the MAPK pathway, as well as phosphorylation of cytoskeletal proteins including FAK, cortactin, p190Rho and p120Ras, leading to cytoskeletal remodeling and migration (48, 139, 146-148). Finally, c-Src prevents EGFR degradation by phosphorylating Cbl, a protein responsible for EGFR endocytosis and degradation, leading to its ubiquitination and proteosomal degradation (149).

c-Src is a known substrate of c-Met following HGF stimulation, and is implicated in transducing signals downstream of the receptor. As previously mentioned, c-Src plays a key role in HGF-induced activation of FAK leading to cytoskeletal remodeling, motility and anchorage independent growth. Furthermore, c-Src along with PI3K has also been reported to play a role in pro-survival signaling via activation of the NF-kB pathway. Finally, c-Src activation can positively feedback on c-Met signaling (62).

Taken together, it can be seen that c-Src is not only activated downstream of EGFR and c-Met in a ligand-dependent manner, but also plays a role in positively interacting with the receptors in potentiating their signaling effects. Furthermore, given the ability of c-Src to participate in a multitude of signaling pathways originating from various receptors and non-receptors, it can lead to transactivation of receptors, thereby mediating signaling crosstalk. The signaling effects mediated by RTKs and non-RTKs are tightly regulated under normal physiological conditions through processes such as receptor internalization (e.g. Cbl mediated endocytosis, ubiqutination and proteosomal degradation of EGFR), activation of regulatory kinases (e.g. CSK or CHK phosphorylating c-Src Y530), phosphatases (e.g. PTPs can dephosphorylate the autophophorylation sites of RTKs leading to receptor inactivation, PTEN attenuates PI3K signaling by converting PIP3 to PIP2) and GAPs, (e.g. Ras-GAPs or GTP activating proteins that hydrolyze Ras-GTP to Ras-GDP, inactivating Ras) serving as important checkpoints (150-154). However, when these signaling proteins are deregulated together with the regulatory proteins keeping them in check, cells undergo uncontrolled growth, proliferation, motility, and invasion and evade apoptosis, which ultimately results in tumorigenesis.

The upcoming sections will discuss the oncogenic potential of EGFR, c-Met and c-Src, their role in human cancers and their complex signaling interactions driving tumour progression.

1.5. DEREGULATION OF RTKS AND NON-RTKS IN CANCER

Given the role of RTKs and non-RTKs in maintaining normal cellular activities, alterations in genes encoding these kinases generate potent oncoproteins that transform

cells through aberrant and deregulated signaling. Some of the major mechanisms leading to their deregulation include: (a) genomic rearrangement such as chromosomal translocations that result in oncogenic fusion proteins [e.g. fusion of chromosomes 9 and 22 generating the Philadelphia chromosome that encodes constitutively active Bcr-Abl oncoprotein, the primary driver of CML (155)], (b) mutations [e.g. gain of function mutations in codons 12, 13 or 61 in Ras leading to constitutively activated Ras (156), loss of function mutations in p53 (157), activating mutations in EGFR that drive non-small cell lung cancer or NSCLC and making tumours "addicted" to EGFR (158)], (c) overexpression of RTKs and non-RTKs resulting from gene amplification [e.g. EGFR/HER2 overexpression in breast cancers, c-Met amplification in NSCLC (26)]. While different mechanisms of alterations exist, the primary outcome remains increased tyrosine kinase activity resulting in uncontrolled cell-cycle progression, invasion and survival leading to cellular transformation.

The upcoming sections highlight the oncogenic role of EGFR, c-Met and c-Src and their ability to drive human cancers.

1.5.1. EGFR in Cancer

Since its discovery in the 1980s (15), EGFR has been one of the best-studied receptors in both molecular biology and cancer biology. Given its role in cell signaling, it is not surprising that deregulation of this receptor leads to pathogenesis. In the 80s, an important clue came from sequencing the *v-erbB* oncogene belonging to the avian erythroblastosis virus (AEV), whose gene product is the truncated form of EGFR (159). This was an important discovery that uncovered EGFR as a proto-oncogene and soon

after, began the search for the oncogenic role of this receptor in human cancers. Today, it is known that EGFR is deregulated in several human cancers including breast, lung, colon, head and neck, brain, prostate, pancreatic and liver, and is one of the most investigated targets for the development of anti-cancer agents (160).

EGFR in cancers can be altered in one or more ways leading to hyperactivation of receptor-mediated signaling that culminates in increased growth, proliferation, invasion and survival. These mechanisms of deregulation include mutations (e.g. point mutations, in-frame deletion), structural alterations, gene amplifications and increased transcriptional activation that result in receptor and/or ligand overexpression and constitutive receptor activation (160).

Although not the predominant form of EGFR deregulation, mutations in the receptor have been identified in specific tumours leading to enhanced growth and cancer progression. A well characterized EGFR mutation is that occurring in glioblastoma multiforme (GBM). Among the primary brain tumours diagnosed, GBM is the most commonly occurring subtype (161). EGFR overexpression due to gene amplification is seen in up to 40% of tumours with about 60-70% of them carrying deletions in exons 2-7 in the gene encoding EGFR. This generates the variant EGFRvIII form, which is lacking part of the extracellular ligand-binding domain and resembles the gene product of the *v-erbB* oncogene. This in-frame deletion confers EGFRvIII with the ability to remain constitutively active and thus contribute towards the oncogenic potential of the receptor. Although previous reports have indicated weak signaling potency of the EGFRvIII receptor, its ability to signal for a longer period of time owing to lack of ligand-dependent receptor endocytosis and internalization could contribute to its tumorigenic role.

Furthermore, EGFRvIII is capable of forming homodimers with EGFR-wt receptor and heterodimers with other members of the EGFR family (e.g. Her2, ErbB3) leading to constitutive signaling via these receptors. Together, these suggest a strong role for EGFR and its variant, EGFRvIII in driving GBM tumours through increased proliferation, survival and invasiveness (162).

Non-small cell lung cancer (SNCLC) is a subtype of lung cancer that is known to have mutations in EGFR. Lung cancer remains the leading cause of cancer related deaths and NSCLC accounts for 70-80% of the cases diagnosed (163). In 2004, two groups independently reported somatic mutations that occur in the EGFR tyrosine kinase domain, which were mainly clustered around exons 18-21 and were detected in a small percentage of patients responding to clinical EGFR inhibitor (164, 165). The two most frequently occurring mutations are the in-frame deletion in exon 19 (del E746-A650) and the point mutation in exon 21 (L858R). Both these mutations occur in the kinase domain of EGFR and are called "activating" mutations since they render the receptor constitutively active by destabilizing its inactive kinase domain conformation. Consequently, tumours expressing these mutant EGFR receptors showed dependence of this receptor for their growth and survival and as a result, exhibited increased sensitivity to EGFR targeted inhibitors (163). While NSCLC remains the major subtype of cancers demonstrating activating EGFR mutations, there have been reports of EGFR mutations in carcinomas of the colon, esophagus, pancreas and the salivary gland (166-168).

While activating mutations have been identified in different tumours, the most common form of deregulation results from EGFR overexpression due to gene amplification or increased transcriptional activation. Tumours that are known to overexpress EGFR

include breast, lung, head and neck, pancreatic, brain, prostate, gastric and ovarian. Furthermore, increased EGFR activity has been noted in some tumours including lung, ovary, colon and prostate due to upregulation of ligand (e.g. TGF-α) production by the stroma or the tumour itself, resulting in paracrine/autocrine receptor activation (160). EGFR is also known to promote migration and invasion and its expression correlates with poor clinical outcome (169, 170). Finally, EGFR also potentiates tumorigenic properties by cooperating with other signaling partners. For instance, EGFR and EGFRvIII cooperate in GBM cells to phosphorylate STAT proteins and potentiate malignant transformation (171). Recently, Tsai *et al.* (172) demonstrated that EGFR and HER2 synergized to promote growth in bladder cancer cells *in vitro* and *in vivo*. EGFR is also known to heterodimerize with HER2 in driving breast cancer progression and promote growth of pancreatic cancer cells (173). Overall, aberrant EGFR signaling results in increased growth, proliferation, survival and invasion and is associated with poor prognosis and clinical outcome (174).

1.5.2. c-Met in cancer

Aberrant c-Met signaling is associated with several tumours including lung, breast, colon, kidney, prostate, hepatocellular, head and neck, brain and ovarian. Deregulated c-Met signaling primarily results from receptor and/or HGF overexpression as well as developing sporadic or germline mutations in the kinase and non-kinase domains of the receptor. The end result is increased and uncontrolled c-Met signaling that promotes growth, proliferation, survival, invasion and metastasis (175, 176).

The discovery of germline mutations in patients with hereditary papillary renal carcinoma or HPRC (a subtype of renal carcinoma) that could be mapped on to the c-Met gene demonstrated a direct malignant role of c-Met in cancers. These mutations were identified as missense mutations in the kinase domain of c-Met that stabilized substrate binding and led to enhanced kinase activity (177). Similar mutations were also found in sporadic papillary renal carcinoma with a lesser frequency (13%) (178). Somatic mutations in the kinase, SEMA (extracellular region) and the juxtamembrane domains have been reported, although rarely, in different cancers including non-small-cell lung, hepatocellular, breast, colorectal, gastric, liver and metastases of head and neck. These mutations lead to enhanced c-Met kinase activity and constitutive activation due to lack of receptor endocytosis (mutations in the juxtamembrane domain prevents Cbl-mediated receptor internalization) (175).

Although several cases of c-Met mutations have been reported in different cancers, the main mode of receptor deregulation remains overexpression resulting from gene amplification, increased transcriptional activation and hypoxia-induced expression. The overexpression of c-Met has been reported in several tumours including breast, lung, prostate, ovarian, head and neck, liver and gastric. Furthermore, enhanced c-Met activity also results from increased ligand-dependent paracrine or autocrine signaling through overexpression of HGF in stroma and within the tumour. HGF overexpression has been reported in tumours including lung, ovarian, head and neck, gastric and liver (175, 179).

In lung adenocarcinomas, overexpression of c-Met and/or HGF correlates with increased tumour growth, metastasis, poor prognosis and resistance to radiation therapy. In breast cancer, c-Met/HGF overexpression correlates with poor prognosis, high proliferative

index and tumour metastasis (175). Furthermore, c-Met is frequently overexpressed in metastatic cancers indicating it is able to not only drive tumour growth and proliferation, but also invasion and metastasis. As an example, c-Met expression increases from 2% to 50% in head and neck cancers as they progress from primary to metastatic tumours. Under normal physiological conditions, HGF/c-Met signaling plays a critical role during embryogenesis in mediating epithelial to mesenchymal (EMT) transition allowing cells to migrate over long distances until they reach their target organ (179). c-Met signaling is also important in regulation of migration and invasion of cells during tissue repair and wound healing processes. Given the ability of the receptor to promote migration and invasion, it is believed that similar pathways play a role in promoting tumour metastasis (28).

Finally, c-Met is also known to engage in signaling crosstalk with other receptors potentiating cancer progression. For instance, c-Met synergizes with HER2 in breast cancer cells to promote invasion (180). c-Met cooperates with IGF-1R to promote migration and invasion of pancreatic cancer cells (181). c-Met also engages in crosstalk with integrins to promote migration and invasion in cells (182). Overall, aberrant c-Met signaling is linked to aggressive metastatic tumours and is associated with poor prognosis (183).

1.5.3. c-Src in cancer

Deregulated c-Src signaling has considerable transforming abilities. c-Src shows elevated activity in breast, lung, prostate, head and neck, colon, pancreatic and ovarian cancer (184). Activating mutations or gene amplifications are rare in the case of c-Src

deregulation. Although the exact mechanism leading to its elevated activity in cancers is unknown, different modes of activation are proposed: (a) increased association with overexpressed or hyperactivated RTKs (e.g. EGFR, c-Met, IGF-1R, PDGFR, VERGF), (b) decreased activity of Csk, the kinase responsible for downregulating c-Src, and (c) upregulation of phosphatases that dephosphorylate Y530, leading to the activation of c-Src (151, 185).

c-Src is an important mediator of tumour cell proliferation and survival through its interactions with RTKs and integrates signaling through the MAPK, PI3K and STAT3 pathways. For instance, c-Src synergizes with EGFR and HER2 to potentiate growth and invasion of breast cancer cells (186-189). c-Src is also known to synergize with EGFR in promoting growth and proliferation in colorectal and head and neck cancer cells (190, 191). c-Src regulates angiogenesis through activating the expression of VEGF (angiogenic factor) under hypoxic conditions (192). c-Src activity is crucial during tumour metastasis due to its ability to regulate the cytoskeleton, migration, adhesion and invasion. The activated FAK/c-Src complex then phosphorylates several other cytoskeletal proteins including paxillin, p130Cas and tensin that are associated with actin filaments and then controls cell migration by promoting focal adhesion formation and turnover (30, 193). c-Src activates epithelial to mesenchymal transition (EMT) through phosphorylation of E-cadherins and disruption of the cadherin-catenin junction, which promotes differentiation and invasion. Additionally, c-Src also promotes invasion through the activation of matrix metalloproteases or MMPs that are proteolytic enzymes required for the digestion of the basement membrane (194, 195).

Taken together, elevated c-Src activity in different cancers drives tumour growth, invasion and metastasis through mediating its pleiotropic effects.

1.6 TARGETING DEREGULATED RTKS AND NON-RTKS IN CANCER

Given the role of RTKs and non-RTKs including EGFR, c-Met and c-Src in driving cancers, tremendous efforts have gone into developing anti-cancer agents targeting these kinases. The last decade has marked significant advances in our knowledge and understanding of the molecular mechanisms controlling tumour growth and progression. In the early 2000s, Bernard Weinstein coined the term "oncogene addiction", which proposed that despite the complexity of signaling networks driving cancer progression, tumour growth might still depend on a particular oncogene whose blockade can lead to potent disruption of growth and induction of apoptosis (196). He further proposed that blockade of a single target might eventually become inadequate and lead to drug resistance since tumours might gain dependency on an alternate signaling circuitry (196). Nonetheless, this became an important concept that helped in the development of targeted therapies based on the ability of specific oncogenes to drive tumours. Experimental evidence was obtained using transgenic mice engineered to overexpress oncogenes (e.g. c-Myc, Bcr-Abl) that led to tumour development but upon deactivation of oncogenes, the tumours regressed (197, 198). Human cancer cell lines were also treated with antisense oligonucleotides against specific driver oncogenes (e.g. K-Ras in pancreatic cancer, HER2 in breast cancer), which completely abrogated growth and proliferation in cells (199, 200). Further validation was obtained through the successful development of imatinib, the first kinase inhibitor against the Bcr-Abl fusion protein, which showed

remarkable clinical response in patients with chronic myelogenous leukemia (CML) (201). Thereafter, several other targeted therapies have been developed and approved for the treatment of different cancers (3, 202).

Targeted therapies currently in clinical use are classified as small molecule tyrosine kinase inhibitors (TKI) or monoclonal antibodies (mAbs). The first class of TKIs consists of ATP analogs that bind the active conformation of the kinase domain and prevent binding of intracellular ATP and subsequent phosphorylation of substrates. The other class of TKIs is not ATP competitive and binds the inactive conformation of the kinase domain. While most TKIs belong to the first class of ATP competitive inhibitors, the Bcr-Abl targeting drugs, imatinib and nilotinib belong to the non-competitive class of TKIs (203).

The next section highlights targeted therapies developed against EGFR, c-Met and c-Src in different cancers.

1.6.1. EGFR targeted therapies

EGFR targeting TKIs and mAbs have been developed and approved for the treatment of different cancers. Gefitinib and erlotinib, EGFR TKIs were approved by the Food and Drug Administration (FDA) for locally advanced or metastatic non-small-cell lung cancer (NSCLC) after failing chemotherapy (204-206). Figure 1.8 illustrates the binding of gefitinib to the EGFR kinase domain [downloaded from PDB, code: 2ITY (207)]. However, it was not until 2004 when two independent groups reported that a subset of NSCLC patients (~10%) receiving gefitinib responded to the drug. Mutational analysis of these tumour samples revealed activating mutations in the EGFR kinase domain (del

E746-A750 in exon 19 and L858R in exon 21) within the population that responded to gefitinib. This indicated that NSCLC tumours in these patients were oncogene addicted to EGFR and subsequent blockade of the receptor led to remarkable clinical response (164, 165). Thus, gefitinib and erlotinib are now indicated for NSCLC patients that have exon 19 or 21 mutations but have wild type K-Ras (another commonly mutated oncogene that mediates resistance to EGFR inhibitors). Furthermore, erlotinib in combination with gemcitabine as first line therapy has also been approved for advanced metastatic pancreatic cancer. Furthermore, cetuximab (EGFR mAb) in combination with chemotherapy or radiotherapy has been approved for head and neck cancer. Panitumumab, another EGFR mAb, and cetuximab in combination with chemotherapy or as single agents when all other therapies fail have been approved for colorectal cancer. Unlike TKIs that block ATP binding in the kinase domain, EGFR monoclonal antibodies block ligand binding to the extracellular domain, promote receptor internalization and lead to antibody and complement-mediated cytotoxicity (206).

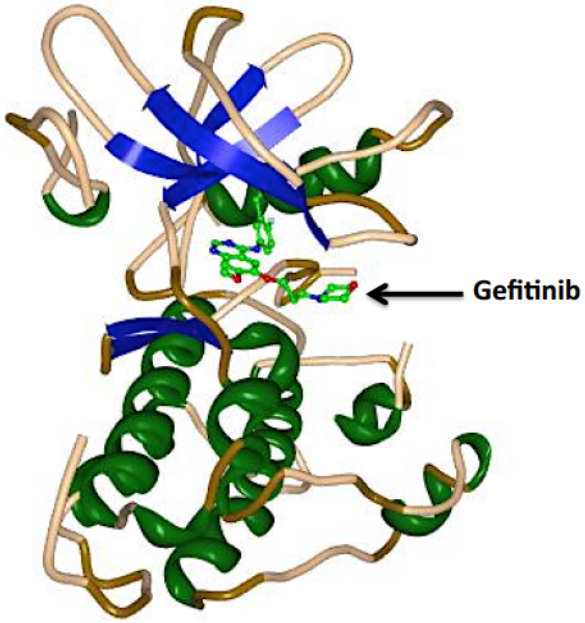

Figure 1.8: Crystal structure of the binding of gefitinib to the EGFR kinase domain [downloaded from PDB, code: 2ITY, (207)]. The N-lobe of the kinase domain consisting primarily of β-sheets is represented in blue, while the C-lobe consisting primarily of α-helices is represented in green.

1.6.2. c-Met targeted therapies

Targeted therapies including monoclonal antibodies and ATP-competitive and non-competitive TKIs have been developed against the c-Met pathway. One of the mechanisms currently being pursued is to evaluate monoclonal antibodies that are designed to bind HGF and prevent it from binding and activating c-Met. Two such antibodies, rilotumumab and ficlatuzumab are in clinical trials. Rolitumumab is currently being evaluated as monotherapy (recurrent glioblastoma, metastatic renal cell carcinoma and ovarian cancer) and combination therapy with chemotherapeutic agents in prostate

cancer or with anti-angiogeneic agents in different solid tumours. Ficlatuzumab is being evaluated as monotherapy and in combination with gefitinib in NSCLC (208).

Another approach has been to design c-Met targeted antibodies that function by blocking ligand binding, mediating receptor internalization and/or inducing antibody-dependent complement cytotoxicity (ADCC). LY2875358, a humanized mAb is in phase I/II clinical trials both as single agent and in combination with erlotinib in NSCLC. Another humanized mAb, H224G11/ABT700 is in phase I clinical trial both as a single agent and in combinations with docetaxel or cetuximab or erlotinib in solid tumour overexpression c-Met. Finally, another c-Met antibody termed Met/Mab or Onartuzumab is being evaluated in phase II clinical trials as combination therapy with chemotherapy or targeted agents in different solid tumours including lung cancer, glioblastomas, metastatic triple negative breast and colon cancers (208).

Finally, c-Met targeting TKIs, both selective and non-selective as well as ATP-competitive and non-competitive have been developed. Crizotinib is a non-selective ATP competitive c-Met TKI, which was originally approved for a subset of NSCLC patients expressing the EML4-ALK fusion protein since crizotinib is also an ALK inhibitor. Figure 1.9 illustrates the binding of crizotinib in the c-Met kinase domain [downloaded from PDB: code 2WGJ (209)]. Currently, crizotinib is currently being evaluated in phase II and III clinical trials. Another non-selective TKI, cabozantinib inhibits c-Met, RET, VEGFR1, VEGFR2, VEGFR3, KIT, FLT-3 and TIE2 and has been recently approved for medullary thyroid carcinoma (210). Tivantinib is a selective non-ATP competitive c-Met TKI that is currently being evaluated in clinical trials against hepatocellular carcinoma as a single agent and in combination with erlotinib in NSCLC (211).

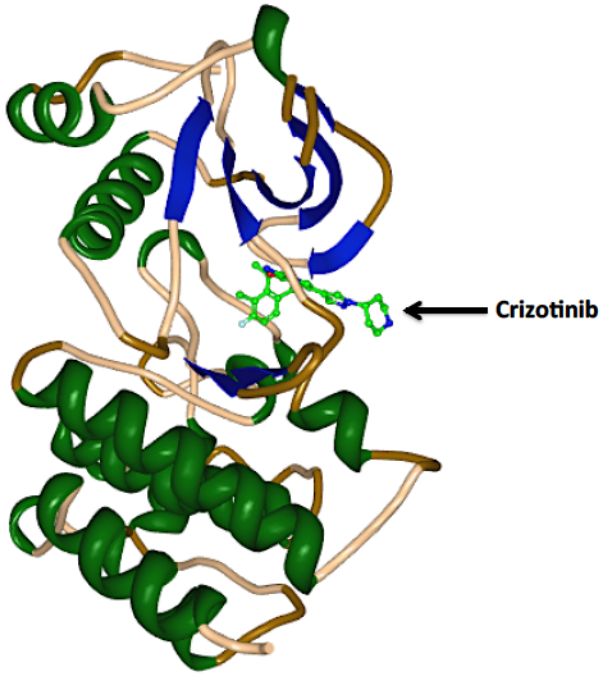

Figure 1.9: Crystal structure of the binding of crizotinib to the c-Met kinase domain [downloaded from PDB, code: 2WGJ (209)]. The N-lobe of the kinase domain consisting primarily of β-sheets is represented in blue, while the C-lobe consisting primarily of α-helices is represented in green.

1.6.3. c-Src targeted therapies

Given the role of c-Src in driving different cancers, dasatinib, a dual c-Src/c-Abl ATP competitive TKI indicated as second line therapy for the treatment of Philadelphia positive CML, was evaluated using preclinical studies on solid tumours. Figure 1.10 illustrates the binding of dasatinib in the c-Src kinase domain [downloaded from PDB: code 3G5D (212)]. Promising outcome from preclinical studies along with a favorable safety profile in phase I clinical trials prompted its further clinical investigation in different solid tumours. Particularly, c-Src being a key regulator of osteoclast-mediated

bone resorption, preclinical data using dasatinib showed a decrease in osteoclast activity and thus bone resorption, which prompted its further evaluation in cancers that metastasize to the bone, particularly prostate and breast cancers. Currently, dasatinib is being evaluated both as monotherapy and in combination with chemotherapy or other targeted therapies in different cancers including lung, breast, prostate, brain (glioblastoma), colon, pancreatic as well as hematological cancers. Saracatinib and bosutinib are other c-Src/Abl TKIs that are also being currently explored as single and combination therapy in clinical trials; however, none of the c-Src inhibitors have been very effective in monotherapy (185, 213).

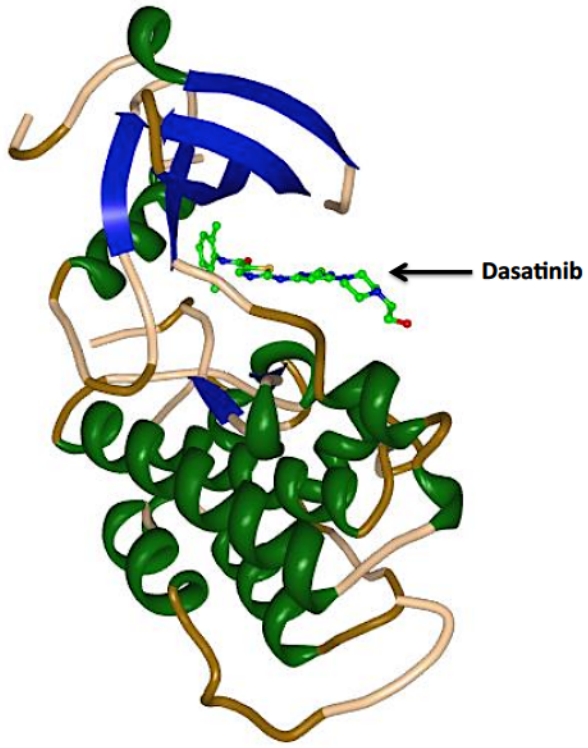

Figure 1.10: Crystal structure of the binding of dasatinib to the c-Src kinase domain [downloaded from PDB, code: 3G5D, (212)]. The N-lobe of the kinase domain consisting primarily of β-sheets is represented in blue, while the C-lobe consisting primarily of α-helices is represented in green.

1.6.4. Molecular subtyping and tumour heterogeneity

Despite their ability to specifically target deregulated kinases in cancer, the clinical response of these TKIs, particularly as single agents, is often only modest. This is especially true when unselected patient populations are treated with the same clinical inhibitor, based on the morphology of the tumour (i.e., colon cancer or non-small-cell lung cancer). The poor clinical response to EGFR inhibitors in unselected patient populations prompted further molecular analysis, which revealed 15 different genetic subtype signatures of NSCLC, including EGFR activating mutations (~13%), EML4-ALK fusions protein expression (~5%), K-Ras mutations (~24%), PIK3CA and PTEN mutations, FGFR-1 and PDGFR-B amplifications (3). Molecular subtyping of tumours in NSCLC has allowed select groups of patients to receive target-specific inhibitors thereby increasing their chances of benefiting from these drugs. Ineffective monotherapy with c-Src inhibitors (i.e., dasatinib) is also partly attributed to carrying out their evaluation in unselected patient populations. However, molecular analysis of colorectal, pancreatic and renal cell carcinoma (RCC) using preclinical studies revealed that cell lines demonstrating elevated c-Src activity were sensitive to c-Src inhibitors including dasatinib and saracatinib (185). Molecular analysis of various tumours has revealed different genetic signatures driving tumour progression in many cancers including colorectal, lung, pancreatic, head and neck, breast, etc. (214-218). Overall, a deeper understanding of the molecular subtypes of tumours has led to a paradigm shift towards therapeutic strategies that are now personalized or customized, thereby allowing patients to achieve maximum clinical response.

The presence of different genetic signatures is a classic example of tumour heterogeneity. Cancer is a complex multi-stage disease that develops through the accumulation of multiple genetic alterations, progressing from a single neoplastic cell to a heterogeneous population of malignant cells forming a tumour mass. Tumour heterogeneity is believed to stem from clonal expansion of cells with genetic instability that were "selected" among others in a Darwinian-manner, which allows for coexistence of different subpopulations of cancer cells with different genetic signatures. Furthermore, heterogeneity is also influenced by morphological changes, differentiation of cancer stem cells, epigenetic changes and dynamic interactions with the tumour microenvironment that play a crucial role in determining the fate of tumour cells (3). Therefore, tumour heterogeneity emphasizes on the need for molecular subtyping to determine appropriate target-specific therapies. However, intratumour heterogeneity is associated with lack of complete drug-response mediated by different acquired or preexisting genetic signatures within the tumour leading to drug resistance (3, 219). The next section describes some of the major mechanisms of resistance to targeted therapies.

1.6.5. Resistance to targeted therapies

Screening of genetic mutations and molecular subtyping of tumours has not only helped target driver oncogenes, but also resulted in a better clinical management of tumour heterogeneity. However, despite these efforts, tumours eventually progress and often metastasize, leading to drug resistance. As depicted in figure 1.11, resistance to targeted therapy can be broadly classified as intrinsic resistance and acquired resistance. Intrinsic resistance is characterized by lack of response to targeted therapies and is further

classified as resulting from tumour-specific alterations (e.g. genetic mutations and alterations) or patient-specific properties (e.g. poor pharmacokinetics, drug-drug interactions). Acquired resistance is characterized by initial response followed by loss of response to targeted therapy, which is believed to be a consequence of selective pressure induced by initial drug treatment. Acquired resistance is primarily classified as resulting from (a) genetic alterations of target oncogene and (b) activation of bypass mechanisms (206, 220). Other mechanisms include change in histopathology of the tumour such as NSCLC transforming to small cell lung cancer (SCLC) or acquisition of epithelial to mesenchymal transition (EMT) (221).

The next section briefly describes the different types of intrinsic and acquired resistance that commonly occurs in cancers.

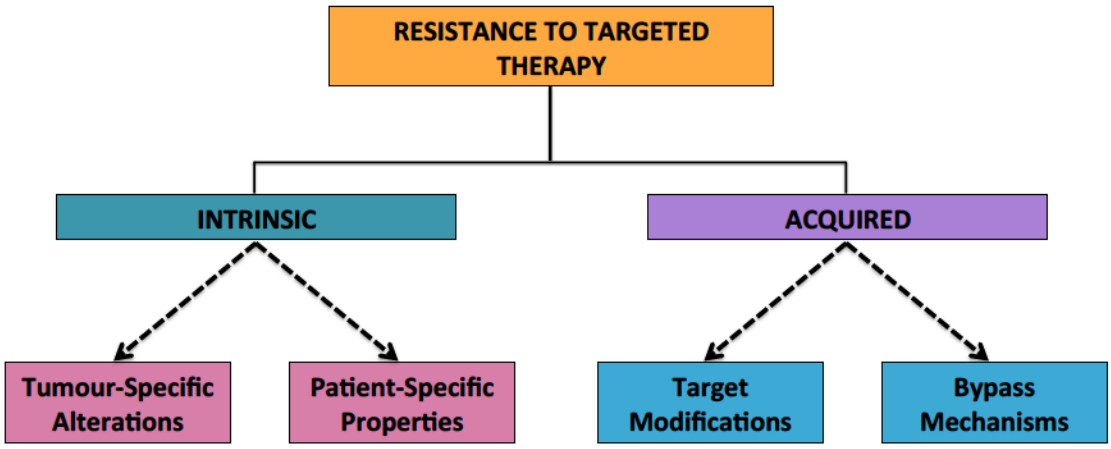

Figure 1.11: Resistance to targeted therapies. Resistance mechanisms are broadly classified as intrinsic or acquired and are further sub-divided into different categories based on their nature or site of origin.

1.6.5.A. Intrinsic Resistance

Intrinsic tumour resistance results from genetic alterations other than those implicated in the driver oncogene, leading to lack of drug response to targeted therapies. For instance, 0.5% of never-smokers with lung adenocarcinoma carried a germline T790M gatekeeper mutation in the kinase domain, thereby not responding to erlotinib or gefitinib (222). Gatekeeper mutations arise from amino acid substitutions that lead to reduced drug binding, while preserving the catalytic activity of the kinase. For instance, the substitution of a threonine (T) for a bulkier methionine (M) at the gatekeeper position creates steric hindrance to the binding of gefitinib or erlotinib while increasing the affinity of ATP-binding and thus retaining EGFR kinase activity (223). In another instance, Gastrointestinal and Stromal Tumours (GIST) demonstrating exon 9 mutations in the c-Kit driver oncogene were resistant to imatinib (a Bcr-Abl/c-Kit/PDGFR TKI approved for the treatment of GIST) (224).

Intrinsic resistance can also occur in a patient-specific manner due to poor pharmacokinetics resulting from altered ADME (absorption, distribution, metabolism and excretion) or drug-drug interactions where one drug induces cytochrome P450 (CYP450) mediated metabolism of the other (e.g. fenofibrate, a drug used to lower cholesterol levels induces CYP3A4, which leads to enhanced metabolism of erlotinib) (220, 225).

1.6.5.B. Acquired Resistance

Acquired resistance to targeted therapy primarily results from target modification or activation of bypass mechanisms. Gene amplification and acquisition of secondary site mutations contribute to target modification and lack of drug response. Gene amplification

of driver oncogenes including EGFR, Bcr-Abl and EML4-ALK have been observed in different tumours that render them insensitive to targeted therapies (220). Secondary mutations such as gatekeeper mutations have been found in "oncogene addicted" cancers treated with specific targeted therapies and mediate resistance to the binding of drugs. Some of these include the T790M mutation in EGFR [resistance to gefitinib/erlotinib (223)], T315I mutation in Bcr-Abl [resistance to imatinib (226)], T670I mutation in c-Kit [resistance to imatinib (227)] and L1196M in EML4-ALK [resistance to crizotinib (228)]. Newer generations of inhibitors capable of binding and inhibiting the kinases despite gatekeeper mutations are in different phases of development (229-232), while some of them have been approved [e.g. dasatinib and nilotinib as second generation drugs for T315I mutant Bcr-Abl in CML (233)].

Another important mechanism of acquired resistance is through the activation of bypass mechanisms leading to continued tumour growth and survival despite targeted therapies inhibiting the driver oncogene. Bypass mechanisms are commonly driven by deregulated receptors (e.g. c-Met, HER2, HER3, IGF-1R, integrins) or non-receptors (e.g. c-Src, K-Ras, PI3K, MEK, ERK1/2, c-Abl, JAK, FAK, STAT3) other than the primary driver oncogene resulting from mutations, gene amplifications and/or elevated activity (234-236). In the case that an alternative RTK (e.g. c-Met) is activated, as a result of gene amplification/overexpression, it will activate the same canonical pathways downstream that promote growth, proliferation, invasion and survival (i.e., MAPK, PI3K/Akt) leading to a phenomenon termed "redundant signaling" wherein therapeutic blockade of one oncogenic pathway is "overcome" by the activation of another (237-241). In another situation, when blockade of RTKs such as EGFR, HER2, c-Met, etc. leads to inhibition

of the MAPK or PI3K/Akt pathways, an alternate pathway, i.e., the JAK/STAT pathway promoting growth and survival is usually activated as a compensatory signaling mechanism, which mediates resistance to the drug (242-244). STAT3 is a commonly deregulated protein in different cancers and is found activated in response to various targeted and chemotherapeutic agents (245-249). Finally, in some cases, mutations in the downstream signaling proteins such as K-Ras, B-Raf (effectors of the MAPK pathway) or PTEN (negative regulator of the PI3K/Akt pathway) leads to constitutive activation of growth and survival pathways, in a manner that is independent of upstream regulation by RTKs, thereby mediating resistance to drugs targeting these receptors (250-256).

Since the primary focus of this thesis is on the oncogenic signaling properties of EGFR, c-Src and c-Met, the upcoming section describes the signaling crosstalk between EGFR, c-Met and c-Src that not only mediates resistance to targeted therapies but also plays a prominent role in driving tumour growth, invasion and survival.

1.6.5.C. Signaling crosstalk and elevated c-Src activity promote tumour growth and mediate resistance to EGFR inhibitors

Previously, the interactive role of c-Src with EGFR has been discussed in the physiological context, wherein c-Src is activated downstream of EGFR in an EGF-dependent manner and is also capable of phosphorylating specific tyrosine residues on EGFR including Y845 and Y920 that result in the activation of the STAT5b, COX-II and PI3K/Akt pathways. This is associated with enhanced EGF-induced DNA synthesis, growth and survival (141, 257). In addition, c-Src is also known to play a role in the transactivation of EGFR by other receptors such GPCRs and integrins (142-144).

Given their signaling interactions and elevated activity in several cancers, it is not surprising that EGFR and c-Src synergize to promote tumour growth and progression. Maa *et al.* (139) demonstrated that in cells overexpressing EGFR, c-Src potentiated DNA synthesis, soft agar growth and tumour formation in nude mice suggesting a synergistic interaction between the two kinases to promoting aggressive tumour progression. Increased c-Src activity has been associated with resistance to EGFR inhibitors in EGFR-driven cancers. EGFR and c-Src are known to be co-expressed in breast cancer and previous work using breast cancer cell lines have demonstrated a synergistic role for the two kinases in promoting enhanced growth, proliferation and tumorigenesis (143). Mueller *et al.* (258) showed using breast cancer cells that c-Met phosphorylation, at least in part, regulated c-Src activation, which in turn mediated EGFR tyrosine kinase independent EGFR phosphorylation and cell proliferation in the presence of gefitinib, suggesting a possible role for c-Met/c-Src in mediating resistance to EGFR TKIs in breast cancer. In another study, Formisano *et al.* (189) reported that the functional interaction of c-Src with EGFR in breast cancer cells might be meditating resistance to lapatinib, a dual EGFR/HER2 TKI.

Zhang *et al.* (259) demonstrated that c-Src phosphorylation was detected in tumour samples from lung cancer (NSCLC) patients and that c-Src promoted survival in EGFR-dependent NSCLC cell lines. Furthermore, they also showed that combined blockade of EGFR and c-Src was synergistic in EGFR-dependent NSCLC cell lines. The role of c-Src has also been implicated in mediating EGFR-TKI resistance in NSCLC cells. Kanda *et al.* (260) established erlotinib resistant NSCLC cell lines that showed increased expression of integrins (β1, α2, α5) and c-Src led to constitutive activation of Akt. They

also demonstrated that silencing of c-Src could restore sensitivity of cells to erlotinib. In another instance, Yoshida *et al.* (261) showed that c-Src activity is elevated in gefitinib-resistant NSCLC cells that have c-Met amplification. They further demonstrated that inhibition of c-Met led to decreased c-Src activity and direct inhibition of c-Src resulted in growth inhibition and induction of apoptosis in these gefitinib resistant NSCLC cells.

High levels of c-Src activity also correlated with cetuximab (EGFR mAb) resistance in colon cancer cells. Resistant cells were shown to have high level of c-Src activity and increased EGFR-dependent HER3 and PI3K activation. However, addition of dasatinib, a c-Src TKI led to re-sensitization of colon cancer cells to cetuximab. Furthermore, combination of EGFR and c-Src inhibitors has shown synergistic effects in *in vitro* models of colon cancer (262). Lu *et al.* (263) showed that c-Src activity is elevated in a cohort of glioblastoma (GBM) tumour samples from patients who also showed high EGFR activity. Furthermore, c-Src was shown to mediate resistance to EGFR mAbs. However, addition of dasatinib increased efficacy of EGFR mAb *in vivo,* in tumours expressing EGFRvIII and exhibiting high c-Src activity (263). c-Src is also known to potentiate the oncogenic effects of EGFR in head and neck squamous cell carcinoma (HNSCC) and its co-expression with EGFR in pancreatic cancers is associated with cancer progression, metastasis and poor clinical prognosis (264, 265).

1.6.5.D. Redundant signaling by c-Met synergizes with EGFR to potentiate tumour progression and resistance to EGFR inhibitors

Elevated c-Met activity due to gene amplification, increased protein synthesis or increased production of the c-Met ligand, HGF in the tumour or stroma in EGFR-

dependent tumours has been associated with resistance to EGFR inhibitors (237, 266). This is mediated by the activation of redundant signaling pathways downstream of c-Met leading to continued tumour growth and progression, despite therapeutic blockade of EGFR.

Amplification of the c-Met gene occurs in about 5% of lung cancer patients and leads to clinical resistance to EGFR TKIs through HER3-mediated activation of the PI3K survival pathway (237). c-Met amplification has also been demonstrated in lung cancer patients with acquired resistance to gefitinib or erlotinib, independent of their EGFR T790M gatekeeper mutational status (267). Yano *et al.* (266) showed that increased HGF production in the tumours/stroma contributes to gefitinib resistance in lung cancers having intrinsic or acquired EGFR mutations, through activation of the c-Met/PI3K/Akt pathway, independent of HER3 activation. Puri *et al.* (268) demonstrated using *in vitro* models of NSCLC cells that EGFR and c-Met synergize to promote growth, proliferation and motility in an EGF and HGF dependent manner. Furthermore, Dulak *et al.* (269) showed that in NSCLC cells that express wild type, non-amplified EGFR and c-Met, EGFR transactivates c-Met in an HGF-independent manner, with c-Src playing a crucial role in mediating this crosstalk. Additionally, they demonstrated that c-Met activation occurred in a delayed manner and was required for potentiating EGFR-induced invasion and motility in NSCLC cells. They proposed that increased c-Met activity resulted from increased EGF-induced transcription and showed that dual-blockade of EGFR and c-Met led to synergistic inhibition of tumour growth and proliferation (269).

As previously mentioned, c-Met amplification has also been observed in treatment-naive lung tumours, mediating primary resistance to EGFR TKIs (270, 271). Currently,

combinations of EGFR and c-Met inhibitors are being evaluated in clinical trials, as a promising new strategy for patients demonstrating intrinsic or acquired resistance to EGFR TKIs through c-Met amplification (272). Increased c-Met activity has also been associated with mediating resistance to cetuximab (EGFR mAb) in head and neck squamous cell carcinoma (HNSCC) (273). Xu *et al.* (274) showed using *in vitro* and *in vivo* models of HNSCC that combined blockade of EGFR and c-Met led to superior growth inhibitory and anti-proliferative effects compared with single RTK targeting. Furthermore, they also demonstrated EGFR-mediated HGF-independent activation of c-Met in HNSCC cells, with c-Src possibly being a candidate mediating crosstalk between the two receptors (274). Stabile *et al.* (275) showed using HNSCC cells overexpression or elevated activity of c-Src mediates resistance to erlotinib (and not cetuximab) by stimulating c-Met activation in an HGF-independent manner. They further demonstrated that addition of a c-Src or a c-Met inhibitor sensitized cells to erlotinib and the addition of a c-Met inhibitor to c-Src overexpressing HNSCC tumours sensitized them to erlotinib *in vivo* and showed increased apoptosis. Together, these underlined a strong rationale for combining a c-Src or a c-Met inhibitor with an EGFR inhibitor to overcome resistance to EGFR TKIs in HNSCC (275). c-Met activation is also known to mediate resistance to EGFR inhibitors in glioblastoma, colorectal, pancreatic and breast cancer cells (276). Furthermore, complex signaling crosstalk between EGFR and c-Met along with the involvement of c-Src has been observed in breast cancer cells, which mediates resistance to EGFR TKIs (258, 277). Finally, there is also supportive evidence for increased EGFR activity mediating resistance to c-Met inhibitors. Kim *et al.* (278) demonstrated that in triple negative breast cancer (TNBC), c-Met expression correlated with EGFR expression

in tumour samples, and in the most drug resistant TNBC cell line, silencing of EGFR sensitized the cells to c-Met inhibition. In c-Met oncogene addicted gastric cancer cells, EGFR activation due to increased TGF-a production mediated resistance to c-Met inhibitors (240).

1.6.6. Underlying rationale for multi-targeting of EGFR, c-Src and c-Met in advanced cancers

It is now increasingly evident that the signaling crosstalk between EGFR, c-Src and c-Met not only leads to synergistic increase in tumour growth, invasion and survival, but also mediates resistance to targeted therapies. While c-Src synergizes with EGFR to promote growth and proliferation, it can also mediate resistance to EGFR targeted therapies by activating other signaling pathways including c-Met and also upon being activated by c-Met (258, 260, 261, 275). c-Met in turn can synergize with EGFR to promote growth, proliferation, invasion and survival when co-expressed, but mediates resistance to EGFR targeted therapies through activation of redundant signaling pathways (237, 268, 269, 274, 276, 277, 279-281). In contrast, EGFR activation in c-Met-addicted cancers can mediate resistance to c-Met inhibitors (240). Importantly, EGFR and c-Met are involved in signaling crosstalk with each other and receptor transactivation with c-Src being a key mediator of these interactions (269, 274, 275, 282, 283). Taken together, these provide a strong rationale for the dual targeting of EGFR and c-Src, EGFR and c-Met as well as the triple targeting of EGFR, c-Met and c-Src to not only abrogate synergistic crosstalk between the kinases, but also effectively block compensatory signaling pathways mediating resistance (Figure 1.12). The upcoming section discusses

the past and current trends in drug discovery and the targeting approach that will be used to inhibit EGFR, c-Src and c-Met in cancers.

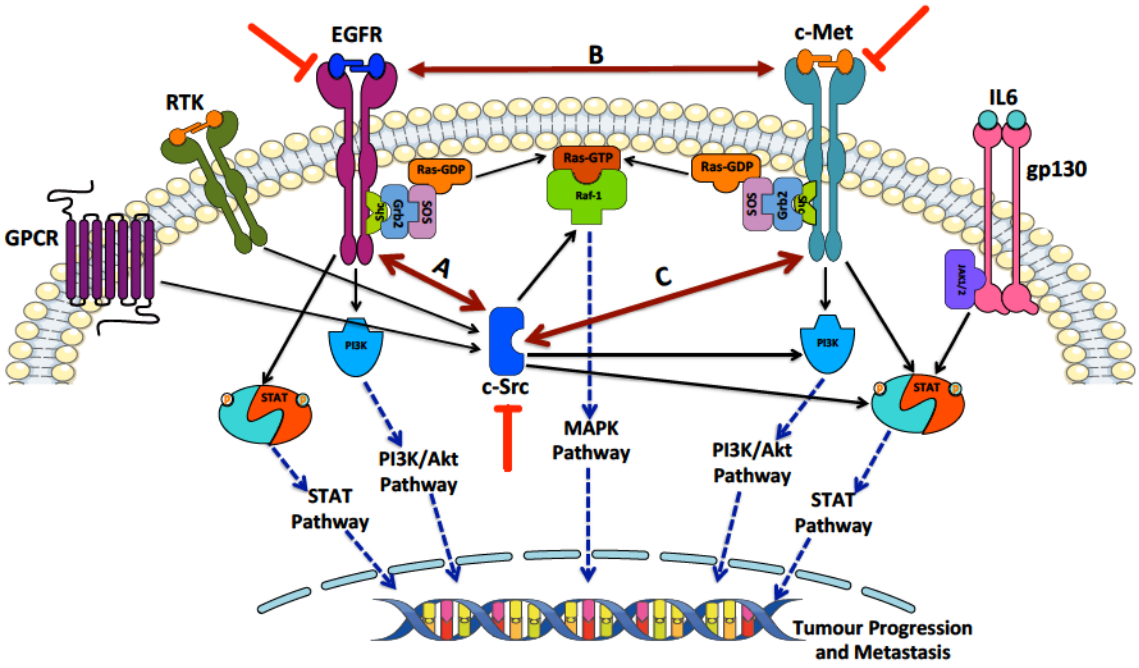

Figure 1.12: Signaling complexity involving the crosstalk between EGFR, c-Met and c-Src and the urgent need for multi-targeting (indicated by red inhibitory signs). In the schematic, **A** represents synergistic crosstalk, ligand independent activation of EGFR by c-Src and resistance to EGFR inhibitors, **B** represents synergistic crosstalk, receptor transactivation and signaling redundancy mediating resistance to EGFR or c-Met inhibitors, and **C** represents synergistic crosstalk, HGF-independent activation of c-Met mediated by c-Src and resistance to targeted therapies.

1.6.7. A shift in the drug discovery paradigm: emergence of polypharmacology

For the longest time, drug discovery has been governed by the "one gene, one disease, one drug" paradigm, which led to the discovery of compounds with a high level of target specificity (284). Although this resulted in the successful development of several drugs,

the field of cancer drug discovery has been crippled by growing clinical attrition rates, particularly in moving from phase II to phase III. The two major reasons for the high rate of drug failure have been largely imputed to the lack of efficacy and poor toxicity profile (1). In addition, recent advances in the field of cancer biology has led to a deeper understanding of the underlying molecular mechanisms driving cancer that is no longer limited to a single dysfunctional gene, which has challenged the one-gene-one-disease paradigm. Genomic studies using single gene knockouts have revealed that only about 19% of the genes are embryonic lethal across various model organisms, and that multiple genes or pathways need to be "disrupted" for a robust or sustained antitumour activity. In addition, the use of systems biology and network analysis of biological pathways has revealed complex signaling nodes with overlapping functionality (285-287).

Taken together, these suggest a large number of redundant and compensatory signaling pathways at play, which has shifted the philosophy of drug discovery towards the development of multi-targeted agents. In general, the multi-targeting approach can be classified as administering: (a) multiple individual drugs (e.g. chemotherapeutic cocktails), (b) multicomponent drugs as single formulations (e.g. single pill formulations), and (c) single drugs with multi-targeted properties (e.g. multi-targeted kinase inhibitors, rationally designed hybrid or chimeric molecules) (284).

The use of classic chemotherapeutic cocktails (e.g. ABVD – adriamycin, bleomycin, vinblastine and dacarbazine for Hodgkin's lymphoma, CHOP – cyclophosphamide, Adriamycin or hydroxy doxorubicin, vincristine or oncovin and prednisone for non-Hodgkin's lymphoma) follows the conventional principles of multi-targeting for achieving sustained antitumour property (288, 289). Similarly, combining different

inhibitors into a single pill has served as an attractive approach in multi-targeting. However, differences in their individual drug properties including pharmacokinetics, biodistribution, solubility and metabolism must be taken into account in order to achieve optimum potency with low toxicity (284).

In order to overcome challenges posed by the use of drug cocktails or multicomponent formulations, the trend of multi-targeting is shifting towards the principles of "polypharmacology", which is based on developing single drugs having specific binding properties towards two or more targets in the cell (284). Unlike some of the small molecule multi-kinase inhibitors (e.g. sorafenib, sunitinib) with serendipitously discovered properties (290), the goal of polypharmacology is to rationally develop compounds with a broad targeting profile that are capable of modulating two or more targets to generate desirable therapeutic effects while exhibiting a favorable safety profile (284). Biological target identification and validation serves as an important step in the developmental stages of multi-targeted drugs, in order to effectively block all the key players involved and delay onset of possible resistance mechanisms. In the recent years, the use of network analysis, systems biology, chemical genomics and RNA-interference technology has aided in the identification of oncogenic targets mediating pleiotropic effects (284, 287, 291-294). This has led to the identification of signaling proteins mediating synergistic crosstalk, redundancy, compensatory activation and drug resistance, which serve as promising candidates for polypharmacology based drug discovery.

Given their role in cancers, we chose to develop rationally designed multi-targeted inhibitors against EGFR, c-Src and c-Met that not only synergize to drive tumour growth

and progression, but also mediate resistance to targeted therapies. In addition, the drug development process was further aided by validating the outcome of blocking two or more of these targets using their respective clinical inhibitors as pharmacological/chemical probes.

The following section reviews the design, synthesis and mechanisms of action of these multi-targeted inhibitors synthesized in our laboratory over the past years. Furthermore, it briefly introduces the first generation of kinase-kinase targeting drugs, which led to the future design and optimization of EGFR-c-Src and EGFR-c-Met dual targeting inhibitors.

1.6.8. Combi-molecules: design, synthesis and mechanism of action

Within the scope of developing rationally designed multi-targeted drugs, our laboratory has extensively studied the design and development of a novel class of compounds termed "combi-molecules" (**I-Tz**) that contain two distinct pharmacophores or targeting arms (e.g. **I** targeting EGFR and **Tz** targeting DNA**)** connected by a linker, and capable of exerting their inhibitory effects on two or more biological targets (Fig. 1.13). Combi-molecules represent a class of chimeric molecules that are capable of inducing divergent targeting of two distinct biological targets, whose combined inhibition leads to additive or synergistic antitumour effects (295-297).

Combi-molecules are broadly classified as type I or type II, as depicted in Figure 1.13. Type I combi-molecules require hydrolysis to generate their two targeted metabolites (**I** + **Tz**) that are designed to inhibit their respective biological targets in the cell (e.g. EGFR and DNA). In contrast, type-II combi-molecules exert their dual inhibitory properties without the requirement for hydrolysis and function as intact structures (**I-Tz**) within the

cell. For over a decade, our laboratory has been specializing in the synthesis of combi-molecules that are capable of inducing tandem blockade of distinct biological targets such as EGFR and DNA, c-Abl and DNA, as well as EGFR, MEK and DNA that can be classified as type I or type II combi-molecules (4, 295, 297-304).

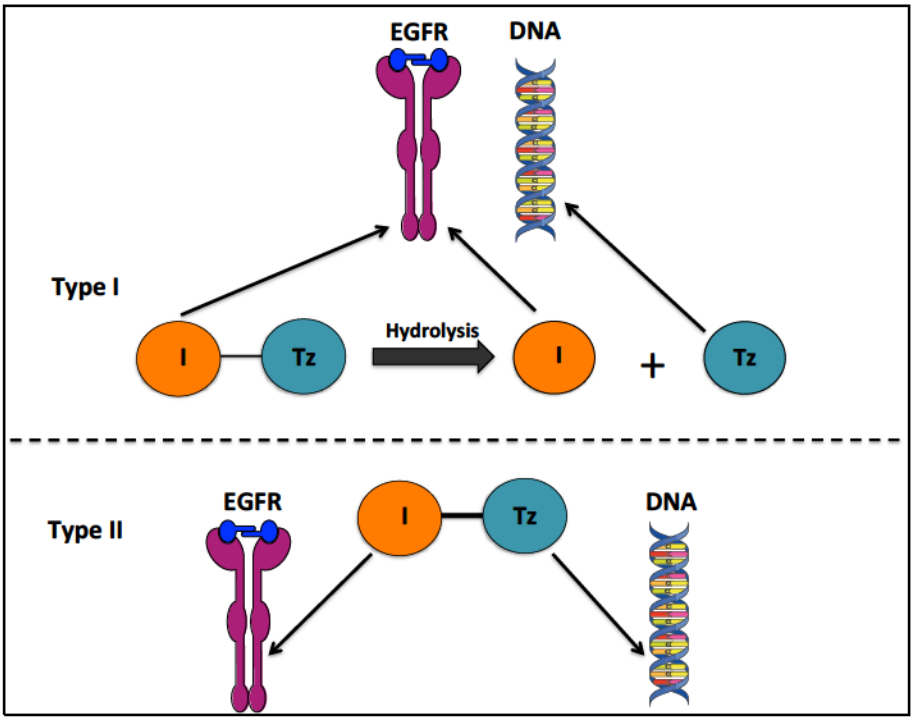

Figure 1.13: The combi-targeting approach. A type-I combi-molecule undergoes hydrolysis to generate its two inhibitory moieties and exert its dual-targeted properties whereas a type-II combi-molecule can exert its dual-inhibitory properties as an intact structure, without the requirement for hydrolysis.

1.6.8.A. Type I combi-molecules

The first type I combi-molecule synthesized was SMA41 in 2001, which was designed to contain an EGFR inhibitor (SMA52) and a DNA damaging agent (methyldiazonium) (see table 1.2 for structure) (4). DNA damage-based cytotoxic therapy has been the mainstay

of cancer treatment for several decades. However, the clinical benefits of chemotherapy are often mitigated by toxicity resulting from chemotherapeutic agents lacking specificity (305). Chemoresistance is mediated by the ability of the cell to repair DNA lesions caused by the drug, which has been another major issue in the clinic (306). EGFR being commonly overexpressed in cancers, and being capable of activating anti-apoptotic signaling, our group hypothesized that the combined targeting of EGFR and DNA would not only enhance targeting specificity through enhanced inhibition of EGFR overexpressing tumours, but would also lead to synergistic blockade of tumour growth and proliferation through inhibition of EGFR and damaging DNA. Furthermore, given the ability of EGFR to induce DNA repair enzymes, it was proposed that an additional advantage of overcoming chemoresistance would be conferred (307, 308). Together, these served as the rationale for the design and development of EGFR-DNA targeting combi-molecules.

The EGFR targeting pharmacophore consists of a 4-anilinoquinazoline moiety, which has been demonstrated through structure-activity relationship (SAR) studies to be a highly selective EGFR tyrosine kinase inhibitor capable of competing with ATP to bind and inhibit the kinase domain (309). Molecular modeling has demonstrated the nitrogen (N) atoms at positions 1 and 3 to form hydrogen bonds with methionine (Met-769) and threonine (Thr-766) residues in the ATP binding pocket. Furthermore, through modeling it has also been suggested that addition of bulky substituents at positions 6 and 7 do not affect the binding of the quinazoline backbone in the EGFR kinase domain (310). This has allowed for the addition of a DNA damaging species via a linker, without compromising the binding activity of the EGFR inhibitor. The DNA damaging species

that was appended to the 6-position of the quinazoline heterocycle was a triazene moiety, which is known to induce DNA damage by alkylating the 6- or 7-position of guanine on the DNA (311). Potent DNA alkylating agents such as temozolomide [a drug approved for the treatment of glioblastoma (312)] are known to be hydrolyzed at neutral pH to a methyldiazonium species that react with guanine to generate an O6 and N7 adduct. Tumour cells that express the O6-methyl guanine methyl transferase (MGMT) enzyme, removes the methyl group from the O6-position of the guanine and are thus resistant to the clinical drug temozolomide (abbreviated henceforth as TEM). However, given its strong DNA alkylating potency, the methyldiazonium species was chosen as the DNA damaging agent to be appended to the quinazoline backbone to generate the first prototype of EGFR-DNA targeting combi-molecule, SMA41. The combi-molecule showed dual targeting potency by inhibiting EGFR kinase activity in an *in vitro* kinase assay and its phosphorylation in a whole cell assay as well as inducing DNA damage. SMA41 showed enhanced anti-proliferative activity compared with SMA52 or TEM indicating that the ability of the combi-molecule to inhibit EGFR and induce DNA damage resulted in its superior potency (4).

With the design and development of SMA41, it was demonstrated that a DNA-damaging species could be grafted on to the quinazoline backbone without losing the inhibitory property of either moiety. Furthermore, SMA41 was used as a model to study the combined effect of inducing growth arrest through the use of an EGFR inhibitor and damaging DNA in cytostatic cells since it has been known that highly proliferative cells are more sensitive towards DNA damaging agents. However, the data indicated that combining SMA52 with TEM was synergistic in nature, further strengthening our basis

for targeting EGFR and DNA (4). Since then, several other combi-molecules with type I targeting properties have been synthesized and evaluated in cancer models both *in vitro* and *in vivo*, a list of which has been presented in table 1.2.

Table 1.2: List of type I combi-molecules (I-Tz) synthesized in our laboratory and their corresponding hydrolysis products (I + Tz).

Type I Combi-molecules	I-Tz	From Targeting Arm (I)	From Targeting Arm (Tz)
SMA-41 (EGFR-DNA)	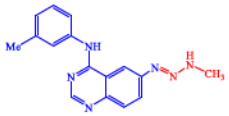	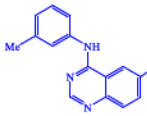 **SMA52**	$N\equiv N^{+}-CH_3$
RB24 (EGFR-DNA)	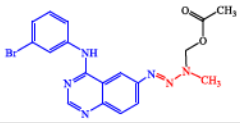	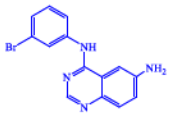	$N\equiv N^{+}-CH_3$
ZRS1 (EGFR-DNA)	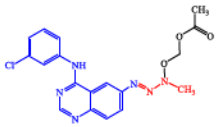	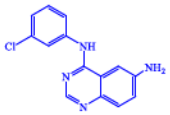	$N\equiv N^{+}-CH_3$
ZRCM5 (BcrAbl-DNA)	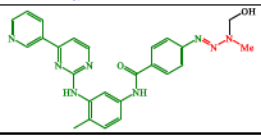	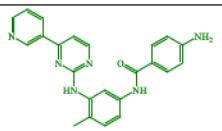	$N\equiv N^{+}-CH_3$

Note: Blue represents the EGFR targeting head, green represents the Bcr-Abl (fusion protein resulting from the the Philadelphia chromosome) targeting head and red represents the DNA damaging species.

1.6.8.B. Subcellular localization of combi-molecules and their hydrolyzed components

Through the course of the work done on combi-molecules, an important revelation came from monitoring the subcellular distribution of type I compounds and their hydrolyzed components. The methyldiazonium species (DNA-damaging) was radiolabeled with ^{14}C

and shown to be distributed everywhere in the cell and alkylated DNA, RNA and proteins, in an unspecific manner. The quinazoline moiety on the other hand being fluorescent was monitored using fluorescence microscopy and was largely distributed in the perinuclear region (with some in the nucleus) and colocalized with EGFR. This suggested that the combi-molecule was brought into close proximity with the nucleus where the methyldiazonium species could easily exert its DNA damaging function (313, 314).

1.6.8.C. Type II combi-molecules

The first type II combi-molecule synthesized was JDD36, which was designed to inhibit EGFR and damage DNA (5). Since the development of this balanced EGFR-DNA targeting combi-molecule, several other type II combi-molecules have been synthesized and evaluated in our laboratory, a list of which is summarized in Table 1.3.

The type II combi-targeting principle was also applied to the synthesis of SB163, the first rationally designed EGFR-c-Src targeting combi-molecule, which was developed based on molecular modeling studies of known X-ray structures of EGFR and c-Src inhibitors (315). The rationale behind developing the first EGFR-c-Src targeting combi-molecule was to induce tandem blockade of both kinases and disrupt the synergistic crosstalk between them in different cancers. A model structure was designed using a phenylaminoquinazoline moiety as the EGFR inhibitory arm and a purine moiety (PP2, a c-Src inhibitor) as the c-Src inhibitory arm, connected by a linker at the N-1 position of PP2. Binding of the molecule to the EGFR and c-Src kinase domains using molecular modeling revealed that PP2 could only be altered on the 9-position without dramatically

altering its kinase binding activity. As previously seen with quinazoline, it can withstand bulky substitutions on the 6-position without affecting its kinase binding activity. Based on these modeling studies, SB163, a chimeric EGFR-c-Src targeting combi-molecule was synthesized, which showed dual kinase inhibitory potency in an *in vitro* kinase assay, although it was a stronger EGFR inhibitor than c-Src (Table 1.3). Despite its inability to demonstrate balanced targeting, it served as the first prototype of a dual kinase-kinase targeting combi-molecule, indicating that a second kinase inhibitory arm could be appended to the EGFR inhibitor, without severely affecting either kinase binding activity (315). Consequently, this paved the path for future design and optimization of other EGFR-c-Src targeting combi-molecules (type I and type II) as well as exploring the possibility of grafting on other kinase inhibitory moieties (e.g. c-Met inhibitor) to the quinazoline backbone to generate EGFR-c-Met targeting combi-molecules.

Table 1.3: List of type II combi-molecules synthesized in our laboratory.

Type II Combi-molecules	**I-Tz**
JDD36 (EGFR-DNA)	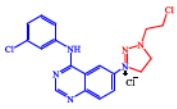
ZR2003 (EGFR-DNA)	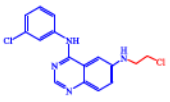
AK04 (BcrAbl-DNA)	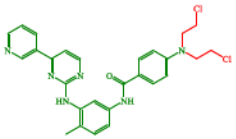
SB163 (EGFR-c-Src)	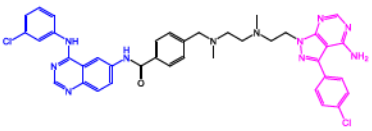

Note: Blue represents the EGFR targeting head, green represents the Bcr-Abl (fusion protein resulting from the Philadelphia chromosome) targeting head, pink represents the c-Src targeting head and red represents the DNA damaging species.

1.6.8.D. The urgency of developing new targeting modalities for the EGFR-c-Src-c-Met signaling interplay

As mentioned earlier, c-Src is an aggressive oncogene that synergizes with EGFR to promote tumour growth, proliferation and resistance to EGFR-targeted therapies. The latter is often also mediated by the activation of c-Met-related signaling pathways. Thus, we believed that in order to abrogate adverse signaling mediated by EGFR, c-Src and c-Met, combi-molecules must be designed that block either EGFR-c-Src or EGFR-c-Met. Here, we wished to focus on the optimization of EGFR-c-Src dual targeting molecules and dissect the interactions between EGFR, c-Met and c-Src, in order to efficiently block their adverse effects. Furthermore, criteria for defining potency of combi-molecules targeting dual or multiple kinases remain to be defined. Here we also analyzed the concept of balanced targeting in our approach, by studying criteria that characterize the potency of combi-molecules and their corresponding equivalent two drug combinations.

1.7 RESEARCH OBJECTIVES

The primary goal of this thesis was to target the signaling crosstalk between EGFR, c-Met and c-Src through: (a) a unimolecular approach to the design and development of EGFR-c-Src and EGFR-c-Met targeting combi-molecules, (b) a multi-kinase approach to abrogate the complex signaling interplay between EGFR, c-Src and c-Met, and (c)

developing a quantitative approach to compare the combination of multiple kinase inhibitors with single multi-targeted molecules.

The thesis focuses on the development of new strategies to block the prosurvival effects mediated by the complex network of signaling mediated by multiple key signaling proteins in refractory tumours. More specifically, as outlined below, three major objectives were pursued therein,

Objective 1: To optimize and elucidate the mechanism of action of the first balanced EGFR-c-Src targeting combi-molecule (Chapters 2 and 3)

Objective 2: To study a multi-kinase approach to block signaling redundancy and compensatory signaling evoked by EGFR, c-Src and c-Met (Chapter 4)

Objective 3: To study a quantitative approach for evaluating equimolar combinations of individual kinase inhibitors (EGFR, c-Met, c-Src) in comparison with single kinase-kinase combi-molecules (e.g. EGFR-c-Src, EGFR-c-Met) synthesized in the context of this thesis (Chapter 5)

1.8. REFERENCES

1. Kola I, Landis J. Can the pharmaceutical industry reduce attrition rates? Nature reviews Drug discovery. 2004;3(8):711-6.
2. Cohen MH, Williams G, Johnson JR, Duan J, Gobburu J, Rahman A, et al. Approval summary for imatinib mesylate capsules in the treatment of chronic myelogenous leukemia. Clinical Cancer Research. 2002;8(5):935-42.
3. Huang M, Shen A, Ding J, Geng M. Molecularly targeted cancer therapy: some lessons from the past decade. Trends in pharmacological sciences. 2014;35(1):41-50.
4. Matheson SL, McNamee J, Jean-Claude BJ. Design of a chimeric 3-methyl-1, 2, 3-triazene with mixed receptor tyrosine kinase and DNA damaging properties: a novel

tumor targeting strategy. Journal of Pharmacology and Experimental Therapeutics. 2001;296(3):832-40.
5. Qiu Q, Domarkas J, Banerjee R, Katsoulas A, McNamee JP, Jean-Claude BJ. Type II combi-molecules: design and binary targeting properties of the novel triazolinium-containing molecules JDD36 and JDE05. Anti-cancer drugs. 2007;18(2):171-7.
6. Hunter T, Cooper JA. Protein-tyrosine kinases. Annual review of biochemistry. 1985;54(1):897-930.
7. Hunter T. The Croonian Lecture 1997. The phosphorylation of proteins on tyrosine: its role in cell growth and disease. Philosophical Transactions of the Royal Society of London B: Biological Sciences. 1998;353(1368):583-605.
8. Schlessinger J. Cell signaling by receptor tyrosine kinases. Cell. 2000;103(2):211-25.
9. Levene P, Alsberg C. The cleavage products of vitellin. Journal of Biological Chemistry. 1906;2(1):127-33.
10. Cohen P. The origins of protein phosphorylation. Nature cell biology. 2002;4(5):E127-E30.
11. Sutherland EW, Science AAftAo, editors. Studies on the mechanism of hormone action1972: American Association for the Advancement of Science.
12. Hunter T, Sefton BM. Transforming gene product of Rous sarcoma virus phosphorylates tyrosine. Proceedings of the National Academy of Sciences. 1980;77(3):1311-5.
13. Ushiro H, Cohen S. Identification of phosphotyrosine as a product of epidermal growth factor-activated protein kinase in A-431 cell membranes. Journal of Biological Chemistry. 1980;255(18):8363-5.
14. Cohen S, Fava RA, Sawyer ST. Purification and characterization of epidermal growth factor receptor/protein kinase from normal mouse liver. Proceedings of the National Academy of Sciences. 1982;79(20):6237-41.
15. Cohen S, Ushiro H, Stoscheck C, Chinkers M. A native 170,000 epidermal growth factor receptor-kinase complex from shed plasma membrane vesicles. Journal of Biological Chemistry. 1982;257(3):1523-31.
16. Anderson D, Koch CA, Grey L, Ellis C, Moran M, Pawson T, editors. Binding of SH2 domains of phospholipase Cγ1, GAP, and Src to activated growth factor receptors1990: American Association for the Advancement of Science.
17. Yarden Y, Schlessinger J. Self-phosphorylation of epidermal growth factor receptor: evidence for a model of intermolecular allosteric activation. Biochemistry. 1987;26(5):1434-42.
18. Yarden Y, Schlessinger J. Epidermal growth factor induces rapid, reversible aggregation of the purified epidermal growth factor receptor. Biochemistry. 1987;26(5):1443-51.
19. Ullrich A, Schlessinger J. Signal transduction by receptors with tyrosine kinase activity. Cell. 1990;61(2):203-12.
20. Gonzatti-Haces M, Seth A, Park M, Copeland T, Oroszlan S, Woude GV. Characterization of the TPR-MET oncogene p65 and the MET protooncogene p140 protein-tyrosine kinases. Proceedings of the National Academy of Sciences. 1988;85(1):21-5.

21. Dean M, Park M, Le Beau MM, Robins TS, Diaz MO, Rowley JD, et al. The human met oncogene is related to the tyrosine kinase oncogenes. 1985.
22. Cooper CS, Park M, Blair DG, Tainsky MA, Huebner K, Croce CM, et al. Molecular cloning of a new transforming gene from a chemically transformed human cell line. Nature. 1983;311(5981):29-33.
23. Park M, Dean M, Kaul K, Braun MJ, Gonda MA, Woude GV. Sequence of MET protooncogene cDNA has features characteristic of the tyrosine kinase family of growth-factor receptors. Proceedings of the National Academy of Sciences. 1987;84(18):6379-83.
24. Kasuga M, Zick Y, Blithe DL, Crettaz M, Kahn CR. Insulin stimulates tyrosine phosphorylation of the insulin receptor in a cell-free system. 1982.
25. Robinson DR, Wu Y-M, Lin S-F. The protein tyrosine kinase family of the human genome. Oncogene. 2000;19(49):5548-57.
26. Blume-Jensen P, Hunter T. Oncogenic kinase signalling. Nature. 2001;411(6835):355-65.
27. Hubbard SR, Mohammadi M, Schlessinger J. Autoregulatory mechanisms in protein-tyrosine kinases. Journal of Biological Chemistry. 1998;273(20):11987-90.
28. Peschard P, Park M. From Tpr-Met to Met, tumorigenesis and tubes. Oncogene. 2007;26(9):1276-85.
29. Neet K, Hunter T. Vertebrate non-receptor protein-tyrosine kinase families. Genes to Cells. 1996;1(2):147-69.
30. Thomas SM, Brugge JS. Cellular functions regulated by Src family kinases. Annual review of cell and developmental biology. 1997;13(1):513-609.
31. Wilks A, Harpur A, Kurban R, Ralph S, Zürcher G, Ziemiecki A. Two novel protein-tyrosine kinases, each with a second phosphotransferase-related catalytic domain, define a new class of protein kinase. Molecular and Cellular Biology. 1991;11(4):2057-65.
32. Firmbach-Kraft I, Byers M, Shows T, Dalla-Favera R, Krolewski J. tyk2, prototype of a novel class of non-receptor tyrosine kinase genes. Oncogene. 1990;5(9):1329-36.
33. Harpur A, Andres A, Ziemiecki A, Aston R, Wilks A. JAK2, a third member of the JAK family of protein tyrosine kinases. Oncogene. 1992;7(7):1347-53.
34. Johnston JA, Kawamura M, Kirken RA, Chen Y-Q, Blake TB, Shibuya K, et al. Phosphorylation and activation of the Jak-3 Janus kinase in response to interleukin-2. 1994.
35. Neet K, Hunter T. Vertebrate non-receptor protein–tyrosine kinase families. Genes to Cells. 1996;1(2):147-69.
36. Schaller MD, Parsons JT. Focal adhesion kinase and associated proteins. Current opinion in cell biology. 1994;6(5):705-10.
37. Heinrich P, Behrmann I, Muller-Newen G, Schaper F, Graeve L. Interleukin-6-type cytokine signalling through the gp130/Jak/STAT pathway1. Biochem j. 1998;334:297-314.
38. Garrett TP, McKern NM, Lou M, Elleman TC, Adams TE, Lovrecz GO, et al. Crystal structure of a truncated epidermal growth factor receptor extracellular domain bound to transforming growth factor α. Cell. 2002;110(6):763-73.

39. Ogiso H, Ishitani R, Nureki O, Fukai S, Yamanaka M, Kim J-H, et al. Crystal structure of the complex of human epidermal growth factor and receptor extracellular domains. Cell. 2002;110(6):775-87.
40. Burgess AW, Cho H-S, Eigenbrot C, Ferguson KM, Garrett TP, Leahy DJ, et al. An open-and-shut case? Recent insights into the activation of EGF/ErbB receptors. Molecular cell. 2003;12(3):541-52.
41. Harris RC, Chung E, Coffey RJ. EGF receptor ligands. Experimental cell research. 2003;284(1):2-13.
42. Massague J. Transforming growth factor-α: a model for membrane-anchored growth factors. J Biol Chem. 1990;265(35):21393-6.
43. Shoyab M, McDonald VL, Bradley JG, Todaro GJ. Amphiregulin: a bifunctional growth-modulating glycoprotein produced by the phorbol 12-myristate 13-acetate-treated human breast adenocarcinoma cell line MCF-7. Proceedings of the National Academy of Sciences. 1988;85(17):6528-32.
44. Toyoda H, Komurasaki T, Uchida D, Takayama Y, Isobe T, Okuyama T, et al. Epiregulin a novel epidermal growth factor with mitogenic activity for rat primary hepatocytes. Journal of Biological Chemistry. 1995;270(13):7495-500.
45. Strachan L, Murison JG, Prestidge RL, Sleeman MA, Watson JD, Kumble KD. Cloning and biological activity of epigen, a novel member of the epidermal growth factor superfamily. Journal of Biological Chemistry. 2001;276(21):18265-71.
46. Domagala T, Konstantopoulos N, Smyth F, Jorissen RN, Fabri L, Geleick D, et al. Stoichiometry, kinetic and binding analysis of the interaction between epidermal growth factor (EGF) and the extracellular domain of the EGF receptor. Growth Factors. 2000;18(1):11-29.
47. Lemmon MA, Bu Z, Ladbury JE, Zhou M, Pinchasi D, Lax I, et al. Two EGF molecules contribute additively to stabilization of the EGFR dimer. The EMBO journal. 1997;16(2):281-94.
48. Jorissen RN, Walker F, Pouliot N, Garrett TP, Ward CW, Burgess AW. Epidermal growth factor receptor: mechanisms of activation and signalling. Experimental cell research. 2003;284(1):31-53.
49. Hubbard SR. Protein tyrosine kinases: autoregulation and small-molecule inhibition. Current opinion in structural biology. 2002;12(6):735-41.
50. Longati P, Bardelli A, Ponzetto C, Naldini L, Comoglio PM. Tyrosines1234-1235 are critical for activation of the tyrosine kinase encoded by the MET proto-oncogene (HGF receptor). Oncogene. 1994;9(1):49-57.
51. Piwnica-Worms H, Saunders KB, Roberts TM, Smith AE, Cheng SH. Tyrosine phosphorylation regulates the biochemical and biological properties of pp60 c-src. Cell. 1987;49(1):75-82.
52. Hubbard SR, Till JH. Protein tyrosine kinase structure and function. Annual review of biochemistry. 2000;69(1):373-98.
53. Yarden Y, Ullrich A. Growth factor receptor tyrosine kinases. Annual review of biochemistry. 1988;57(1):443-78.
54. Hubbard SR. Crystal structure of the activated insulin receptor tyrosine kinase in complex with peptide substrate and ATP analog. The EMBO journal. 1997;16(18):5572-81.

55. Gotoh N, Tojo A, Hino M, Yazaki Y, Shibuya M. A highly conserved tyrosine residue at codon 845 within the kinase domain is not required for the transforming activity of human epidermal growth factor receptor. Biochemical and biophysical research communications. 1992;186(2):768-74.
56. Zhang X, Gureasko J, Shen K, Cole PA, Kuriyan J. An allosteric mechanism for activation of the kinase domain of epidermal growth factor receptor. Cell. 2006;125(6):1137-49.
57. Abe M, Kuroda Y, Hirose M, Watanabe Y, Nakano M, Handa T. Inhibition of autophosphorylation of epidermal growth factor receptor by small peptides in vitro. British journal of pharmacology. 2006;147(4):402-11.
58. Tamagnone L, Artigiani S, Chen H, He Z, Ming G-l, Song H-j, et al. Plexins are a large family of receptors for transmembrane, secreted, and GPI-anchored semaphorins in vertebrates. Cell. 1999;99(1):71-80.
59. Yazdani U, Terman JR. The semaphorins. Genome Biol. 2006;7(3):211.
60. Kozlov G, Perreault A, Schrag JD, Park M, Cygler M, Gehring K, et al. Insights into function of PSI domains from structure of the Met receptor PSI domain. Biochemical and biophysical research communications. 2004;321(1):234-40.
61. Bork P, Doerks T, Springer TA, Snel B. Domains in plexins: links to integrins and transcription factors. Trends in biochemical sciences. 1999;24(7):261-3.
62. Organ SL, Tsao M-S. An overview of the c-MET signaling pathway. Therapeutic advances in medical oncology. 2011;3(1 suppl):S7-S19.
63. Zhu H, Naujokas MA, Park M. Receptor chimeras indicate that the met tyrosine kinase mediates the motility and morphogenic responses of hepatocyte growth/scatter factor. Cell Growth and Differentiation-Publication American Association for Cancer Research. 1994;5(4):359-66.
64. Stella MC, Comoglio PM. HGF: a multifunctional growth factor controlling cell scattering. The international journal of biochemistry & cell biology. 1999;31(12):1357-62.
65. Gherardi E, Sandin S, Petoukhov MV, Finch J, Youles ME, Öfverstedt L-G, et al. Structural basis of hepatocyte growth factor/scatter factor and MET signalling. Proceedings of the National Academy of Sciences of the United States of America. 2006;103(11):4046-51.
66. Mizuno S, Nakamura T. HGF–MET cascade, a key target for inhibiting cancer metastasis: The impact of NK4 discovery on cancer biology and therapeutics. International journal of molecular sciences. 2013;14(1):888-919.
67. Basilico C, Arnesano A, Galluzzo M, Comoglio PM, Michieli P. A high affinity hepatocyte growth factor-binding site in the immunoglobulin-like region of Met. Journal of Biological Chemistry. 2008;283(30):21267-77.
68. Chiara F, Michieli P, Pugliese L, Comoglio PM. Mutations in the met oncogene unveil a “dual switch” mechanism controlling tyrosine kinase activity. Journal of Biological Chemistry. 2003;278(31):29352-8.
69. Ponzetto C, Bardelli A, Zhen Z, Maina F, dalla Zonca P, Giordano S, et al. A multifunctional docking site mediates signaling and transformation by the hepatocyte growth factor/scatter factor receptor family. Cell. 1994;77(2):261-71.

70. Trusolino L, Bertotti A, Comoglio PM. MET signalling: principles and functions in development, organ regeneration and cancer. Nature reviews Molecular cell biology. 2010;11(12):834-48.
71. Brown MT, Cooper JA. Regulation, substrates and functions of src. Biochimica et Biophysica Acta (BBA)-Reviews on Cancer. 1996;1287(2):121-49.
72. Resh MD. Interaction of tyrosine kinase oncoproteins with cellular membranes. Biochimica et Biophysica Acta (BBA)-Reviews on Cancer. 1993;1155(3):307-22.
73. Koch CA, Anderson D, Moran MF, Ellis C, Pawson T. SH2 and SH3 domains: elements that control interactions of cytoplasmic signaling proteins. Science. 1991;252(5006):668-74.
74. Cohen GB, Ren R, Baltimore D. Modular binding domains in signal transduction proteins. Cell. 1995;80(2):237-48.
75. Martin GS. The hunting of the Src. Nature reviews Molecular cell biology. 2001;2(6):467-75.
76. Liu X, Brodeur SR, Gish G, Songyang Z, Cantley LC, Laudano AP, et al. Regulation of c-Src tyrosine kinase activity by the Src SH2 domainv. 1993.
77. Cooper JA, Gould KL, Cartwright CA, Hunter T. Tyr527 is phosphorylated in pp60c-src: implications for regulation. Science. 1986;231(4744):1431-4.
78. Roussel RR, Brodeur SR, Shalloway D, Laudano AP. Selective binding of activated pp60c-src by an immobilized synthetic phosphopeptide modeled on the carboxyl terminus of pp60c-src. Proceedings of the National Academy of Sciences. 1991;88(23):10696-700.
79. Nada S, Okada M, MacAuley A, Cooper JA, Nakagawa H. Cloning of a complementary DNA for a protein-tyrosine kinase that specifically phosphorylates a negative regulatory site of p60c-src. 1991.
80. Chong Y-P, Mulhern TD, Cheng H-C. C-terminal Src kinase (CSK) and CSK-homologous kinase (CHK)—endogenous negative regulators of Src-family protein kinases: Mini Review. Growth Factors. 2005;23(3):233-44.
81. Wenqing X, Harrison S, Eck M. Three-dimensional structure of the tyrosine kinase c-Src. Nature. 1997;385(6617):595-602.
82. Boggon TJ, Eck MJ. Structure and regulation of Src family kinases. Oncogene. 2004;23(48):7918-27.
83. Xu W, Doshi A, Lei M, Eck MJ, Harrison SC. Crystal structures of c-Src reveal features of its autoinhibitory mechanism. Molecular cell. 1999;3(5):629-38.
84. Bjorge JD, Jakymiw A, Fujita DJ. Selected glimpses into the activation and function of Src kinase. Oncogene. 2000;19(49):5620-35.
85. Csiszár Á. Structural and functional diversity of adaptor proteins involved in tyrosine kinase signalling. Bioessays. 2006;28(5):465-79.
86. Pelicci G, Lanfrancone L, Grignani F, McGlade J, Cavallo F, Forni G, et al. A novel transforming protein (SHC) with an SH2 domain is implicated in mitogenic signal transduction. Cell. 1992;70(1):93-104.
87. Lowenstein E, Daly R, Batzer A, Li W, Margolis B, Lammers R, et al. The SH2 and SH3 domain-containing protein GRB2 links receptor tyrosine kinases to ras signaling. Cell. 1992;70(3):431-42.

88. Weidner KM, Arakaki N, Hartmann G, Vandekerckhove J, Weingart S, Rieder H, et al. Evidence for the identity of human scatter factor and human hepatocyte growth factor. Proceedings of the National Academy of Sciences. 1991;88(16):7001-5.
89. Schlessinger J. SH2/SH3 signaling proteins. Current opinion in genetics & development. 1994;4(1):25-30.
90. Shuai K, Horvath CM, Huang LHT, Qureshi SA, Cowburn D, Darnell JE. Interferon activation of the transcription factor Stat91 involves dimerization through SH2-phosphotyrosyl peptide interactions. Cell. 1994;76(5):821-8.
91. Escobedo JA, Navankasattusas S, Kavanaugh WM, Milfay D, Fried VA, Williams LT. cDNA cloning of a novel 85 kd protein that has SH2 domains and regulates binding of PI3-kinase to the PDGF β-receptor. Cell. 1991;65(1):75-82.
92. Dhillon A, Hagan S, Rath O, Kolch W. MAP kinase signalling pathways in cancer. Oncogene. 2007;26(22):3279-90.
93. Roberts P, Der C. Targeting the Raf-MEK-ERK mitogen-activated protein kinase cascade for the treatment of cancer. Oncogene. 2007;26(22):3291-310.
94. Batzer A, Rotin D, Urena J, Skolnik E, Schlessinger J. Hierarchy of binding sites for Grb2 and Shc on the epidermal growth factor receptor. Molecular and cellular biology. 1994;14(8):5192-201.
95. Sakaguchi K, Okabayashi Y, Kido Y, Kimura S, Matsumura Y, Inushima K, et al. Shc phosphotyrosine-binding domain dominantly interacts with epidermal growth factor receptors and mediates Ras activation in intact cells. Molecular Endocrinology. 1998;12(4):536-43.
96. Sasaoka T, Langlois WJ, Leitner JW, Draznin B, Olefsky JM. The signaling pathway coupling epidermal growth factor receptors to activation of p21ras. Journal of Biological Chemistry. 1994;269(51):32621-5.
97. Fixman ED, Fournier TM, Kamikura DM, Naujokas MA, Park M. Pathways downstream of Shc and Grb2 are required for cell transformation by the tpr-Met oncoprotein. Journal of Biological Chemistry. 1996;271(22):13116-22.
98. Pelicci G, Giordano S, Zhen Z, Salcini A, Lanfrancone L, Bardelli A, et al. The motogenic and mitogenic responses to HGF are amplified by the Shc adaptor protein. Oncogene. 1995;10(8):1631-8.
99. Morrison D, Heidecker G, Rapp U, Copeland TD. Identification of the major phosphorylation sites of the Raf-1 kinase. Journal of Biological Chemistry. 1993;268(23):17309-16.
100. Hibino K, Shibata T, Yanagida T, Sako Y. Activation Kinetics of RAF Protein in the Ternary Complex of RAF, RAS-GTP, and Kinase on the Plasma Membrane of Living Cells SINGLE-MOLECULE IMAGING ANALYSIS. Journal of Biological Chemistry. 2011;286(42):36460-8.
101. Marais R, Light Y, Paterson H, Marshall C. Ras recruits Raf-1 to the plasma membrane for activation by tyrosine phosphorylation. The EMBO journal. 1995;14(13):3136.
102. Fabian J, Daar I, Morrison D. Critical tyrosine residues regulate the enzymatic and biological activity of Raf-1 kinase. Molecular and cellular biology. 1993;13(11):7170-9.

103. Williams NG, Roberts TM, Li P. Both p21ras and pp60v-src are required, but neither alone is sufficient, to activate the Raf-1 kinase. Proceedings of the National Academy of Sciences. 1992;89(7):2922-6.
104. van der Geer P, Wiley S, Gish GD, Pawson T. The Shc adaptor protein is highly phosphorylated at conserved, twin tyrosine residues (Y239/240) that mediate protein–protein interactions. Current Biology. 1996;6(11):1435-44.
105. Chang F, Steelman L, Lee J, Shelton J, Navolanic P, Blalock W, et al. Signal transduction mediated by the Ras/Raf/MEK/ERK pathway from cytokine receptors to transcription factors: potential targeting for therapeutic intervention. Leukemia. 2003;17(7):1263-93.
106. Vivanco I, Sawyers CL. The phosphatidylinositol 3-kinase–AKT pathway in human cancer. Nature Reviews Cancer. 2002;2(7):489-501.
107. Martini M, De Santis MC, Braccini L, Gulluni F, Hirsch E. PI3K/AKT signaling pathway and cancer: an updated review. Annals of medicine. 2014;46(6):372-83.
108. Thorpe LM, Yuzugullu H, Zhao JJ. PI3K in cancer: divergent roles of isoforms, modes of activation and therapeutic targeting. Nature Reviews Cancer. 2015;15(1):7-24.
109. Fruman DA, Rommel C. PI3K and cancer: lessons, challenges and opportunities. Nature reviews Drug discovery. 2014;13(2):140-56.
110. Vanhaesebroeck B, Stephens L, Hawkins P. PI3K signalling: the path to discovery and understanding. Nature reviews Molecular cell biology. 2012;13(3):195-203.
111. Carpenter CL, Auger K, Chanudhuri M, Yoakim M, Schaffhausen B, Shoelson S, et al. Phosphoinositide 3-kinase is activated by phosphopeptides that bind to the SH2 domains of the 85-kDa subunit. Journal of Biological Chemistry. 1993;268(13):9478-83.
112. Kim H-H, Sierke SL, Koland JG. Epidermal growth factor-dependent association of phosphatidylinositol 3-kinase with the erbB3 gene product. Journal of Biological Chemistry. 1994;269(40):24747-55.
113. Stover DR, Becker M, Liebetanz J, Lydon NB. Src phosphorylation of the epidermal growth factor receptor at novel sites mediates receptor interaction with Src and P85α. Journal of Biological Chemistry. 1995;270(26):15591-7.
114. Mattoon DR, Lamothe B, Lax I, Schlessinger J. The docking protein Gab1 is the primary mediator of EGF-stimulated activation of the PI-3K/Akt cell survival pathway. BMC biology. 2004;2(1):24.
115. Liu X, Marengere L, Koch C, Pawson T. The v-Src SH3 domain binds phosphatidylinositol 3'-kinase. Molecular and Cellular Biology. 1993;13(9):5225-32.
116. Sarbassov DD, Guertin DA, Ali SM, Sabatini DM. Phosphorylation and regulation of Akt/PKB by the rictor-mTOR complex. Science. 2005;307(5712):1098-101.
117. Vara JÁF, Casado E, de Castro J, Cejas P, Belda-Iniesta C, González-Barón M. PI3K/Akt signalling pathway and cancer. Cancer treatment reviews. 2004;30(2):193-204.
118. Bromberg JF. Activation of STAT proteins and growth control. Bioessays. 2001;23(2):161-9.
119. Calò V, Migliavacca M, Bazan V, Macaluso M, Buscemi M, Gebbia N, et al. STAT proteins: from normal control of cellular events to tumorigenesis. Journal of cellular physiology. 2003;197(2):157-68.
120. Pensa S, Regis G, Boselli D, Novelli F, Poli V. STAT1 and STAT3 in tumorigenesis: two sides of the same coin? 2000.

121. Quesnelle KM, Boehm AL, Grandis JR. STAT-mediated EGFR signaling in cancer. Journal of cellular biochemistry. 2007;102(2):311-9.
122. Shuai K, Stark GR, Kerr IM, Darnell J. A single phosphotyrosine residue of Stat91 required for gene activation by interferon-gamma. Science. 1993;261(5129):1744-6.
123. Kaptein A, Paillard V, Saunders M. Dominant negative stat3 mutant inhibits interleukin-6-induced Jak-STAT signal transduction. Journal of Biological Chemistry. 1996;271(11):5961-4.
124. Gouilleux F, Wakao H, Mundt M, Groner B. Prolactin induces phosphorylation of Tyr694 of Stat5 (MGF), a prerequisite for DNA binding and induction of transcription. The EMBO journal. 1994;13(18):4361.
125. Levy DE, Darnell J. Stats: transcriptional control and biological impact. Nature reviews Molecular cell biology. 2002;3(9):651-62.
126. Park OK, Schaefer TS, Nathans D. In vitro activation of Stat3 by epidermal growth factor receptor kinase. Proceedings of the National Academy of Sciences. 1996;93(24):13704-8.
127. Leaman DW, Pisharody S, Flickinger TW, Commane MA, Schlessinger J, Kerr IM, et al. Roles of JAKs in activation of STATs and stimulation of c-fos gene expression by epidermal growth factor. Molecular and Cellular Biology. 1996;16(1):369-75.
128. David M, Wong L, Flavell R, Thompson SA, Wells A, Larner AC, et al. STAT activation by epidermal growth factor (EGF) and amphiregulin Requirement for the EGF receptor kinase but not for tyrosine phosphorylation sites or JAK1. Journal of Biological Chemistry. 1996;271(16):9185-8.
129. Cao X, Tay A, Guy GR, Tan Y. Activation and association of Stat3 with Src in v-Src-transformed cell lines. Molecular and Cellular Biology. 1996;16(4):1595-603.
130. Yu C-L, Meyer DJ, Campbell GS, Larner AC, Carter-Su C, Schwartz J, et al. Enhanced DNA-binding activity of a Stat3-related protein in cells transformed by the Src oncoprotein. Science. 1995;269(5220):81-3.
131. Chaturvedi P, Reddy MR, Reddy EP. Src kinases and not JAKs activate STATs during IL-3 induced myeloid cell proliferation. Oncogene. 1998;16(13):1749-58.
132. Wang Y-Z, Wharton W, Garcia R, Kraker A, Jove R, Pledger W. Activation of Stat3 preassembled with platelet-derived growth factor beta receptors requires Src kinase activity. Oncogene. 2000;19(17):2075-85.
133. Garcia R, Bowman TL, Niu G, Yu H, Minton S, Muro-Cacho CA, et al. Constitutive activation of Stat3 by the Src and JAK tyrosine kinases participates in growth regulation of human breast carcinoma cells. Oncogene. 2001;20(20):2499-513.
134. Boccaccio C, Andò M, Tamagnone L, Bardelli A, Michieli P, Battistini C, et al. Induction of epithelial tubules by growth factor HGF depends on the STAT pathway. Nature. 1998;391(6664):285-8.
135. Carpenter RL, Lo H-W. STAT3 target genes relevant to human cancers. Cancers. 2014;6(2):897-925.
136. Luttrell D, Luttrell L, Parsons S. Augmented mitogenic responsiveness to epidermal growth factor in murine fibroblasts that overexpress pp60c-src. Molecular and cellular biology. 1988;8(1):497-501.
137. Wilson LK, Luttrell DK, Parsons JT, Parsons SJ. pp60c-src tyrosine kinase, myristylation, and modulatory domains are required for enhanced mitogenic

responsiveness to epidermal growth factor seen in cells overexpressing c-src. Molecular and cellular biology. 1989;9(4):1536-44.
138. Tice DA, Biscardi JS, Nickles AL, Parsons SJ. Mechanism of biological synergy between cellular Src and epidermal growth factor receptor. Proceedings of the National Academy of Sciences. 1999;96(4):1415-20.
139. Maa M-C, Leu T-H, McCarley DJ, Schatzman RC, Parsons SJ. Potentiation of epidermal growth factor receptor-mediated oncogenesis by c-Src: implications for the etiology of multiple human cancers. Proceedings of the National Academy of Sciences. 1995;92(15):6981-5.
140. Kloth MT, Laughlin KK, Biscardi JS, Boerner JL, Parsons SJ, Silva CM. STAT5b, a mediator of synergism between c-Src and the epidermal growth factor receptor. Journal of Biological Chemistry. 2003;278(3):1671-9.
141. Ishizawar R, Parsons SJ. c-Src and cooperating partners in human cancer. Cancer cell. 2004;6(3):209-14.
142. Moro L, Dolce L, Cabodi S, Bergatto E, Erba EB, Smeriglio M, et al. Integrin-induced epidermal growth factor (EGF) receptor activation requires c-Src and p130Cas and leads to phosphorylation of specific EGF receptor tyrosines. Journal of Biological Chemistry. 2002;277(11):9405-14.
143. Biscardi JS, Ishizawar RC, Silva CM, Parsons SJ. Tyrosine kinase signalling in breast cancer: epidermal growth factor receptor and c-Src interactions in breast cancer. Breast Cancer Research. 2000;2(3):203.
144. Prenzel N, Zwick E, Leserer M, Ullrich A. Tyrosine kinase signalling in breast cancer: Epidermal growth factor receptor-convergence point for signal integration and diversification. Breast Cancer Research. 2000;2(3):184.
145. Wu W, Graves LM, Gill GN, Parsons SJ, Samet JM. Src-dependent phosphorylation of the epidermal growth factor receptor on tyrosine 845 is required for zinc-induced Ras activation. Journal of Biological Chemistry. 2002;277(27):24252-7.
146. Chang J-H, Gill S, Settleman J, Parsons SJ. c-Src regulates the simultaneous rearrangement of actin cytoskeleton, p190RhoGAP, and p120RasGAP following epidermal growth factor stimulation. The Journal of Cell Biology. 1995;130(2):355-68.
147. Weernink PAO, Rijksen G. Activation and translocation of c-Src to the cytoskeleton by both platelet-derived growth factor and epidermal growth factor. Journal of Biological Chemistry. 1995;270(5):2264-7.
148. Rodier J-M, Vallés AM, Denoyelle M, Thiery JP, Boyer B. pp60c-src is a positive regulator of growth factor-induced cell scattering in a rat bladder carcinoma cell line. The Journal of cell biology. 1995;131(3):761-73.
149. Bao J, Gur G, Yarden Y. Src promotes destruction of c-Cbl: implications for oncogenic synergy between Src and growth factor receptors. Proceedings of the National Academy of Sciences. 2003;100(5):2438-43.
150. Yarden Y. The EGFR family and its ligands in human cancer: signalling mechanisms and therapeutic opportunities. European journal of cancer. 2001;37:3-8.
151. Sen B, Johnson FM. Regulation of SRC family kinases in human cancers. Journal of signal transduction. 2011;2011.
152. Tonks NK. Protein tyrosine phosphatases: from genes, to function, to disease. Nature Reviews Molecular Cell Biology. 2006;7(11):833-46.

153. Song MS, Salmena L, Pandolfi PP. The functions and regulation of the PTEN tumour suppressor. Nature reviews Molecular cell biology. 2012;13(5):283-96.
154. Colicelli J. Human RAS superfamily proteins and related GTPases. Science's STKE: signal transduction knowledge environment. 2004;2004(250):RE13.
155. Nowell PC, Hungerford DA. Chromosome studies in human leukemia. II. Chronic granulocytic leukemia. Journal of the National Cancer Institute. 1961;27(5):1013-35.
156. Prior IA, Lewis PD, Mattos C. A comprehensive survey of Ras mutations in cancer. Cancer research. 2012;72(10):2457-67.
157. Olivier M, Hollstein M, Hainaut P. TP53 mutations in human cancers: origins, consequences, and clinical use. Cold Spring Harbor perspectives in biology. 2010;2(1):a001008.
158. Gazdar A. Activating and resistance mutations of EGFR in non-small-cell lung cancer: role in clinical response to EGFR tyrosine kinase inhibitors. Oncogene. 2009;28:S24-S31.
159. Downward J, Yarden Y, Mayes E, Scrace G, Totty N, Stockwell P, et al. Close similarity of epidermal growth factor receptor and v-erb-B oncogene protein sequences. 1984.
160. Yarden Y, Sliwkowski MX. Untangling the ErbB signalling network. Nature reviews Molecular cell biology. 2001;2(2):127-37.
161. Holland EC. Glioblastoma multiforme: the terminator. Proceedings of the National Academy of Sciences. 2000;97(12):6242-4.
162. Gan HK, Kaye AH, Luwor RB. The EGFRvIII variant in glioblastoma multiforme. Journal of Clinical Neuroscience. 2009;16(6):748-54.
163. da Cunha Santos G, Shepherd FA, Tsao MS. EGFR mutations and lung cancer. Annual Review of Pathology: Mechanisms of Disease. 2011;6:49-69.
164. Paez JG, Jänne PA, Lee JC, Tracy S, Greulich H, Gabriel S, et al. EGFR mutations in lung cancer: correlation with clinical response to gefitinib therapy. Science. 2004;304(5676):1497-500.
165. Lynch TJ, Bell DW, Sordella R, Gurubhagavatula S, Okimoto RA, Brannigan BW, et al. Activating mutations in the epidermal growth factor receptor underlying responsiveness of non–small-cell lung cancer to gefitinib. New England Journal of Medicine. 2004;350(21):2129-39.
166. Barber TD, Vogelstein B, Kinzler KW, Velculescu VE. Somatic mutations of EGFR in colorectal cancers and glioblastomas. New England Journal of Medicine. 2004;351(27):2883-.
167. Kwak EL, Jankowski J, Thayer SP, Lauwers GY, Brannigan BW, Harris PL, et al. Epidermal growth factor receptor kinase domain mutations in esophageal and pancreatic adenocarcinomas. Clinical Cancer Research. 2006;12(14):4283-7.
168. Dahse R, Driemel O, Schwarz S, Dahse J, Kromeyer-Hauschild K, Berndt A, et al. Epidermal growth factor receptor kinase domain mutations are rare in salivary gland carcinomas. British journal of cancer. 2009;100(4):623-5.
169. Lu Z, Jiang G, Blume-Jensen P, Hunter T. Epidermal growth factor-induced tumor cell invasion and metastasis initiated by dephosphorylation and downregulation of focal adhesion kinase. Molecular and cellular biology. 2001;21(12):4016-31.
170. Wells A. Tumor invasion: role of growth factor-induced cell motility. Advances in cancer research. 1999;78:31-101.

171. Fan Q-W, Cheng CK, Gustafson WC, Charron E, Zipper P, Wong RA, et al. EGFR phosphorylates tumor-derived EGFRvIII driving STAT3/5 and progression in glioblastoma. Cancer cell. 2013;24(4):438-49.
172. Tsai Y-C, Ho P-Y, Tzen K-Y, Tuan T-F, Liu W-L, Cheng A-L, et al. Synergistic Blockade of EGFR and HER2 by New-Generation EGFR Tyrosine Kinase Inhibitor Enhances Radiation Effect in Bladder Cancer Cells. Molecular cancer therapeutics. 2015;14(3):810-20.
173. Larbouret C, Gaborit N, Chardès T, Coelho M, Campigna E, Bascoul-Mollevi C, et al. In pancreatic carcinoma, dual EGFR/HER2 targeting with cetuximab/trastuzumab is more effective than treatment with trastuzumab/erlotinib or lapatinib alone: implication of receptors' down-regulation and dimers' disruption. Neoplasia. 2012;14(2):121-30.
174. Normanno N, De Luca A, Bianco C, Strizzi L, Mancino M, Maiello MR, et al. Epidermal growth factor receptor (EGFR) signaling in cancer. Gene. 2006;366(1):2-16.
175. Sierra JR, Tsao M-S. c-MET as a potential therapeutic target and biomarker in cancer. Therapeutic advances in medical oncology. 2011;3(1 suppl):S21-S35.
176. Ma PC, Tretiakova MS, MacKinnon AC, Ramnath N, Johnson C, Dietrich S, et al. Expression and mutational analysis of MET in human solid cancers. Genes, Chromosomes and Cancer. 2008;47(12):1025-37.
177. Schmidt L, Duh F-M, Chen F, Kishida T, Glenn G, Choyke P, et al. Germline and somatic mutations in the tyrosine kinase domain of the MET proto-oncogene in papillary renal carcinomas. Nature genetics. 1997;16(1):68-73.
178. Schmidt L, Junker K, Nakaigawa N, Kinjerski T, Weirich G, Miller M, et al. Novel mutations of the MET proto-oncogene in papillary renal carcinomas. Oncogene. 1999;18(14):2343-50.
179. Birchmeier C, Birchmeier W, Gherardi E, Woude GFV. Met, metastasis, motility and more. Nature reviews Molecular cell biology. 2003;4(12):915-25.
180. Khoury H, Naujokas MA, Zuo D, Sangwan V, Frigault MM, Petkiewicz S, et al. HGF converts ErbB2/Neu epithelial morphogenesis to cell invasion. Molecular biology of the cell. 2005;16(2):550-61.
181. Bauer TW, Somcio RJ, Fan F, Liu W, Johnson M, Lesslie DP, et al. Regulatory role of c-Met in insulin-like growth factor-I receptor–mediated migration and invasion of human pancreatic carcinoma cells. Molecular cancer therapeutics. 2006;5(7):1676-82.
182. Trusolino L, Comoglio PM. Scatter-factor and semaphorin receptors: cell signalling for invasive growth. Nature Reviews Cancer. 2002;2(4):289-300.
183. Viticchiè G, Muller PA. c-Met and Other Cell Surface Molecules: Interaction, Activation and Functional Consequences. Biomedicines. 2015;3(1):46-70.
184. Irby RB, Yeatman TJ. Role of Src expression and activation in human cancer. Oncogene. 2000;19(49):5636-42.
185. Zhang S, Yu D. Targeting Src family kinases in anti-cancer therapies: turning promise into triumph. Trends in pharmacological sciences. 2012;33(3):122-8.
186. Belsches-Jablonski AP, Biscardi JS, Peavy DR, Tice DA, Romney DA, Parsons SJ. Src family kinases and HER2 interactions in human breast cancer cell growth and survival. Oncogene. 2001;20(12):1465-75.
187. Peiro G, Ortiz-Martinez F, Gallardo A, Perez-Balaguer A, Sanchez-Paya J, Ponce J, et al. Src, a potential target for overcoming trastuzumab resistance in HER2-positive breast carcinoma. British journal of cancer. 2014.

188. Nautiyal J, Majumder P, Patel BB, Lee FY, Majumdar AP. Src inhibitor dasatinib inhibits growth of breast cancer cells by modulating EGFR signaling. Cancer letters. 2009;283(2):143-51.
189. Formisano L, Nappi L, Rosa R, Marciano R, D'Amato C, D'Amato V, et al. Epidermal growth factor-receptor activation modulates Src-dependent resistance to lapatinib in breast cancer models. Breast Cancer Research. 2014;16(3):R45.
190. Kopetz S. Targeting SRC and epidermal growth factor receptor in colorectal cancer: rationale and progress into the clinic. Gastrointestinal cancer research: GCR. 2007;1(4 Suppl 2):S37.
191. Koppikar P, Choi S-H, Egloff AM, Cai Q, Suzuki S, Freilino M, et al. Combined inhibition of c-Src and epidermal growth factor receptor abrogates growth and invasion of head and neck squamous cell carcinoma. Clinical Cancer Research. 2008;14(13):4284-91.
192. Schenone S, Manetti F, Botta M. SRC inhibitors and angiogenesis. Current pharmaceutical design. 2007;13(21):2118-28.
193. Mitra SK, Schlaepfer DD. Integrin-regulated FAK–Src signaling in normal and cancer cells. Current opinion in cell biology. 2006;18(5):516-23.
194. Kim LC, Song L, Haura EB. Src kinases as therapeutic targets for cancer. Nature Reviews Clinical Oncology. 2009;6(10):587-95.
195. Yeatman TJ. A renaissance for SRC. Nature Reviews Cancer. 2004;4(6):470-80.
196. Weinstein IB. Addiction to oncogenes--the Achilles heal of cancer. Science. 2002;297(5578):63-4.
197. Felsher DW, Bishop JM. Reversible tumorigenesis by MYC in hematopoietic lineages. Molecular cell. 1999;4(2):199-207.
198. Huettner CS, Zhang P, Van Etten RA, Tenen DG. Reversibility of acute B-cell leukaemia induced by BCR–ABL1. Nature genetics. 2000;24(1):57-60.
199. Aoki K, Yoshida T, Matsumoto N, Ide H, Sugimura T, Terada M. Suppression of Ki-ras p21 levels leading to growth inhibition of pancreatic cancer cell lines with Ki-ras mutation but not those without Ki-ras mutation. Molecular carcinogenesis. 1997;20(2):251-8.
200. Colomer R, Lupu R, Bacus S, Gelmann E. erbB-2 antisense oligonucleotides inhibit the proliferation of breast carcinoma cells with erbB-2 oncogene amplification. British journal of cancer. 1994;70(5):819.
201. Hochhaus A, Kreil S, Corbin A, La Rosee P, Muller M, Lahaye T, et al. Molecular and chromosomal mechanisms of resistance to imatinib (STI571) therapy. Leukemia. 2002;16(11):2190-6.
202. Hojjat-Farsangi M. Small-molecule inhibitors of the receptor tyrosine kinases: promising tools for targeted cancer therapies. International journal of molecular sciences. 2014;15(8):13768-801.
203. Zhang J, Yang PL, Gray NS. Targeting cancer with small molecule kinase inhibitors. Nature Reviews Cancer. 2009;9(1):28-39.
204. Cohen MH, Williams GA, Sridhara R, Chen G, Pazdur R. FDA drug approval summary: gefitinib (ZD1839)(Iressa®) tablets. The oncologist. 2003;8(4):303-6.
205. Cohen MH, Johnson JR, Chen Y-F, Sridhara R, Pazdur R. FDA drug approval summary: erlotinib (Tarceva®) tablets. The oncologist. 2005;10(7):461-6.

206. Chong CR, Jänne PA. The quest to overcome resistance to EGFR-targeted therapies in cancer. Nature medicine. 2013;19(11):1389-400.
207. Yun C-H, Boggon TJ, Li Y, Woo MS, Greulich H, Meyerson M, et al. Structures of lung cancer-derived EGFR mutants and inhibitor complexes: mechanism of activation and insights into differential inhibitor sensitivity. Cancer cell. 2007;11(3):217-27.
208. Vigna E, Comoglio P. Targeting the oncogenic Met receptor by antibodies and gene therapy. Oncogene. 2014.
209. Cui JJ, Tran-Dubé M, Shen H, Nambu M, Kung P-P, Pairish M, et al. Structure based drug design of crizotinib (PF-02341066), a potent and selective dual inhibitor of mesenchymal–epithelial transition factor (c-MET) kinase and anaplastic lymphoma kinase (ALK). Journal of medicinal chemistry. 2011;54(18):6342-63.
210. Elisei R, Schlumberger MJ, Müller SP, Schöffski P, Brose MS, Shah MH, et al. Cabozantinib in progressive medullary thyroid cancer. Journal of Clinical Oncology. 2013;31(29):3639-46.
211. Blumenschein GR, Mills GB, Gonzalez-Angulo AM. Targeting the hepatocyte growth factor–cMET axis in cancer therapy. Journal of Clinical Oncology. 2012;30(26):3287-96.
212. Getlik Mu, Grütter C, Simard JR, Klüter S, Rabiller M, Rode HB, et al. Hybrid compound design to overcome the gatekeeper T338M mutation in cSrc#. Journal of medicinal chemistry. 2009;52(13):3915-26.
213. Puls LN, Eadens M, Messersmith W. Current status of SRC inhibitors in solid tumor malignancies. The oncologist. 2011;16(5):566-78.
214. Allison KH. Molecular Pathology of Breast Cancer What a Pathologist Needs to Know. American journal of clinical pathology. 2012;138(6):770-80.
215. Eroles P, Bosch A, Pérez-Fidalgo JA, Lluch A. Molecular biology in breast cancer: intrinsic subtypes and signaling pathways. Cancer treatment reviews. 2012;38(6):698-707.
216. Hensing T, Chawla A, Batra R, Salgia R. A personalized treatment for lung cancer: molecular pathways, targeted therapies, and genomic characterization. Systems Analysis of Human Multigene Disorders: Springer; 2014. p. 85-117.
217. Collisson EA, Sadanandam A, Olson P, Gibb WJ, Truitt M, Gu S, et al. Subtypes of pancreatic ductal adenocarcinoma and their differing responses to therapy. Nature medicine. 2011;17(4):500-3.
218. Riaz N, Morris LG, Lee W, Chan TA. Unraveling the molecular genetics of head and neck cancer through genome-wide approaches. Genes & Diseases. 2014;1(1):75-86.
219. McGranahan N, Swanton C. Biological and therapeutic impact of intratumor heterogeneity in cancer evolution. Cancer cell. 2015;27(1):15-26.
220. Lovly CM, Shaw AT. Molecular pathways: resistance to kinase inhibitors and implications for therapeutic strategies. Clinical Cancer Research. 2014;20(9):2249-56.
221. Sequist LV, Waltman BA, Dias-Santagata D, Digumarthy S, Turke AB, Fidias P, et al. Genotypic and histological evolution of lung cancers acquiring resistance to EGFR inhibitors. Science translational medicine. 2011;3(75):75ra26-75ra26.
222. Girard N, Lou E, Azzoli CG, Reddy R, Robson M, Harlan M, et al. Analysis of genetic variants in never-smokers with lung cancer facilitated by an Internet-based blood collection protocol: a preliminary report. Clinical Cancer Research. 2010;16(2):755-63.

223. Kobayashi S, Boggon TJ, Dayaram T, Jänne PA, Kocher O, Meyerson M, et al. EGFR mutation and resistance of non–small-cell lung cancer to gefitinib. New England Journal of Medicine. 2005;352(8):786-92.
224. Heinrich MC, Corless CL, Demetri GD, Blanke CD, von Mehren M, Joensuu H, et al. Kinase mutations and imatinib response in patients with metastatic gastrointestinal stromal tumor. Journal of Clinical Oncology. 2003;21(23):4342-9.
225. Mir O, Blanchet B, Goldwasser F. Drug-induced effects on erlotinib metabolism. New England Journal of Medicine. 2011;365(4):379-80.
226. Gorre ME, Mohammed M, Ellwood K, Hsu N, Paquette R, Rao PN, et al. Clinical resistance to STI-571 cancer therapy caused by BCR-ABL gene mutation or amplification. Science. 2001;293(5531):876-80.
227. Tamborini E, Pricl S, Negri T, Lagonigro M, Miselli F, Greco A, et al. Functional analyses and molecular modeling of two c-Kit mutations responsible for imatinib secondary resistance in GIST patients. Oncogene. 2006;25(45):6140-6.
228. Katayama R, Khan TM, Benes C, Lifshits E, Ebi H, Rivera VM, et al. Therapeutic strategies to overcome crizotinib resistance in non-small cell lung cancers harboring the fusion oncogene EML4-ALK. Proceedings of the National Academy of Sciences. 2011;108(18):7535-40.
229. Cross DA, Ashton SE, Ghiorghiu S, Eberlein C, Nebhan CA, Spitzler PJ, et al. AZD9291, an irreversible EGFR TKI, overcomes T790M-mediated resistance to EGFR inhibitors in lung cancer. Cancer discovery. 2014;4(9):1046-61.
230. Janjigian YY, Smit EF, Groen HJ, Horn L, Gettinger S, Camidge DR, et al. Dual inhibition of EGFR with afatinib and cetuximab in kinase inhibitor–resistant EGFR-mutant lung cancer with and without T790M mutations. Cancer discovery. 2014;4(9):1036-45.
231. Rothschild SI. Ceritinib—a second-generation ALK inhibitor overcoming resistance in ALK-rearranged non-small cell lung cancer. Translational Lung Cancer Research. 2014;3(6):379.
232. Song Z, Wang M, Zhang A. Alectinib: a novel second generation anaplastic lymphoma kinase (ALK) inhibitor for overcoming clinically-acquired resistance. Acta Pharmaceutica Sinica B. 2015;5(1):34-7.
233. Jabbour E, Kantarjian H, Cortes J. Use of Second-and Third-Generation Tyrosine Kinase Inhibitors in the Treatment of Chronic Myeloid Leukemia: An Evolving Treatment Paradigm. Clinical Lymphoma Myeloma and Leukemia. 2015.
234. Holohan C, Van Schaeybroeck S, Longley DB, Johnston PG. Cancer drug resistance: an evolving paradigm. Nature Reviews Cancer. 2013;13(10):714-26.
235. Sun C, Bernards R. Feedback and redundancy in receptor tyrosine kinase signaling: relevance to cancer therapies. Trends in biochemical sciences. 2014;39(10):465-74.
236. Logue JS, Morrison DK. Complexity in the signaling network: insights from the use of targeted inhibitors in cancer therapy. Genes & development. 2012;26(7):641-50.
237. Engelman JA, Zejnullahu K, Mitsudomi T, Song Y, Hyland C, Park JO, et al. MET amplification leads to gefitinib resistance in lung cancer by activating ERBB3 signaling. science. 2007;316(5827):1039-43.

238. Guix M, Faber AC, Wang SE, Olivares MG, Song Y, Qu S, et al. Acquired resistance to EGFR tyrosine kinase inhibitors in cancer cells is mediated by loss of IGF-binding proteins. The Journal of clinical investigation. 2008;118(7):2609.
239. Yonesaka K, Zejnullahu K, Okamoto I, Satoh T, Cappuzzo F, Souglakos J, et al. Activation of ERBB2 signaling causes resistance to the EGFR-directed therapeutic antibody cetuximab. Science translational medicine. 2011;3(99):99ra86-99ra86.
240. Qi J, McTigue MA, Rogers A, Lifshits E, Christensen JG, Jänne PA, et al. Multiple mutations and bypass mechanisms can contribute to development of acquired resistance to MET inhibitors. Cancer research. 2011;71(3):1081-91.
241. Zhang S, Huang W-C, Li P, Guo H, Poh S-B, Brady SW, et al. Combating trastuzumab resistance by targeting SRC, a common node downstream of multiple resistance pathways. Nature medicine. 2011;17(4):461-9.
242. von Manstein V, Yang CM, Richter D, Delis N, Vafaizadeh V, Groner B. Resistance of cancer cells to targeted therapies through the activation of compensating signaling loops. Current signal transduction therapy. 2013;8(3):193.
243. Wang Y, van Boxel-Dezaire AH, Cheon H, Yang J, Stark GR. STAT3 activation in response to IL-6 is prolonged by the binding of IL-6 receptor to EGF receptor. Proceedings of the National Academy of Sciences. 2013;110(42):16975-80.
244. Byers LA, Sen B, Saigal B, Diao L, Wang J, Nanjundan M, et al. Reciprocal regulation of c-Src and STAT3 in non-small cell lung cancer. Clinical Cancer Research. 2009;15(22):6852-61.
245. Siveen KS, Sikka S, Surana R, Dai X, Zhang J, Kumar AP, et al. Targeting the STAT3 signaling pathway in cancer: role of synthetic and natural inhibitors. Biochimica et Biophysica Acta (BBA)-Reviews on Cancer. 2014;1845(2):136-54.
246. Yu H, Pardoll D, Jove R. STATs in cancer inflammation and immunity: a leading role for STAT3. Nature Reviews Cancer. 2009;9(11):798-809.
247. Huang S, Chen M, Shen Y, Shen W, Guo H, Gao Q, et al. Inhibition of activated Stat3 reverses drug resistance to chemotherapeutic agents in gastric cancer cells. Cancer letters. 2012;315(2):198-205.
248. Sen B, Peng S, Woods DM, Wistuba I, Bell D, El-Naggar AK, et al. STAT5A-mediated SOCS2 expression regulates Jak2 and STAT3 activity following c-Src inhibition in head and neck squamous carcinoma. Clinical Cancer Research. 2012;18(1):127-39.
249. Lee H-J, Zhuang G, Cao Y, Du P, Kim H-J, Settleman J. Drug resistance via feedback activation of Stat3 in oncogene-addicted cancer cells. Cancer cell. 2014;26(2):207-21.
250. Eser S, Schnieke A, Schneider G, Saur D. Oncogenic KRAS signalling in pancreatic cancer. British journal of cancer. 2014;111(5):817-22.
251. Markman B, Javier Ramos F, Capdevila J, Tabernero J. EGFR and KRAS in colorectal cancer. Advances in clinical chemistry. 2010;51:72.
252. Riely GJ, Marks J, Pao W. KRAS mutations in non–small cell lung cancer. Proceedings of the American Thoracic Society. 2009;6(2):201-5.
253. Davies H, Bignell GR, Cox C, Stephens P, Edkins S, Clegg S, et al. Mutations of the BRAF gene in human cancer. Nature. 2002;417(6892):949-54.

254. Papa A, Wan L, Bonora M, Salmena L, Song MS, Hobbs RM, et al. Cancer-associated PTEN mutants act in a dominant-negative manner to suppress PTEN protein function. Cell. 2014;157(3):595-610.
255. Chalhoub N, Baker SJ. PTEN and the PI3-kinase pathway in cancer. Annual review of pathology. 2009;4:127.
256. Yamada KM, Araki M. Tumor suppressor PTEN: modulator of cell signaling, growth, migration and apoptosis. Journal of cell science. 2001;114(13):2375-82.
257. Sato K-i. Cellular functions regulated by phosphorylation of EGFR on Tyr845. International journal of molecular sciences. 2013;14(6):10761-90.
258. Mueller KL, Hunter LA, Ethier SP, Boerner JL. Met and c-Src cooperate to compensate for loss of epidermal growth factor receptor kinase activity in breast cancer cells. Cancer research. 2008;68(9):3314-22.
259. Zhang J, Kalyankrishna S, Wislez M, Thilaganathan N, Saigal B, Wei W, et al. SRC-family kinases are activated in non-small cell lung cancer and promote the survival of epidermal growth factor receptor-dependent cell lines. The American journal of pathology. 2007;170(1):366-76.
260. Kanda R, Kawahara A, Watari K, Murakami Y, Sonoda K, Maeda M, et al. Erlotinib resistance in lung cancer cells mediated by integrin β1/Src/Akt-driven bypass signaling. Cancer research. 2013;73(20):6243-53.
261. Yoshida T, Okamoto I, Okamoto W, Hatashita E, Yamada Y, Kuwata K, et al. Effects of Src inhibitors on cell growth and epidermal growth factor receptor and MET signaling in gefitinib-resistant non-small cell lung cancer cells with acquired MET amplification. Cancer science. 2010;101(1):167-72.
262. Lieu C, Kopetz S. The SRC family of protein tyrosine kinases: a new and promising target for colorectal cancer therapy. Clinical colorectal cancer. 2010;9(2):89-94.
263. Lu KV, Zhu S, Cvrljevic A, Huang TT, Sarkaria S, Ahkavan D, et al. Fyn and SRC are effectors of oncogenic epidermal growth factor receptor signaling in glioblastoma patients. Cancer research. 2009;69(17):6889-98.
264. Kalyankrishna S, Grandis JR. Epidermal growth factor receptor biology in head and neck cancer. Journal of Clinical Oncology. 2006;24(17):2666-72.
265. Nagaraj NS, Washington MK, Merchant NB. Combined blockade of Src kinase and epidermal growth factor receptor with gemcitabine overcomes STAT3-mediated resistance of inhibition of pancreatic tumor growth. Clinical Cancer Research. 2011;17(3):483-93.
266. Yano S, Wang W, Li Q, Matsumoto K, Sakurama H, Nakamura T, et al. Hepatocyte growth factor induces gefitinib resistance of lung adenocarcinoma with epidermal growth factor receptor–activating mutations. Cancer research. 2008;68(22):9479-87.
267. Bean J, Brennan C, Shih J-Y, Riely G, Viale A, Wang L, et al. MET amplification occurs with or without T790M mutations in EGFR mutant lung tumors with acquired resistance to gefitinib or erlotinib. Proceedings of the National Academy of Sciences. 2007;104(52):20932-7.
268. Puri N, Salgia R. Synergism of EGFR and c-Met pathways, cross-talk and inhibition, in non-small cell lung cancer. Journal of carcinogenesis. 2008;7(1):9.

269. Dulak AM, Gubish CT, Stabile LP, Henry C, Siegfried JM. HGF-independent potentiation of EGFR action by c-Met. Oncogene. 2011;30(33):3625-35.
270. Benedettini E, Sholl LM, Peyton M, Reilly J, Ware C, Davis L, et al. Met activation in non-small cell lung cancer is associated with de novo resistance to EGFR inhibitors and the development of brain metastasis. The American journal of pathology. 2010;177(1):415-23.
271. Cappuzzo F, Jänne P, Skokan M, Finocchiaro G, Rossi E, Ligorio C, et al. MET increased gene copy number and primary resistance to gefitinib therapy in non-small-cell lung cancer patients. Annals of oncology. 2009;20(2):298-304.
272. Sharma N, Adjei AA. In the clinic: ongoing clinical trials evaluating c-MET-inhibiting drugs. Therapeutic advances in medical oncology. 2011;3(1 suppl):S37-S50.
273. Wheeler DL, Huang S, Kruser TJ, Nechrebecki MM, Armstrong EA, Benavente S, et al. Mechanisms of acquired resistance to cetuximab: role of HER (ErbB) family members. Oncogene. 2008;27(28):3944-56.
274. Xu H, Stabile LP, Gubish CT, Gooding WE, Grandis JR, Siegfried JM. Dual blockade of EGFR and c-Met abrogates redundant signaling and proliferation in head and neck carcinoma cells. Clinical Cancer Research. 2011;17(13):4425-38.
275. Stabile LP, He G, Lui VWY, Thomas SM, Henry C, Gubish CT, et al. c-Src activation mediates erlotinib resistance in head and neck cancer by stimulating c-Met. Clinical Cancer Research. 2013;19(2):380-92.
276. Sohn J, Liu S, Parinyanitikul N, Lee J, Hortobagyi GN, Mills GB, et al. cMET Activation and EGFR-Directed Therapy Resistance in Triple-Negative Breast Cancer. Journal of Cancer. 2014;5(9):745.
277. Mueller KL, Yang Z-Q, Haddad R, Ethier SP, Boerner JL. EGFR/Met association regulates EGFR TKI resistance in breast cancer. Journal of molecular signaling. 2010;5(1):8.
278. Kim YJ, Choi JS, Seo J, Song JY, Eun Lee S, Kwon MJ, et al. MET is a potential target for use in combination therapy with EGFR inhibition in triple-negative/basal-like breast cancer. International Journal of Cancer. 2014;134(10):2424-36.
279. Stabile LP, Rothstein ME, Keohavong P, Lenzner D, Land SR, Gaither-Davis AL, et al. Targeting of both the c-Met and EGFR pathways results in additive inhibition of lung tumorigenesis in transgenic mice. Cancers. 2010;2(4):2153-70.
280. Yamamoto N, Mammadova G, Song RX-D, Fukami Y, Sato K-i. Tyrosine phosphorylation of p145met mediated by EGFR and Src is required for serum-independent survival of human bladder carcinoma cells. Journal of cell science. 2006;119(22):4623-33.
281. Zucali P, Ruiz MG, Giovannetti E, Destro A, Varella-Garcia M, Floor K, et al. Role of cMET expression in non-small-cell lung cancer patients treated with EGFR tyrosine kinase inhibitors. Annals of oncology. 2008;19(9):1605-12.
282. Jo M, Stolz DB, Esplen JE, Dorko K, Michalopoulos GK, Strom SC. Cross-talk between epidermal growth factor receptor and c-Met signal pathways in transformed cells. Journal of Biological Chemistry. 2000;275(12):8806-11.
283. Reznik TE, Sang Y, Ma Y, Abounader R, Rosen EM, Xia S, et al. Transcription-dependent epidermal growth factor receptor activation by hepatocyte growth factor. Molecular Cancer Research. 2008;6(1):139-50.

284. Hopkins AL. Network pharmacology: the next paradigm in drug discovery. Nature chemical biology. 2008;4(11):682-90.
285. Zambrowicz BP, Sands AT. Modeling drug action in the mouse with knockouts and RNA interference. Drug Discovery Today: TARGETS. 2004;3(5):198-207.
286. Winzeler EA, Shoemaker DD, Astromoff A, Liang H, Anderson K, Andre B, et al. Functional characterization of the S. cerevisiae genome by gene deletion and parallel analysis. science. 1999;285(5429):901-6.
287. Morrow JK, Tian L, Zhang S. Molecular networks in drug discovery. Critical Reviews™ in Biomedical Engineering. 2010;38(2).
288. Canellos GP, Anderson JR, Propert KJ, Nissen N, Cooper MR, Henderson ES, et al. Chemotherapy of advanced Hodgkin's disease with MOPP, ABVD, or MOPP alternating with ABVD. New England Journal of Medicine. 1992;327(21):1478-84.
289. Fisher RI, Gaynor ER, Dahlberg S, Oken MM, Grogan TM, Mize EM, et al. Comparison of a standard regimen (CHOP) with three intensive chemotherapy regimens for advanced non-Hodgkin's lymphoma. New England Journal of Medicine. 1993;328(14):1002-6.
290. Giordano S, Petrelli A. From single-to multi-target drugs in cancer therapy: when aspecificity becomes an advantage. Current medicinal chemistry. 2008;15(5):422-32.
291. Boran AD, Iyengar R. Systems approaches to polypharmacology and drug discovery. Current opinion in drug discovery & development. 2010;13(3):297.
292. Masoudi-Nejad A, Mousavian Z, Bozorgmehr JH. Drug-target and disease networks: polypharmacology in the post-genomic era. Silico Pharm. 2013;1:17.
293. Dar AC, Das TK, Shokat KM, Cagan RL. Chemical genetic discovery of targets and anti-targets for cancer polypharmacology. Nature. 2012;486(7401):80-4.
294. Knight ZA, Lin H, Shokat KM. Targeting the cancer kinome through polypharmacology. Nature Reviews Cancer. 2010;10(2):130-7.
295. Brahimi F, Matheson SL, Dudouit F, Mcnamee JP, Tari AM, Jean-Claude BJ. Inhibition of epidermal growth factor receptor-mediated signaling by “combi-triazene” BJ2000, a new probe for combi-targeting postulates. Journal of Pharmacology and Experimental Therapeutics. 2002;303(1):238-46.
296. Huang Y, Rachid Z, Jean-Claude BJ. MGMT Is a Molecular Determinant for Potency of the DNA-EGFR–Combi-Molecule ZRS1. Molecular Cancer Research. 2011;9(3):320-31.
297. Ait-Tihyaty M, Rachid Z, Larroque-Lombard A-L, Jean-Claude BJ. ZRX1, the first EGFR inhibitor-capecitabine based combi-molecule, requires carboxylesterase-mediated hydrolysis for optimal activity. Investigational new drugs. 2013;31(6):1409-23.
298. Banerjee R, Rachid Z, Qiu Q, McNamee J, Tari A, Jean-Claude B. Sustained antiproliferative mechanisms by RB24, a targeted precursor of multiple inhibitors of epidermal growth factor receptor and a DNA alkylating agent in the A431 epidermal carcinoma of the vulva cell line. British journal of cancer. 2004;91(6):1066-73.
299. Brahimi F, Rachid Z, Qiu Q, McNamee JP, Li YJ, Tari AM, et al. Multiple mechanisms of action of ZR2002 in human breast cancer cells: A novel combi-molecule designed to block signaling mediated by the ERB family of oncogenes and to damage genomic DNA. International journal of cancer. 2004;112(3):484-91.
300. Rachid Z, Katsoulas A, Williams C, Larroque A-L, McNamee J, Jean-Claude BJ. Optimization of novel combi-molecules: identification of balanced and mixed bcr-

abl/DNA targeting properties. Bioorganic & medicinal chemistry letters. 2007;17(15):4248-53.
301. Katsoulas A, Rachid Z, McNamee JP, Williams C, Jean-Claude BJ. Combi-targeting concept: an optimized single-molecule dual-targeting model for the treatment of chronic myelogenous leukemia. Molecular cancer therapeutics. 2008;7(5):1033-43.
302. Huang Y, Rachid Z, Peyrard L, Senhaji Mouhri Z, Williams C, Jean-Claude BJ. Positional Isomerization of A Non-Cleavable Combi-Molecule Dramatically Altered Tumor Cell Response Profile. Chemical biology & drug design. 2015;85(2):153-62.
303. Katsoulas A, Rachid Z, Brahimi F, McNamee J, Jean-Claude BJ. Cytokinetics and mechanism of action of AKO4: a novel nitrogen mustard targeted to bcr-abl. Leukemia research. 2005;29(5):565-72.
304. Larroque-Lombard AL, Todorova M, Qiyu Q, Jean-Claude B. Synthesis and Studies on Three-Compartment Flavone-Containing Combi-Molecules Designed to Target EGFR, DNA, and MEK. Chemical biology & drug design. 2011;77(5):309-18.
305. Cheung-Ong K, Giaever G, Nislow C. DNA-damaging agents in cancer chemotherapy: serendipity and chemical biology. Chemistry & biology. 2013;20(5):648-59.
306. Karran P. Mechanisms of tolerance to DNA damaging therapeutic drugs. Carcinogenesis. 2001;22(12):1931-7.
307. Liccardi G, Hartley JA, Hochhauser D. EGFR nuclear translocation modulates DNA repair following cisplatin and ionizing radiation treatment. Cancer research. 2011;71(3):1103-14.
308. Bai J, Guo X-G, Bai X-P. Epidermal growth factor receptor-related DNA repair and radiation-resistance regulatory mechanisms: a mini-review. Asian Pac J Cancer Prev. 2012;13(10):4879-81.
309. Denny WA, Rewcastle GW, Bridges AJ, Fry DW, Kraker AJ. STRUCTURE-ACTIVITY RELATIONSHIPS FOR 4-ANILINOQUINAZOLINES AS POTENT INHIBITORS AT THE ATP BINDING SITE OF THE EPIDERMAL GROWTH FACTOR RECEPTOR IN VITRO. Clinical and experimental pharmacology and physiology. 1996;23(5):424-7.
310. Rewcastle GW, Bridges AJ, Fry DW, Rubin JR, Denny WA. Tyrosine kinase inhibitors. 12. Synthesis and structure-activity relationships for 6-substituted 4-(phenylamino) pyrimido [5, 4-d] pyrimidines designed as inhibitors of the epidermal growth factor receptor. Journal of medicinal chemistry. 1997;40(12):1820-6.
311. Abdulnur S, Flurry R. Effect of guanine alkylation on mispairing. Nature. 1976;264(5584):369-70.
312. Friedman HS, Kerby T, Calvert H. Temozolomide and treatment of malignant glioma. Clinical Cancer Research. 2000;6(7):2585-97.
313. Matheson SL, Brahimi F, Jean-Claude BJ. The combi-targeting concept: intracellular fragmentation of the binary epidermal growth factor (EGFR)/DNA targeting "combi-triazene" SMA41. Biochemical pharmacology. 2004;67(6):1131-8.
314. Todorova MI, Larroque A-L, Dauphin-Pierre S, Fang Y-Q, Jean-Claude BJ. Subcellular distribution of a fluorescence-labeled combi-molecule designed to block epidermal growth factor receptor tyrosine kinase and damage DNA with a green fluorescent species. Molecular cancer therapeutics. 2010;9(4):869-82.

315. Barchéchath S, Williams C, Saade K, Lauwagie S, Jean-Claude B. Rational design of multitargeted tyrosine kinase inhibitors: a novel approach. Chemical biology & drug design. 2009;73(4):380-7.

CHAPTER 2

BIOLOGICAL EFFECTS OF AL622, A MOLECULE RATIONALLY DESIGNED TO RELEASE AN EGFR AND A c-SRC KINASE INHIBITOR

Anne-Laure Larroque-Lombard, Na Ning*, Suman Rao, Sylvia Lauwagie, Ruba Halaoui, Laëtitia Coudray, Ying Huang, and Bertrand J. Jean-Claude*

* The two authors contributed equally to the work

Cancer Drug Research Laboratory, Department of Medicine, Division of Medical Oncology, McGill University Health Center/Royal Victoria Hospital, 687 Pine Avenue West Rm. M-719, Montreal, Quebec, H3A 1A1 Canada

2.1. ABSTRACT

In breast cancer cells expressing c-Src and EGFR, a control of one of the two oncogenes over proliferation and invasion is observed whereas in others, the synergistic interaction between them is required for tumour progression. With the purpose of developing molecules with the highest probability for blocking the adverse effects of these two oncogenes, we designed AL622, which contains a quinazoline head targeted to EGFR and a linker that bridges it to the PP2-like for targeting c-Src. In case the entire molecule would not be capable of blocking c-Src, we designed AL622 to hydrolyze to an intact c-Src-targeting PP2 molecule. After confirming its binary c-Src-EGFR targeting potency of AL622, we analyzed its potency in isogenic NIH3T3 cells tranfected with EGFR and HER2 and human breast cancer cells known to be dominated by c-Src function. The results showed that in EGFR/HER-2 driven cells, it was more potent than PP2 and its activity was in the same range as the latter in more c-Src-driven cells. Its ability to block motility and invasion was comparable with that of PP2 and corresponding combinations, indicating that AL622 could be a better antitumour agent in cells where c-Src and/or EGFR play a role.

2.2. INTRODUCTION

Tumour progression is characterized by a variety of signaling pathways often subverted by the mutation or overexpression of genes encoding key signaling proteins. Disordered expression of several growth factor receptors is not only associated with enhanced growth signaling, but also with tumour invasiveness. In the latter process, receptor tyrosine kinases can interact with non-receptor tyrosine kinases to promote motility and invasion (1, 2). One such interaction has already been reported for the epidermal growth factor receptor (EGFR) and the non-receptor tyrosine kinase c-Src (3). Recent studies showed that activation of c-Src in some breast cancer cell lines led to phosphorylation of EGFR on Tyr845 and that the downstream effect is transduced through the STAT3/5 pathway (4, 5). A significant body of work has now accumulated to suggest that EGFR and c-Src may contribute to an aggressive phenotype in some tumours (6). Recently with the purpose of inducing a tandem and targeted blockade of EGFR and c-Src, we designed a series of agents containing a PP2-like warhead directed at c-Src and a gefitinib-like moiety targeted to EGFR. PP2 (see Fig. 2.1) is an aminopurine inhibitor of c-Src (7) and the quinazoline moiety of gefitinib is known to anchor into the ATP site of EGFR (8). Studies on this series of molecules revealed that compounds such as SB163 (Fig. 2.1) (9) have a strong EGFR inhibitory property but moderate c-Src targeting potential. The reduced c-Src targeting potency of SB163 was believed to be due to the bulkiness of the linker attached to the 6-position of the aminopurine PP2-like moiety (9). To circumvent this problem, we recently re-designed the molecule to release an intact PP2 molecule and a 7-substituted aminoquinazoline capable of blocking EGFR activation. Here we study the cytokinetics of one such compound AL622 wherein the hydrolysable linker is

branched to the 6-aminopurine through an amide bond. It was expected that due to the electron deficiency of the pyridine linker, the amide bond could be readily hydrolyzed in the intracellular milieu.

Here we analyzed the degradation, the growth inhibitory potency as well as the mixed EGFR- c-Src targeting properties of this novel type of combi-molecule. Furthermore, given the significant role of c-Src and EGFR in invasion and motility, we analyzed the ability of AL622 to block these processes in breast cancer cells using the wound healing and Boyden Chamber assays.

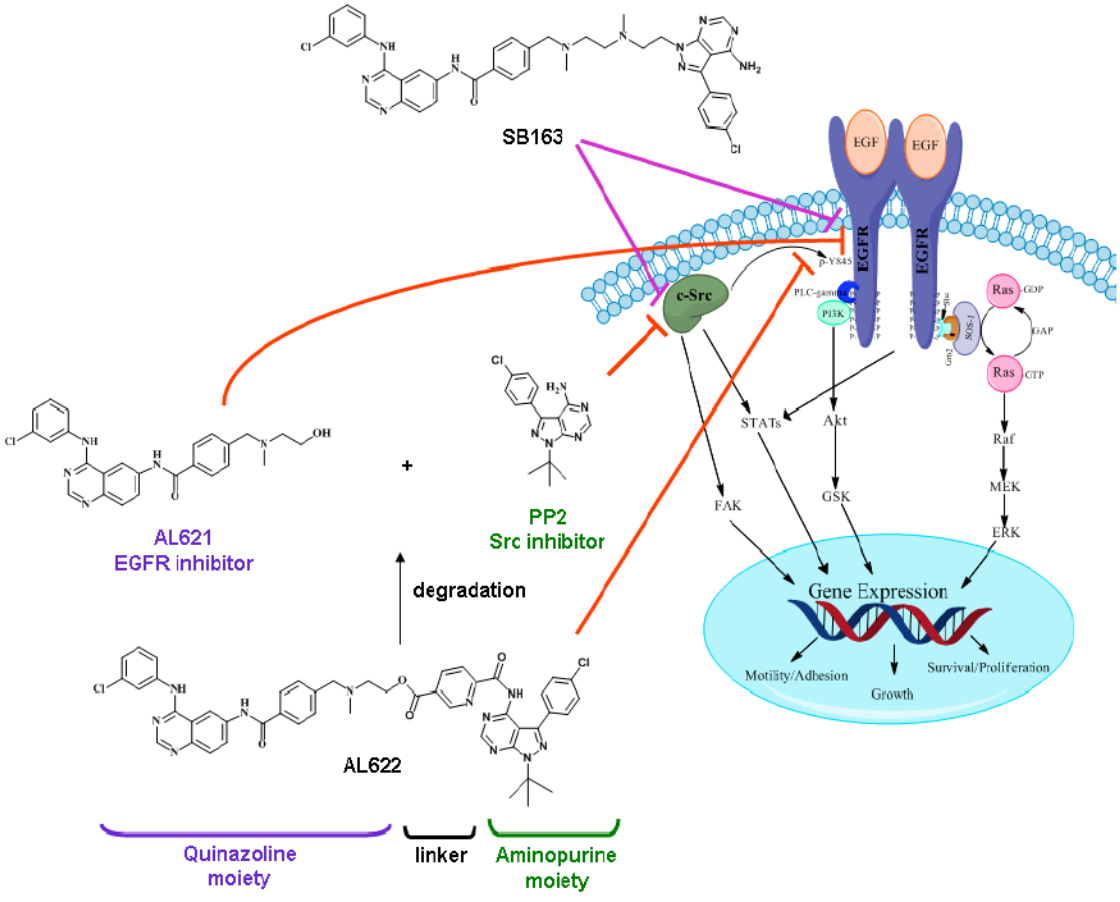

Figure 2.1. Schematic representation of crosstalk between different membrane receptors such as EGFR and the non-receptor tyrosine kinase c-Src.

2.3. MATERIALS AND METHODS

2.3.1. Chemistry

^{1}H NMR spectra and ^{13}C NMR spectra were recorded on a Varian 300, 400 or 500 MHz spectrometer. Chemical shifts are given as δ values in parts per million (ppm) and are referenced to the residual solvent proton or carbon peak. Mass spectrometry was performed by the McGill University Mass spectroscopy Center and electrospray ionization (ESI) spectra were performed on a Finnigan LC QDUO spectrometer. Data are reported as m/z (intensity relative to base peak = 100). All chemicals were purchased from Sigma-Aldrich.

Compound 2.

To a solution of PP2 (0.5 g, 1.66 mmol) in dry THF (10 mL) at 0 ºC. NaH (60% oil dispersion) (80 mg, 1.2 eq) was added portionwise. After 30 min, a solution of methyl 6-(chlorocarbonyl)nicotinate (0.66 g, 2 eq.), , in THF (5 mL) was added dropwise at 0 ºC. The mixture was subsequently kept under argon for 24 h, after which it was evaporated to give a green-blue crude powder (1.2g), which was purified by silica gel chromatography column (CH_2Cl_2/MeOH 9/1 to 85/15) to give **2** as pure white powder (0.4g, 52%). ^{1}H NMR (400 MHz, *DMSO-d_6*) d ppm 1.82 (s, 9H), 3.93 (s, 3H), 7.42 (d, *J* = 8.4 Hz, 2H), 7.71 (br s, 2H), 7.98 (d, *J* = 8 Hz, 1H), 8.46 (dd, *J* = 8 Hz, *J* = 2 Hz, 1H), 8.86 (s, 1H), 8.99 (s, 1H), 11.07 (br s, 1H).

Compound 3.

Compound **2** (0.4 g, 0.87 mmol) was dissolved in THF/CH_2Cl_2 (1/1) mixture (10 mL) at room temperature and potassium trimethylsilanoate (0.56 g, 5 eq.) was added. A white precipitate appeared within a few minutes and the mixture was further stirred at room

temperature under argon for 2h30 after which it was evaporated to dryness. The resulting solid was triturated in ethyl ether, collected by filtration and redissolved in water. The pH of the solution was adjusted to 1 with HCl 1N and the product extracted three times with ethyl acetate. The organic phase was then dried over $MgSO_4$, filtered and evaporated to give **3** as a pure white solid (0.28 mg, 71%). ^{1}H NMR (400 MHz, *DMSO-d_6*) d ppm 1.82 (s, 9H), 7.43 (d, *J* = 8.2 Hz, 2H), 7.70 (d, *J* = 8.2 Hz, 2H), 7.97 (d, *J* = 8.2 Hz, 1H), 8.44 (d, *J* = 8.2 Hz, 1H), 8.87 (s, 1H), 8.97 (s, 1H), 11.06 (s, 1H).

Compound 5.

6-Amino-4-[(3-chlorophenyl)amino]quinazoline **4** (7.4 mmol, 2.0 g) was dissolved in dry THF (40 mL) containing pyridine (0.9 mL, 1.5 eq) and triethylamine (1.6 mL, 1.5 eq.) at 0 ºC. A solution of 4-chloromethylbenzoyl chloride (2.1 g, 1.5 eq.) in dry THF (5 mL) was added dropwise. After 2 h at room temperature, the reaction mixture was concentrated *in vacuo*. The resulting green solid was washed with aqueous HCl (1N) and aqueous K_2CO_3 (10%). Additional washings with water, CH_2Cl_2 and Et_2O gave a green solid, which was subsequently dried *in vacuo* to afford compound **5** as a yellow-green solid (2.33 g, 74 % yield). ^{1}H NMR (400 MHz, DMSO-d_6): δ 5.86 (s, 2 H), 7.15 (dd, *J* = 8.0 Hz, *J* = 1.0 Hz, 1 H), 7.40 (t, *J* = 8.0 Hz, 1 H), 7.63 (d, *J* = 8.5 Hz, 2 H), 7.82 (d, *J* = 8.0 Hz, 2 H), 8.00-8.08 (m, 4 H), 8.60 (s, 1 H), 8.91 (d, *J* = 2.0 Hz, 1 H), 9.97 (s, 1 H), 10.67 (s, 1 H).

Compound 6.

To compound **5** (1.0 g, 2.36 mmol) in DMF (10 mL) was added potassium iodide (0.43 g, 1.1 eq.) followed by 2-methylaminoethanol (0.57 mL, 3 eq.) at room temperature under argon. After 3 h at 70 °C under argon, the DMF was azeotroped with heptane to give a

brown paste, which was triturated in water. The resulting pale orange solid was filtered, dried *in vacuo* to give compound **6** (1 g, 92 %).^{1}H NMR (400 MHz, DMSO-d_6): δ 2.17 (s, 3H), 2.44 (t, *J* = 6.4 Hz, 2H), 3.51 (q, *J* = 9.2 Hz, *J* = 5.6 Hz, 2H), 3.58 (s, 2H), 4.44 (t, *J* = 5.6 Hz, 1H), 7.14 (dd, *J* = 8.0 Hz, *J* = 1.4 Hz, 1 H), 7.39 (t, *J* = 8.0 Hz, 1 H), 7.49 (d, *J* = 8.4 Hz, 2 H), 7.81 (d, *J* = 9.4 Hz, 2 H), 7.99 (d, *J* = 8.4 Hz, 2 H), 8.02-8.07 (m, 2 H), 8.60 (s, 1 H), 8.90 (d, *J* = 2.4 Hz, 1 H), 9.95 (s, 1 H), 10.58 (s, 1 H).

Compound 7 (AL622).

To a solution of **3** (0.54 g, 1.2 mmol) and **6** (0.55 g, 1 eq in DMF (10 mL) were added dicyclohexyl carbodiimide (DCC) (0.37 g, 1.5 eq.), hydroxybenzotriazole (HOBt) (0.24 g, 1.5 eq.) and dimethylaminopyridine (DMAP) (15 mg, 0.1 eq.). A white precipitate appeared within a few minutes and the mixture was further stirred at room temperature for 48h under argon. The precipitate was filtered through celite and the DMF evaporated *in vacuo*. The resulting paste was redissolved in ethyl acetate and washed with water and brine. The organic layer was removed and dried over $MgSO_4$, to give a crude brown solid (1.6 g), which was further purified by silica gel chromatography column (CH_2Cl_2/MeOH 95/5 to 9/1). Further purification r by preparative TLC (silica plate, CH_2Cl_2/MeOH 9/1) gave **7** as a pure pale yellow solid (0.37g, 35%). ^{1}H NMR (400 MHz, DMSO-d_6): δ 1.78 (s, 9H), 2.32 (s, 3H), 2.78 (t, *J* = 5.0 Hz, 2H), 3.66 (s, 2H), 4.48 (t, *J* = 5.0 Hz, 2H), 7.13 (dd, *J* = 8.0 Hz, *J* = 1.5 Hz, 1 H), 7.37 (t, *J* = 8.5 Hz, 1 H), 7.40 (d, *J* = 8.4 Hz, 2H), 7.45 (d, *J* = 8.4 Hz, 2 H), 7.67 (br s, 1H), 7.71 (d, *J* = 8.8 Hz, 2H), 7.78 (dd, *J* = 8.5 Hz, *J* = 1.5 Hz, 1 H), 7.90 (d, *J* = 8.4 Hz, 2 H), 7.96 (dd, *J* = 8.5 Hz, *J* = 1.8 Hz, 1 H), 8.03-8.06 (m, 2 H), 8.44 (dd, *J* = 8.5 Hz, *J* = 1.8 Hz, 1 H), 8.56 (s, 1 H), 8.76 (br s, 1H), 8.85 (d, *J* = 1.6 Hz, 1 H), 8.92 (s, 1H), 9.86 (s, 1 H), 10.51 (s, 1 H), 11.01 (br s, 1H); ^{13}C NMR (100

MHz, DMSO-d_6)) δ 168.8, 165.9, 165.7, 164.2, 157.7 (2C), 154.6, 154.5, 153.6, 151.8, 149.0, 147.2, 143.8, 141.4, 141.3, 139.4, 137.3 (2C), 133.8, 133.3, 133.1 (2C), 131.9, 130.8, 130.4, 129.1(2C), 128.6 (2C), 128.1 (2C), 123.3, 123.1, 121.8, 120.7, 115.7, 113.8, 105.0 (2C), 63.7, 61.5, 61.1, 55.3, 42.9, 29.2 (3C); ESI *m/z* 916.23 (MNa^+ with ^{35}Cl, ^{35}Cl).

2.3.2. Drug treatment

AL622 was designed and synthesized in our laboratory. PP2 was also synthesized in our laboratory following the methods already described in the literature (10) and Iressa® (gefitinib, AstraZeneca) was purchased from the Royal Victoria Hospital pharmacy and extracted from pills in our laboratory. In all assays, drugs were dissolved in DMSO and the concentration of DMSO never exceeded 0.2% (v/v). Subsequently compounds were diluted in sterile media (DMEM or RPMI-1640) containing 10% fetal bovine serum (FBS) prior to addition to cells.

2.3.3. Cell culture

4T1 murine breast cancer cells (generous gift from Dr. Thierry Muanza, Jewish General Hospital, Montreal, Canada) were maintained as a monolayer in RPMI-1640 with 4.5g/L of glucose, 2 mM L-glutamine,10 mM of sodium pyruvate, 10 mM HEPES, 10% FBS and 100 μg/mL penicillin-streptomycin cell culture. The human breast carcinoma MDA-MB-231 cell line was obtained from American Type Culture Collection (ATCC, Manassas, VA). Mouse fibroblast cells NIH 3T3 wild type, NIH3T3-Her14 (transfected with erbB1/EGFR gene) and NIH3T3-Neu (transfected with erbB2/Her2 gene) were

provided by Dr.Moulay Aloui-Jamali (Jewish General Hospital, Montreal, Canada). Cells were maintained in Dulbecco Modified Eagle's Medium (DMEM) supplemented with 10% FBS, 10 mM HEPES, 2 mM L-glutamine and 100 μg/mL penicillin/streptomycin (all reagent purchased from Wisent Inc., St-Bruno, Canada). All cells were grown in a humidified incubator with 5% carbon dioxide at 37°C.

2.3.4. Enzyme Binding Assay

The EGFR, c-Src, Abl and c-Met kinase assays are similar to the one described by Brahimi *et al.* (11). Briefly, the kinase reaction was performed in 96-well plates (Nunc Maxisorp) coated with PGT (poly L-glutamic acid L-tyrosine, 4:1) and incubated at 37ºC for 48 h using 4.5 ng/well EGFR or c-Src (Biomol, PA). PGT served as the substrate to be phosphorylated by EGFR and c-Src in the presence of ATP (50 μM) when stimulated by EGF (100 μg/mL). Following drug addition (range 0.0001-10 μM), phosphorylation of EGFR or c-Src was initiated by supplementing the reaction with ATP. The phosphorylated substrate was detected using an HRP-conjugated anti-phosphotyrosine antibody (Santa Cruz Biotechnology, CA). The signal was developed by the addition of 3, 3', 5, 5'-tetramethylbenzidine peroxidase substrate (Kierkegaard and Perry Laboratories, Gaithersberg, MD) and the colorimetric reaction was monitored at 450 nm using a microplate reader ELx808 (BioTek Instruments). The IC_{50} values were calculated using GraphPad Prism (GraphPad Software, Inc., San Diego, CA).

2.3.5. *In vitro* Growth Inhibition Studies

Growth inhibitory activities were evaluated using the sulforhodamine B (SRB) assay (12). 4T1 and MDA-MB-231 were plated at approximately 5000 cells per well in 96 well plates and cells were allowed to attach for 24 h. Thereafter, cells were exposed to different drug concentrations for five days to determine basal growth inhibition. Subsequently, cells were fixed with 10% ice-cold trichloroacetic acid for 60 min at 4°C, stained with sulforhodamine B (SRB 0.4%) for 4 h at room temperature, rinsed with 1% acetic acid and allowed to dry overnight. The resulting colored residue was dissolved in Tris base (10 mM, pH 10-10.5) and the optical density recorded at 492 nm using a microplate reader ELx808. The results were analyzed using GraphPad Prism (GraphPad Software, Inc., San Diego, CA) and the sigmoidal dose response curve was used to determine IC_{50} values. Each point represents the average of at least three independent experiments run in triplicate.

2.3.6. Wound Healing Assay

Breast cancer cell lines 4T1 and MDA-MB-231 were plated in 6-well plates and incubated overnight (37°C, 5% CO_2). A cross scratch was made in the middle of the cell monolayer. The cells were then washed twice with PBS, and the media was changed to fresh RPMI-1640 or DMEM. Cells were incubated without or in the presence of the drug at 12.5 μM and 25 μM concentrations. The images were captured at time 0 and at regular intervals of 24, 48 and 96 h to monitor cell migration using a Leica DM IL inverted fluorescence microscope (10X).

2.3.7. Matrigel invasion assay

The invasive property of breast cancer cells was determined using the two-compartment Boyden chamber assay (13). Cells were added onto polycarbonate transwell filter (8 μm pore size), which is a Matrigel-coated membrane separating the top and bottom chambers (50 μg/filter). A total of 5 x 10^4 4T1 breast cancer cells resuspended in DMEM starvation medium were added to the upper chamber and the insert was placed in a 24-well plate containing DMEM starvation media either without or with 10% FBS and 20 ng/mL TGF-α as a chemo-attractant. AL622, PP2, gefitinib and equimolar doses of PP2 and gefitinib were added to both the upper and lower chambers and the cells were incubated at 37°C for 4 h. Medium was removed and cells on both side of the filter were fixed with 3.7% paraformaldehyde (Sigma-Aldrich Canada Ltd) for 1 hour, thereafter stained with 0.1% crystal violet solution for 30 min and the cells on the upper surface of the filters were carefully removed with a cotton-tipped applicator and two washes with PBS. Cells that passed across the Matrigel transwell filter toward the lower surface were counted in three randomly selected nonoverlapping fields (4X objective). The average cells counted from three independent experiments were reported and representative images were photographed.

2.3.8. Fluorescence microscopy imaging for intracellular localization of combi-molecule

4T1 breast cancer cells were seeded in 6-well plates (1 x 10^6 cells/well) and grown in RPMI-1640 with 10% FBS for 24 h. Cells were then treated with three different concentrations (15 μM, 25 μM and 50 μM) of AL622 or PP2. Cells were observed by

fluorescence microscopy every hour for the appearance of blue fluorescence (excitation 294 nm, emission 451 nm) resulting from the release of free PP2 after AL622 degradation into its two moieties. Images were recorded at 5 and 24 h after incubation.

2.3.9. Autophosphorylation Assay (Western Blot)

MDA-MB-231 cells (up to 1 x 10^6 cells/well) were plated in 6-well plates and pre-incubated in DMEM with 10% FBS at 37 °C for 24 h. Following overnight starvation, cells were exposed for 2 h to a dose range of each drug and subsequently cells were washed and stimulated with EGF (50 ng/mL) for 15 min at 37 ºC. Cells were washed, detached by scraping in ice-cold PBS and collected by centrifugation for 2 min at 8000 rpm. Pelleted cells were re-suspended in cold lysis buffer [50 mM Tris-HCl pH 7.5; 150 mM NaCl; 1% Nonidet P-40, 1 mM EDTA; 5 mM NaF; 1 mM Na3VO4; protease inhibitor tablet (Roche Biochemicals, Laval, Canada)]. Lysates were kept on ice for 30 min and collected by centrifugation at 10,000 rpm for 20 min at 4 °C. The concentration of protein was determined using the Bio-Rad protein assay kit (Bio-Rad laboratories, Hercules, CA). Equal amounts of proteins were loaded, resolved on 10% SDS-PAGE and thereafter transferred to a polyvinylidene difluoride membrane (Milipore, Bedford, MA). Membranes were blocked with 5% milk in TBST (20 mM Tris-HCl, 137 mM NaCl, 0.1% Tween 20) for 2 h at room temperature followed by incubation with anti-phosphotyrosine antibody (clone 4G10, Upstate; 1:1000) at 4°C overnight. After three 10-min washes with TBST, blots were incubated with secondary HRP-conjugated goat anti-mouse antibody (Jackson ImmunoResearch Laboratories) for 1 hour in TBST solution. The membranes were subsequently incubated with anti-phospho-c-Src, total c-Src antibody (Cell

Signaling Technology) and total EGFR (sc-03, Santa Cruz, CA). Immunoblot bands were visualized using ECL kit and enhanced chemiluminescence system (Amersham Pharmacia Biotech, Buckinghamshire).

2.3.10. Degradation analysis of the combi-molecule AL622 by high-performance liquid chromatography (HPLC)

4T1 breast cancer cells were seeded in 6-well plates (1 x 10^6 cells/well) and grown in RPMI-1640 with 10% FBS for 24 h. Cells were then treated with different concentrations of AL622 or PP2 at 37 ºC for 5h and 24h. The cells were washed with ice-cold PBS to remove extracellular drug. Cells were scraped with 1 mL of methanol and the resulting mixture centrifuged at 10,000 rpm for 6 min. The supernatant was collected and evaporated to dryness. The resulting residue was reconstituted in a smaller of methanol (100 μL). The HPLC analyses were performed with a Cogent C18 series column (150mmx4.6mm) and the elutions achieved with 88% aqueous methanol at a 1 mL/min flow rate. Analyses were performed using a Thermoquest P4000 equipped with a UV2000 detector and a AS300. autosampler

2.4. RESULTS

2.4.1. Chemical synthesis

The synthesis of the molecule AL622 (**7**) proceeded according to Schemes 1, 2 and 3. Following activation with NaH, PP2 (**1**) obtained according to a method described in the literature (10), was treated with an excess of methyl 6-(chlorocarbonyl)nicotinate to give **2**, whose methyl ester was removed in the presence of potassium silanoate base to give acid **3** (Scheme 2.1). Alcohol **6** (AL621) was synthesized as described in Scheme 2.2. Briefly, the anilinoaminoquinazoline **4** (18) was coupled with 4-(chloromethyl) benzoyl chloride in the presence of pyridine and triethylaminnve to give **5,** which was further treated with an excess of (2-methyl)aminoethanol to provide compound **6**. As depicted in Scheme 2.3, coupling of **3** with **6** in the presence of DCC, HOBt and DMAP gave **7** (AL622).

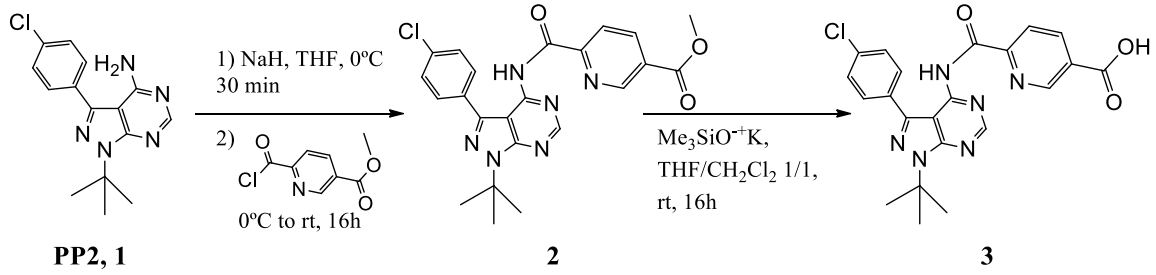

Scheme 2.1. Synthesis pathway of intermediate **3**.

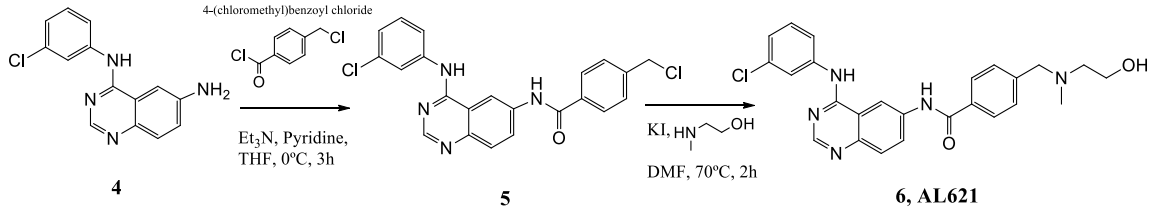

Scheme 2.2. Synthesis pathway of intermediate **6**.

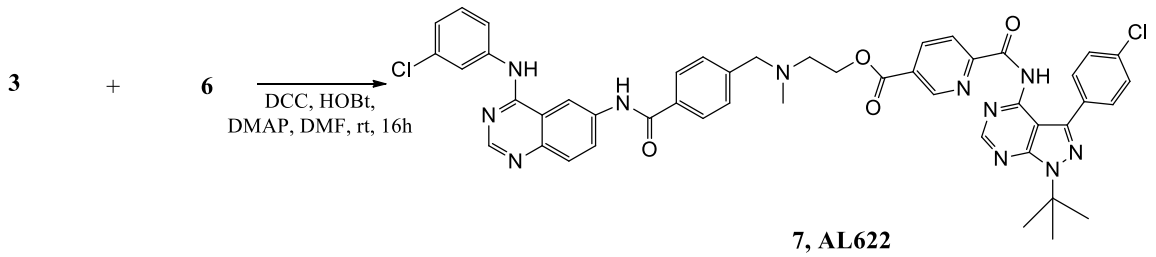

Scheme 2.3. Synthesis pathway of the combi-molecule **AL622**, **7**.

2.4.2. Hydrolysis

The central strategy employed in the design of AL622 was based on the use of a linker capable of releasing both the EGFR and the c-Src inhibitors upon hydrolysis. As depicted in figure 1, AL622 was designed to contain a cleavable p-dicarboxylic acid ester group that links it to the EGFR inhibitory moiety and a hydrolysable amide that carries the PP2 moiety. The synthesis of AL622 will be reported elsewhere.

Analysis of AL622 hydrolysis in 4T1 mouse mammary cells revealed that its two primary metabolites were AL621 and PP2. After a 5 h drug exposure, the release of PP2 from AL622 was analyzed by fluorescence microscopy (Fig. 2.2). PP2 fluoresces in the blue. The results showed that within the first 5 h, blue florescence was detectable inside the cells reaching a significantly high intensity 24 h later. PP2 released from AL622 could be observed in the perinuclear region. In contrast, PP2 administered alone did not show a significant perinuclear distribution.

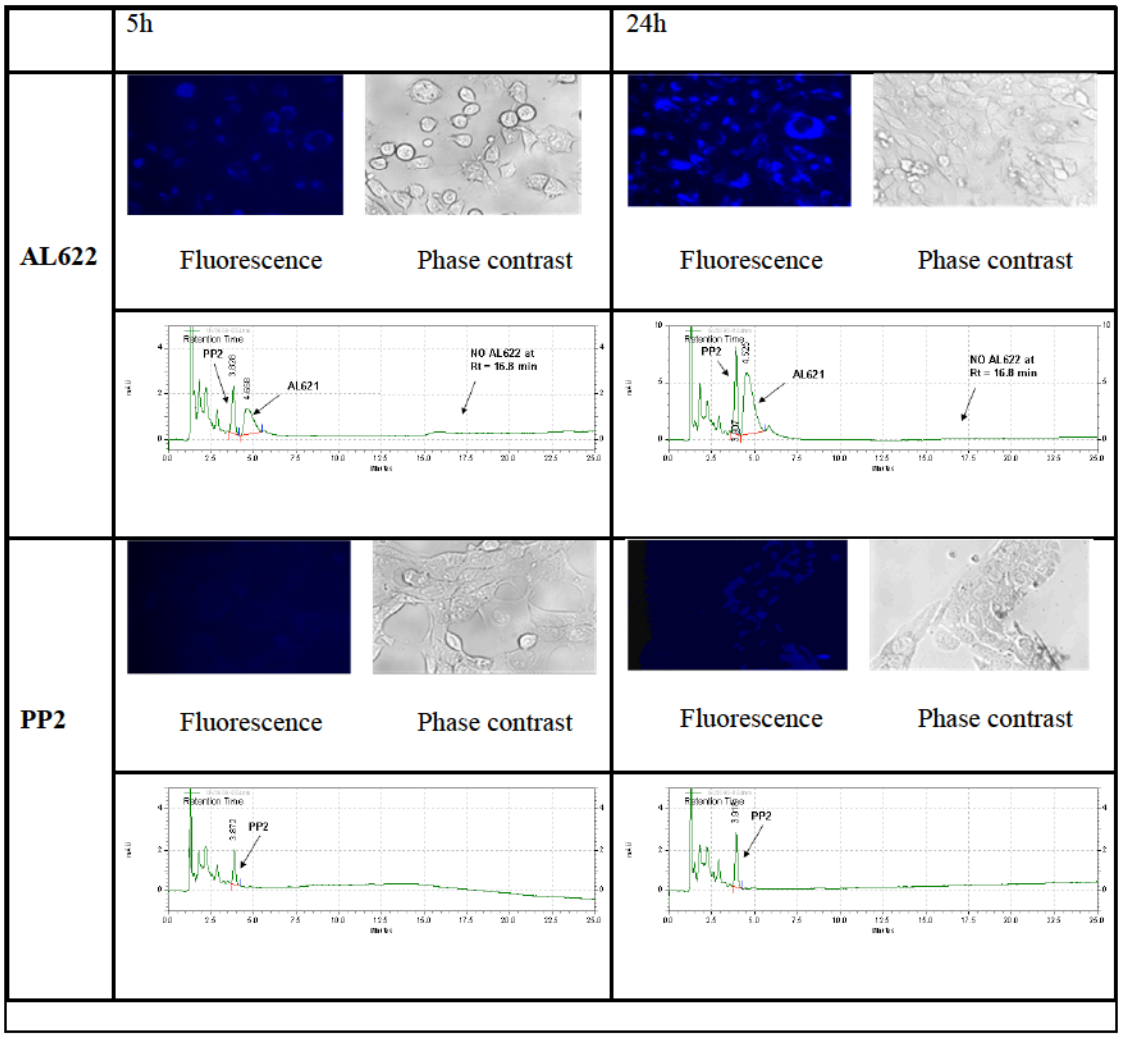

Figure 2.2. Fluorescence microscopy imaging of intracellular localization of combi-molecule. 4T1 breast cancer cells were treated with three different concentrations of AL622 and PP2 for various time periods (5 and 24 h). The intracellular distribution of PP2 was observed by fluorescence microscopy.

2.4.3. EGFR- c-Src inhibitory potency

The ability of AL622 to block EGFR and c-Src tyrosine kinase activity was studied in an ELISA (Fig. 2.3A and B). While gefitinib showed IC_{50} in the nM range (24 nM), despite its bulkiness, AL622 induced a dose dependent inhibition of EGFR TK (IC_{50} of 0.6 µM).

In addition to being a prodrug for the potent c-Src inhibitor PP2 (IC_{50}, 0.188 μM), it was also able to induce c-Src TK inhibition on its own (IC_{50} values of 1.099 μM).

2.4.4. EGFR-c-Src competitive binding at various ATP concentrations and kinase selectivity.

From the EGFR and c-Src inhibition studies to determine the IC50 of AL622, it appeared that it was a *ca*. 2-fold stronger inhibitor of EGFR than c-Src. In order to further ascertain this difference in potency, we performed an activity study with our ELISA using OD that reflects the level of substrate phosphorylation by EGFR and c-Src. Significant lost of inhibitory activity was observed for c-Src at much lower concentrations of ATP (e.g 10 mM ATP) than for EGFR (e.g. 250 mM) (Fig. 2.3C) indicating that AL622 (intact structure) has a much stronger affinity for EGFR than for c-Src. This was further corroborated by comparison with other kinases (e.g. c-Met, Abl). As shown in figure 2.3D, AL622 while retaining strong inhibitory potency against c-Src and Abl, was more selective for EGFR.

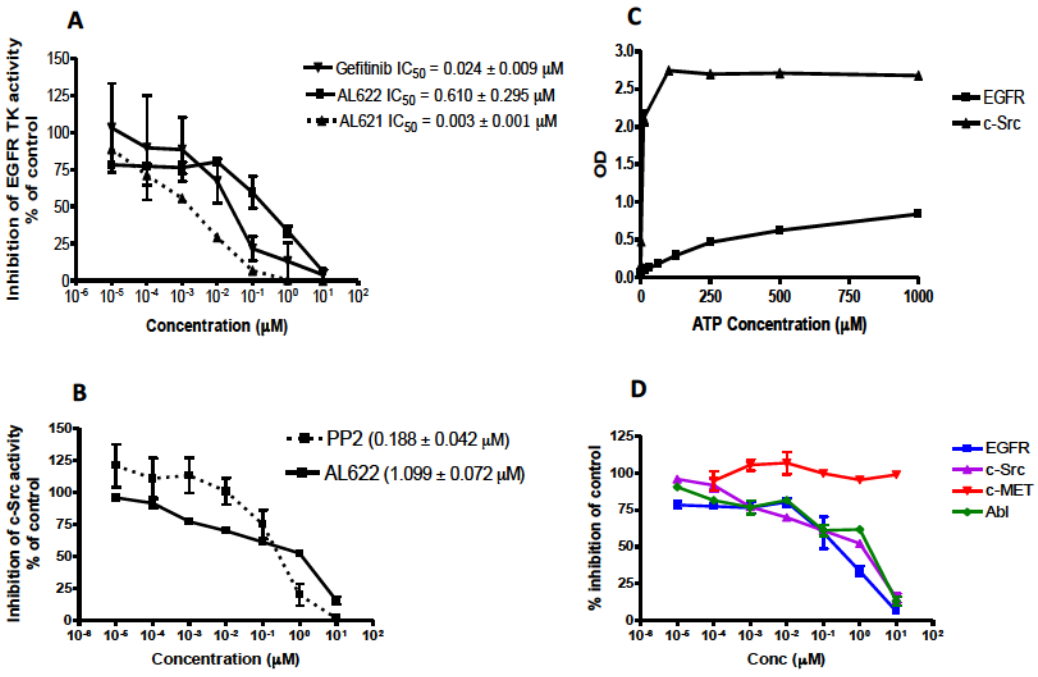

Figure 2.3. Enzyme inhibition assay of AL622 in comparison with gefitinib and PP2. **A**) Inhibition of EGFR and **B**) inhibition of c-Src**.** Ninety-six-well plates were coated with PGT (poly L-glutamic acid L-tyrosine), which served as the substrate to be phosphorylated by EGFR and c-Src in the presence of ATP (50 µM) when stimulated by EGF (100 µg/mL). Dose dependent inhibition by the drugs was observed by adding a chemiluminescent agent and measuring absorbance at 450 nm. **C**) EGFR and c-Src activity at various ATP concentrations and AL622 (1 mM) in an ELISA-based competitive ATP binding assay. Lost of inhibitory activity was observed for c-Src at lower concentrations of ATP than for EGFR. **D**) Inhibition of receptor and non-receptor tyrosine kinases by AL622 in an ELISA-based competitive ATP binding assay.

2.4.5. Whole cell EGFR- c-Src inhibitory potency

The ability of AL622 to block phosphorylation of EGFR and c-Src in whole cells was studied in the MDA-MB-231 cell line, which is known to express the latter two

oncogenes. The results showed that AL622 was capable of inducing strong inhibition of c-Src phosphorylation in MDA-MB-231 at doses ranging from 3.125 to 25 mM, (Fig. 2.4). Analysis of EGFR phosphorylation revealed that AL622 was capable of inducing a dose-dependent inhibition of EGFR TK with almost 100% inhibition of phosphorylation at a concentration as low as 0.1 mM. By contrast, at a 3 time higher concentration (0.3 mM), PP2 induced a moderate level of EGFR phosphorylation. It is worth noting that while the isolated enzyme assays showed noticeable difference between EGFR and c-Src inhibitory activities for intact AL622, in the 3.125-25 mM range at which inhibition of growth, motility and invasion experiments were performed, the two kinases were maximally inhibited (Fig 2.4D).

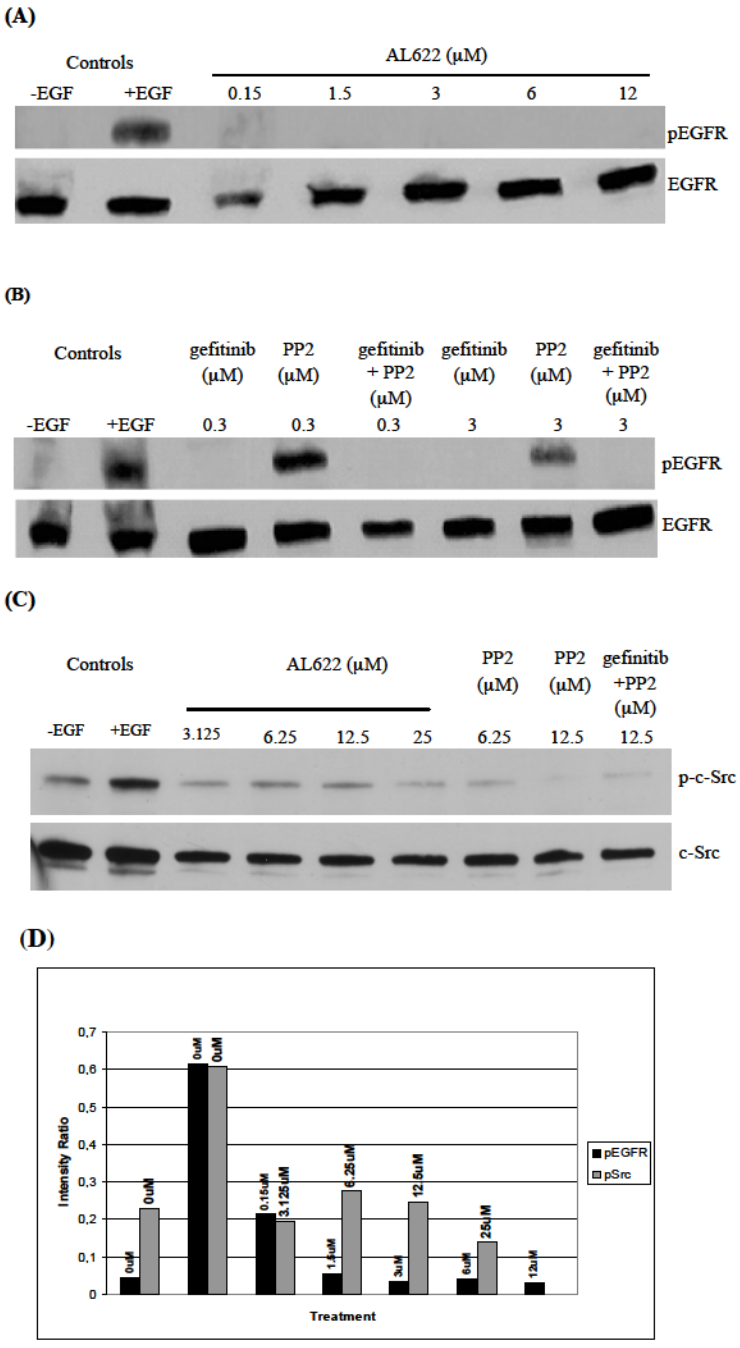

Figure 2.4. Dose-dependent inhibition of EGFR and c-Src phosphorylation in MDA-MB-231 cells upon treatment with AL622 (**A** and **C**), gefitinib, PP2 and gefitinib+PP2 (**B**). Western Blot analysis was performed using serum starved cells. Cells were treated with the drugs for 2 h followed by EGF (50 ng/mL) stimulation for 20 min. In (A) and (B)

phospho-EGFR was determined by probing with pY99 mouse monoclonal primary antibody and an HRP-conjugated goat anti-mouse secondary antibody. In (**C**) Phospho-c-Src levels were determined using the pY416 c-Src (rabbit) primary antibody and the HRP-conjugated goat-anti-rabbit secondary antibody. Total EGFR and c-Src levels were determined using anti-EGFR and c-Src antibodies to check for equal protein loading. (**D**) Levels of phosphorylation of EGFR and c-Src quantitated by band intensity ratio (kinase/loading control) resulting from densitometric analysis of (A) and (C).

2.5.6. Effect of AL622 on cell motility

The ability of AL622 to block cell motility was studied on 4T1 and MDA-MB-231 cells (Fig. 2.5). The results showed that AL622 prevented repopulation of the wound in a dose-dependent manner with levels of inhibition slightly less strong than the combination of gefitinib plus PP2 or PP2 alone. The potency of the AL622 in blocking wound healing was equivalent to that of PP2.

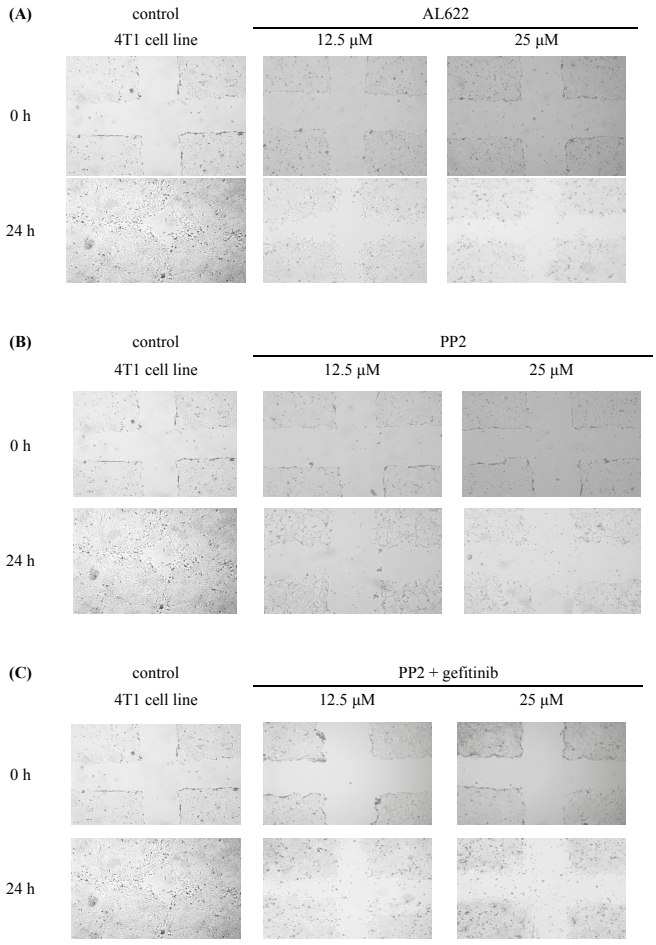

Figure 2.5. Wound healing assay of untreated and treated 4T1 cells. Cells were treated with 12.5 and 25 µM of AL622, PP2 or PP2+gefitinib were observed at 0 h and 24 h after treatment. The control cells showed almost complete wound closure.

2.5.7. Effect of AL622 on cell invasiveness

The ability of AL622 to block cell invasiveness was studied in 4T1 cells which invaded the matrigel in the presence of serum (Fig. 2.6). The results showed that at the lower dose

AL622 induced more significant blockade of invasion than gefitinib (P<0.001), PP2 (P<0.001) and the combination of these two drugs (gefitinib+PP2) (P<0.001).

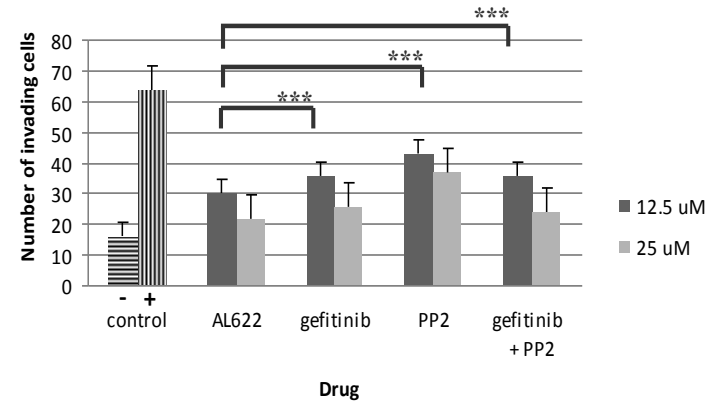

Figure 2.6. Invasive capacity of 4T1 breast cancer cells treated with AL622, gefitinib and PP2. The cells were incubated with the drug at 37 °C for 4 h.

2.5.8. Oncogene-selective growth inhibitory potency

In order to evaluate the targeting contribution of the EGFR warhead of AL622, we evaluated its potency and selectivity on ErbB oncogene transfected cells. Using NIH3T3 cells transfected with ErbB1 (Her14/EGFR) and ErbB2 (Neu) genes, we showed that AL622, gefitinib and PP2 were capable of inducing selective inhibition of the oncogene transfected cells (Fig. 2.7). However, of all the drugs tested and corresponding combinations (e.g. gefitinib+PP2), AL622 was the most selective; with minimal growth inhibitory effect against the normal NIH3T3 wild type cells.

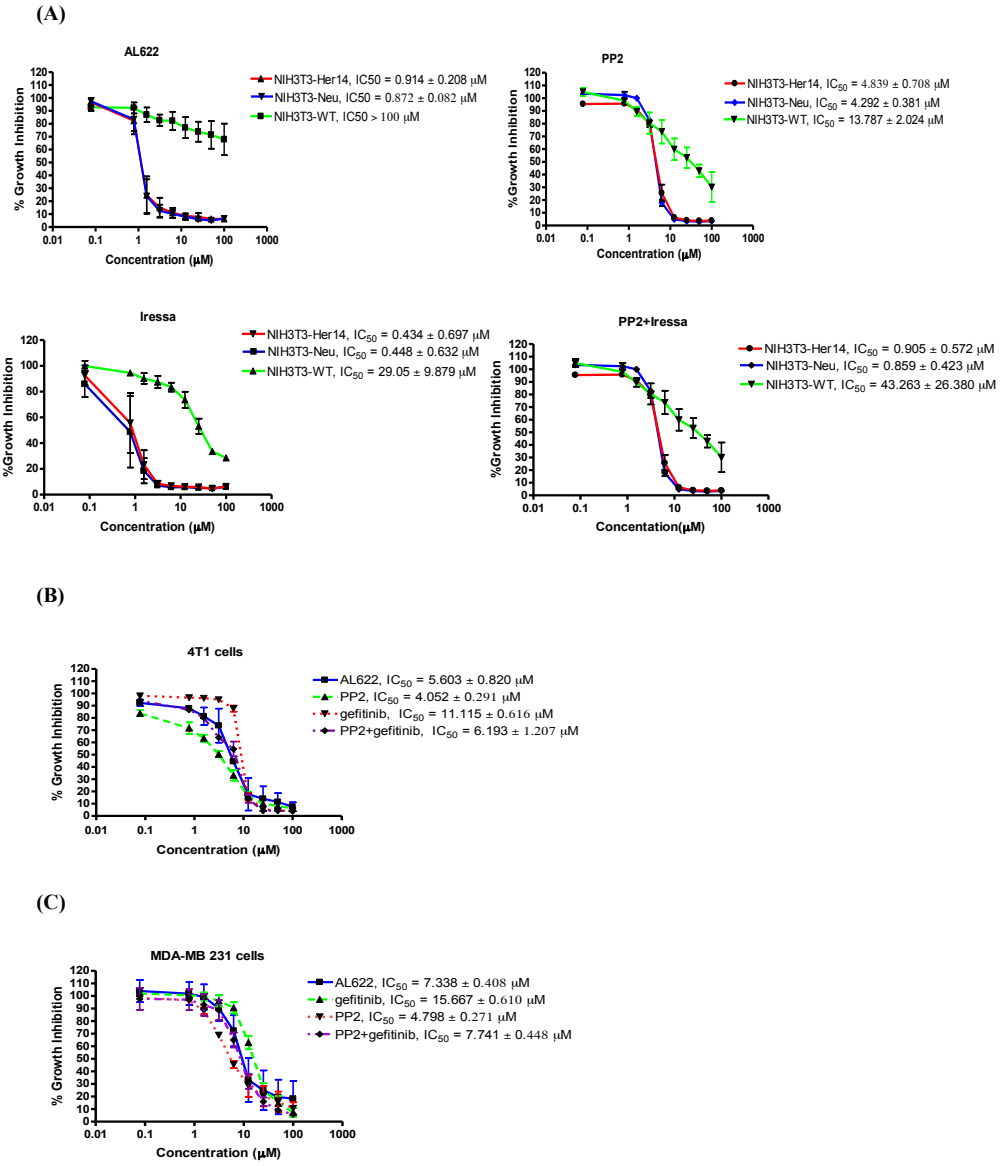

Figure 2.7. Growth inhibition assay of different cell lines treated with AL622, PP2, gefitinib and PP2+ gefitinib. Approximately 5000 cells were allowed to attach for 24 h and exposed to drug treatment for 5 days during. Growth inhibition was determined using the SRB assay. (A) NIH3T3 wild type and transfected, (B) 4T1 cells and (C) MDA-MB-231 cells.

2.6. DISCUSSION

The design of AL622 stemmed from previous work on the combi-targeting concept that sought to prepare multitargeted molecules to interfere with multiple signaling pathways in tumour cells (9, 14). These molecules termed “combi-molecules” are now classified into two major groups: type I and type II (15). Type I combi-molecules are designed to be hydrolyzed in order to generate their binary targeting functions: (e.g. EGFR and DNA), while type II combi-molecules do not require hydrolysis to generate their EGFR-DNA targeting function (16, 17). In our search for potent EGFR TK and c-Src TK cross-targeting compound, we recently designed and synthesized SB163, a type II combi-molecule in which a basic linker was flanked by a quinazoline ring on one hand and an aminopurine analogue of PP2 on the other (Fig. 2.1) [9]. Studies on the latter molecule showed that it could significantly block EGFR, but possessed a weak c-Src inhibitory activity (IC50 = 3 mM). Thus, we re-designed the molecules to release an intact c-Src inhibitor and a quinazoline derivative that retained EGFR inhibitory potency.

The c-Src inhibitory potency of inhibitors of the same class as PP2 is extremely sensitive to structural alteration. Molecular modeling suggested the 9-position of the purine ring to be the best substitution position for retention of optimal c-Src TK activity. When we replaced the tert-butyl group of PP2 by an ethylamino linker as in SB163 (Fig. 2.1), c-Src inhibitory potency decreased by 3-fold when compared with PP2. In this study, we rationalized that a type I combi-molecule strategy (18) would lead to a prodrug capable of releasing upon hydrolysis, intact PP2 and the 6-substituted anilinoquinazoline, which usually retains significant EGFR inhibitory activity. As described herein, this strategy has led to the synthesis of the first prodrug, which in addition to being EGFR and c-Src

inhibitor on its own (EGFR inhibition IC_{50} = 0.610 μM and c-Src inhibition = 1.099 μM) is capable of releasing two different kinase inhibitors: PP2 and AL621. The results suggest that AL622 is clearly a rationally designed drug for "mix-targeting" EGFR and c-Src. Here we used the selective EGFR inhibitor (gefitinib) and the selective c-Src inhibitor PP2 as control drugs to assess the binary cytokinetic profile of AL622. We used the sensitivity of highly invasive breast cancer cells 4T1 and MDA-MB-231 to PP2 and to the highly EGFR-selective inhibitor gefitinib. PP2 was used as a reference to assess the c-Src dependence of the potency of AL622 and gefitinib, as a reference for its EGFR-dependence.

In growth inhibition assays, AL622 was equipotent with PP2 against the 4T1 cells whose growth and invasion strongly depend on c-Src. It was slightly more potent against MDA-MB-231 cells in which c-Src and EGFR are known to synergize to promote growth (19, 20). Importantly, c-Src and EGFR were found to be strongly inhibited at concentrations markedly lower than IC50 for growth inhibition in these cells. In NIH3T3 mouse fibroblast cells transfected with EGFR or HER2 whose growth strongly depends on EGFR or HER2, AL622 was significantly more potent than PP2 but less potent than gefitinib. Interestingly, the dominance of the potency of AL622 over PP2, gefitinib and the corresponding combination PP2+gefitinib was seen only in the invasion assay. Recently, EGFR and c-Src was shown to cooperatively promote aberrant invasive behavior in immortalized breast cells (6). Perhaps, in this case, due to the requirement for both EGFR and c-Src to promote invasion, the dual mechanism of action of AL622 led to a more pronounced effect. The superior potency of AL622 when compared with

equimolar addition of individual drugs (PP2+gefitinib) may be due to a greater level or released bioactive species inside the cells when administered via a prodrug than as a combination of individual drugs. Indeed fluorescence microscopy showed that higher intensity of blue fluorescence associated with PP2 was seen when AL622 was administered than when PP2 was given alone.

The results presented herein indicate that blockade of c-Src in the cells is sufficient to induce a significant levels of growth inhibitory activity and reduction of motility. Tandem blockade of EGFR and c-Src with either AL622 or combination of individual molecules did not enhance these activities, suggesting that c-Src is the dominant oncogene controlling both proliferation and motility in these cells. It is now known that c-Src can phosphorylate EGFR at Y845 and this is associated with mitogenic signaling through a pathway in which only STAT5 has been identified (5, 21). Previous work by Biscardi *et al.* (5) showed that transfection of CH101/2 cells with a Y845F mutant form of EGFR led to ablation of EGF-stimulated DNA synthesis in the latter cells, suggesting that c-Src activation plays an important role in the growth of EGFR-expressing cells. Additional blockade of EGFR by AL622 and the individual drug combination gefitinib+PP2 did not enhance inhibition of motility. The activity of the two types of combinations (AL622 and PP2+gefitinib) was comparable with that of the c-Src inhibitor PP2 alone. This response may also be due to the fact that c-Src is the major player in regulating motility in these cells, a role that is now suspected to be exerted through the PI3K pathway.

One particular and important observation is the markedly selective potency of AL622 in NIH3T3 ErbB transfectants. PP2 that primarily targets c-Src was the least selective of the

panel. Gefitinib also induced a dose dependent growth inhibition in the wild type. The decreased potency of AL622 in these non-transformed cells may be due to decreased intracellular metabolism of AL622 when compared with their transformed counterpart. Further studies are ongoing to prove this point.

The results *in toto* suggest that AL622 is a potent combi-drug that releases an intact c-Src and an EGFR inhibitor inside the cells. Its significant anti-invasive properties warrant further evaluation *in vivo*, in a model wherein c-Src synergizes with EGFR to promote invasion.

2.7. ACKNOWLEDGMENT

We would like to thank the Canadian Institutes of Health Research (CIHR) Team Grant for financial support. Dr. Na Ning thanks the National Science Council of China for financial support. Dr. Anne-Laure Larroque-Lombard thanks the CIHR and the Drug Development Training Program (DDTP) for her post-doctoral fellowship training award. Dr. Ying Huang thanks the MUHC Research Institute for her post-doctoral fellowship training award.

2.8. REFERENCES

1. Summy JM, Gallick GE. Src family kinases in tumor progression and metastasis. Cancer Metastasis Rev. 2003;22(4):337-58.
2. Yeatman TJ. A renaissance for SRC. Nat Rev Cancer. 2004;4(6):470-80.
3. Nautiyal J, Majumder P, Patel BB, Lee FY, Majumdar AP. Src inhibitor dasatinib inhibits growth of breast cancer cells by modulating EGFR signaling. Cancer Lett. 2009;283(2):143-51.

4. Boerner JL, Demory ML, Silva C, Parsons SJ. Phosphorylation of Y845 on the epidermal growth factor receptor mediates binding to the mitochondrial protein cytochrome c oxidase subunit II. Mol Cell Biol. 2004;24(16):7059-71.
5. Biscardi JS, Maa M-C, Tice DA, Cox ME, Leu T-H, Parsons SJ. c-Src-mediated phosphorylation of the epidermal growth factor receptor on Tyr845 and Tyr1101 is associated with modulation of receptor function. Journal of Biological Chemistry. 1999;274(12):8335-43.
6. Dimri M, Naramura M, Duan L, Chen J, Ortega-Cava C, Chen G, et al. Modeling breast cancer-associated c-Src and EGFR overexpression in human MECs: c-Src and EGFR cooperatively promote aberrant three-dimensional acinar structure and invasive behavior. Cancer Res. 2007;67(9):4164-72.
7. Hanke JH, Gardner JP, Dow RL, Changelian PS, Brissette WH, Weringer EJ, et al. Discovery of a novel, potent, and Src family-selective tyrosine kinase inhibitor. Study of Lck- and FynT-dependent T cell activation. J Biol Chem. 1996;271(2):695-701.
8. Barker AJ, Gibson KH, Grundy W, Godfrey AA, Barlow JJ, Healy MP, et al. Studies leading to the identification of ZD1839 (iressa): an orally active, selective epidermal growth factor receptor tyrosine kinase inhibitor targeted to the treatment of cancer. Bioorganic & medicinal chemistry letters. 2001;11(14):1911-4.
9. Barchechath S, Williams C, Saade K, Lauwagie S, Jean-Claude B. Rational design of multitargeted tyrosine kinase inhibitors: a novel approach. Chem Biol Drug Des. 2009;73(4):380-7.
10. Hanefeld U, Rees CW, White AJP, Williams DJ. One-pot synthesis of tetrasubstituted pyrazoles - proof of regiochemistry. Journal of the Chemical Society, Perkin Transactions 1: Organic and Bio-Organic Chemistry. 1996(13):1545-52.
11. Brahimi F, Matheson SL, Dudouit F, McNamee JP, Tari AM, Jean-Claude BJ. Inhibition of epidermal growth factor receptor-mediated signaling by "Combi-Triazene" BJ2000, a new probe for Combi-Targeting postulates. J Pharmacol Exp Ther. 2002;303(1):238-46.
12. Skehan P, Storeng R, Scudiero D, Monks A, McMahon J, Vistica D, et al. New colorimetric cytotoxicity assay for anticancer-drug screening. J Natl Cancer Inst. 1990;82(13):1107-12.
13. Jallal H, Valentino ML, Chen G, Boschelli F, Ali S, Rabbani SA. A Src/Abl kinase inhibitor, SKI-606, blocks breast cancer invasion, growth, and metastasis in vitro and in vivo. Cancer Res. 2007;67(4):1580-8.
14. Banerjee R, Huang Y, McNamee JP, Todorova M, Jean-Claude BJ. The combi-targeting concept: selective targeting of the epidermal growth factor receptor- and Her2-expressing cancer cells by the complex combi-molecule RB24. J Pharmacol Exp Ther. 2010;334(1):9-20.
15. Qiu Q, Domarkas J, Banerjee R, Merayo N, Brahimi F, McNamee JP, et al. The Combi-Targeting Concept: In vitro and In vivo Fragmentation of a Stable Combi-Nitrosourea Engineered to Interact with the Epidermal Growth Factor Receptor while Remaining DNA Reactive. Clin Cancer Res. 2007;13(1):331-40.
16. Rachid Z, Brahimi F, Domarkas J, Jean-Claude BJ. Synthesis of half-mustard combi-molecules with fluorescence properties: correlation with EGFR status. Bioorganic & medicinal chemistry letters. 2005;15(4):1135-8.

17. Rachid Z, Brahimi F, Katsoulas A, Teoh N, Jean-Claude BJ. The Combi-Targeting Concept: Chemical Dissection of the Dual Targeting Properties of a Series of "Combi-Triazenes". J Med Chem. 2003;46(20):4313-21.
18. Qiu Q, Domarkas J, Banerjee R, Katsoulas A, McNamee JP, Jean-Claude BJ. Type II combi-molecules: design and binary targeting properties of the novel triazolinium-containing molecules JDD36 and JDE05. Anti-Cancer Drugs. 2007;18(2):171-7.
19. Biscardi JS, Belsches AP, Parsons SJ. Characterization of human epidermal growth factor receptor and c-Src interactions in human breast tumor cells. Mol Carcinog. 1998;21(4):261-72.
20. Biscardi JS, Ishizawar RC, Silva CM, Parsons SJ. Tyrosine kinase signalling in breast cancer: epidermal growth factor receptor and c-Src interactions in breast cancer. Breast Cancer Res. 2000;2(3):203-10.
21. Silva CM. Role of STATs as downstream signal transducers in Src family kinase-mediated tumorigenesis. Oncogene. 2004;23(48):8017-23.

CONNECTING TEXT

Through the work done in the previous chapter, we demonstrated the first cleavable EGFR-c-Src targeting combi-molecule that underwent hydrolysis to generate its two inhibitory moieties, AL621 targeting EGFR and PP2 targeting c-Src. Although this molecule showed strong EGFR inhibitory potency, it remained a weak c-Src inhibitor, thereby generating an unbalanced combi-molecule. We thus undertook an optimization study that sought to design and develop combi-molecules with strong and balanced EGFR and c-Src inhibitory properties. Moreover, given the labile nature of the pyrazolopyrimidine backbone of PP2, which is highly sensitive to substituent changes, we decided to pursue future design and synthesis using the thiazolylaminopyrimidine scaffold of the dual c-Abl/c-Src kinase inhibitor, dasatinib, currently approved for the treatment of Chronic Myelogenous Leukemia (CML). This chapter highlights the optimization of EGFR-c-Src targeting combi-molecules and describes the mechanism of action and targeting modality of a novel EGFR-c-Src targeting combi-molecule, AL776 *in vitro* and *in vivo.*

CHAPTER 3

TARGET MODULATION BY A KINASE INHIBITOR ENGINEERED TO INDUCE A TANDEM BLOCKADE OF THE EPIDERMAL GROWTH FACTOR RECEPTOR (EGFR) AND C-SRC: THE CONCEPT OF TYPE III COMBI-TARGETING

Suman Rao[1], Anne-Laure Larroque-Lombard[1], Lisa Peyrard[1], Cédric Thauvin[1], Zakaria Rachid,[1] Christopher Williams[2], Bertrand J. Jean-Claude[1]*

[1]Cancer Drug Research Laboratory, Department of Medicine, Division of Medical Oncology, McGill University Health Center/Royal Victoria Hospital, 687 Pine Avenue West Rm. M7.19, Montreal, Quebec, H3A 1A1 Canada

[2]Chemical Computing Group Inc., 1010 Sherbooke St. West, Suite #910, Montreal, QC, H3A 2R7 Canada

3.1. ABSTRACT

Cancer cells are characterized by a complex network of interrelated and compensatory signaling driven by multiple kinases that reduce their sensitivity to targeted therapy. Therefore, strategies directed at inhibiting two or more kinases are required to robustly block the growth of refractory tumour cells. Here we report on a novel strategy to promote sustained inhibition of two oncogenic kinases (Kin-1 and Kin-2) by designing a molecule K1-K2, termed "combi-molecule", to induce a tandem blockade of Kin-1 and Kin-2, as an intact structure and to be further hydrolyzed to two inhibitors K1 and K2 directed at Kin-1 and Kin-2, respectively. We chose to target EGFR (Kin-1) and c-Src (Kin-2), two tyrosine kinases known to synergize to promote tumour growth and progression. Variation of K1-K2 linkers led to AL776, our first optimized EGFR-c-Src targeting prototype. Here we showed that: (a) AL776 blocked EGFR and c-Src as an intact structure using an *in vitro* kinase assay (IC_{50} EGFR = 0.12 μM and IC_{50} c-Src = 3 nM), (b) it could release K1 (AL621, a nanomolar EGFR inhibitor) and K2 (dasatinib, a clinically approved Abl/c-Src inhibitor) by hydrolytic cleavage both *in vitro* and *in vivo,* (c) it could robustly inhibit phosphorylation of EGFR and c-Src (0.25-1 μM) in cells, (d) it induced 2-4 fold stronger growth inhibition than gefitinib or dasatinib and apoptosis at concentrations as low as 1 μM, and, (e) blocked motility and invasion at sub-micromolar doses in the highly invasive 4T1 and MDA-MB-231 cells. Despite its size (MW = 1032), AL776 blocked phosphorylation of EGFR and c-Src in 4T1 tumours *in vivo*. We now termed this new targeting model consisting of designing a kinase inhibitor K1-K2 to target Kin-1 and Kin-2, and to further release two inhibitors K1 and K2 of the latter kinases, "type III combi-targeting".

3.2. INTRODUCTION

Current trend in cancer drug discovery is towards the design of multi-targeted agents (1). This trend is driven by the observation that the attrition rates in the development of multi-targeted agents are significantly lower than that of single-targeted agents (2). Indeed analysis of 974 anticancer agents from 1995 to 2007, in developmental phases (phase I to registration) led to an overall attrition rate of 82%. However, this rate fell to only 52% when the analysis was restricted to a subset of multi-targeted kinase inhibitors (2). The clinical efficacy of multi-targeted agents is partly imputed to their ability to induce a tandem blockade of multiple targets that drive tumour progression and resistance to apoptosis in refractory tumours. However, despite the acknowledged potency of multi-targeted drugs, their rational design to inhibit specific oncogenic targets remains a tremendous challenge (3). In the past, in the context of a novel multi-targeted approach termed "combi-targeting", we designed inhibitors termed "combi-molecules" that can block targets as divergent as tyrosine kinase receptors and genomic DNA. We demonstrated their ability to kill tumour cells by blocking receptor phosphorylation, damaging DNA and down-regulating DNA repair proteins (4, 5). We classified such molecules as type I (i.e., those that require hydrolysis to fully exhibit their dual potency) and type II (i.e., those that could induce DNA damage and a tandem blockade of receptor mediated signaling without requirement for hydrolysis). As depicted in figure 3.1A, the type I molecule I-Tz was designed to release an EGFR tyrosine kinase inhibitor (I) and a DNA damaging species Tz (step 1). I-Tz was also designed to interact with EGFR as an intact structure (step 2) (6-8). Conversely, I-Tz in its type II form is designed to inhibit EGFR tyrosine kinase and damage DNA without requirement for hydrolysis (Fig. 3.1B,

steps 1 and 2) (9, 10). While this classification includes several types of agents directed at the epidermal growth factor receptor (EGFR) and DNA, the demonstration of the approach with two different tyrosine kinase targets remained a challenge (11-13). Here, we designed a rational approach to give rise to a novel type of chimeric kinase inhibitor, that reconciles the type I and II targeting models. As shown in figure 3.1C (step 1), to target a cell expressing kinase 1 (Kin-1) and kinase 2 (Kin-2), we wish to design the molecule K1-K2 to behave like a type I targeted molecule, by conferring it a hydrolysable linker, which upon hydrolysis will release free K1 and K2 (inhibitors of kinases 1 and 2 respectively). In addition, the molecule is designed to possess an intrinsic dual K1/K2 targeting property as an intact molecule, thereby behaving as a type II molecule (Fig. 3.1C, steps 2 and 3). The expected advantage of the latter property lies in the fact that in the event that the hydrolysis of K1-K2 is slow inside the tumour cell, the intact structure can still induce a tandem blockade of the oncogenic targets Kin-1 and Kin-2. Overall, this novel targeting approach, which is now designated as type III combi-targeting, is designed to induce multispecies dynamic inside the cells with the dual tyrosine kinase Kin-1 and Kin-2 inhibition as a constant. Here we challenge this concept using an optimized molecule AL776, which was designed to block a receptor tyrosine kinase, EGFR, as Kin-1, and a non-receptor tyrosine kinase, c-Src, as Kin-2.

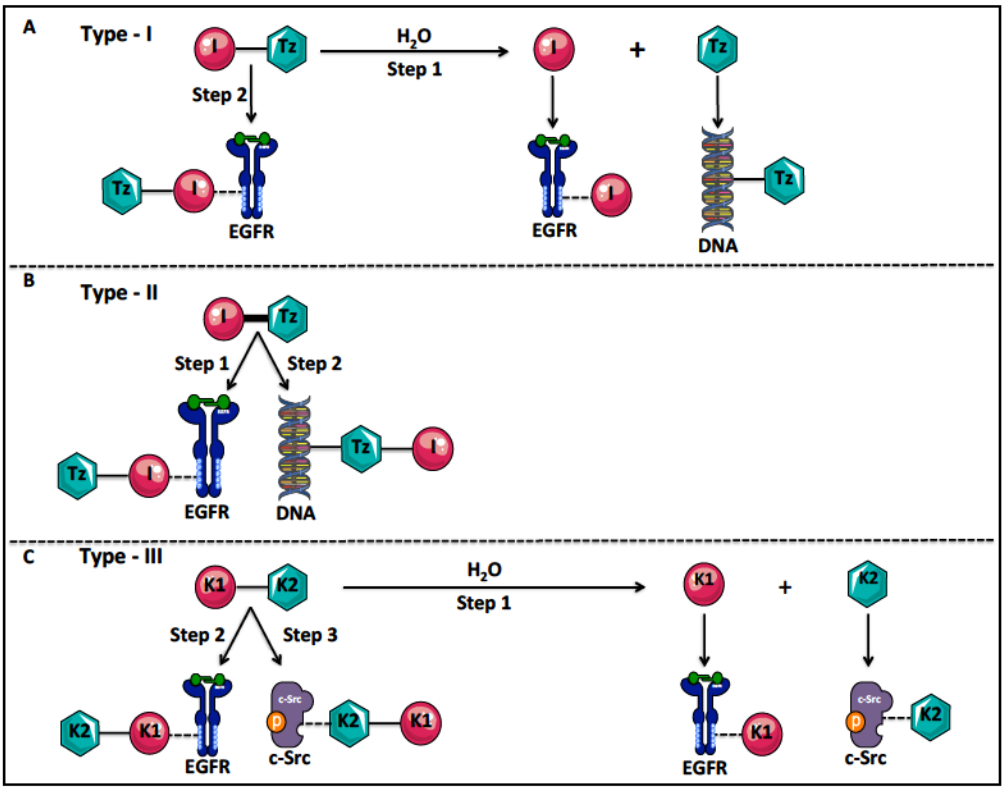

Figure 3.1: Prototypes of type-I, type-II and the novel type-III targeting molecules. (**A**) The type-I molecule (I-Tz) was designed to contain an EGFR tyrosine kinase inhibitor (I) and a DNA alkylating triazene (Tz) moiety bridged by a hydrolysable linker. The type-I molecule can inhibit EGFR as an intact structure (step 2), or upon undergoing hydrolysis to release the two moieties (I + Tz), but the molecule is only capable of targeting DNA through the release of its Tz moiety (step 1). (**B**) The type-II molecule was designed to contain the EGFR tyrosine kinase inhibitor (I) and the DNA alkylating triazene moiety (Tz) connected via a non-hydrolysable linker. This type-II molecule is capable of targeting both EGFR and DNA as an intact structure through each of its targeting arm (steps 1 and 2). (**C**) The novel type-III molecule (K1-K2) is designed to contain two tyrosine kinase inhibitors connected via a hydrolysable linker where K1 is targeted to Kin-1 (EGFR) and K2 to Kin-2 (c-Src). This molecule is "programmed" to

exhibit both type-I and type-II like properties by inhibiting its two targets both as an intact structure (steps 2, 3) as well as upon undergoing hydrolysis to release inhibitors of EGFR and c-Src (step 1).

EGFR (Kin-1) and its family members are often overexpressed in many solid tumours including breast, lung, head and neck, prostate and colon and are associated with aggressive tumour progression and poor prognosis (14, 15). EGFR belongs to the HER family of receptor tyrosine kinases (RTKs) that consists of EGFR (HER1), HER2, HER3 and HER4. Upon ligand binding (e.g. EGF, TGF-α), the receptor undergoes homo/hetero-dimerization with its family members (or other RTKs) and activates several downstream signaling pathways including Ras-Raf-MAPK, PI3K/Akt and the signal transducer and activators of transcription (STAT), that are known to drive tumour growth, proliferation, survival and angiogenesis (16, 17).

c-Src, our secondary target (Kin-2), is another important signaling protein activated downstream of EGFR. It is overexpressed in many solid tumours and is implicated in their growth, progression and metastasis (18). Growth factor receptors other than EGFR including c-Met, PDGFR, IGF-1 receptor and several other membrane proteins including integrins, GPCRs, cytokine receptors are known to activate c-Src (18). It has been demonstrated that tumours overexpressing both EGFR and c-Src have increased EGF-mediated DNA synthesis, soft agar growth, increased phosphorylation of receptor-binding proteins (Shc, PLC-γ) and increased tumourigenesis in nude mice (19). Furthermore, it has also been shown that c-Src is responsible for the phosphorylation of a novel tyrosine residue, Y845 (a non-autophosphorylation site in the activation lip of the

kinase domain) on EGFR, which leads to enhanced EGF-mediated DNA synthesis (20). In addition, previous work by Bao *et al.* (21) demonstrated that c-Src prevents c-Cbl mediated endocytosis and ubiquitination of EGFR, thereby prolonging its signaling at the cell surface. Overall, EGFR and c-Src synergize to promote tumour growth and progression (20, 22), and as a result, these deleterious interactions between the two kinases represent an appropriate multi-signaling context to challenge the new type III combi-targeting model.

Here we describe the synthesis, multispecies dynamics and the mechanism of action of the optimized prototype K1-K2 targeting molecule, AL776. We also report on its ability to modulate the two targets EGFR (Kin-1) and c-Src (Kin-2) *in vivo*.

3.3. MATERIALS AND METHODS

"Animal studies were carried out according to protocol # 4934 approved by the McGill Facility Animal Care Committee (FACC)"

3.3.1. Chemistry

1H NMR spectra were recorded on a Varian 300 or 400 MHz spectrometer. Chemical shifts are given as δ values in parts per million (ppm) and are referenced to the residual solvent proton peak. Mass spectrometry was performed by the McGill University Mass spectroscopy Center and electrospray ionization (ESI) spectra were performed on a Finnigan LC QDUO spectrometer. Data are reported as m/z (intensity relative to base peak = 100). Elemental analyses were carried out by GCL & Chemisar Laboratories (Guelph, Ontario, Canada). All chemicals were purchased from Sigma-Aldrich.

Compound 1

To a solution of dasatinib (200 mg, 0.4 mmol) in dry dimethylformamide (DMF) (10 mL) at room temperature, an excess of succinic anhydride (41 mg, 4 mol, 10 eq.) with a catalytic quantity of dimethylaminopyridine (DMAP) (10 mg, 0.08 mmol, 0.2 eq.) was added. The mixture was subsequently heated at 50°C under argon. The DMF was azeotroped after 18h with heptane to give a white-yellow solid, which was dissolved in acidic water. The acidic aqueous solution was alkalinized to pH 4-5 with dropwise addition of NaOH 4M.The white precipitate that formed was filtered and dried under vacuum to give compound **1** as a pure white powder (218 mg, 90%)^{1}H NMR (400 MHz, *DMSO-d_6*) d ppm 2.22 (s, 3H), 2.38 (s, 3H), 2.42 to 2.48 (m, 4H), 2.57 (t, J = 5.7 Hz, 2H), 3.21 to 3.38 (m, 4H), 3.43 to 3.56 (m, 4H), 4.14 (t, J = 5.7 Hz, 2H), 6.03 (s, 1H), 7.19 to 7.31 (m, 2H), 7.38 (d, J = 5.9 Hz, 1H), 8.20 (s, 1 H), 9.86 (s, 1 H), 11.46 (s, 1 H), 12.23 (bs, 1H).

Compound VII (AL776)

To a solution of **1** (218 mg, 0.37 mmol) and **AL621** (12) (171 mg, 1 eq) in dry DMF (3.6 mL) were added 1-ethyl-3-(3-dimethylaminopropyl) carbodiimide (EDCI) (78 µL, 1.2 eq.), hydroxybenzotriazole (HOBt) (60 mg, 1.2 eq.) and 4-dimethylaminopyridine DMAP (4.5 mg, 0.1 eq.). A precipitate appeared within a few minutes and the resulting brown mixture was further stirred at room temperature for 18h under argon. The DMF was azeotroped with heptane to give a crude solid, which was triturated in water, after which the resulting precipitate was filtered and dried. The resulting solid (440 mg) was purified by silica gel chromatography column (CH_2Cl_2/MeOH 9/1). Further purification by

preparative thin layer chromatography (TLC) (silica plate, CH_2Cl_2/MeOH 9/1, two successive elutions) gave **VII** (AL776) as a pure white powder (136 mg, 36%).

^{1}H NMR (300 MHz, *DMSO-d_6*) d ppm 2.19 (s, 3H), 2.21 (s, 3H), 2.37 (s, 3H), 2.41 to 2.47 (m, 4H), 2.52 to 2.64 (m, 8H), 3.42 to 3.53 (m, 4H), 3.59 (s, 2H), 4.05 to 4.20 (m, 4H), 6.01 (s, 1H), 7.14 (d, J = 9.4 Hz, 1H), 7.19 to 7.31 (m, 2H), 7.34 to 7.53 (m, 4H), 7.77 to 7.89 (m, 2H), 7.94 to 8.11 (m, 4H), 8.20 (s, 1 H), 8.59 (s, 1H), 8.90 (s, 1H), 9.86 (s, 1 H), 9.95 (s, 1H), 10.59 (s, 1 H), 10.58 (s, 1H), ESI *m/z* 1031.29 (MNa^+ with ^{35}Cl, ^{35}Cl). Anal. ($C_{51}H_{52}Cl_2N_{12}O_6S$) C, H, N.

3.3.2. Cell culture

The cell lines used in the *in vitro* studies of AL776 included the mouse fibroblast NIH3T3 panel consisting of wild type (NIH3T3-WT) and cells transfected with EGFR (NIH3T3-Her14), the mouse mammary tumour cell line 4T1 as well as the triple negative human breast cancer cell line MDA-MB-231. The NIH3T3 wild type and Her14 (EGFR transfected) cells were a generous gift from Dr. Moulay Alaoui-Jamali (Lady Davis Institute for Medical Research Sir Mortimer B. Davis, Jewish General Hospital, Montreal, Canada). MDA-MB-231 human breast cancer cell line was purchased from American Type Culture Collection (ATCC, Manassas, VA, USA). 4T1 cells were a generous gift from Dr. Thierry Muanza (Department of Oncology, Division of Radiation Oncology, Jewish General Hospital, Montreal, Canada), originally isolated by Dr. Fred Miller (Karmanos Cancer Institute, MI, USA) (23). All cell lines were maintained in Dulbecco Modified Eagle's Medium (DMEM) supplemented with 10% FBS, 10 mM HEPES, 2 mM L-glutamine, gentamycin sulfate and fungizone (all reagents purchased

from Wisent Inc., St-Bruno, Canada) and were grown in a humidified incubator with 5% carbon dioxide at 37°C.

3.3.3. Drug Treatment

The K1-K2 molecules including AL776 were synthesized in our laboratory. Iressa (gefitinib, AstraZeneca) and dasatinib (Sprycel) were purchased from the Royal Victoria Hospital pharmacy (Montreal, Canada) and extracted from pills in our laboratory. All drugs were dissolved in DMSO to obtain a concentration of 10 mM (or lower). Drug dilutions were carried out under sterile conditions using DMEM (10% FBS or serum-free) medium and the final concentration of DMSO never exceeded 1 % (v/v).

3.3.4. Kinetic analysis of AL776 *in vitro* and *in vivo*

3.3.4.A. Absorption kinetics analysis in NIH3T3-Her14 (EGFR) cells

NIH3T3-Her14 cells were seeded in 6-well plates (1 x 10^6 cells/well) and grown in DMEM with 10% FBS for 24 h. Cells were then treated with 25 µM of AL776 and incubated at 37ºC for 1h, 2h, 6h, 24h or 48h. The media was collected and extracted using twice the volume of methanol, on ice and centrifuged for 20 min at 13,000 rpm at 4°C. The resulting supernatant was filtered, evaporated to dryness and reconstituted with 100 µL of methanol. Cells were collected using trypsin and the cell pellet obtained was rinsed once with PBS and lysed with methanol (500 µL /tube) on ice for 1h. The lysate was centrifuged at 13,000 rpm for 20 min at 4°C and the resulting supernatant was collected into a separate tube and the remaining pellet was subjected to lysis two more times (250 µL /tube). The supernatant from each lysis step were pooled all together,

filtered, evaporated to dryness and resuspended in 100 μL of methanol before further analyzing the samples. HPLC analysis was performed using a ACE 5 C18 5 μm column (150 mmx4.6 mm) under elution conditions of gradient 70-75% methanol:water for the first 5 min and isocratic methanol elution until 30 min, using a 0.75 mL/min flow rate. Analyses were performed using a Thermoquest P4000 equipped with a UV2000 detector and an AS300 Autosampler.

3.3.4.B. Liquid chromatography-mass spectrometry (LC-MS) analysis of the hydrolysis of AL776 *in vivo*

CD-1 mice were divided into groups of three and treated with 80 mg/kg of AL776, injected intraperitoneally (i.p) or intravenously (i.v). Mice were sacrificed and their plasma was collected for further analysis after 0, 5, 15 and 30 min after drug treatment. Plasma samples were extracted using twice the volume of methanol and lysed at 13,000 rpm for 30 min at 4°C. The resulting supernatant from each sample was collected, filtered and evaporated to dryness before reconstituting in 100 μL of methanol. LC-MS analyses were performed on a Synapt G2-S instrument coupled with an Acquity UPLC Class I system both from Waters. Elution rate was set at 500 μL/min using an Eclipse XDB C8, 3.5 um, 2.1 x 100 mm chromatographic column from Agilent Technologies. The experiments were performed with the following eluents: 0.1% aqueous formic acid (eluent A) and methanol (eluent B). The initial mobile phase was 30% B, which was maintained for 0.2 min at the beginning of the run. The following gradient elution was subsequently applied: 30 to 50% B from 0.2 to 4 min; 50 to 80% B from 4 to 10 min; held at 80% B from 10 to 11 min. Thereafter, eluent B was decreased to 30% in 0.2 min

and held constant for up to 15 min to allow the column to equilibrate. Each sample was diluted with methanol in order to avoid detector saturation and 3 mL aliquots of the resulting solutions were injected. Analyses were performed with the electrospray interface in positive ion mode and mass spectra acquired from m/z 100 to 1200. For accurate mass determination, Leucine Enkephalin was used as lock mass. The MassLynx software was used for instrument control, data acquisition and data processing.

3.3.5. *In vitro* kinase assay

The EGFR and c-Src kinase assays were performed in 96-well plates (NuncMaxisorp) coated with PGT (poly L-glutamic acid L-tyrosine, 4:1, Sigma Aldrich, MO, USA) and incubated at 37ºC for 48h prior to using. PGT served as the substrate to be phosphorylated by EGFR (Enzo Life Sciences Inc, NY, USA, Signal Chem, Richmond, Canada) and c-Src (Enzo Life Sciences Inc, NY, USA, Signal Chem, Richmond, Canada) in the presence of ATP (50 μM). A dose range of drugs (**I-VII**, gefitinib or dasatinib) was added to compete with ATP to bind and inhibit the ATP-binding site in the kinase domain of EGFR or c-Src. To each well, 15 ng of EGFR (20 μg/ml) or 6 ng of c-Src (0.1 μg/μl) were added. The phosphorylated substrate was detected using an HRP-conjugated anti-phosphotyrosine antibody (Santa Cruz Biotechnology, CA). The signal was developed by the addition of 3, 3', 5, 5'-tetramethylbenzidine peroxidase substrate (Kierkegaard and Perry Laboratories, Gaithersburg, MD) and the colorimetric reaction was monitored at 450 nm using a microplate reader ELx808 (BioTek Instruments). The IC_{50} values were calculated using GraphPad Prism 6.0 (GraphPadSoftware, Inc., San Diego, CA). Each experiment was carried out at least three times, in duplicate.

3.3.6. Molecular Modeling

AL776 was modeled in the EGFR kinase pocket using the Protein Data Bank (PDB) structure (24) with code 1M17 downloaded from www.rcsb.org. The quinazoline portion of bound erlotinib in 1M17 was used as a template to construct and minimize a bound pose of AL776. Minimizations were carried out in the MOE 2013.08 (25) software using the Amber10:EHT forcefield with R-Field electrostatics. AL776 was also modeled in the c-Src kinase pocket using the PDB structure 3G5D (26). AL776 was constructed and minimized in 3G5D staring with the bound dasatinib ligand as the template. The modeling was carried out in the MOE 2013.08 software using the Amber10:EHT forcefield and R-Field electrostatics for minimizations.

3.3.7. Growth inhibition assay

Growth inhibition was measured in cells using the sulforhodamine B (SRB) assay (27). NIH3T3 (wildtype and EGFR transfected), MDA-MB-231 and 4T1 cell lines were grown in 10% FBS containing media (DMEM) were plated (2000-5000 cells/well) in 96-well plates and allowed to attach overnight (37°C, 5% CO_2). Twenty-four hours later, they were treated with a dose range of drugs (**I-VII**, gefitinib and dasatinib) or media (for control) and allowed to grow in the incubator for the next 120h (5 days) at 37°C. At the end of this 5-day treatment period, they were fixed in 50% trichloroacetic acid (TCA) for 2-3h at 4°C, washed four times under cold tap water and stained with sulforhodamine B (0.4%) overnight at room temperature. The plates were subsequently rinsed with 1% acetic acid, and allowed to dry overnight. The stained cells were then dissolved using 10 mM Tris-Base and the plates were read using a microplate reader ELx808 at 492 nm. The

results were analyzed using GraphPad Prism 6.0 (GraphPadSoftware, Inc., San Diego, CA) and the sigmoidal dose response curve was used to determine IC_{50} values. Each experiment was carried out at least four times, in triplicate.

3.3.8. Wound-healing assay

MDA-MB-231 and 4T1 cells were plated in 6-well plates (500,000 cells/well) and allowed to attach overnight (37°C, 5% CO_2). The following day, media was removed and a cross scratch was made in the middle of the cell monolayer. Cells were washed twice with PBS, and treated with 100 nM of drugs (AL776, dasatinib, gefitinib) or just media (control) for a period of 24 hours. The scratch was visualized at two different time points (0 and 24h) using the Leica DM IL inverted microscope (10X) and images were obtained using the Leica DFC300FX camera.

3.3.9. Boyden chamber invasion assay

The invasive property of MDA-MB-231 and 4T1 cells was determined using the Boyden-chamber invasion assay. Cells suspended in serum-free media were plated (120-150,000 cells/well) onto polycarbonate transwell inserts (8 μm pore size, BD Biosciences) coated with matrigel (6%) (BD Biosciences), separating the top and bottom chambers (50 μl/filter). The cells were allowed to attach for a few hours and subsequently, serum-free media with or without drugs (AL776, dasatinib, gefitinib) was added to the top chambers of the inserts, whereas 10% FBS containing complete media with or without drugs was added to the bottom chambers creating a chemo-attractive gradient. The invasive property of cells was observed 24h after treatment by fixing cells in formalin and staining with

0.1% crystal violet (Sigma-Aldrich Canada Ltd). Cells attached on the upper surface of the insert (top chamber) were removed by gently scraping away with a cotton swab, whereas those that invaded onto the lower side of the insert were observed using a microscope (Leica DM IL inverted microscope, 10X). Images of five non-overlapping fields of invading cells were captured using the Leica DFC300FX camera and quantification was done using the Scion Image Analysis (3.53.0.0) software and ImageJ 1.46r software. The results were expressed in terms of percentage of invading cells relative to control and the bar graphs represent the average of three independent experiments.

3.3.10. Western blot

NIH3T3-Her14 and 4T1 cells grown in 10% FBS containing media were plated (~ 1 x 10^6 cells/well) in 6-well plates and allowed to attach overnight (37°C, 5% CO_2). The cells were rinsed twice with PBS twenty-four hours later and starved overnight on addition of serum-free media. Thereafter, they were treated with different doses of AL776 for 2 hours, washed with PBS (twice) and stimulated with 50 ng/ml EGF for 30 min at 37ºC. Cells were washed, detached by scraping in ice-cold PBS and collected by centrifugation for 15 min at 3000 rpm. Cell pellets were re-suspended in cold lysis buffer 50 mM Tris-HCl pH 7.5; 150 mM NaCl; 1% Nonidet P-40, 1 mM EDTA; 5 mM NaF; 1 mM Na_3VO_4; protease inhibitor tablet (Roche Biochemicals, Laval, Canada)]. Lysates were kept on ice for 1 h and collected by centrifugation at 13,000 rpm for 20 min at 4°C. The concentration of protein was determined using the Bio-Rad protein assay kit (Bio-Rad laboratories, Hercules, CA). Equal amounts of proteins were loaded, resolved on 10%

SDS-PAGE and thereafter transferred to a polyvinylidenedifluoride (PVDF) membrane (Milipore, Bedford, MA). Membranes were blocked with 5% milk in TBST (20 mM Tris-HCl, 137 mM NaCl, 0.1% Tween 20) overnight at 4°C followed by incubation with phosphotyrosine antibodies such as phospho-EGFR Y1068 (Cell Signaling Technology, USA, 1:4000) and phospho-Src Y416 (Cell Signaling Technology, USA, 1:1000) in 5% milk, at 4°C overnight. The membranes were washed with TBST and incubated with respective secondary antibodies for 1h at room temperature in 5% blocking solution. After incubation with antibodies against phosphotyrosines, the membranes were stripped using the Restore Stripping buffer (Thermo Scientific, Rockford, IL, United States) and probed for total EGFR (Santa Cruz, CA, USA) and total Src (Cell Signaling Technology, USA) antibodies along with GAPDH or beta-actin (Santa Cruz, CA, USA) antibodies. Immunoblot bands were visualized using ECL kit and enhanced chemiluminescence system (GE Healthcare).

3.3.11. Characterization of apoptosis using flow cytometry

NIH3T3 cell lines (wild type and EGFR transfected) were plated in 6-well plates (500,000 cells/well) and allowed to grow overnight (37°C, 5% CO_2). The next day, fresh media with or without different doses of drugs (AL776, dasatinib, gefitinib) were added to the cells and incubated for a period of 48 hours. They were subsequently collected using trypsin (Wisent Inc., St-Bruno, Canada), centrifuged (2000 rpm, 5 min), rinsed with PBS and centrifuged again to obtain a cell pellet. The pellet was re-suspended in binding buffer (1X) and prior to being analyzed, annexin V-FITC and PI stains (eBioscience, San Diego, CA, USA) were added to the cells and incubated for 15 min in the dark at 4°C.

Annexin V–FITC and PI binding were analyzed with a Becton Dickinson FACScan. Data were collected using logarithmic amplification of both the FL1 (FITC) and FL2 (PI) channels. Quadrant analysis of coordinate dot plots was done with CellQuestPro software. The experiment was carried out three times.

3.3.12. *In vivo* efficacy and pharmacodynamics

In vivo efficacy and pharmacodynamic studies were carried out in female Balb/c mice (Charles River Laboratories, USA) strictly in accordance with the protocol (#4934) approved by the Facility Animal Care Committee (FACC), McGill University. Mice were implanted with 4T1 mammary tumour cells, 15 million cells/flank (suspended in 200 μL PBS), subcutaneously. For the efficacy study, once the tumours reached an average size of 80 mm^3, the mice were randomized into groups of 6 (n = 6) and treated (intravenously, i.v, once/day) with vehicle (20% + cremophor + 20% ethanol + 60% saline) or 40 mg/kg of AL776. Tumour growth was monitored for the next two weeks by measuring tumour volumes using the formula [4/3*3.14*L/2*(W/2)^2] alternate days, along with the body weight.

For the pharmacodynamic study, female Balb/c mice bearing 4T1 tumours were divided into groups of four and treated with vehicle (20% cremophor + 20% ethanol + 60% saline), AL776 (40 mg/kg) or combination of gefitinib + dasatinib (20mg/kg each). Mice were sacrificed 1h or 24h after treatment and their tumours were collected and snap frozen at -80°C for further analysis using western blots. Tumours were crushed using a mortar/pestle chilled using liquid nitrogen and lysed with RIPA buffer diluted to a 1X concentration and supplemented with 1mM PMSF (Cell Signaling Technology, USA).

Western blot analysis was carried out with the tumour samples, similar to the method described earlier.

3.3.13. Statistical Significance

Statistical significance for *in vitro* assays was carried out using the unpaired, two-tailed student t-test with $p < 0.05$ indicating significance. For the *in vivo* pharmacodynamic experiments, statistical significance was determined using multiple t-test (Holm-Sidak method, with alpha = 5.0%). Each row was analyzed individually, without assuming a consistent SD. P value < 0.05 was considered statistically significant. GraphPad Prism 6.0 (GraphPadSoftware, Inc., San Diego, CA) was used for statistical analysis.

3.4. RESULTS

3.4.1. Design and kinase inhibition by K1-K2 molecular prototypes

A series of K1-K2 molecules designed and synthesized in our laboratory is presented in figure 3.2A. The quinazoline backbone being highly tolerant of bulky substituents at the 6-position (28), was chosen as the EGFR targeting scaffold. This scaffold is common to many clinical inhibitors of EGFR including gefitinib, erlotinib, lapatinib and afatinib and is known to anchor into the ATP binding site of the receptor (29). In the past, we found the pyrazolo pyrimidine class of inhibitors of c-Src to be extremely sensitive to substituent changes (11). Therefore, we selected the thiazolylaminopyrimidine backbone of dasatinib, a clinically approved and potent inhibitor of Abl and c-Src, as the c-Src targeting scaffold (30). To facilitate intracellular hydrolysis, we selected ester- or carbonate-based linkers between K1 and K2. This led to the structures shown in figure

3.2A, with IC_{50} values for EGFR and c-Src inhibition measured by an *in vitro* kinase assay. Of all the linkers studied, the succinic acid one led to the most potent dual EGFR-c-Src targeting molecule. The latter, AL776 showed an IC_{50} of 0.12 µM for EGFR kinase inhibition and 3 nM for c-Src kinase inhibition (Fig. 3.2B). Therefore, AL776 was selected as our K1-K2 prototype in the study.

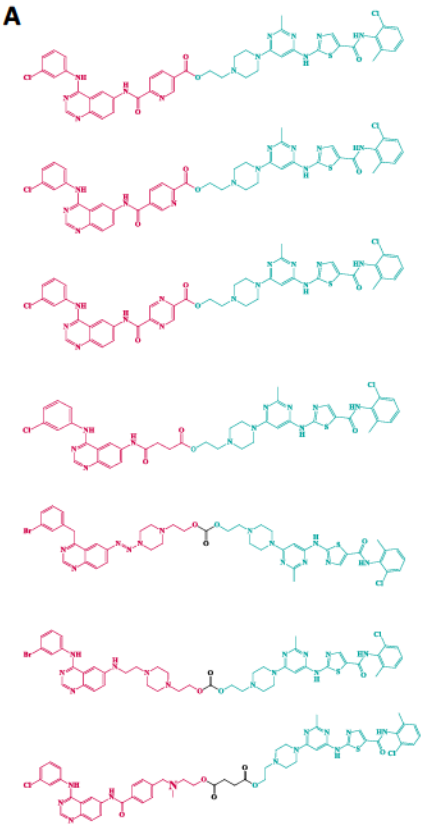

B

	EGFR	c-Src
I	4.3 ± 0.4 µM	0.2 ± 0.01 µM
II	26.6 ± 15.4 µM	0.07 ± 0.01 µM
III	0.6 ± 0.2 µM	< 0.1 nM
IV	0.4 ± 0.1 µM	0.008 ± 0.003 µM
V	0.9 ± 0.2 µM	0.03 ± 0.003 µM
VI	1.1 ± 0.3 µM	0.04 ± 0.01 µM
VII (AL776)	0.12 ± 0.1 µM	0.003 ± 0.002 µM
Gefitinib	0.02 ± 0.007 µM	> 1 µM
Dasatinib	> 1 µM	< 0.001 µM

Figure 3.2: **Series of EGFR-c-Src targeting type III molecules and their kinase inhibitory potency *in vitro*.** (**A**) EGFR-c-Src targeting type III molecules were designed and synthesized in our laboratory using quinazoline moieties (red) as the EGFR targeting head and dasatinib as the c-Src inhibitory arm (green), connected through different hydrolysable linkers. (**B**) *In vitro* kinase assay was used to determine the potency of each molecule in the series to competitively bind and inhibit the ATP binding pocket of the

tyrosine kinase domains of EGFR and c-Src. Gefitinib and dasatinib were used as control drugs for comparison, and the IC_{50} values of kinase inhibition were determined using the GraphPad Prism 6.0 software. Each value represents the average IC_{50} from three independent experiments, carried out in duplicate.

3.4.2. Synthesis of AL776

The synthesis of AL776 proceeded according to figure 3.3. Dasatinib was treated with an excess of succinic anhydride to give compound **1**, which was coupled with AL621 (a potent EGFR tyrosine kinase inhibitor with IC_{50} = 3 nM (12)) in the presence of EDCI, HOBt and DMAP to give **VII** (AL776) as an analytically pure white powder following purification by preparative TLC. We predicted that the hydrolysis of AL776 would restore its primary synthetic elements (i.e. AL621 as K1 and dasatinib as K2).

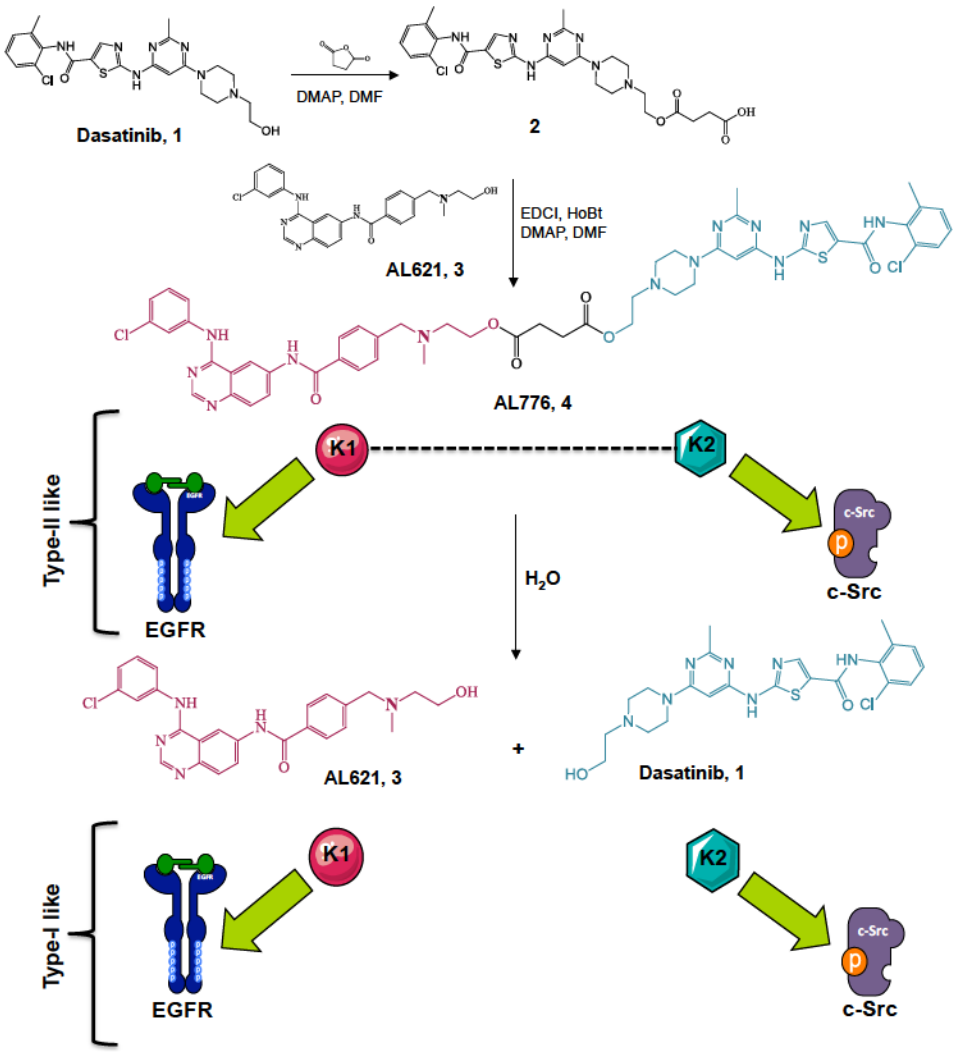

Figure 3.3: Synthesis and hydrolysis of AL776, the lead K1-K2 prototype targeting EGFR and c-Src. The synthesis of AL776 was carried out in our laboratory according to the steps indicated above. The resulting type III K1-K2 molecule is designed to undergo hydrolysis inside the cells and release a potent EGFR tyrosine kinase inhibitor (K1) termed AL621 and a potent c-Src tyrosine kinase inhibitor (K2) dasatinib (type I). AL776 is also capable of exerting its dual inhibitory property by directly interacting with each target as an intact molecule (type II).

3.4.3. Kinetics of hydrolysis of AL776 *in vitro* and *in vivo*

The kinetics of hydrolysis of AL776 was studied both *in vitro* using NIH3T3-Her14 (EGFR transfected) cells and *in vivo* in CD-1 mice following i.p. and i.v. injection. *In vitro*, high performance liquid chromatography (HPLC) analysis of the extracellular medium and isolated whole cells revealed that AL776 was stable enough to slowly diffuse into the cells with minimal extracellular decomposition. As shown in figure 3.4A, 24-48h later, AL776 was detectable inside the cells but not in the extracellular medium, indicating that the absorption equilibrium was shifted towards intracellular retention of the molecule. AL776 slowly degraded inside the cells and liquid chromatography-mass spectrometry (LC-MS) analysis confirmed that the two released metabolites were AL621 and dasatinib (Fig. 3.4B). The observation of detectable levels of AL776 as long as 48h after treatment indicates that, as predicted, in addition to the individual metabolites K1 and K2 released inside the cells, intact K1-K2 may also contribute to their response to drug treatment. A representative spectrum is shown in figure 3.4B with m/z corresponding to the major metabolites along with intact AL776.

Having studied the hydrolysis of AL776 *in vitro*, we sought to determine whether its degradation profile *in vivo* would parallel that *in vitro*. Mice were injected i.v. and i.p. with 80 mg/kg of AL776 and plasma collected at early time points. The results showed following i.p. injection, only the major metabolites were detected with no intact AL776 found in plasma. Therefore, the study was focused on i.v. injection where intact AL776 could be tracked at the earlier time points. Following i.v. injection, AL776 rapidly disappeared from the plasma with barely detectable levels as early as 30 min post-administration. However, after 30 min (see Fig. 3.4C), abundant levels of its two major

metabolites (AL621 and dasatinib) were detected (Fig. 3.4C). Furthermore, LC-MS analysis showed that AL776 was not only cleaved to release AL621 (K1) + dasatinib (K2) but also generated metabolites carrying a succinic acid moiety, which we refer to as AL621-L (K1-L) and dasatinib-L (K2-L). Thus, as predicted, the major products of hydrolysis of AL776 were AL621 and dasatinib, which could be detected both *in vitro* and *in vivo*. In addition, since the levels of acidic metabolites AL621-L and dasatinib-L decreased rapidly, we believe that they were either eliminated or eventually converted to AL621 and dasatinib as proposed in figure 3.5.

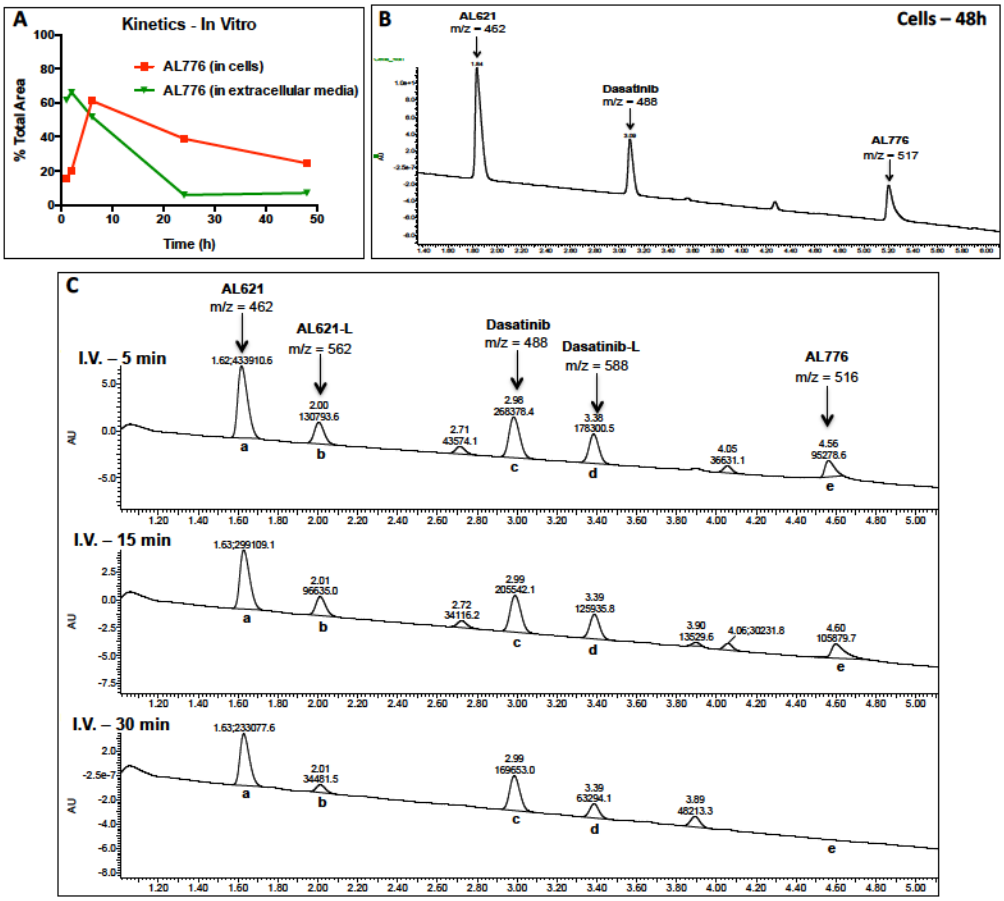

Figure 3.4: *In vitro* and *in vivo* hydrolysis of AL776 using high performance liquid chromatography (HPLC) and mass spectrometry (MS) analyses. (**A**) The kinetics of entry into the cells and degradation of AL776 inside the cells were monitored using

HPLC analysis. NIH3T3-Her14 (EGFR transfected) cells were treated with 25 μM of AL776 for 1h, 2h, 6h, 24h and 48h, after which the cells and the corresponding extracellular media were collected and processed according to the procedure described in the Materials and Method section. The area under the curve (AUC) for the AL776 peak was determined and its percentage compared with all the other peaks was calculated and plotted. (**B**) A representative spectrum obtained from liquid chromatography (LC)-mass spectrometry (MS) analysis in cells treated with AL776 for 48h is shown with m/z = 462 (AL621), m/z = 488 (dasatinib) and m/2z = 517 (AL776). (**C**) The kinetics of AL776 hydrolysis in the plasma of CD-1 mice injected with 80 mg/kg of the drug was monitored 5, 15 and 30 min post-administration. LC-MS chromatograms at different time points with m/z values for intact AL776 and its metabolites are shown: m/z = 462 for AL621, m/z = 562 for AL621-L (succinic acid linked-AL621), m/z = 488 for dasatinib, m/z = 588 for dasatinib-L (succinic acid linked-dasatinib), m/2z = 516 for AL776.

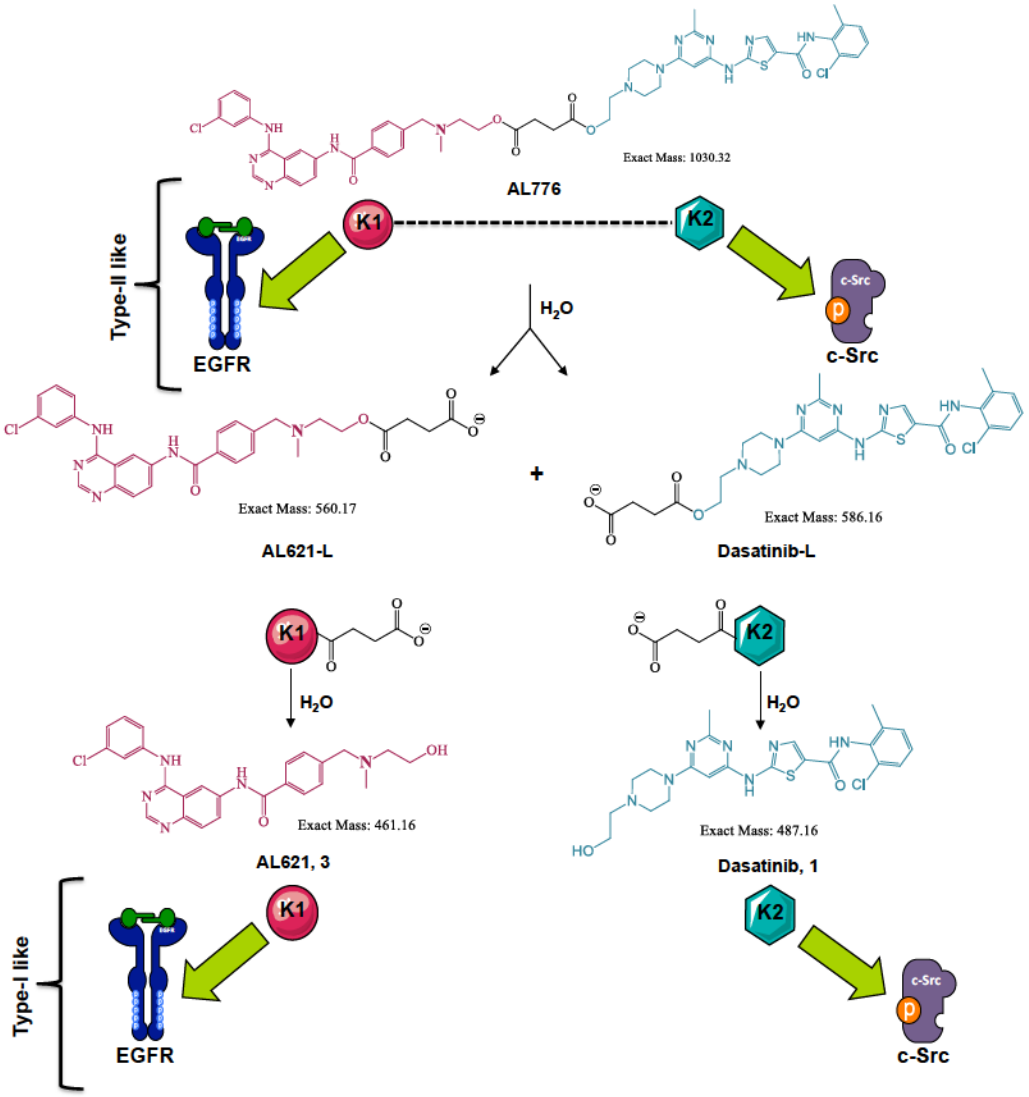

Figure 3.5: Schematic representation of AL776 hydrolysis and its hydrolyzed metabolites. Based on LC-MS characterization of the metabolites of AL776 both *in vitro* and *in vivo*, the hydrolytic scheme of AL776 is modified to represent all the major metabolites. The K1-K2 molecule undergoes hydrolysis to generate the acidic forms of AL621 and dasatinib (AL621-L and dasatinib-L), which are further metabolized to AL621 (K1 or EGFR inhibitor) and dasatinib (K2 or c-Src inhibitor).

3.4.4. Molecular modeling and mode of binding of AL776 in the EGFR and c-Src kinase pocket

One of the primary requirements of the K1-K2 prototype is to possess strong inhibitory potency against Kin-1 and Kin-2, both as an intact molecule as well as upon undergoing hydrolysis to release K1 directed at Kin-1 and K2 at Kin-2. Having found that AL776 (K1-K2) in an *in vitro* kinase assay possessed dual EGFR and c-Src targeting property as an intact structure, it was important to determine how it could probably bind to the EGFR and c-Src kinase domain. Thus, molecular modeling was used to map the binding of the intact structure to EGFR or c-Src. AL776 was modeled in the EGFR kinase pocket using the 1M17 Protein Data Bank (PDB) structure as a starting point. The quinazoline portion of bound erlotinib (24) in 1M17 was used as a template to construct and minimize a bound pose of AL776. Despite the large size of AL776, the quinazoline moiety could bind to the 1M17 structure in a pose analogous to erlotinib. In this pose the linker-dasatinib portion of AL776 points out of the ATP binding pocket towards solvent, allowing for conformational flexibility. Furthermore, the tertiary alkyl nitrogen atom of AL776 is in a position such that the protonated form can interact via a hydrogen-bond/ionic interaction with the carboxylate group of Asp776. A sample pose of AL776 showing the N+-Asp776 interaction is given in figure 3.6A.

AL776 was also modeled in the c-Src kinase pocket using the PDB structure 3G5D (26), It was constructed and minimized in 3G5D starting with the bound dasatinib ligand as the template. The dasatinib portion of AL776 is in the same position as dasatinib in 3G5D, and maintains the same protein-ligand non-bonded interactions as dasatinib. The linker-quinazoline portion of AL776 is solvent exposed and makes no

specific interactions with the c-Src ATP-binding pocket. A conformational search performed on the linker-quinazoline portion of AL776 produced many diverse conformations, none of which shows any specific H-bond or electrostatic interaction between AL776 atoms and c-Src residues. Thus, when bound to c-Src, the dasatinib portion of AL776 can adopt a binding mode identical to that of dasatinib in 3G5D, while the linker-quinazoline portion of the AL776 is free to adopt a number of conformations, none of which appear particularly favored due to a specific interaction with residues at the mouth of the c-Src ATP binding pocket. A sample pose of AL776 modeled in 3G5D is given in 3.6B.

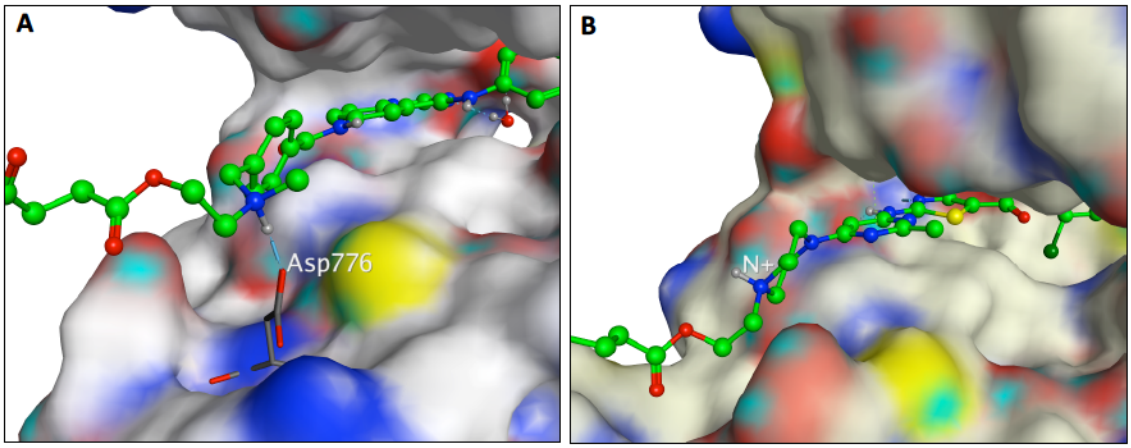

Figure 3.6: Molecular modeling of AL776. (**A**) AL776 modeled in the EGFR kinase-binding pocket using the Protein Data Bank (PDB) with code 1M17. The quinazoline moiety can bind to the hinge region in a manner analogous to erlotinib, while the linker-dasatinib portion of AL776, exposed to solvent, can adopt a number of conformations. The protonated form of the tertiary amine in AL776 can interact with Asp776. (**B**) AL776 modeled in the c-Src pocket using the PDB with code 3G5D. The dasatinib moiety of AL776 binds to the hinge portion of the c-Src ATP binding pocket in a pose identical to

dasatinib while the linker-quinazoline portion of AL776 points out into solvent and can adopt many conformations.

3.4.5. Target modulation and effect on growth inhibition, survival and invasion in cells

3.4.5.A Downregulation of EGFR and c-Src phosphorylation by AL776

The contribution of the multiple species in the cells to inhibition of EGFR and c-Src phosphorylation was analyzed by immunoblot assay in NIH3T3-Her14 mouse fibroblast cells transfected with EGFR (Fig. 3.7A) and in the highly invasive 4T1 mammary tumour cells (Fig. 3.7B). Cells were treated with different concentrations of AL776 for two hours followed by stimulation with EGF (50 ng/ml) for 30 minutes. The results showed that AL776 induced a dose-dependent inhibition of both EGFR and c-Src phosphorylation with maximal inhibition at a concentration as low as 1 μM. The results obtained from the kinetics of hydrolysis of AL776 inside the cells after 2h are consistent with the presence of intact AL776 along with AL621 and dasatinib (supplementary figure S3.1).

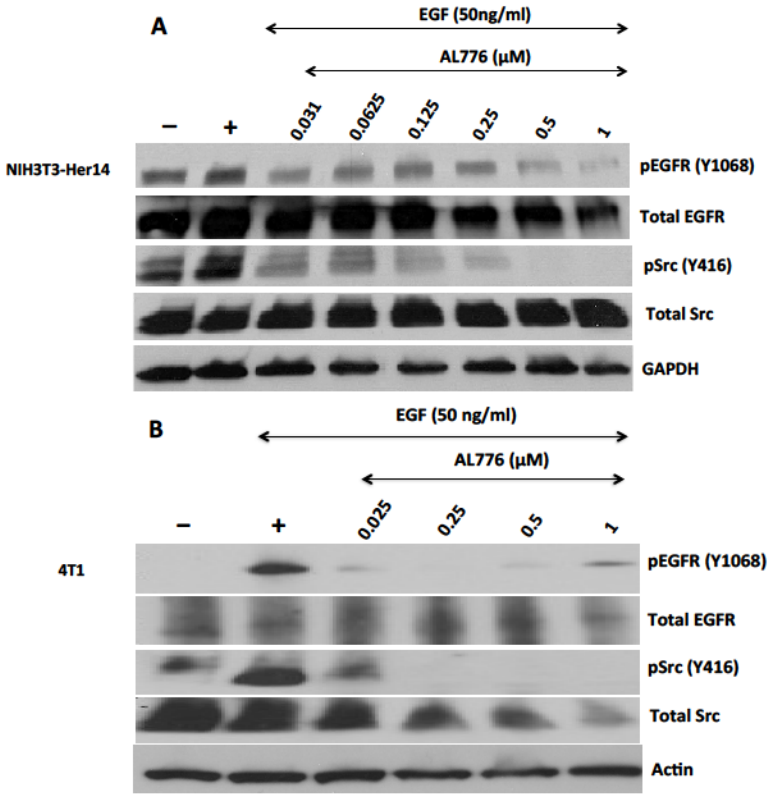

Figure 3.7: Target modulation using western blot analysis. (**A**) NIH3T3-Her14 (EGFR transfected cells) and (**B**) 4T1 mouse mammary tumour cells were starved using serum-free medium for 24h and treated with varying concentrations of AL776 for 2h. The drug was removed from the medium and the cells were stimulated with 50 ng/ml of EGF for 30 min. Cells were extracted, lysed and western blot analysis was carried out according to the protocol described in the Materials and Methods section. Membranes were probed with phospho-EGFR (Y1068), phospho-Src (Y416), total EGFR, Src and housekeeping (Actin or GAPDH) antibodies.

3.4.5.B Anti-motility and anti-invasive properties of AL776

c-Src being a key tyrosine kinase in the signaling pathways associated with motility and invasion, we thought it of interest to evaluate the effects of AL776 on motility and

invasion using the wound-healing and the Boyden chamber assay respectively. These experiments were performed in the highly invasive 4T1 and MDA-MB-231 breast cancer cell lines. Both cell lines were used in these assays due to their high levels of c-Src expression, which is a key oncogene in driving tumour invasion and metastasis (31, 32). The assay was carried out by exposing the cells to the drug for 24h, a time point at which 50% of intact AL776 was found in the cells. Wound-healing assay results showed that AL776 at 0.1 µM blocked wound-closure after a 24h drug exposure in both cell lines (Fig. 3.8A and B). Boyden chamber invasion assay results showed that AL776, like dasatinib, strongly inhibited invasion at a concentration as low as 0.1 µM. However, gefitinib was mostly unable to block invasion at such low doses (Fig. 3.8C and D), indicating that c-Src and not EGFR is primarily responsible for the invasive properties of these cells.

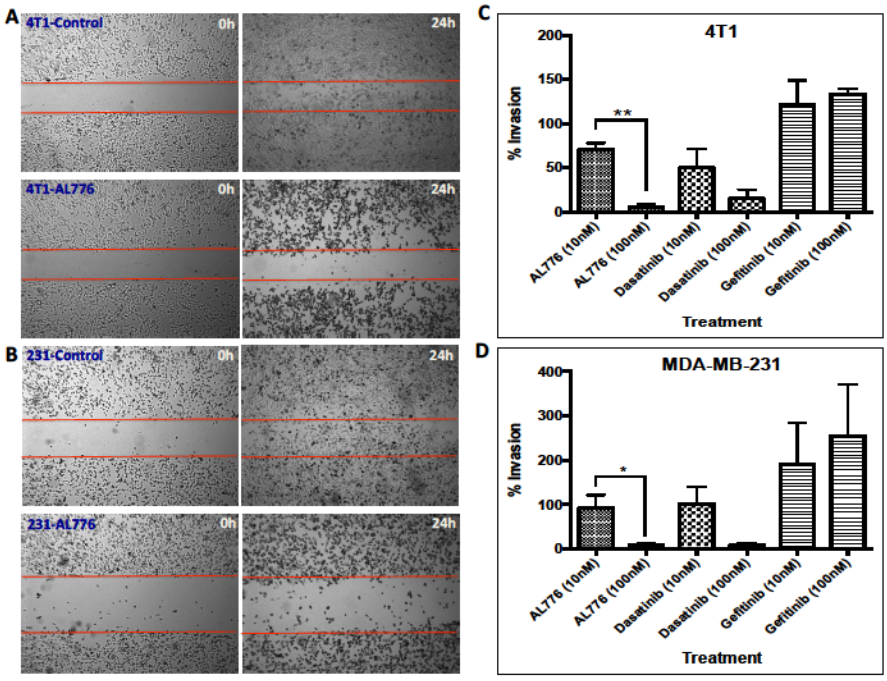

Figure 3.8: Anti-motility and anti-invasive properties of AL776 in 4T1 mouse mammary tumour and MDA-MB-231 triple negative breast cancer cell lines. (A)

4T1 and (**B**) MDA-MB-231 cells were treated with 100 nM of AL776 or control drugs gefitinib or dasatinib for a period of 24h and the wound-closure (scratch) was monitored at both 0h and 24h time points. (**C**) 4T1 or (**D**) MDA-MB-231 cells were treated with varying doses of AL776 (in comparison with dasatinib or gefitinib) for a period of 24h in a Boyden Chamber invasion assay. Cells were plated in serum-free media (top chamber) and allowed to invade across the layer of matrigel towards media containing 10% FBS (bottom chamber) through chemotaxis. Drugs were added to both the top and bottom chambers to maintain a uniform distribution. Cells were fixed, stained and quantified to generate the percentage of invading cells across the matrigel in comparison with untreated control cells. The histograms represent the average ± SEM of three independent experiments. Statistical analysis was performed using the unpaired two-tailed t-test and p values were obtained ($p < 0.05$ is significant): 4T1 ** ($p = 0.001$), MDA-MB-231 * ($p < 0.05$).

3.4.5.C *Growth inhibitory and apoptotic properties of AL776*

One of the premises of designing multi-targeted molecules is to induce pleiotropic effects without losing selectivity for the primary targets. Having shown that AL776 was capable of blocking invasion, we tested the ability of its multi-targeted properties to translate into selective growth inhibition and apoptosis in different cell lines. .

Its growth inhibitory property was tested by treating the NIH3T3 wild type, Her14 (EGFR transfected), MDA-MB-231 and 4T1 cell lines with a dose range of AL776 or gefitinib or dasatinib for a period of 5 days and the IC_{50} values for growth inhibition were determined. The results showed that AL776 induced strong growth inhibition in NIH3T3-

Her14 cells with an IC_{50} of 0.18 μM and showed 2-4 fold higher potency compared with clinical drugs gefitinib or dasatinib. In MDA-MB-231 and 4T1 cell lines, it induced strong growth inhibition, like dasatinib, with IC_{50} values in the sub-micromolar range (Fig. 3.9A). More importantly, AL776 was selectively more potent in NIH3T3 cells transfected to overexpress EGFR when compared with their wild type counterpart (Fig. 3.9B).

The ability of AL776 to induce apoptosis was assessed using NIH3T3 wild type and EGFR transfected cells treated with 0.5, 1 or 5 μM doses of AL776, gefitinib or dasatinib for a period of 48h and analyzed using flow cytometry. Total apoptosis induced in these cells was calculated as the sum of the percentage of early (annexin V staining) and late apoptosis (annexin V + PI staining). The results showed that while all three drugs were selectively cytotoxic towards EGFR transfected cells, AL776 induced a higher level of apoptosis than gefitinib or dasatinib at the 1μM dose (Fig. 3.9C, D). Interestingly, HPLC analysis showed that 48h after drug exposure, while a major part of AL776 had undergone hydrolysis to release its two inhibitory arms (AL621 and dasatinib), a small percentage of the intact molecule was still present inside the cells (Fig. 3.4B). This indicated that inhibition of EGFR and c-Src could not only be mediated by AL621 and dasatinib, but also by intact AL776.

A

	AL776 (μM)	Dasatinib (μM)	Gefitinib (μM)
NIH3T3 – Wt	7.6 ± 3.0	16.4 ± 5.2	12.6 ± 2.1
NIH3T3 – Her14	0.18 ± 0.03	0.81 ± 0.3	0.35 ± 0.04
4T1	0.07 ± 0.01	0.05 ± 0.02	8.2 ± 1.8
MDA-MB-231	0.05 ± 0.004	0.02 ± 0.01	15.1 ± 1.9

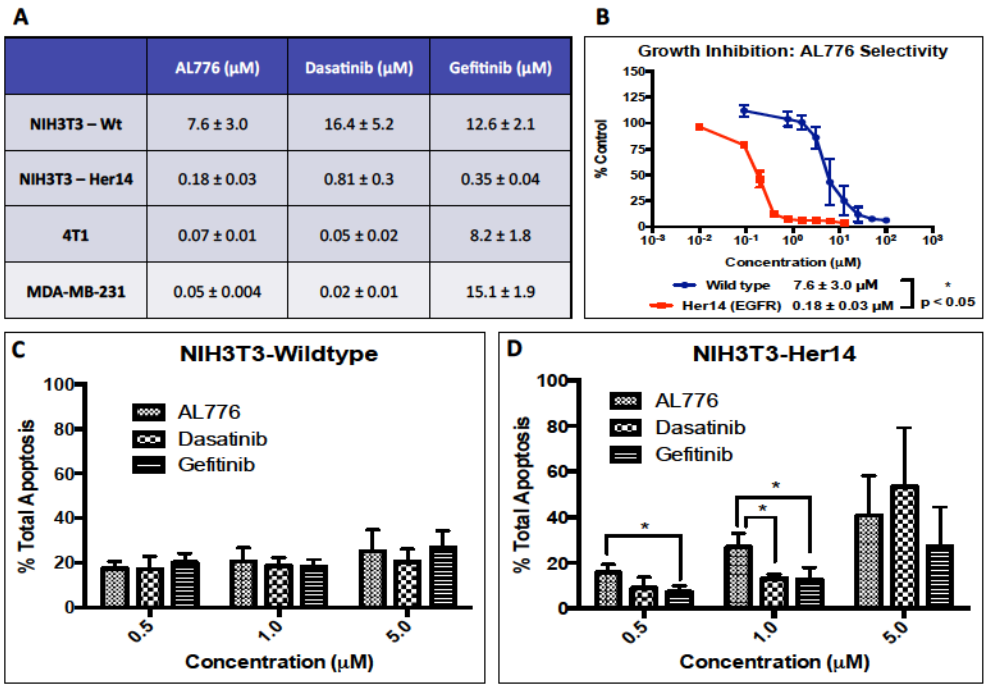

Figure 3.9: Growth inhibitory and apoptotic properties of AL776. (**A**) Growth inhibition was carried out in NIH3T3 wild type and Her14 (EGFR transfected), 4T1 and MDA-MB-231 cell lines using the sulforhodamine B (SRB) assay. Cells were treated with varying doses of AL776, gefitinib or dasatinib for a period of 5 days following which cells were fixed, stained and quantified. Each experiment was repeated at least four times and carried out in triplicates. (**B**) Comparison of the growth inhibition curves and corresponding IC_{50} values of AL776 in the isogenic NIH3T3 wild type and EGFR transfected cell lines. Each point represents the average ± SEM of five independent experiments carried out in triplicates. The difference between their average IC_{50} values was statistically significant with $p < 0.05$. (**C**, **D**) Annexin V and propidium iodide staining (PI) of cells was used to determine the percentage of apoptosis (early + late) induced by AL776, gefitinib and dasatinib. Cells were treated with different doses of AL776 for 48h, collected, stained and analyzed using flow cytometry. The histogram

represents the average ± SEM of three independent experiments with $p < 0.05$ in the NIH3T3-EGFR transfected cell line.

3.4.6. Target modulation *in vivo*

Having shown that this new K1-K2 prototype could be hydrolyzed into the major bioactive species *in vivo* and to strongly block EGFR (Kin-1) and c-Src (Kin-2) phosphorylation *in vitro,* we sought to determine whether it could modulate its two targets in a tumour model *in vivo.* This was performed in comparison with the administration of the two free clinical inhibitors (gefitinib and dasatinib) targeting Kin-1 (EGFR) and Kin-2 (c-Src) using the mouse 4T1 cells in which we have shown the two targets to be modulated *in vitro* (Fig. 3.7B). The results showed that administration of AL776 (40 mg/kg) induced strong blockade of EGFR and c-Src phosphorylation *in vivo* 1h post-administration in a manner similar to the gefitinib + dasatinib combination. This was consistent with the observed inhibition of the two targets *in vitro*. Furthermore, *in vivo*, phosphorylation of the downstream phospho-protein ERK1/2 was strongly inhibited by AL776 and the 2-drug combination 1h post-administration. Inhibitions of phosphorylation of EGFR, c-Src and ERK1/2 by AL776 were reversed 24 h post-treatment but partially retained in mice treated with the two drug combinations (Fig. 3.10 A, B and supplementary figure S3.4).

The ability of target modulation by AL776 to translate into inhibition of tumour growth was monitored by treating Balb/c mice bearing 4T1 tumours with 40 mg/kg of AL776 (i.v. injection) for 5 days. The results showed that AL776 was unable to block tumour growth (Fig. 3.10C) and animals treated with equivalent doses of gefitinib + dasatinib

(given 20 mg/kg each, i.v.) experienced toxicities that precluded data collection. At the end of the study, tumour masses from control versus AL776 treated groups were weighed and there was no difference observed (Fig. 3.10D).

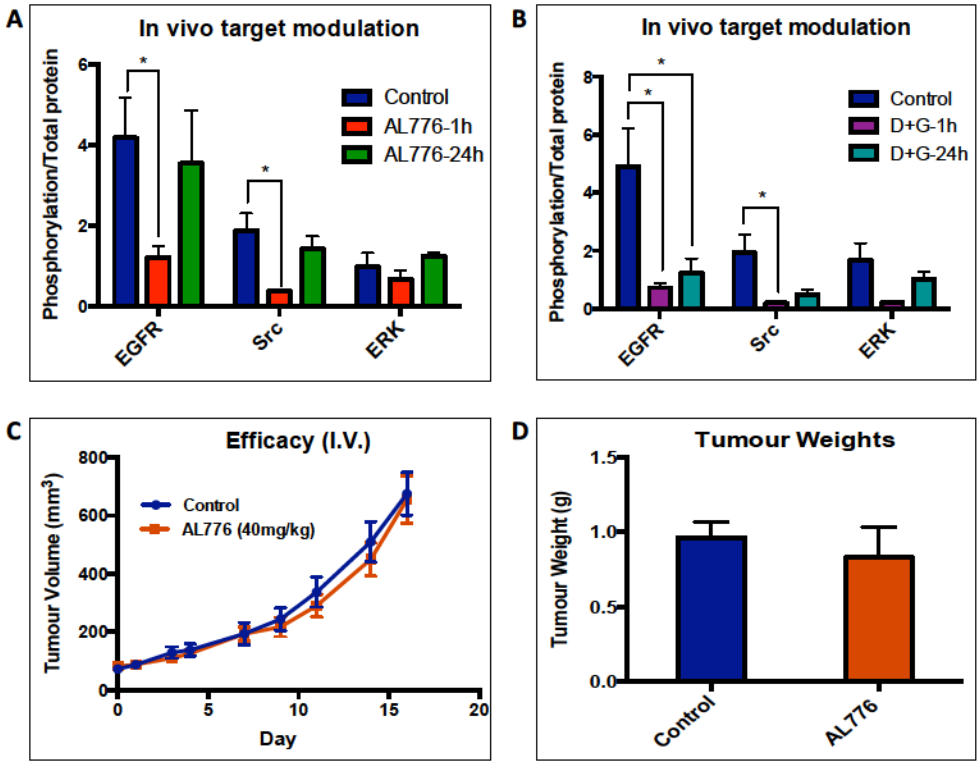

Figure 3.10: Pharmacodynamics in 4T1 tumours. (**A**, **B**) Female Balb/c mice (n = 4) bearing 4T1 tumours were treated with 40 mg/kg of AL776, 20 mg/kg each of gefitinib + dasatinib or vehicle and sacrificed 1h and 24h after drug administration (intravenous, i.v). Tumours were collected and western blot analysis was used to detect inhibition of phosphorylation of EGFR, c-Src and ERK1/2 by the drug, at different time points. The bands were quantified and represented as histograms and as a ratio of phospho-protein/total protein. Statistical significance was determined using multiple t-test and $p < 0.05$ was considered significant. (**C**) Efficacy study was carried out in female Balb/c mice (n = 6) bearing 4T1 tumours and treated with 40 mg/kg of AL776 or vehicle administered IV (once/day) for 5 consecutive days. Tumour growth was monitored for two weeks by

measuring tumour volume on alternate days. Graphs representing the average tumour volumes ± SEM of the two groups are shown. (**D**) On the last day of the study, tumours were collected and their average ± SEM weight (g) from AL776 treated and the control groups (n = 6) are plotted as histograms.

3.5. DISCUSSION

Over the past decade, while targeted therapy focused on single-drug-single-gene strategies, the field of polypharmacology emerged with a new paradigm shifting approach towards tumour targeting that consists of a one-drug-multiple gene approach (33, 34). Within the same context, we initiated a concept termed "combi-targeting" that sought to rationally design molecules to either degrade to generate multiple bioactive species (type I) or to hit two targets without any requirement for hydrolytic cleavage (type II). While we demonstrated the feasibility of these two approaches with molecular prototypes targeting DNA and EGFR (7, 10), their application to the targeting of two different kinases (e.g. Kin-1 and Kin-2) remained a challenge. Molecular prototypes designed to induce a tandem inhibition of EGFR and c-Src lacked inhibitory potency against either kinase as an intact molecule (11, 12). Therefore it was not possible to prove the principle that consists of designing the K1-K2 molecule to hit the two targets without the requirement for hydrolysis and to be further hydrolyzed to release two potent inhibitors of Kin-1 and Kin-2 (see figure 3.1). Here, we sought to synthesize a potent dual EGFR-c-Src targeting prototype by introducing the thiazolylaminopyrimidine moiety as the c-Src tyrosine kinase inhibitor (TKI) while retaining the quinazoline head as the EGFR TKI and by altering the linkers (structures **I-VII**). It is important to mention here that the c-Src

TKI dasatinib induces significant off-target inhibition of kinases including Bcr-Abl, members of the c-Src family of kinases and certain receptor tyrosine kinases including c-Kit, PDGFR-α, β and vascular endothelial growth factor receptor 2 (35, 36) which may advantageously enhance the spectrum of potency of our combi-targeting compound in cells that harbor multiple compensatory pathways. Within the series of combi-targeting molecules (K1-K2) synthesized, we identified AL776 with IC_{50} values of 0.12 μM for EGFR and 3 nM for c-Src as an intact molecule, both IC_{50} concentrations being known to be associated with clinically active drugs (37, 38). Thus, AL776 was selected as a prototype to verify the type III combi-targeting postulates.

Hydrolysis studies have indeed shown that in cells, a fraction of the molecule remained intact (type II), as long as 48h post-treatment, while another portion was converted to EGFR and c-Src TKI (type I). These results indicate that indeed, up to 48h post-treatment, at least three major species were present, AL776 (K1-K2), AL621 (K1) and dasatinib (K2) in the cells. Evaluation of the biological impact of this multi-species milieu showed that a 2h drug exposure could induce both EGFR and c-Src blockade in whole cells. The presence of multiple hydrolytic products of AL776 in the cells indicate that dual inhibition of EGFR and c-Src in cells could primarily result from both type-I and type-II like mechanism, as highlighted in figure 3.1C. Evidence that the intact structure could induce strong EGFR and c-Src targeting potency in an ATP-competitive manner, is given by the enzyme assay in which the exposure time was only 8 minutes (assay time) at room temperature. Furthermore, molecular modeling confirmed the ability of AL776 to anchor in the ATP site of each kinase as an intact molecule. Also, the

relative stability of AL776 in the intracellular milieu suggests that it can modulate its targets by a type II targeting mechanism (i.e. it does not require hydrolysis for generating its dual targeting properties). These results *in toto* confirmed AL776 as the first type III molecular probe of the combi-targeting postulates.

It is important to outline the fact that AL776, our K1-K2 prototype, could release the EGFR TKI AL621 (K1) with published IC_{50} value for EGFR kinase inhibition of 3 nM [*ca.* 40-fold more potent than the intact AL776 (K1-K2)] (12). This property further strengthens the EGFR inhibitory potency of the parental K1-K2. Likewise, the potency of dasatinib (K2) remained in the nanomolar range (Fig. 3.2B). Thus, AL776 behaves like a prodrug of potent EGFR and c-Src inhibitors. Interestingly, analysis of the biological consequences of this property in isogenic cells expressing EGFR and c-Src (NIH3T3-EGFR transfected) showed that of all the binary targeting molecules tested, AL776 was the most potent on the EGFR transfectant (supplementary figure S3.2), indicating high levels of EGFR selectivity. More importantly, the growth inhibitory potency of AL776 was 2-4 fold stronger than that of gefitinib (a nanomolar inhibitor of EGFR) and dasatinib (a low nanomolar inhibitor of c-Src). This superior effect of AL776, as evidenced by its ability to strongly block EGFR and c-Src phosphorylation in the cells, may be due to its ability to disrupt the synergistic interaction between EGFR and c-Src required to promote growth (19). Interestingly, AL776 exhibited cytotoxic effects evidenced by its ability to induce high levels of apoptosis. Perhaps this may be secondary to the inhibition of EGFR and c-Src in the cells, two kinases that are known to activate the anti-apoptotic PI3K/Akt pathway (39-43).

EGFR and c-Src are known to promote motility and invasion in cells (44-46). However our results showed that targeting c-Src alone with dasatinib was sufficient to induce anti-invasive and anti-motility effects in the same range as AL776. We believe that this is due to the fact that c-Src is the main driver of invasion in these cells, thereby leading to a non-consequential contribution of the strong EGFR inhibitory potency of AL776 and its released potent EGFR TKI, AL621. In corroboration, gefitinib alone showed 2-3-fold weaker anti-invasive effects than dasatinib.

Having proven the feasibility and potency of type III targeting *in vitro*, we subsequently tested our hypothesis *in vivo*. Interestingly, the metabolism of AL776 *in vivo* mimicked its intracellular degradation but with significantly faster kinetics and detectable levels of multiple species resulting from its partial hydrolysis or metabolism. The formation of the latter metabolites (AL621-L, Dasatinib-L and other unknown structures) may significantly enhance the multispecies dynamics *in vivo*. The rapid cleavage of AL776, which could only be detected at the early time points following i.v. injection may be mediated by the elevated levels of esterases known to be present in mouse plasma (47, 48). However it is important to note that following its complete disappearance (30 min), abundant levels of the two major metabolites (AL621 and dasatinib) were still present in the plasma. While the rapid degradation of AL776 *in vivo* does not support its ability to induce significant type II targeting in tumours *in vivo,* its dual targeting properties may still be supported by the major metabolites (e.g. AL621 and dasatinib) that it releases in the plasma. Indeed 1h after injection of AL776 both c-Src and EGFR phosphorylation were significantly inhibited in the tumours *in vivo* ($p < 0.05$) but these effects were reversed 24h post-injection and this did not translate into tumour growth inhibition.

These results together with our *in vitro* data suggest that in order for type III targeting to be achievable *in vivo*, the rate of hydrolytic cleavage of AL776 must be slower. Further, structural modifications of the linker are required to achieve this goal.

In summary, here we described the first prototype of multi-targeted molecule of type III and our results suggest that it was a suitable probe for the demonstration of this novel targeting mechanism *in vitro*. Briefly, as depicted in figure 3.11. K1-K2 penetrates the cells by passive diffusion where, through its ability to behave like a type II molecule, it can induce a tandem inhibition of EGFR and c-Src as an intact structure, or as a type I molecule whereby its intracellular hydrolysis leads to K1 targeted to EGFR and K2, targeted to c-Src. A fraction of K1-K2 could be hydrolyzed through a type I mechanism extracellularly, in which case, the released K1 and K2 could freely diffuse into the cells. Similarly, *in vivo,* the K1-K2 molecule and its metabolites were observed after i.v. injection. These multiple species are capable of inhibiting the two targets in a dose-dependent manner and modulate their phosphorylation status both *in vitro* and *in vivo*. Further work is required to ameliorate the *in vivo* potency of this novel type III combi-targeting approach.

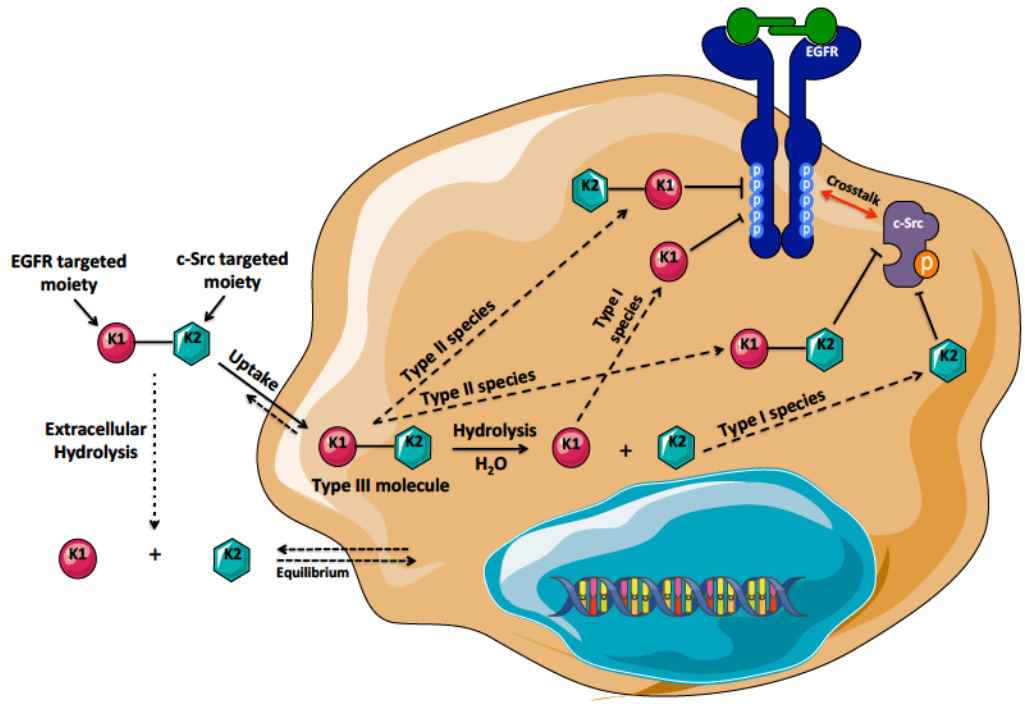

Figure 3.11: Schematic representation of type III combi-targeting mechanism with EGFR (K1) and c-Src (K2) as the kinase targets. Upon entering the cells, K1-K2 binds and inhibits its targets, EGFR and c-Src, both as an intact molecule and as a prodrug whose hydrolysis leads to the release of inhibitors of EGFR (K1) and c-Src (K2). The multiple bioactive species generated inside the cells inhibit both the targeted receptor and non-receptor tyrosine kinases, ultimately leading to inhibition of downstream signaling pathways associated with tumour growth and progression.

3.6. CONLCUSION

It is now increasingly recognized that the overall attrition rate in the development of multi-targeted kinase inhibitors is significantly low when compared with other types of drugs. This is believed to be due to the ability of such drugs to modulate multiple targets in the tumour cell. Here we demonstrated a novel approach to rationally design inhibitors to block two different kinases. We conclusively showed that a molecule could be

designed as K1-K2 to block the two tyrosine kinases (Kin-1 and Kin-2) as an intact structure (K1-K2) and upon undergoing hydrolysis to release two potent inhibitors (K1 + K2) of Kin-1 and Kin-2, respectively. We showed that the two targets (EGFR and c-Src) were modulated *in vitro* and *in vivo* by our first prototype. While amenable *in vivo,* further work is required to overcome the bioavailability hurdles posed by the rapid hydrolysis of the resulting molecule. Our novel approach referred to as "type III combi-targeting" is the first targeting model to lead to a "prodrug-like" molecule with dual kinase activity, which is further "programmed" to generate even more potent inhibitors of these kinases (Kin-1 and Kin-2), upon hydrolysis.

3.7. ACKNOWLEDGEMENT

We are grateful to Dr. Alexandra Furtos from the University of Montreal, for carrying out the LC-MS analysis and Nadim Saade (Department of Chemistry, McGill University) for mass spectra analyses. We would also like to acknowledge Eric Massicotte from the Institut de Recherches Cliniques de Montréal (IRCM) for his help with flow cytometry analysis, and Rosalie Michaud from the Animal Research Center, McGill University for her help with the *in vivo* work. We would also like to acknowledge Servier Medical Art for the cell template of figure 3.11.

3.8. REFERENCES

1. Knight ZA, Lin H, Shokat KM. Targeting the cancer kinome through polypharmacology. Nat Rev Cancer. 2010;10(2):130-7.
2. Walker I, Newell H. Do molecularly targeted agents in oncology have reduced attrition rates? Nat Rev Drug Discov. 2009;8(1):15-6.
3. Reddy AS, Zhang S. Polypharmacology: drug discovery for the future. Expert Rev Clin Pharmacol. 2014;6(1):41-7.

4. Todorova MI, Larroque AL, Dauphin-Pierre S, Fang YQ, Jean-Claude BJ. Subcellular distribution of a fluorescence-labeled combi-molecule designed to block epidermal growth factor receptor tyrosine kinase and damage DNA with a green fluorescent species. Mol Cancer Ther. 2010;9(4):869-82.
5. Banerjee R, Huang Y, Qiu Q, James J, Belinsky G, Jean-Claude BJ. The combi-targeting concept: mechanism of action of the pleiotropic combi-molecule RB24 and discovery of a novel cell signaling-based combination principle Cell Signal. 2011;4:630-40.
6. Banerjee R, Huang Y, McNamee JP, Todorova M, Jean-Claude BJ. The combi-targeting concept: selective targeting of the epidermal growth factor receptor- and Her2-expressing cancer cells by the complex combi-molecule RB24. J Pharmacol Exp Ther. 2010;334(1):9-20.
7. Banerjee R, Rachid Z, McNamee J, Jean-Claude BJ. Synthesis of a Prodrug Designed To Release Multiple Inhibitors of the Epidermal Growth Factor Receptor Tyrosine Kinase and an Alkylating Agent: A Novel Tumor Targeting Concept. J Med Chem. 2003;46(25):5546-51.
8. Larroque-Lombard AL, Todorova M, Golabi N, Williams C, Jean-Claude BJ. Synthesis and Uptake of Fluorescence-Labeled Combi-molecules by P-Glycoprotein-Proficient and -Deficient Uterine Sarcoma Cells MES-SA and MES-SA/DX5. J Med Chem 2010;53 (5):2104-13.
9. Brahimi F, Rachid Z, McNamee JP, Alaoui-Jamali MA, Tari AM, Jean-Claude BJ. Mechanism of action of a novel "combi-triazene" engineered to possess a polar functional group on the alkylating moiety: Evidence for enhancement of potency. Biochem Pharm. 2005;70(4):511-9.
10. Rachid Z, Brahimi F, Domarkas J, Jean-Claude BJ. Synthesis of half-mustard combi-molecules with fluorescence properties: correlation with EGFR status. Bioorganic & medicinal chemistry letters. 2005;15(4):1135-8.
11. Barchechath S, Williams C, Saade K, Lauwagie S, Jean-Claude B. Rational design of multitargeted tyrosine kinase inhibitors: a novel approach. Chem Biol Drug Des. 2009;73(4):380-7.
12. Larroque-Lombard A-L, Ning N, Rao S, Lauwagie S, Coudray L, Huang Y, et al. Biological effects of AL622, a molecule rationally designed to release an EGFR and a SRC kinase inhibitor. Chemical Biology & Drug Design. 2012;80:981-91.
13. Larroque-Lombard A-L, Todorova M, Qiu Q, Jean-Claude BJ. Synthesis and studies on three-compartment flavone-containing combi-molecules designed to target EGFR, DNA and MEK. Chemical Biology & Drug Design. 2011;77(5):309–18.
14. Modjtahedi H, Dean C. The receptor for EGF and its ligands: expression, prognostic value and target for therapy in cancer (review). International Journal of Oncology. 1994;4(2):277-96.
15. Normanno N, De Luca A, Bianco C, Strizzi L, Mancino M, Maiello MR, et al. Epidermal growth factor receptor (EGFR) signaling in cancer. Gene. 2006;366(1):2-16.
16. Seshacharyulu P, Ponnusamy MP, Haridas D, Jain M, Ganti AK, Batra SK. Targeting the EGFR signaling pathway in cancer therapy. Expert Opin Ther Targets. 2013;16(1):15-31.

17. Ono M, Kuwano M. Molecular mechanisms of epidermal growth factor receptor (EGFR) activation and response to gefitinib and other EGFR-targeting drugs. Clin Cancer Res. 2006;12(24):7242-51.
18. Irby RB, Yeatman TJ. Role of Src expression and activation in human cancer. Oncogene. 2000;19(49):5636-42.
19. Maa MC, Leu TH, McCarley DJ, Schatzman RC, Parsons SJ. Potentiation of epidermal growth factor receptor-mediated oncogenesis by c-Src: implications for the etiology of multiple human cancers. Proc Natl Acad Sci U S A. 1995;92(15):6981-5.
20. Biscardi JS, Maa M-C, Tice DA, Cox ME, Leu T-H, Parsons SJ. c-Src-mediated phosphorylation of the epidermal growth factor receptor on Tyr845 and Tyr1101 is associated with modulation of receptor function. J Biol Chem 1999;274(12):8335-43.
21. Bao J, Gur G, Yarden Y. Src promotes destruction of c-Cbl: implications for oncogenic synergy between Src and growth factor receptors. Proc Natl Acad Sci U S A. 2003;100(5):2438-43.
22. Nautiyal J, Majumder P, Patel BB, Lee FY, Majumdar AP. Src inhibitor dasatinib inhibits growth of breast cancer cells by modulating EGFR signaling. Cancer Lett. 2009;283(2):143-51.
23. Heppner GH, Miller FR, Shekhar PM. Nontransgenic models of breast cancer. Breast Cancer Research. 2000;2(5):331.
24. Stamos J, Sliwkowski MX, Eigenbrot C. Structure of the Epidermal Growth Factor Receptor Kinase Domain Alone and in Complex with a 4-Anilinoquinazoline Inhibitor. J Biol Chem. 2002;277(48):46265-72.
25. Molecular Operating Environment (MOE) CCGI, 1010 Sherbooke St. West, Suite #910, Montreal, QC, Canada, H3A 2R7, 2013.
26. Getlik M, Grutter C, Simard JR, Kluter S, Rabiller M, Rode HB, et al. Hybrid compound design to overcome the gatekeeper T338M mutation in cSrc. J Med Chem. 2009;52(13):3915-26.
27. Skehan P, Storeng R, Scudiero D, Monks A, McMahon J, Vistica D, et al. New colorimetric cytotoxicity assay for anticancer-drug screening. J Natl Cancer Inst. 1990;82(13):1107-12.
28. Larroque A-L, Peori B, Williams C, Fang YQ, Qiu Q, Rachid Z, et al. Synthesis of water soluble bis-triazenoquinazolines: an unusual predicted mode of binding to the epidermal growth factor receptor tyrosine kinase. Chemical Biology & Drug Design. 2008;71(4):374-9.
29. Solca F, Dahl G, Zoephel A, Bader G, Sanderson M, Klein C, et al. Target binding properties and cellular activity of afatinib (BIBW 2992), an irreversible ErbB family blocker. Journal of Pharmacology and Experimental Therapeutics. 2012;343(2):342-50.
30. Lombardo LJ, Lee FY, Chen P, Norris D, Barrish JC, Behnia K, et al. Discovery of N-(2-chloro-6-methyl- phenyl)-2-(6-(4-(2-hydroxyethyl)- piperazin-1-yl)-2-methylpyrimidin-4- ylamino)thiazole-5-carboxamide (BMS-354825), a dual Src/Abl kinase inhibitor with potent antitumor activity in preclinical assays. J Med Chem. 2004;47(27):6658-61.
31. Tanjoni I, Walsh C, Uryu S, Tomar A, Nam JO, Mielgo A, et al. PND-1186 FAK inhibitor selectively promotes tumor cell apoptosis in three-dimensional environments. Cancer. 2010;9(10):764-77.

32. Tryfonopoulos D, Walsh S, Collins DM, Flanagan L, Quinn C, Corkery B, et al. Src: a potential target for the treatment of triple-negative breast cancer. Ann Oncol. 2011;22(10):2234-40.
33. Dar AC, Das TK, Shokat KM, Cagan RL. Chemical genetic discovery of targets and anti-targets for cancer polypharmacology. Nature. 2012;486(7401):80-4.
34. Fortin S, Berube G. Advances in the development of hybrid anticancer drugs. Expert Opin Drug Discov. 2013;8(8):1029-47.
35. Zhang J, Yang PL, Gray NS. Targeting cancer with small molecule kinase inhibitors. Nature Reviews Cancer. 2009;9(1):28-39.
36. Karaman MW, Herrgard S, Treiber DK, Gallant P, Atteridge CE, Campbell BT, et al. A quantitative analysis of kinase inhibitor selectivity. Nature biotechnology. 2008;26(1):127-32.
37. Brahimi F, Matheson SL, Dudouit F, McNamee JP, Tari AM, Jean-Claude BJ. Inhibition of epidermal growth factor receptor-mediated signaling by "Combi-Triazene" BJ2000, a new probe for Combi-Targeting postulates. J Pharmacol Exp Ther. 2002;303(1):238-46.
38. Neto C, Fernandes C, Oliveira MC, Gano L, Mendes F, Kniess T, et al. Radiohalogenated 4-anilinoquinazoline-based EGFR-TK inhibitors as potential cancer imaging agents. Nucl Med Biol. 2012;39(2):247-60.
39. Irwin ME, Bohin N, Boerner JL. Src family kinases mediate epidermal growth factor receptor signaling from lipid rafts in breast cancer cells. Cancer. 2011;12(8):718-26.
40. Schlessinger J. Cell signaling by receptor tyrosine kinases. Cell. 2000;103(2):211-25.
41. Garcia R, Bowman TL, Niu G, Yu H, Minton S, Muro-Cacho CA, et al. Constitutive activation of Stat3 by the Src and JAK tyrosine kinases participates in growth regulation of human breast carcinoma cells. Oncogene. 2001;20(20):2499-513.
42. Courtney KD, Corcoran RB, Engelman JA. The PI3K pathway as drug target in human cancer. J Clin Oncol. 2010;28(6):1075-83.
43. Li H, Schmid-Bindert G, Wang D, Zhao Y, Yang X, Su B, et al. Blocking the PI3K/AKT and MEK/ERK signaling pathways can overcome gefitinib-resistance in non-small cell lung cancer cell lines. Adv Med Sci 2011;56(2):275-84.
44. Kim LC, Song L, Haura EB. Src kinases as therapeutic targets for cancer. Nat Rev Clin Oncol. 2009;6(10):587-95.
45. Yeatman TJ. A renaissance for SRC. Nat Rev Cancer. 2004;4(6):470-80.
46. Koppikar P, Choi SH, Egloff AM, Cai Q, Suzuki S, Freilino M, et al. Combined inhibition of c-Src and epidermal growth factor receptor abrogates growth and invasion of head and neck squamous cell carcinoma. Clin Cancer Res. 2008;14(13):4284-91.
47. Bahar FG, Ohura K, Ogihara T, Imai T. Species difference of esterase expression and hydrolase activity in plasma. Journal of pharmaceutical sciences. 2012;101(10):3979-88.
48. Hunter RL, Strachan DS. The esterases of mouse blood. Annals of the New York Academy of Sciences. 1961;94(3):861-7.

3.9. SUPPLEMENTARY FIGURES

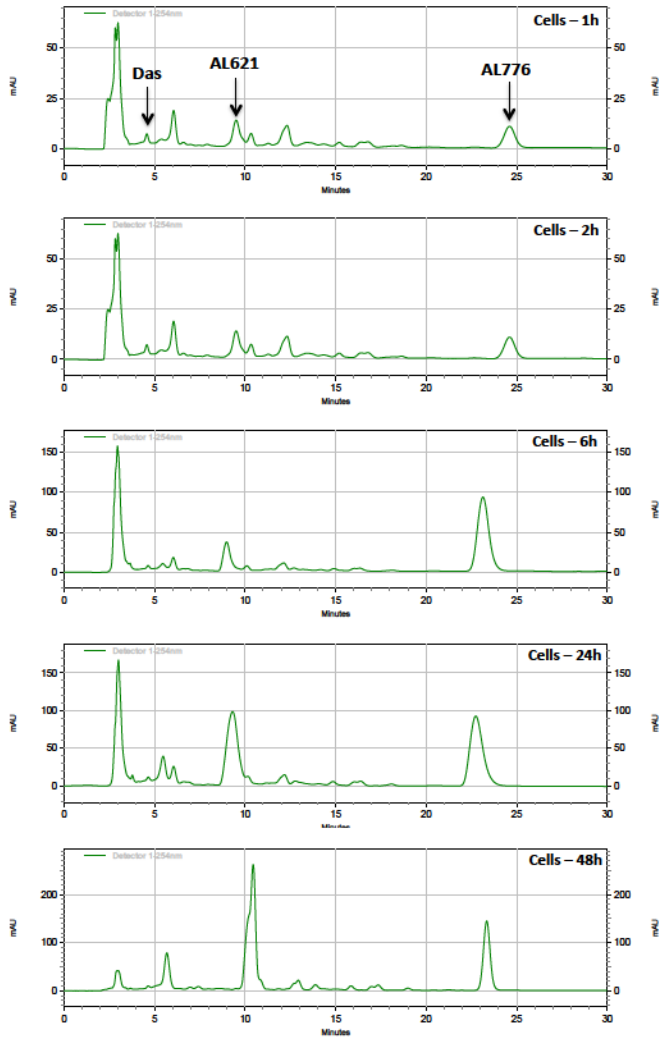

Figure S3.1: High performance liquid chromatography (HPLC) analysis of the hydrolysis of AL776 inside the cells. The intracellular hydrolysis of AL776 was studied by treating NIH3T3-Her14 (EGFR transfected) cells with 25 μM of AL776 for 1, 2, 6, 24 and 48h. The HPLC spectra show the slow internalization and degradation products (AL621 and dasatinib) obtained from AL776 hydrolysis mediated by intracellular esterases.

	WT (μM)	HER14 (EGFR) (μM)
1	> 10	> 10
2	> 10	0.37 ± 0.01
3	1.4 ± 0.4	0.36 ± 0.00
4	17.5 ± 2.2	0.37 ± 0.06
5	> 100	0.3 ± 0.03
6	54.1 ± 6.4	0.6 ± 0.01
7 (AL776)	7.6 ± 3.0	0.18 ± 0.03
Gefitinib	12.6 ± 2.1	0.35 ± 0.04
Dasatinib	16.4 ± 5.2	0.8 ± 0.3

Figure S3.2: **Growth inhibition in NIH3T3 wild type and Her14 (EGFR-transfected) cell lines**. The growth inhibitory property of each EGFR-c-Src targeting molecule in the series was determined using the sulforhodamine B (SRB) assay. Gefitinib and dasatinib were used as control drugs for comparison, and the IC_{50} values for growth inhibition were determined using the GraphPad Prism 6.0 software.

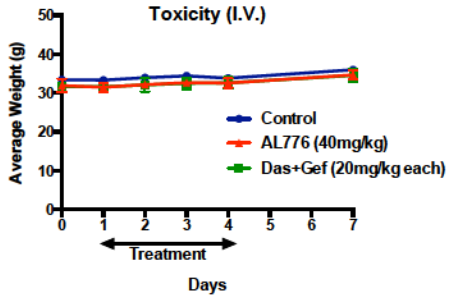

Figure S3.3: Toxicity of AL776 *in vivo*. The toxicity of (**A**) AL776 (40 mg/kg) and the combination of (**B**) gefitinib + dasatinib (20 mg/kg each) was determined in CD-1 mice (n = 3) treated with the drug (intravenous, i.v.) for 4 consecutive days. The effect of toxicity was determined by monitoring the average body weight (g) of each treated group compared with the vehicle control. Greater than 15% weight loss was considered toxic.

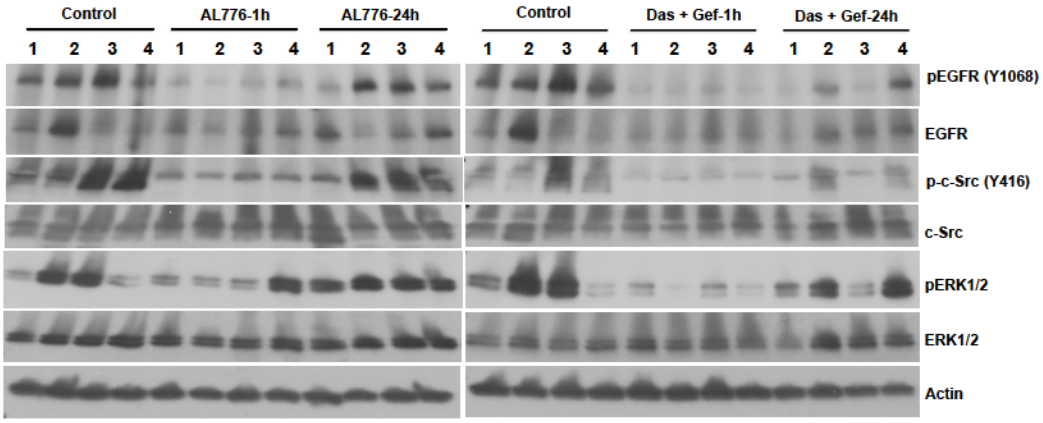

Figure S3.4: Pharmacodynamics of AL776. Female Balb/c mice (n = 4) with 4T1 mammary tumours were treated with (**A**) 40 mg/kg of AL776 or the combination of (**B**) gefitinib + dasatinib (20 mg/kg each) compared with the vehicle control. Mice were sacrificed 1h or 24h after drug exposure and the tumours were collected, processed and inhibition of phosphorylated proteins (EGFR, c-Src, ERK1/2) was assessed using western blots.

CONNECTING TEXT

The previous chapter highlighted the design and development of Kin1-Kin2 targeting combi-molecules engineered to induce tandem blockade of two kinases overexpressed in cancer cells. Optimization and synthesis of compounds **I** - **VII** (AL776), led to the first "type III" combi-molecule, AL776, that could not only induce blockade of Kin1 (EGFR) and Kin2 (c-Src) as an intact structure, but also hydrolyzed to generate potent inhibitors of the two kinases (AL621 or K1 targeting EGFR and dasatinib or K2 targeting c-Src), inside the cells. This study successfully demonstrated the feasibility of developing combi-molecules capable of inducing tandem blockade of two different kinases (e.g. EGFR and c-Src) overexpressed in cancer cells. Importantly, it led to the development of a novel targeting principle (i.e., type III) that is further applicable in the context of inhibiting other receptor and non-receptor tyrosine kinases driving tumour growth and progression through a complex network of signal transduction pathways. One such signaling crosstalk is known to occur between EGFR and another receptor tyrosine kinase (RTK), c-Met, which is often co-expressed with EGFR in several cancers driving synergistic growth, proliferation, invasion and survival as well as mediating resistance to EGFR inhibitors. Furthermore, c-Src, which has been previously demonstrated to synergize with EGFR, is known to play a role in the signaling crosstalk between the two receptors promoting tumour progression and mediating drug resistance. Thus, in the upcoming chapter, we wished to further dissect the signaling interplay between EGFR, c-Met and c-Src using their respective clinical kinase inhibitors (small molecules inhibitors) as pharmacological probes, prior to designing and evaluating the potency of Kin1-Kin2 targeting combi-molecules (e.g. EGFR-c-Src, EGFR-c-Met) on these cancer cells. Our purpose was also

to identify the key kinases to be targeted in order to abrogate the signaling interplay between RTKs EGFR and c-Met and the non-RTK c-Src.

CHAPTER 4

PHARMACOLOGICAL PROBING OF SIGNALING REDUNDANCY MEDIATED BY RECEPTOR AND NON-RECEPTOR TYROSINE KINASES REVEALED ACHILLES' HEELS IN CASTRATE RESISTANT PROSTATE CANCER

Suman Rao[1], Ben Allal[2], Anne-Laure Larroque-Lombard[1], Etienne Chatelut[2], Jean-Pierre Delord[2], Bertrand Jean-Claude[1]*

[1] : Research Institute – McGill University Health Center (MUHC), 1001 Decarie Blvd, Block E, Montreal, Quebec, H4A 3J1, Canada

[2] : Institut Universitaire du Cancer Toulouse – Oncopole, 1 avenue Irène Joliot-Curie, 31059 TOULOUSE Cedex 9, France

4.1. ABSTRACT

In a selected subset of advanced prostate cancer cells, we sought to identify a targeting modality for abrogating tumour resistance due to the complex interplay between c-Met, EGFR and c-Src. Our strategy was to block c-Met, EGFR and c-Src tyrosine kinase functions with their respective clinical kinase inhibitors *in vitro* and *in vivo*. Referring to the c-Met-related pathways as target pathway 1 "T1", EGFR "T2" and c-Src "T3", we analyzed the ability of two or more drug combinations to modulate their corresponding target phosphorylation and induce growth inhibition in prostate cancer cells. The results showed that dual targeting of c-Met (T1) and EGFR (T2) with crizotinib + gefitinib, abrogated signaling redundancy between the two receptors and led to sustained inhibition of c-Src phosphorylation, cell growth and invasion. By contrast, direct inhibition of c-Src (T3) by adding dasatinib to the crizotinib + gefitinib modality (3-drug combination), resulted in strong and delayed re-phosphorylation of c-Src, and did not significantly enhance growth inhibitory and anti-invasive potency. All targeting modalities (2- or 3-drug combinations) induced STAT3 phosphorylation. However, additional blockade of JAK1/2-STAT3 (T4) with ruxolitinib (4-drug combination), although leading to sustained blockade of STAT3 phosphorylation, did not significantly enhance growth inhibitory potency ($p > 0.05$). Despite the multiplicity of targets involved in signaling redundancy and compensatory signaling, targeting two key signaling proteins (e.g. c-Met-EGFR, EGFR-c-Src or c-Met-c-Src) may suffice to induce potent growth inhibition, thereby representing the Achilles' heels of these refractory tumours.

4.2. INTRODUCTION

Solid tumours are characterized by the overexpression of several receptor tyrosine kinases (RTKs) including EGFR, HER2, c-Met, PDGFR and VEGFR (1-5). Interaction of these receptors with other downstream signaling proteins including GTPases, serine/threonine and lipid kinases (e.g. Ras, Raf, MEK, ERK1/2, PI3K, Akt), non-receptor tyrosine kinases or non-RTKs (e.g. c-Src, c-Abl, JAK1/2), transcription factors (STAT3, β-catenin, c-Myc) lead to a complex interplay that drives tumour progression and reduces tumour sensitivity to treatment. Over the past decade, several kinase inhibitors designed to target and block signaling mediated by RTKs and non-RTKs have been introduced in the clinical management of solid tumours (6, 7). In many cases, their effects have been mitigated not only by gatekeeper mutations at the target ATP binding site, but also by compensatory signaling (8, 9). The phrase "compensatory signaling¨, which is now commonly used in signaling studies, refers to a situation where in response to the inhibition of one pathway, the cells activate one or more pathways leading to its survival (10). A typical example includes activation of the STAT3 pathway, a transcription factor overexpressed in several solid tumours mediating survival, in response to kinase inhibitors and other chemotherapeutic agents (11-15). Another type of compensatory mechanism involves the co-expression of receptors that activate signaling through identical pathways. This phenomenon termed "signaling redundancy" is known to induce resistance to kinase inhibitors. A typical example is resistance to EGFR tyrosine kinase inhibitors (TKIs) gefitinib and erlotinib, in non-small cell lung cancer (NSCLC), which is associated with the overexpression of c-Met that can activate the MAPK and PI3K/Akt pathways despite strong blockade of EGFR functions by these

inhibitors (16). Other examples of signaling redundancy leading to EGFR TKI resistance include the co-activation of the insulin receptor IGF-1R in squamous carcinoma cells and HER2 in colorectal cancer cells (17, 18). However, despite our increasingly clear understanding of compensatory signaling, scant attention has been paid to the design of targeting modalities to block their adverse effects. Recently, we reported on a novel molecular strategy to abrogate the deleterious interactions between c-Src and EGFR using a kinase inhibitor engineered to induce a tandem blockade of these two proteins (19). Furthermore, the involvement of c-Src in the signaling crosstalk between c-Met and EGFR has been previously indicated (20-22). Given the involvement of c-Met in signaling redundancy with EGFR and taking into account our own work on targeting crosstalks between EGFR and c-Src, we surmised that blocking c-Src concomitantly with EGFR and c-Met might enhance growth inhibitory and anti-invasive properties.

The intricate nature of the interplay between c-Met, EGFR and c-Src and associated pathways *a priori*, inspires the use of multiple inhibitors to block the network of signaling that they evoke. However, we surmised that a detailed analysis of the modulation the EGFR-c-Met-c-Src axis with kinase inhibitors might lead to a clinically achievable therapeutic modality. Thus, this study sought to identify critical pathways to be targeted with a minimal number of drugs, to effectively abrogate the adverse effects of c-Met-, EGFR- and c-Src-mediated signaling. As depicted in Figure 4.1, to define the Achilles' heels of this complex interplay, we analyzed four canonical pathways designated herein as T1 for c-Met-, T2 for EGFR-, T3 for c-Src-, and T4 for the JAK1/2-STAT3 pathway. The latter has been shown, in many studies, to be activated in response

to a large number of kinase inhibitors (15). Here using kinase inhibitors as probes, we first sought to identify cell types with signaling redundancy associated with c-Met and EGFR. Superior activity of drug-combination *versus* drug alone was used as an indirect insight into signaling redundancy in these cells. Among the cell lines chosen, breast cancer and prostate cancer cells responded to the dual targeting of EGFR and c-Met. Given the paucity of studies on the signaling redundancy between c-Met and EGFR in prostate cancer, this work focused exclusively on the subset of prostate cancer cells (DU145 and PC3) that showed enhanced growth inhibition upon treatment with a combination of c-Met and EGFR inhibitors. Within the clinical limit of the number of drugs for combination therapy, our search for the Achilles' heels to be targeted, focused on analyzing the single targeting of T1, T2, T3, T4, the dual targeting of T1 + T2, T1 + T3, T1 + T4, T2 + T3, T2 + T4, T3 + T4, the triple targeting of T1 + T2 + T3, T1 + T2 + T4, T1 + T3 + T4, T2 +T3 + T4, T1 + T2 + T3 and the 4-drug combinations targeting T1 + T2 + T3 + T4. c-Src being our primary non-RTK target of the signaling interplay, our approach was to study signaling responses associated with dasatinib (a c-Src TKI) treatment alone and in multi-drug combinations. We found that targeting one or more of the pathways (e.g. T1, T2, T3) resulted in activation of T4 (STAT3 pathway). However, compensatory induction of T4 had no effects on cell viability. By contrast, targeting T1 + T2 + T3 did evoke compensatory signaling via T3 (c-Src activation) and T4 (STAT3), but did induce strong growth inhibitory potency. Further blockade of T4 in addition to T1 + T2 + T3 did not lead to any significant enhancement of activity. Importantly, tandem blockade of the two receptors (i.e., T1 + T2) did not induce compensatory signaling via T3 (i.e. no c-Src reactivation) and resulted in strong growth inhibitory and anti-invasive

properties. *In vitro*, tandem targeting of multiple pathways (i.e., T1 + T2 + T3, T1 + T2 + T3 + T4) appeared to be equieffective with dual RTK-RTK and RTK-non-RTK targeting (i.e., T1 + T2, T2 + T3, T3 + T4). Thus the effects of the three dual targeting modalities were compared *in vivo* where they were found to induce equipotent and significant antitumour activities. These results indicate that the signaling redundancy between c-Met and EGFR or the crosstalks between these two receptors with c-Src (i.e, EGFR-c-Src, c-Met-c-Src) are the Achilles' heels to be targeted for effective growth inhibitory and anti-invasive potency in these cells that co-express EGFR, c-Met and c-Src.

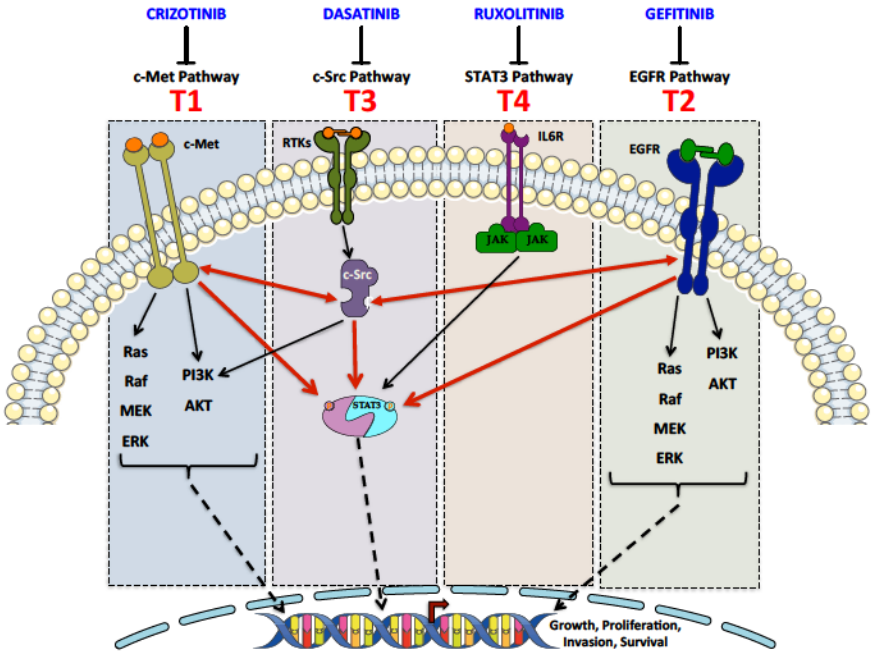

Figure 4.1: Targeting the signaling interplay between c-Met, EGFR, c-Src and STAT3 using pharmacological inhibitors. Scheme showing the signaling crosstalk between receptor and non-receptor tyrosine kinases promoting growth, proliferation, invasion and survival in cancer cells. Clinically approved tyrosine kinase inhibitors including crizotinib, gefitinib, dasatinib and ruxolitinib were used to target the c-Met

(designated as T1), EGFR (T2), c-Src (T3) and JAK1/2-STAT3 (T4) pathways, respectively.

4.3. MATERIALS AND METHODS

4.3.1. Cell culture

Breast cancer (MDA-MB-231, BT549, MDA-MB-468), non-small-cell lung cancer (A549, H2170) and prostate cancer cells (DU145, PC3 and 22RV1) were used. PC3 and 22RV1 cells were a generous gift from Dr Amina Zoubeidi (University of British Columbia, Canada), while the remaining cell lines were purchased from ATCC (USA). Cells were maintained in DMEM supplemented with 10% FBS, 10mM HEPES, 2mM L-glutamine, gentamycin sulfate and fungizone (Wisent Inc., Canada).

4.3.2. Drug treatment

Clinical inhibitors crizotinib (PharmaBlock, USA), gefitinib (Royal Victoria Hospital pharmacy, Montreal, Canada), dasatinib (Ark Pharm Inc., USA) and ruxolitinib (Selleckchem, USA) were used and dissolved in DMSO to obtain a concentration of 40mM and lower. DMSO in media never exceeded 1% v/v.

4.3.3. Growth inhibition assay

Cells were plated and treated with drugs (single, equimolar or equieffective combinations) for 5 days. Growth inhibition was carried out using the sulforhodamine B (SRB) assay (23). Plates were read using a microplate reader ELx808 (Biotek, USA) at

492nm. Combination index values (CI) were calculated according to the Chou-Talalay method (24) and the average CI from three independent experiments were reported.

4.3.4. Boyden chamber invasion assay

Cells were plated onto polycarbonate transwell inserts (8μm pore size, BD Biosciences) coated with matrigel (6%) (BD Biosciences, USA) in serum-free media with the bottom chamber containing 10%-FBS media. Cells were treated with drugs for 24h and fixed in formalin, stained with 0.1% crystal violet (Sigma-Aldrich Canada Co., Canada) and five non-overlapping images of the invading cells were captured using the Leica DFC300FX camera and quantified using the ImageJ 1.46r software (National Institute of Health, USA).

4.3.5. Apoptosis

Cells were plated and treated with drugs for 48h and apoptosis analysis was carried out according to the protocol previously described by Rao S *et al* (19).

4.3.6. Western blot

Cells were plated and then treated under basal (10% FBS) or starvation-stimulation (EGF + HGF, 20ng/ml each) conditions. Western blot analysis was carried out according to the protocol previously described by Rao S *et al.* (19). All antibodies were purchased from New England Biolabs, Canada except total EGFR and β-actin (Santa Cruz, USA).

4.3.7. *In vivo*

Male Swiss Nude mice, Jackson model (Charles River laboratories, France) were used after approval from Claudius Regaud Institute animal ethics committee and housed according to the European Laboratory Animal Science Association standards. Mice were implanted with DU145 prostate cancer cells, 15 million cells on each flank, subcutaneously. At 200 mm^3 tumour size, mice were randomized into groups of 8 and treated once/day (orally) with vehicle (20% cremophor + 20% ethanol + 60% dextrose, 10% w/v) or the following drug combinations: crizotinib (50mg/kg) + gefitinib (50mg/kg), crizotinib (50mg/kg) + dasatinib (10mg/kg) or gefitinib (50mg/kg) + dasatinib (10mg/kg). Tumour volume was calculated according to the formula, [(L^2*W)/2].

4.3.8. Statistical Analysis

One-way ANOVA or student t-test (unpaired, one-tailed) analysis was used to calculate significance. All results were analyzed using GraphPad Prism 6.0 (GraphPadSoftware, Inc., USA).

4.4. RESULTS

4.4.1. Screening for signaling redundancy by pharmacological probing of cancer cell lines

In order to identify cell lines responding to the dual inhibition of EGFR and c-Met, we screened a panel of advanced cancer cell lines using kinase inhibitors as probes in a growth inhibition assay. Crizotinib was used to inhibit c-Met and gefitinib EGFR. Cell lines co-expressing EGFR and c-Met including breast cancer cells (MDA-MB-231,

MDA-MB-468 and BT549), prostate cancer cells (DU145, PC3 and 22RV1) and non-small-cell lung cancer cells (A549 and H2170) were evaluated (25-31). The results showed that amongst all the cell lines screened in the panel, MDA-MB-468, DU145 and PC3 were the only ones found to exhibit 2-3 fold greater sensitivity to dual c-Met and EGFR targeting when compared with single drug alone (Fig. 4.2A). Given the paucity of data available on c-Met and EGFR redundancy in prostate cancer, the subset of prostate cancer cell lines DU145, PC3 and 22RV1 were selected for further investigation. Within this subset, the androgen-receptor positive 22RV1 cells did not respond to the dual targeting of c-Met + EGFR and was analyzed for comparison only. The androgen receptor negative castrate resistant prostate cancer (CRPC) cell lines, DU145 and PC3 were moderately sensitive to crizotinib alone (DU145: 6.5 ± 1.0μM, PC3: 4.9 ± 1.6μM) and gefitinib alone (DU145: IC50 = 9.3 ± 1.1μM, PC3: 22.1 ± 5.2μM). However, dual inhibition of c-Met and EGFR using an equimolar combination of crizotinib + gefitinib significantly enhanced potency by 2-3-fold (DU145: 2.3 ± 0.4μM and PC3: 2.0 ± 0.3μM) (Fig. 4.2A). These results stimulated our interest in performing a molecular analysis of the signaling redundancy mediated by c-Met and EGFR in these cells and their interplay with c-Src.

4.4.2. Abrogation of the redundancy mediated by EGFR and c-Met and the interplay with c-Src kinase: signaling analysis in prostate cancer cells

Through the use of kinase inhibitors as pharmacological probes, we obtained indirect evidence of the potential signaling redundancy between EGFR and c-Met in the CRPC cell lines. In order to gain direct evidence of this redundancy, we inhibited the two

receptors (T1 + T2) upstream and probed for signaling pathways downstream using western blot analysis. Our results showed that treatment with crizotinib alone led to blockade of c-Met and c-Src phosphorylation without affecting EGFR, ERK1/2 and Akt phosphorylation (Fig. 4.2B). Likewise, gefitinib did not inhibit c-Met or Akt but blocked EGFR, c-Src and ERK1/2 phosphorylation. However, treatment with the equieffective combination of crizotinib + gefitinib, led to potent inhibition of EGFR, c-Met, c-Src, ERK1/2 and Akt phosphorylation. These results suggest that EGFR and c-Met are engaged in signaling redundancy in these cells and that c-Src participates in the signaling interplay between the latter two receptors (Fig. 4.2B).

c-Src (T3) activation being common with signaling associated with the two receptors, we sought to modulate its effect using the IC50 dose of dasatinib obtained from a growth inhibition assay (Fig. 4.S1) in order to determine whether it participates in the signaling redundancy. The results showed that while dasatinib alone induced potent inhibition of c-Src, this did not lead to inhibition of c-Met, EGFR, ERK1/2 or Akt phosphorylation. However, when dasatinib was added to the combination of crizotinib + gefitinib, (i.e. tandem blockade of T1 + T2 + T3), there was complete and potent inhibition of c-Met, EGFR, c-Src, ERK1/2 and Akt phosphorylation in both cell lines (Fig. 4.2B).

4.4.3. Growth factor-dependent activation of c-Src and reversibility of inhibition under conditions where signaling redundancy between c-Met and EGFR was inhibited

As mentioned earlier, blockade of c-Met and EGFR led to downregulation of c-Src phosphorylation. In order to determine whether c-Src remained continuously or

transiently activated, we monitored its kinetics of phosphorylation downstream of EGFR and c-Met stimulation with their respective ligands, EGF and HGF. The results showed that c-Src phosphorylation peaked at 6h and gradually decreased over time in both cell lines, indicating that perhaps c-Src activation increased in response to growth factor-activated EGFR and c-Met (Fig. 4.2C). Thus, we surmised that biological response associated with the modulation of c-Met and EGFR may have some dependence on c-Src activation. Therefore, we sought to study the effects of blocking EGFR and c-Met using the dual-combination of crizotinib + gefitinib (Fig. 4.2D) on c-Src phosphorylation. The results showed that upon EGF + HGF stimulation and treatment with the equieffective combination of crizotinib + gefitinib, there was gradual and sustained inhibition of c-Src, which was maintained up to 24h with concomitant blockade of c-Met and EGFR phosphorylation up to 24h (Fig. 4.2D). While the dual blockade of c-Met and EGFR led to sustained inhibition of c-Src, the effect of direct inhibition of c-Src under these conditions remained to be evaluated. Thus, we analyzed the kinetics of c-Src inhibition upon treatment with dasatinib alone and dasatinib in combination with crizotinib + gefitinib. Surprisingly, under both conditions, c-Src remained transiently inhibited (up to 2h) with delayed reactivation between 6-24h. This effect was particularly pronounced in DU145 cells (Fig. 4.2D) and indicates that perhaps some compensatory signaling is activated in response to c-Src inhibition.

A	Breast Cancer			Prostate Cancer			Lung Cancer	
	MDA-MB-231	BT549	MDA-MB-468	DU145	PC3	22RV1	A549	H2170
C	1.2 ± 0.1	1.5 ± 0.03	1.0 ± 0.08	6.5 ± 1.0	4.9 ± 1.6	0.5 ± 0.02	2.0 ± 0.3	3.9 ± 0.6
G	> 10	> 10	5.4 ± 0.6	9.3 ± 1.1	22.1 ± 5.2	47.8 ± 4.8	17.1 ± 4	1.8 ± 0.3
C + G	1.0 ± 0.001	1.5 ± 0.2	0.3 ± 0.03	2.3 ± 0.4	2.0 ± 0.3	0.8 ± 0.08	1.3 ± 0.3	1.2 ± 0.5

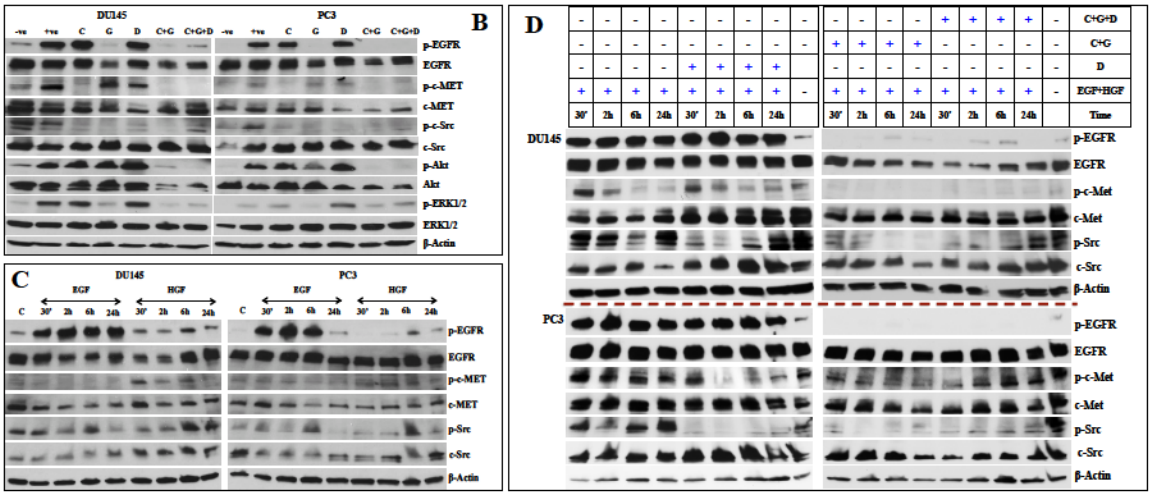

Figure 4.2: (A) IC50 (μM) values of growth inhibition carried out on a panel of breast, prostate and lung cancer cell lines using crizotinib (targeting c-Met), gefitinib (targeting EGFR) and the equimolar combination of the two drugs. Each value represents the average of at least two independent experiments. **(B)** Western blot analysis of the blockade of signaling redundancy between c-Met and EGFR and evaluating the role of c-Src in the receptor interplay using single or equieffective combinations of drugs. **(C)** Western blot analysis of the kinetics of activation of c-Src under EGF (20ng/ml) or HGF (20ng/ml) stimulatory conditions. **(D)** Western blot analysis of the kinetics of c-Met, EGFR and c-Src inhibition under conditions of EGF + HGF (20ng/ml each) stimulation and treatment with single and equieffective combinations of drugs. C = crizotinib, G = gefitinib and D = dasatinib.

4.4.4. Growth inhibitory, anti-invasive and apoptotic properties mediated by tandem targeting of signaling pathways

4.4.4.A. Growth inhibitory potency

Thus far, we have demonstrated using signaling analysis that dual inhibition of c-Met + EGFR (T1 + T2) led to potent blockade of signaling pathways downstream, including the MAPK, PI3K/Akt and c-Src, which are known to promote growth, invasion and survival in cells. We thus evaluated the growth inhibitory, anti-invasive and apoptotic properties mediated by the dual-blockade of T1 + T2. Furthermore, due to the activation of c-Src downstream of c-Met and EGFR and its ability to synergize with both receptors to promote growth and invasion (32-35), we analyzed the effects of blocking T1 + T3 (c-Met + c-Src) and T2 + T3 (EGFR + c-Src). The Chou-Talalay method was used to calculate the combination indices (CI) and determine whether drug combinations were synergistic (CI < 1), additive (CI = 1) or antagonistic (CI > 1) (24). The results showed that the equieffective combination of crizotinib + gefitinib synergistically blocked the growth of DU145 (CI = 0.5) and PC3 cells (CI = 0.2). Likewise, the dual combinations of crizotinib + dasatinib and gefitinib + dasatinib were also synergistic (Fig. 4.3A).

Given the surprising reactivation of c-Src observed in the triple combination designed to target T1 + T2 + T3, we sought to determine the growth inhibitory potency induced by the combination of crizotinib + gefitinib + dasatinib. The CI values for the three-drug combination were also synergistic in both cell lines (CI = 0.3 in DU145 and CI = 0.2 in PC3) (Fig. 3A). More importantly, there was no significant difference between the IC50 values of the equieffective combinations of drugs targeting T1 + T2 (DU145: 3.7 ± 0.7μM, PC3: 2.8 ± 0.9μM), T2 + T3 (DU145: 1.7 ± 0.5μM, PC3: 1.8 ± 0.7μM), T1 + T3

(DU145: 1.8 ± 0.4μM, PC3: 0.9 ± 0.05μM) or T1 + T2 + T3 (DU145: 1.4 ± 0.2μM, PC3: 1.3 ± 0.5μM), indicating that reactivation of c-Src in the triple combination was perhaps inconsequential (Fig. 4.3A).

4.4.4.B Anti-invasive properties

Besides driving growth and proliferation, EGFR and c-Met are also known to promote invasion and metastasis (36, 37). We thus evaluated the anti-invasive properties of blocking the two receptors, T1 + T2, in prostate cancer cells using the Boyden chamber invasion assay (38). Furthermore, c-Src being a major player in driving motility and invasion in cells, we evaluated the anti-invasive outcome of blocking c-Src alone (T3) as well as in combination with c-Met and EGFR, leading to the blockade of T1 + T3 and T2 + T3.

The results showed that the equieffective combination of crizotinib + gefitinib targeting T1 + T2, resulted in 2-3 fold stronger anti-invasive properties in DU145 ($p < 0.0001$) when compared with either single drug alone. No significant difference was seen in PC3 cells, indicating that this effect is cell specific ($p > 0.05$). Blockade of T1 (c-Met) alone did not lead to inhibition of invasion, but blockade of T2 (EGFR) alone led to moderate anti-invasive properties in both cell lines. Furthermore, while inhibition of c-Src (T3) induced equal potency as dual receptor blockade (T1 + T2), tandem inhibition of c-Met and c-Src (T1 + T3) or EGFR and c-Src (T2 + T3), resulted in even stronger anti-invasive properties when compared with T1, T2, T3 or T1 + T2 (e.g. DU145: $p < 0.01$) (Fig. 3B,C). In order to determine whether signaling reactivation associated with the triple combination had an effect on inducing potent anti-invasive properties, we evaluated the

triple drug combination of crizotinib + gefitinib + dasatinib targeting T1 + T2 + T3 in this assay. The results showed that the triple combination exhibited similar activity as the dual combinations of crizotinib + dasatinib targeting T1 + T3 and gefitinib + dasatinib targeting T2 + T3 (Fig. 4.3B,C), indicating that like their growth inhibitory potency, blockade of c-Src reactivation did not significantly enhance anti-invasive potency.

4.4.4.C. Induction of apoptosis

Given the role of EGFR, c-Met and c-Src in activating the PI3K/Akt pathway, we thought it of relevance to analyze the level of apoptosis induced upon tandem inhibition of all three kinases (39-41). The results showed that in PC3 cells, blockade of T1 (c-Met), T2 (EGFR), T3 (c-Src) or T1 + T2 did not induce significant levels of apoptosis compared with the control (Fig. 4.3E). In DU145 cells, blockade of T1 + T2 induced 2-3 fold greater levels of apoptosis compared with the control ($p = 0.02$) (Fig. 4.3D). Furthermore, in both cell lines, blockade of T1 + T2 + T3 induced significantly higher levels of apoptosis compared with the control (DU145: $p = 0.03$, PC3: $p = 0.006$). Importantly, there was no significant difference ($p > 0.05$) in apoptotic activity between crizotinib + gefitinib or crizotinib + gefitinib + dasatinib (Fig. 3D, E), indicating that blockade of c-Src, in addition to modulating the signaling redundancy between c-Met and EGFR did not enhance the apoptotic potency in cells.

A	IC50 (μM)		CI	
	DU145	PC3	DU145	PC3
C + G	3.7 ± 0.7	2.8 ± 0.9	0.5	0.2
G + D	1.7 ± 0.5	1.8 ± 0.7	0.4	0.2
C + D	1.8 ± 0.4	0.9 ± 0.05	0.6	0.5
C + G + D	1.4 ± 0.2	1.3 ± 0.5	0.3	0.2

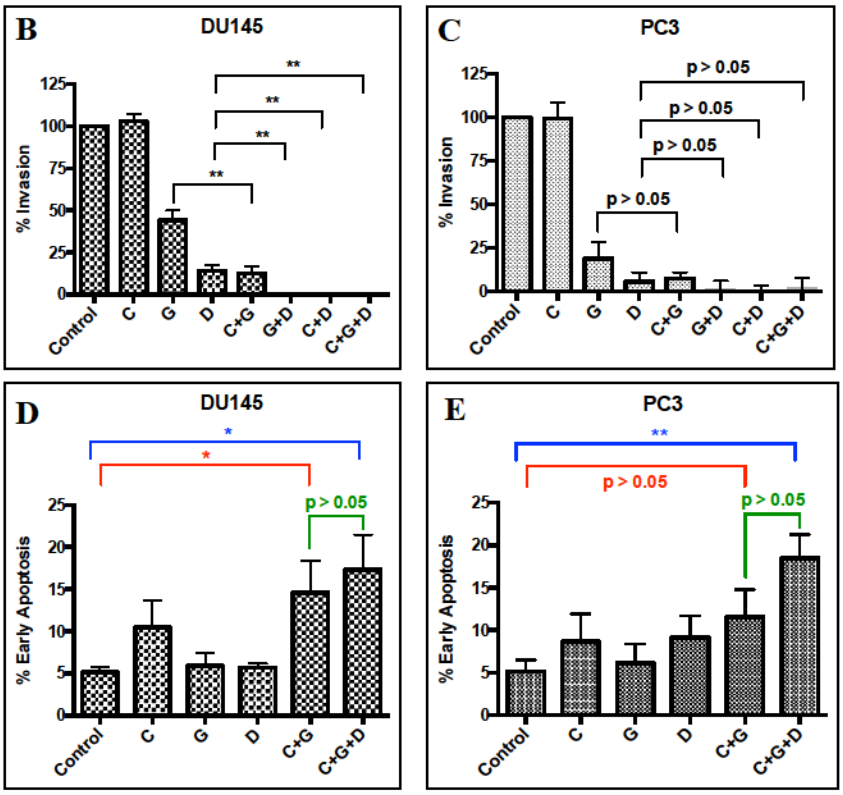

Figure 4.3: (A) IC50 (μM) and combination index (CI) values of growth inhibition assay using equieffective drug combinations targeting c-Met, EGFR and c-Src. CI values were calculated using the Chou-Talalay method where CI < 1 indicates synergy, CI = 1 is additive and CI > 1 is antagonistic. Each value represents the average of at least three independent experiments. Boyden chamber invasion assay in **(B)** DU145 and **(C)** PC3 cells using equieffective doses of drugs. Each value represents the average of at least three independent experiments. Statistical significance between treated groups was calculated one-way ANOVA (**** indicates $p < 0.0001$, ** $p < 0.01$ and $p > 0.05$ is not

significant). Characterization of apoptosis in **(D)** DU145 and **(E)** PC3 cells after treatment with equieffective doses of drugs. Each value represents the average of at least three independent experiments. Statistical significance was calculated using one-tailed student t-test (* indicates $p < 0.05$ and ** $p < 0.001$). C = crizotinib, G = gefitinib and D = dasatinib.

4.4.5. STAT3 activation and compensatory signaling

It is now known that STAT3 can be activated downstream of c-Met, EGFR and c-Src (35, 42). Moreover, given the role of STAT3 compensatory signaling in response to kinase inhibitors, we thought it of interest to investigate its role in the c-Met, EGFR and c-Src interplay, following exposure to crizotinib, gefitinib, dasatinib and their corresponding combinations. As depicted in Figure 4.1, the STAT3 pathway is designated as T4. The results showed that exposure of cells to crizotinib, gefitinib or dasatinib targeting T1, T2 and T3 respectively, primarily inhibited STAT3 phosphorylation at 30 min post-treatment. However, a delayed reactivation began 2h later, indicating the possible activation of a compensatory signaling pathway. It is noteworthy that exposure to the c-Src inhibitor, dasatinib, led to massive reactivation of STAT3, which represents further evidence of the marked propensity of inhibition of T3 (c-Src) to induce compensatory signaling (Fig. 4.4A).

In order to challenge the role of STAT3 activation in the signaling interplay between c-Met, EGFR and c-Src, we targeted JAK1/2, which is a key activator of STAT3 in the JAK/STAT pathway. This was performed with a known clinical inhibitor of JAK1/2, ruxolitinib. The results showed that STAT3 phosphorylation was inhibited in a dose

dependent manner with maximum inhibition seen at the 1μM concentration in both cell lines (Fig. 4.4B).

Having demonstrated that inhibiting the JAK1/2 kinases upstream led to potent inhibition of STAT3 downstream, we further determined whether ruxolitinib could block STAT3 reactivation under crizotinib + gefitinib + dasatinib treatment. This led to combination patterns T1 + T2 + T3 + T4, which was compared with T1 + T2 + T3 using signaling analysis. The results showed that crizotinib + gefitinib + dasatinib potently blocked STAT3 phosphorylation up to 6h with reactivation seen between 24-48h. When ruxolitinib (1μM) was added to this combination, there was potent and sustained inhibition of STAT3 phosphorylation with no reactivation even after 48h, in both cell lines (Fig. 4.4C). This indicated that JAK1/2 was the pathway through which STAT3 was reactivated when cells were exposed to gefitinib, crizotinib, dasatinib or a corresponding combination.

Having successfully identified JAK1/2-STAT3 as being the compensatory signaling pathway activating STAT3, we evaluated the growth inhibitory potency of blocking it in addition to the two and three-drug combinations targeting T1, T2 and T3. The results showed that while ruxolitinib alone (targeting T4) was a poor inhibitor of growth in cells (DU145: 36.4 ± 4.5μM, PC3: 46.6 ± 15.4μM, Fig. 4.S2A), its equieffective combination with crizotinib + gefitinib and crizotinib + gefitinib + dasatinib was synergistic (CI50 values ≤ 0.3) (Fig. 4.4D). However, the CI for a 4-drug combination and the IC50 values were not significantly different from those obtained previously for 2-drug combinations crizotinib + gefitinib targeting T1 + T2 or the 3-drug combination crizotinib + gefitinib +

dasatinib targeting T1 + T2 + T3 (Fig. 4.4E, F, G). This indicates that the additional blockade of JAK1/2-STAT3 (T4) that led to a four-drug combination did not significantly enhance growth inhibitory activity ($p > 0.05$). Furthermore, the addition of ruxolitinib to dasatinib was antagonistic (CI = 1.5) in DU145 and resulted in significantly higher IC50 values when combined with crizotinib + dasatinib (DU145: $p < 0.001$, PC3: $p < 0.01$) or gefitinib + dasatinib (DU145: $p < 0.01$, PC3: $p > 0.05$) in both cell lines (Fig. 4.S2B-D).

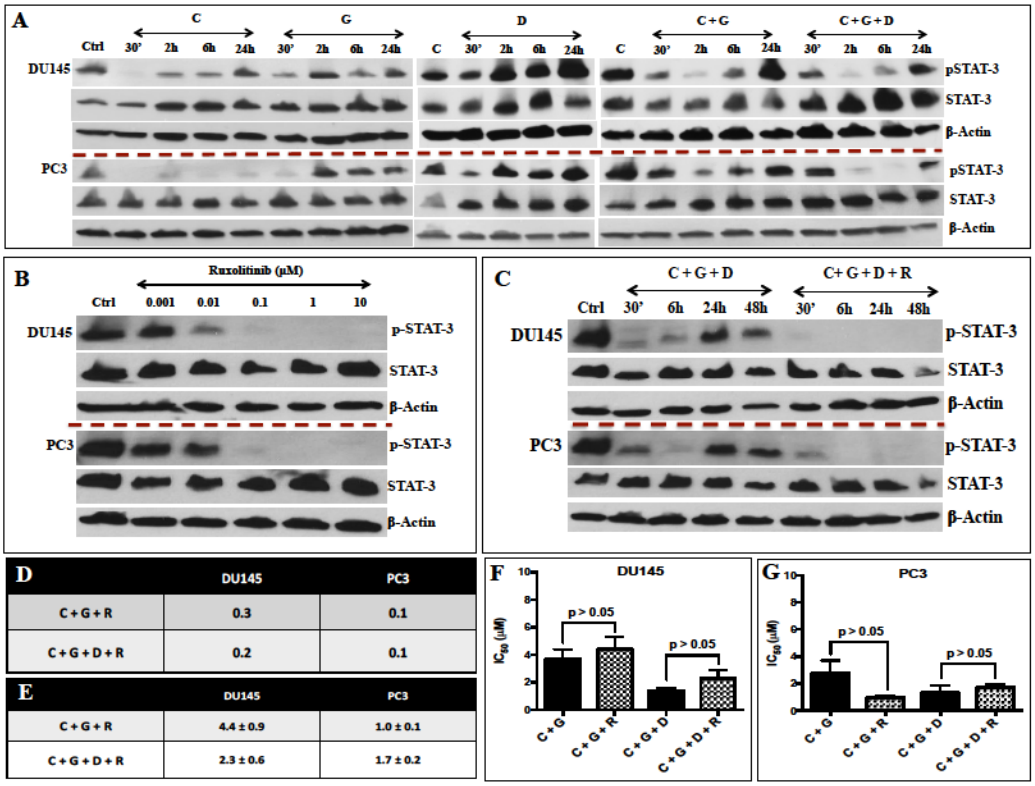

Figure 4.4: **(A)** Western blot analysis of the kinetics of STAT3 inhibition and reactivation in DU145 and PC3 cells treated with equieffective doses of drugs under basal growth conditions. **(B)** Western blot analysis for the dose-dependent inhibition of STAT3 phosphorylation upon treatment with ruxolitinib, a JAK1/2 inhibitor. **(C)** Western blot analysis showing the kinetics of STAT3 inhibition and reactivation upon triple

targeting of T1 (c-Met) + T2 (EGFR) + T3 (c-Src) and quadruple targeting of T1 + T2 + T3 + T4 (JAK1/2/STAT3). **(D)** Combination index (CI) and **(E)** IC50 (μM) values of growth inhibition assay using equieffective drug combinations targeting c-Met, EGFR, c-Src and the JAK1/2/STAT3 pathway. Each value represents the average of at least three independent experiments. **(F)** Histograms representing average IC50 (μM) values of growth inhibition assay using equieffective drug combinations. Each value represents the average of at least three independent experiments. Statistical significance was calculated using one-way ANOVA and $p > 0.05$ implies no significance. C = crizotinib, G = gefitinib, D = dasatinib and R = ruxolitinib.

4.4.6. In vivo activity of two-drug combinations targeting c-Met, EGFR and c-Src

Thus far, our results indicated that in a two-drug combination, inhibition of c-Met and EGFR led to a sustained downregulation of c-Src. In contrast, direct inhibition of c-Src by adding dasatinib to the dual crizotinib + gefitinib combination led to initial inhibition, followed by strong reactivation of c-Src and STAT3. Despite the activation of compensatory signaling, the two- and three-drug combinations were equipotent in inducing growth inhibitory, anti-invasive and apoptotic properties. Furthermore, the 4-drug combination blocking the compensatory signaling activated by JAK1/2 did not enhance growth inhibition. Thus, it appears that the blockade of compensatory signaling added to the number of drugs to be combined, without significantly improving growth inhibitory outcomes. Thus, the two drug combinations, crizotinib + gefitinib, crizotinib + dasatinib and gefitinib + dasatinib, were compared *in vivo* (Fig. 4.5A). Indeed, all three showed significant tumour growth inhibitory activity *in vivo* in a DU145 xenograft model

($p < 0.01$) (Fig. 4.5B). Interestingly, all three combinations showed nearly the same level of growth inhibitory activity with no significant difference between them ($p > 0.05$). These results indicate that dual targeting of RTK-RTK and RTK-non-RTK may be the optimal targeting modality both *in vitro* and *in vivo*.

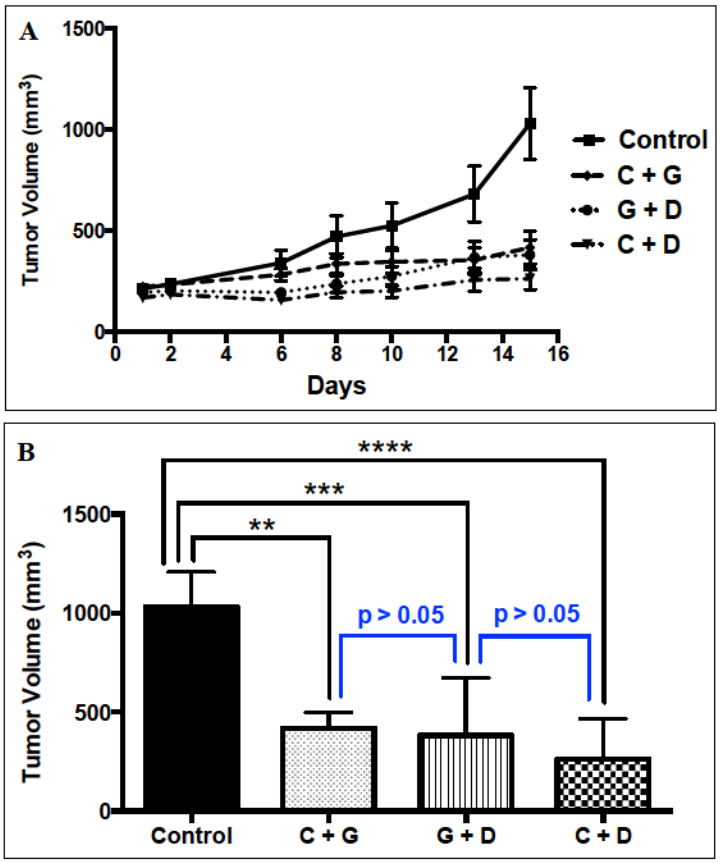

Figure 4.5: (A) Tumour growth curves representing *in vivo* efficacy in a DU145 xenograft model. Male Swiss nude mice (n = 8) bearing tumours on each flank (2 tumours/mouse) were treated with combinations of crizotinib + gefitinib (50mg/kg each), gefitinib (50mg/kg) + dasatinib (10mg/kg), crizotinib (50mg/kg) + dasatinib (10mg/kg) or vehicle administered once daily, orally, for a period of 10 days. **(B)** Histograms represent the average tumour volume ± SEM at the end of the study (day 15) for each group. Statistical significance was calculated using one-way ANOVA (** $p < 0.01$, ***p

< 0.001, ****p < 0.0001 and p > 0.05 indicates no significance). C = crizotinib, G = gefitinib and D = dasatinib.

4.5. DISCUSSION

A complex network of signaling pathways driven by RTKs and non-RTKs characterizes advanced solid tumours and the direct relationship between these pathways and growth or proliferation has made these kinases ideal candidates for selective tumour targeting (43, 44). However, the complexity of these signaling pathways is such that inhibition of one kinase pathway does not suffice to induce sustained growth inhibition. This is believed to be due to several phenomena involving compensatory signaling that have begun to be identified. One such event is signaling redundancy. Here we have not only analyzed signaling redundancy associated with c-Met and EGFR, but also drug-induced compensatory signaling evoked by non-RTKs (e.g. c-Src and JAK1/2) in metastatic CRPC cells (i.e., DU145 and PC3). Although blockade of these mechanisms, i.e. compensatory signaling, appears to require the combinations of multiple kinase inhibitors, we hypothesized that some key signaling pathways, which we refer to as Achilles' heels, could be targeted to induce sustained growth inhibition and this might deter from the use of complex drug cocktails to block the deleterious effects of these networks of signaling. Thus, we analyzed signaling responses associated with key kinases, using their corresponding clinical inhibitors as probes to modulate their interactions. We found that DU145 and PC3 cells responded to the dual blockade of c-Met and EGFR, which was required for complete inhibition of both the MAPK and PI3K/Akt pathways associated with the two receptors. However, previous work by

Parsons and our group have shown that c-Src can synergize with EGFR to promote growth and invasion (19, 45-47). We thus thought it of interest to analyze its role in the signaling redundancy mediated by c-Met and EGFR. Indeed, activation of both receptors led to a time-dependent increase in c-Src phosphorylation and dual blockade of c-Met and EGFR led to potent and sustained inhibition of c-Src. However, downregulation of the signaling redundancy, concomitant with direct blockade of c-Src (triple targeting) revealed interesting dynamics around its phosphorylation. While temporarily inhibited, there was a delayed reactivation of c-Src 6-24h later, especially in DU145 cells, indicating that some compensatory signaling is at play in the process. Negative feedback loops are known to play a crucial role in the reactivation of signaling pathways, which could potentially explain the reactivation of c-Src upon inhibition with dasatinib, both as a single drug and in combination with crizotinib + gefitinib (48). Further analysis revealed that STAT3 was another compensatory pathway activated upon treatment with all kinase inhibitors (as single drug or in combination), with anomalously strong induction of STAT3 phosphorylation seen when cells were treated with dasatinib. Previous reports in the literature suggest that inhibition of c-Src can activate STAT3 via the JAK1/2 pathway (11). It was proposed that c-Src inhibition led to downregulation of SOCS2, a negative regulator of JAK1/2, thus leading to activation of JAK1/2 and subsequent activation of STAT3 (49). A similar feedback mechanism has been implicated in the reactivation of STAT3 upon inhibition of EGFR (50). Thus, this can provide a rational explanation for the activation of STAT3 under conditions where c-Src and EGFR are inhibited.

Given the importance of the JAK1/2-STAT3 pathway in survival, we thought it of interest to determine whether blockade of the latter pathway would further sensitize the cells to the abrogation of the c-Met-EGFR-c-Src interplay. This led to a 4-drug cocktail, which surprisingly, did not further enhance growth inhibitory activity, indicating that perhaps despite its activation, the JAK1/2-STAT3 pathway does not play an effective role in the survival of these cells following kinase inhibition. This result is in agreement with a similar observation by Lee *et al.* (15) who suggested that the inconsequential effect of STAT3 activation might be related to a competitive kinetics between cell death and survival. They suggest that the cells may be engaged in a death pathway that is activated at a faster rate than the compensatory STAT3 survival pathway. While we do not have experimental evidence to support their proposed mechanism, these observations allowed us to question the use of complex cocktails to downregulate multiple signaling pathways as a therapeutic strategy. Furthermore, the strong antagonism observed with the tandem targeting of c-Src and the JAK1/2-STAT3 pathway suggests a complex crosstalk between the two and deters us from using their respective inhibitors in combination. Indeed, in this study, we analyzed the effect of blocking several targeting pathways (T1, T2, T3, T4) using single, dual, triple and 4-drug combinations of kinase inhibitors. Abrogation of the signaling redundancy between c-Met and EGFR with two drugs seemed to lead to sustained inhibition of the MAPK, PI3K/Akt and c-Src pathways. Furthermore, despite induction of compensatory c-Src phosphorylation by its direct inhibitor dasatinib, all the 2-drug combinations including crizotinib + dasatinib (T1 + T3), gefitinib + dasatinib (T2 + T3) and crizotinib + gefitinib (T1 + T2) led to potent inhibition of growth and invasion in CRPC cells, and they were equipotent with the 3-drug combination of crizotinib +

gefitinib + dasatinib (T1 + T2 + T3). This led to the conclusion that modulating the c-Met-EGFR signaling redundancy was a more clinically amenable approach than the 3- and 4-drug combinations. Thus, we evaluated its effect *in vivo* with other 2-drug combinations such as crizotinib + dasatinib (targeting T1 + T3) or gefitinib + dasatinib (targeting T2 + T3). Indeed significant *in vivo* activity was observed with all the two-drug combinations in blocking tumour growth in a DU145 xenograft model. This provides further evidence that dual targeting of two key elements of the interplay can be therapeutically useful.

In summary, as depicted in Figure 4.6, using kinase inhibitors as probes, we identified the signaling redundancy between c-Met and EGFR (T1 + T2) as well as the crosstalk between c-Met and c-Src (T1 + T3) or EGFR and c-Src (T2 + T3) as the Achilles' heel of the CRPC cells. Further attempt to enhance the effect of targeting c-Met-EGFR by additional blockade of c-Src using its direct inhibitor (dasatinib) led to activation of compensatory signaling via c-Src and STAT3. While the true biological significance of these compensatory signaling pathways remains to be elucidated, they do not affect growth inhibitory or anti-invasive potency associated with the blockade of signaling redundancy between c-Met and EGFR or the crosstalk between c-Met and c-Src or EGFR and c-Src. This suggests that the use of complex cocktails for abrogating signaling interplay might not be a requirement for therapeutic outcomes. Our results led to the conclusion that the limitation of the number of targeted pathways to two may be the most recommended therapeutic strategy in castrate resistant prostate tumours co-expressing c-Met, EGFR and c-Src.

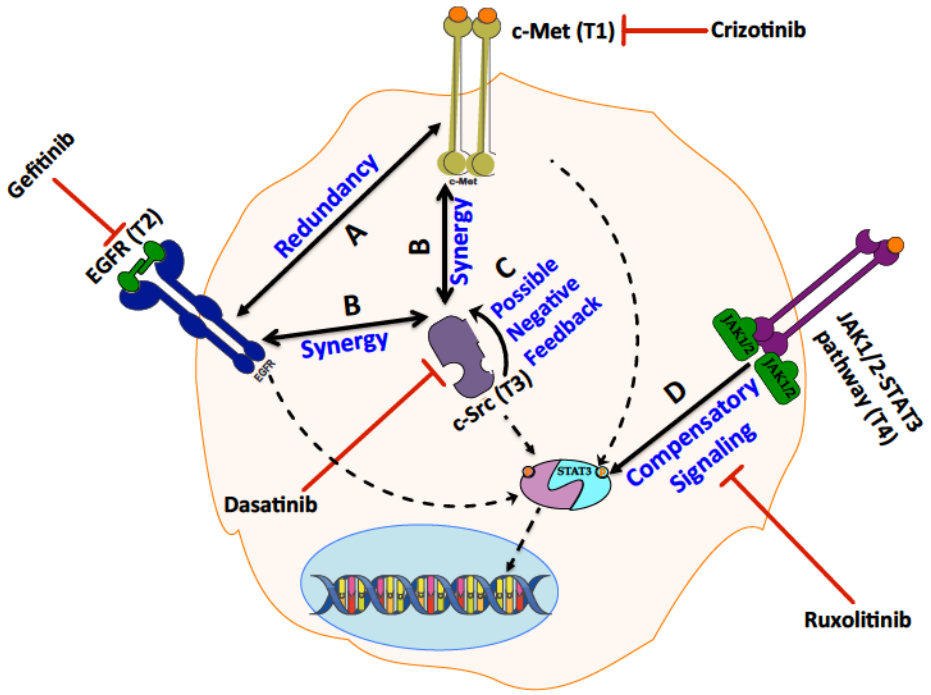

Figure 4.6: Snapshot of signaling crosstalk between receptor and non-receptor tyrosine kinases and the compensatory signaling pathways activated upon treatment with kinase inhibitors in castrate resistant prostate cancer (CRPC) cells. Targeting A (i.e., signaling redundancy between c-Met and EGFR when c-Met is amplified) or B (synergistic crosstalk between c-Met and c-Src or EGFR and c-Src) is the "Achilles' heel" of this interplay. Additional blockade of C (negative feedback activation of c-Src in the presence of dasatinib) or D (reactivation of STAT3 through JAK1/2 compensatory signaling) did not enhance the overall potency.

4.6. ACKNOWLEDGEMENT

We are grateful to Eric Massicotte from the Institut de Recherches Cliniques de Montréal (IRCM) for his help with carrying out the flow cytometry (apoptosis) analysis.

4.7. REFERENCES

1. Nicholson R, Gee J, Harper M. EGFR and cancer prognosis. European Journal of Cancer. 2001;37:9-15.
2. Normanno N, De Luca A, Bianco C, Strizzi L, Mancino M, Maiello MR, et al. Epidermal growth factor receptor (EGFR) signaling in cancer. Gene. 2006;366(1):2-16.
3. Gherardi E, Birchmeier W, Birchmeier C, Woude GV. Targeting MET in cancer: rationale and progress. Nature Reviews Cancer. 2012;12(2):89-103.
4. Heldin C-H. Targeting the PDGF signaling pathway in tumor treatment. Cell Commun Signal. 2013;11(1):97.
5. Goel HL, Mercurio AM. VEGF targets the tumour cell. Nature Reviews Cancer. 2013;13(12):871-82.
6. Arora A, Scholar EM. Role of tyrosine kinase inhibitors in cancer therapy. Journal of Pharmacology and Experimental Therapeutics. 2005;315(3):971-9.
7. Zhang J, Yang PL, Gray NS. Targeting cancer with small molecule kinase inhibitors. Nature Reviews Cancer. 2009;9(1):28-39.
8. Logue JS, Morrison DK. Complexity in the signaling network: insights from the use of targeted inhibitors in cancer therapy. Genes & development. 2012;26(7):641-50.
9. Chong CR, Jänne PA. The quest to overcome resistance to EGFR-targeted therapies in cancer. Nature medicine. 2013;19(11):1389-400.
10. von Manstein V, Yang CM, Richter D, Delis N, Vafaizadeh V, Groner B. Resistance of Cancer Cells to Targeted Therapies Through the Activation of Compensating Signaling Loops. Current signal transduction therapy. 2013;8(3):193.
11. Byers LA, Sen B, Saigal B, Diao L, Wang J, Nanjundan M, et al. Reciprocal regulation of c-Src and STAT3 in non-small cell lung cancer. Clinical Cancer Research. 2009;15(22):6852-61.
12. Chiu H-C, Chou D-L, Huang C-T, Lin W-H, Lien T-W, Yen K-J, et al. Suppression of Stat3 activity sensitizes gefitinib-resistant non small cell lung cancer cells. Biochemical pharmacology. 2011;81(11):1263-70.
13. Huang S, Chen M, Shen Y, Shen W, Guo H, Gao Q, et al. Inhibition of activated Stat3 reverses drug resistance to chemotherapeutic agents in gastric cancer cells. Cancer letters. 2012;315(2):198-205.
14. Lee E-S, Ko K-K, Joe Y, Kang S-G, Hong Y-K. Inhibition of STAT3 reverses drug resistance acquired in temozolomide-resistant human glioma cells. Oncology letters. 2011;2(1):115-21.
15. Lee H-J, Zhuang G, Cao Y, Du P, Kim H-J, Settleman J. Drug resistance via feedback activation of Stat3 in oncogene-addicted cancer cells. Cancer cell. 2014;26(2):207-21.
16. Engelman JA, Zejnullahu K, Mitsudomi T, Song Y, Hyland C, Park JO, et al. MET amplification leads to gefitinib resistance in lung cancer by activating ERBB3 signaling. science. 2007;316(5827):1039-43.
17. Guix M, Faber AC, Wang SE, Olivares MG, Song Y, Qu S, et al. Acquired resistance to EGFR tyrosine kinase inhibitors in cancer cells is mediated by loss of IGF-binding proteins. The Journal of clinical investigation. 2008;118(7):2609.

18. Yonesaka K, Zejnullahu K, Okamoto I, Satoh T, Cappuzzo F, Souglakos J, et al. Activation of ERBB2 signaling causes resistance to the EGFR-directed therapeutic antibody cetuximab. Science translational medicine. 2011;3(99):99ra86-99ra86.
19. Rao S, Larroque-Lombard A-L, Peyrard L, Thauvin C, Rachid Z, Williams C, et al. Target Modulation by a Kinase Inhibitor Engineered to Induce a Tandem Blockade of the Epidermal Growth Factor Receptor (EGFR) and c-Src: The Concept of Type III Combi-Targeting. PloS one. 2015;10(2).
20. Dulak AM, Gubish CT, Stabile LP, Henry C, Siegfried JM. HGF-independent potentiation of EGFR action by c-Met. Oncogene. 2011;30(33):3625-35.
21. Xu H, Stabile LP, Gubish CT, Gooding WE, Grandis JR, Siegfried JM. Dual blockade of EGFR and c-Met abrogates redundant signaling and proliferation in head and neck carcinoma cells. Clinical Cancer Research. 2011;17(13):4425-38.
22. Mueller KL, Hunter LA, Ethier SP, Boerner JL. Met and c-Src cooperate to compensate for loss of epidermal growth factor receptor kinase activity in breast cancer cells. Cancer research. 2008;68(9):3314-22.
23. Skehan P, Storeng R, Scudiero D, Monks A, McMahon J, Vistica D, et al. New colorimetric cytotoxicity assay for anticancer-drug screening. J Natl Cancer Inst. 1990;82(13):1107-12.
24. Chou T-C, Talalay P. Quantitative analysis of dose-effect relationships: the combined effects of multiple drugs or enzyme inhibitors. Advances in enzyme regulation. 1984;22:27-55.
25. Subik K, Lee J-F, Baxter L, Strzepek T, Costello D, Crowley P, et al. The expression patterns of ER, PR, HER2, CK5/6, EGFR, Ki-67 and AR by immunohistochemical analysis in breast cancer cell lines. Breast cancer: basic and clinical research. 2010;4:35.
26. Yamasaki F, Johansen MJ, Zhang D, Krishnamurthy S, Felix E, Bartholomeusz C, et al. Acquired resistance to erlotinib in A-431 epidermoid cancer cells requires down-regulation of MMAC1/PTEN and up-regulation of phosphorylated Akt. Cancer research. 2007;67(12):5779-88.
27. Reshetnikova G, Troyanovsky S, Rimm DL. Definition of a direct extracellular interaction between Met and E-cadherin. Cell biology international. 2007;31(4):366-73.
28. Puri N, Salgia R. Synergism of EGFR and c-Met pathways, cross-talk and inhibition, in non-small cell lung cancer. Journal of carcinogenesis. 2008;7(1):9.
29. Sohn J, Liu S, Parinyanitikul N, Lee J, Hortobagyi GN, Mills GB, et al. cMET Activation and EGFR-Directed Therapy Resistance in Triple-Negative Breast Cancer. Journal of Cancer. 2014;5(9):745.
30. El Sheikh SS, Domin J, Abel P, Stamp G, Lalani E-N. Phosphorylation of both EGFR and ErbB2 is a reliable predictor of prostate cancer cell proliferation in response to EGF. Neoplasia. 2004;6(6):846-53.
31. Humphrey PA, Zhu X, Zarnegar R, Swanson PE, Ratliff TL, Vollmer RT, et al. Hepatocyte growth factor and its receptor (c-MET) in prostatic carcinoma. The American journal of pathology. 1995;147(2):386.
32. Koppikar P, Choi S-H, Egloff AM, Cai Q, Suzuki S, Freilino M, et al. Combined inhibition of c-Src and epidermal growth factor receptor abrogates growth and invasion of head and neck squamous cell carcinoma. Clinical Cancer Research. 2008;14(13):4284-91.

33. Lotz M, Wang HH-F, Cance W, Matthews J, Pories S. Epidermal growth factor stimulation can substitute for c-Src overexpression in promoting breast carcinoma invasion. Journal of Surgical Research. 2003;109(2):123-9.
34. Sen B, Peng S, Saigal B, Williams MD, Johnson FM. Distinct interactions between c-Src and c-Met in mediating resistance to c-Src inhibition in head and neck cancer. Clinical Cancer Research. 2011;17(3):514-24.
35. Organ SL, Tsao M-S. An overview of the c-MET signaling pathway. Therapeutic advances in medical oncology. 2011;3(1 suppl):S7-S19.
36. Bonaccorsi L, Marchiani S, Muratori M, Forti G, Baldi E. Gefitinib ('IRESSA', ZD1839) inhibits EGF-induced invasion in prostate cancer cells by suppressing PI3 K/AKT activation. Journal of cancer research and clinical oncology. 2004;130(10):604-14.
37. Han Y, Luo Y, Zhao J, Li M, Jiang Y. Overexpression of c‐Met increases the tumor invasion of human prostate LNCaP cancer cells in vitro and in vivo. Oncology letters. 2014;8(4):1618-24.
38. Boyden S. The chemotactic effect of mixtures of antibody and antigen on polymorphonuclear leucocytes. The Journal of experimental medicine. 1962;115(3):453-66.
39. Scaltriti M, Baselga J. The epidermal growth factor receptor pathway: a model for targeted therapy. Clinical Cancer Research. 2006;12(18):5268-72.
40. Peruzzi B, Bottaro DP. Targeting the c-Met signaling pathway in cancer. Clinical Cancer Research. 2006;12(12):3657-60.
41. Thomas SM, Brugge JS. Cellular functions regulated by Src family kinases. Annual review of cell and developmental biology. 1997;13(1):513-609.
42. Johnston PA, Grandis JR. STAT3 signaling: anticancer strategies and challenges. Molecular interventions. 2011;11(1):18.
43. Zhang DY, Ye F, Gao L, Liu X, Zhao X, Che Y, et al. Proteomics, pathway array and signaling network-based medicine in cancer. Cell Div. 2009;4:20.
44. Werner HM, Mills GB, Ram PT. Cancer Systems Biology: a peek into the future of patient care? Nature Reviews Clinical Oncology. 2014;11(3):167-76.
45. Kloth MT, Laughlin KK, Biscardi JS, Boerner JL, Parsons SJ, Silva CM. STAT5b, a mediator of synergism between c-Src and the epidermal growth factor receptor. Journal of Biological Chemistry. 2003;278(3):1671-9.
46. Belsches AP, Haskell MD, Parsons SJ. Role of c-Src tyrosine kinase in EGF-induced mitogenesis. Front Biosci. 1997;2:d501-d18.
47. Larroque‐Lombard AL, Ning N, Rao S, Lauwagie S, Halaoui R, Coudray L, et al. Biological Effects of AL622, a Molecule Rationally Designed to Release an EGFR and ac‐Src Kinase Inhibitor. Chemical biology & drug design. 2012;80(6):981-91.
48. Chandarlapaty S. Negative feedback and adaptive resistance to the targeted therapy of cancer. Cancer discovery. 2012;2(4):311-9.
49. Sen B, Peng S, Woods DM, Wistuba I, Bell D, El-Naggar AK, et al. STAT5A-mediated SOCS2 expression regulates Jak2 and STAT3 activity following c-Src inhibition in head and neck squamous carcinoma. Clinical Cancer Research. 2012;18(1):127-39.

50. Wu K, Chang Q, Lu Y, Qiu P, Chen B, Thakur C, et al. Gefitinib resistance resulted from STAT3-mediated Akt activation in lung cancer cells. Oncotarget. 2013;4(12):2430.

4.8. SUPPLEMENTARY FIGURES

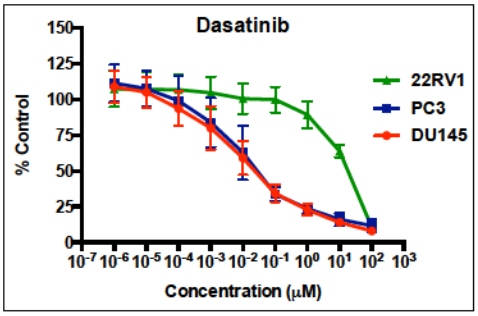

	DU145	PC3	22RV1
Dasatinib	0.04 ± 0.01	0.05 ± 0.03	15.1 ± 1.8

Figure 4.S1: Growth inhibition assay with dasatinib and its IC50 values (μM) in prostate cancer cell lines.

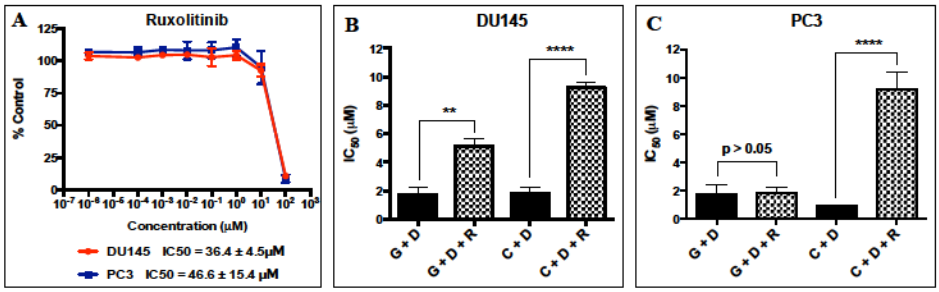

D	IC50 (μM)		CI	
	DU145	PC3	DU145	PC3
C + R	10.3 ± 0.3	11.5 ± 0.2	0.5	0.6
G + R	7.9 ± 1.2	4.0 ± 0.9	0.4	0.1
D + R	25.0 ± 3.0	16.0 ± 1.3	1.5	0.8
C + G + R	4.4 ± 0.9	1.0 ± 0.1	0.3	0.1
G + D + R	5.1 ± 0.5	1.8 ± 0.4	0.4	0.1
C + D + R	9.2 ± 0.3	9.2 ± 1.2	0.7	0.6
C + G + D + R	2.3 ± 0.6	1.7 ± 0.2	0.2	0.1

Figure 4.S2: (A) IC50 (μM) values of growth inhibition assay on prostate cancer cells using ruxolitinib (JAK1/2 inhibitor). **(B, C)** Average histograms representing IC50 (μM) values (± SEM) for equieffective combinations of drugs in a growth inhibition assay. Statistical significance was calculated using one-way ANOVA and $p > 0.05$ indicates no significance. **(D)** Table summarizing the IC50 (μM) and CI values for single, dual, triple and quadruple combinations with ruxolitinib in growth inhibition assay. Each value represents the average of at least three independent experiments in **A-D**. C = crizotinib, G = gefitinib, D = dasatinib and R = ruxolitinib.

CONNECTING TEXT

In the previous chapter, we uncovered the signaling redundancy between c-Met and EGFR as well as their ability to synergize to promote growth, proliferation, invasion and survival in castrate resistant prostate cancer cells. Furthermore, we also demonstrated their synergistic crosstalk with c-Src in driving growth and proliferation of prostate cancer cells, both *in vitro* and *in vivo*. Finally, we also elucidated the activation of the compensatory JAK1/2-STAT3 pathway and showed that complex cocktails of drugs involving 3 or 4 inhibitors are not required for optimum growth inhibitory potency. Targeting two of the kinases involved in adverse signaling (e.g. EGFR-c-Src, EGFR-c-Met or c-Met-c-Src) seem to be sufficient and these targets were designated as the Achilles' heels of these advanced metastatic prostate cancer cells.

Overall, through the use of equimolar and equieffective combinations of clinical inhibitors, we demonstrated the strong antitumour potency associated with dual targeting of kinases, further lending support to the design and development of combi-molecules targeting EGFR-c-Src or EGFR-c-Met. While median-effect calculations proposed by Chou and Talalay determines the potency of equieffective drug combinations, little is known about methods to evaluate the potency of equimolar drug combinations, or their unimolecular analogs such as hybrid or combi-molecules. Thus, in the next chapter, we not only designed novel EGFR-c-Met targeting combi-molecules, but also developed simple models to predict the potency of equimolar drug combinations and their unimolecular analogs on a given cell system. We discovered new relationships that allowed to better describing the notion of "balanced targeting" and we established

quantitative parameters to validate the use of a single combi-molecule instead of a simple equimolar 2-drug combination.

CHAPTER 5

QUANTITATIVE ANALYSIS OF THE POTENCY OF EQUIMOLAR TWO-DRUG COMBINATIONS AND COMBI-MOLECULES INVOLVING KINASE INHIBITORS AGAINST HUMAN TUMOUR CELLS: THE CONCEPT OF BALANCED TARGETING

Suman Rao[1], Benoît Thibault[1], Lisa Peyrard[1], Anne-Laure Larroque-Lombard[1], Martin Rupp[1], Cedric Thauvin[1], Bertrand J. Jean-Claude[1]

[1]The Research Institute of the McGill University Health Center (MUHC), 1001 Decarie Blvd, Block E, Montreal, Quebec, H4A 3J1, Canada

5.1. ABSTRACT

The median-effect principle proposed by Chou and Talalay has proven the most effective approach to parameterize interactions between two or more agents given in combination. However, this method cannot be used to evaluate the effectiveness of equimolar drug combinations, which are now comparative references for dual targeting molecular design. Here, using data acquired through the development of a novel class of hybrid molecules termed "combi-molecules" designed to block two kinases (e.g. EGFR-c-Src, EGFR-c-Met), we discovered new relationships that can be derived to establish potency indices for equimolar and dual targeted molecules. We found that if the fold-difference (defined as **κ**) between the IC50 of the two individual kinase inhibitors was > 6, the IC50 of their corresponding equimolar combinations resembled that of the more potent inhibitor. Hence, the "combi-targeting" of the two kinases was considered "imbalanced" and the combination "ineffective". However, if **κ** was ≤ 6, the IC50 of the combination fell below that of each individual drug. Hence, the combination was considered "effective" and the targeting "balanced". Effectiveness could be parameterized using a potency index **ε**, which linearly increased with **κ** (R^2=0.95). The observed data allowed to establish that **ε** < 5 indicated balanced targeting and > 5 imbalanced targeting. We also established that hybrid or combi-molecules should be compared with equimolar combinations only under balanced conditions and proposed a new parameter **Ω** for validating their effectiveness. A given multi-targeted drug is said to be effective if **Ω,** defined as a fraction of its IC50 over that of its corresponding balanced equimolar combination, is less than 1.

5.2. INTRODUCTION

The implication of several signaling proteins in a complex network of signal transduction pathways is a commonly occurring event in advanced cancers. These signaling interactions between growth factor receptors including the epidermal growth factor receptor (EGFR), hepatocyte growth factor receptor (c-Met), platelet derived growth factor receptor (PDGFR), vascular endothelial growth factor receptor (VEGFR), etc. and cytoplasmic non-receptor tyrosine kinases and transcription factors (c-Src, c-Abl, JAKs, STAT3, β-catenin, etc.) not only synergize to promote tumour growth, survival and metastasis, but also mediate resistance to targeted therapies through the activation of compensatory signaling pathways (1-3). Thus in recent years, strategies designed to overcome resistance mediated by compensatory signaling have involved the use of a multi-targeted approach (4, 5). Within this context, over the past decade, we developed a novel approach termed "combi-targeting" that sought to design agents designated as "combi-molecules" capable of inducing tandem blockade of two divergent biological targets (e.g. EGFR and DNA) (6-9). Further work on the concept led to the synthesis of molecules rationally designed to target two oncogenic tyrosine kinases involved in adverse signaling (10, 11). More specifically, we demonstrated the feasibility of combi-molecules capable of blocking c-Src and EGFR as intact molecules and further degrading to two intact inhibitors of the two targets. Such types of molecules capable of behaving as dual targeting agents, while being a prodrug of two active inhibitors, were designated as type III targeting molecules. This designation was chosen to distinguish them from their type I and type II predecessors (12). Type I combi-molecules are designed to block only one target as an intact molecule and require hydrolysis to be able to block their secondary

target (8, 13-15). Type II combi-molecules are dual targeting molecules that do not require hydrolysis to hit their two targets (16, 17). The targeting mode that is referred to as type II is the most commonly used approach in the literature and the resulting molecules are often referred to as hybrid or chimeric molecules (18, 19). Regardless of how they are referred to, combi- or hybrid molecules are considered to be carriers of two or more equimolar agents generating two or more distinct effects, each of which being associated with one of the moieties of the parent molecule. Thus, their potency is often evaluated in comparison with equimolar combinations of agents acting by the same mechanisms of action (20-22).

Recent efforts toward inducing a tandem blockade of multiple signaling pathways have added interest in the use of equimolar combinations. We and others have frequently used them as reference for studying the biological effects of newly designed hybrid molecules (11, 15, 22-24). More recently, we used them as pharmacological tools to identify and block signaling nodes mediated by EGFR, c-Met and c-Src in tumour cells [Rao *et al.* 2015, under review (45)]. Despite the extensive use of equimolar combinations as reference for multi-targeted drugs and current interest in combinations of targeted agents, little is known about criteria to define the magnitude of potency of mixtures of two drugs administered *in vitro* in an equimolar combination modality.

In the past, Chou and Talalay (25) demonstrated that the type of interactions between two or more drugs combined in an equieffective ratio could be parameterized by the median effect principle, whereby the combination index (CI) is used to define synergy when the value is < 1, additivity when the value is 1 and antagonism when the value is > 1 (25-27). However, such calculations cannot be performed under conditions where the drugs

are combined in an equimolar ratio, a condition that is best suited for comparisons with hybrid drugs or combi-molecules (22, 23, 28, 29). In this study, using current and past data acquired from our kinase-kinase and kinase-DNA targeting programs, we propose a quantitative model based on simple mathematical equations for determining the degree of effectiveness of an equimolar drug combination and also exploited their similarity to hybrid drug and combi-molecules to propose attrition criteria for developing combi-molecules.

The approach we chose to study was to target tyrosine kinases such as c-Src, c-Met, EGFR, which are known to be involved in a complex signaling interplay. Here we first determined the IC50 values for growth inhibition induced by their clinical inhibitors both as single agents and equimolar combinations against human cancer cell lines of various histological origins and subsequently analyzed the trends of the IC50 values of these combinations in comparison with individual drugs. For studying the parameterization of the potency of combi-molecules in comparison with equimolar combinations of individual kinase inhibitors, we used the AL-series of EGFR-c-Src targeting molecules (Fig. 5.5A) (12) and for the newly synthesized EGFR-c-Met targeting, LP121 (Fig. 5.5A). We found a linear correlation between the fold-difference between the IC50 values of drugs alone and a new proposed parameter for effectiveness referred to as **ε**. Based upon the analyzed data, we proposed that combinations are considered effective when **ε** < 5, a range under which the two tyrosine kinase inhibitors are considered to be targeted in a balanced fashion. Likewise, we propose that a hybrid or combi-molecule can be considered effective in a given cell system when its IC50 for growth inhibition is lower or equal to that of a combination with **ε** value < 5.

5.3. MATERIALS AND METHODS

5.3.1. Combi-molecule synthesis

The EGFR-c-Src combi-molecules AL660, AL690, AL692 and AL739 and the EGFR-c-Met targeting combi-molecule, LP121 were synthesized according to the methods described in the supplementary section. AL776 was synthesized according to methods previously described in Rao *et al.,* 2015 (12).

5.3.2. Cell culture

The human cancer cell lines used in the present study include breast (MDA-MB-231, BT549, MDA-MB-468), prostate (DU145, PC3 and 22RV1), lung (A549, A427, A427-MGMT, H2170, H1975 and HCC827), Chinese hamster lung cancer cells (VC8 and VC8-MGMT), ovarian (IGROV-1, SKOV-3, EFO-21, A2780 and OVCAR-3), head & neck (UM22A), NIH3T3 wild type (Wt), EGFR (Her14) and Her2 (Neu) transfected cells, and mouse mammary tumour 4T1 cells. The prostate cancer cells were a generous gift from Dr. Amina Zoubeidi (Vancouver Prostate Centre, Department of Urologic Sciences, University of British Columbia). 4T1, U87 and U87-MGMT cells were a generous gift from Dr. Thierry Muanza (Department of Oncology, Division of Radiation Oncology, Jewish General Hospital, Montreal, Canada). 4T1 cells were originally isolated by Dr. Fred Miller (Karmanos Cancer Institute, MI, USA) (30). The NIH3T3 panel of cells was a generous gift from Dr. Moulay Alaoui-Jamali (Lady Davis Institute for Medical Research Sir Mortimer B. Davis, Jewish General Hospital, Montreal, Canada). IGROV-1 cells were a generous gift from the Gustave Roussy Institute (Villejuif, France). A2780 cells were purchased from Sigma Aldrich (France). V79 and

V79 MGMT were kindly given by Dr. Bernd Kaina (Institute of Toxicology, University Medical Center, Mainz, Germany). A427-MGMT were obtained from American Type Culture Collection (ATCC, VA, USA) and transfected with MGMT in our lab (7). The remaining cell lines were purchased from the ATCC. H1975, HCC827, IGROV-1, SKOV-3, EFO-21, A2780 and OVCAR-3 cells were maintained in RPMI-1640 medium. The remaining cell lines were maintained in Dulbecco Modified Eagle's Medium (DMEM). Both media were supplemented with 10% FBS, 10mM HEPES, 2mM L-glutamine, gentamycin sulfate and fungizone (all reagents purchased from Wisent Inc., St-Bruno, Canada). Cells were grown in a humidified incubator with 5% CO_2 at 37°C.

5.3.3 Drug Treatment

Crizotinib was purchased from PharmaBlock USA, Inc. (CA, USA), gefitinib from the Royal Victoria Hospital (Montreal, Canada) pharmacy and extracted from pills in our laboratory. Dasatinib was purchased from Ark Pharm Inc., USA. Temozolomide was extracted form Temodal pills purchased form Merck/Schering Plough, USA. All drugs were dissolved in DMSO to obtain a concentration of 40mM or lower. Drug dilutions were carried out under sterile conditions using RPMI or DMEM (10% FBS) medium and the final concentration of DMSO never exceeded 1% (v/v).

5.3.4. Growth Inhibition Assay

Sulforhodamine B assay was used to measure growth inhibition in cells (31). Cells were plated (5000-10,000 cells/well) and 24h later treated with a dose range of single or combinations of drugs. After 5 days of treatment, cells were fixed in 50% trichloroacetic

acid (TCA) for 2-3h at 4°C, washed 4 times under cold tap water and stained with SRB (0.4 %) for 2h-overnight at room temperature. Plates were rinsed with 1% acetic acid, and allowed to dry overnight, stained cells were dissolved in 10mM Tris-Base and the plates were read using a microplate reader ELx808 (492 nm). GraphPad Prism 6.0 (GraphPadSoftware, Inc., San Diego, CA) was used for data processing. Each experiment was repeated at least twice, in triplicate.

5.3.5. *In Vitro* Kinase Assay

EGFR and c-Met *in vitro* kinase assays were carried out in 96-well plates (Nunc Maxisorp) coated with PGT (poly L-glutamic acid L-tyrosine, 4:1, Sigma Aldrich, MO, USA) and incubated at 37ºC for 48h. PGT was the substrate to be phosphorylated by EGFR (Enzo Life Sciences Inc, NY, USA, Signal Chem, Richmond, Canada) or c-Met (BPS Bioscience, CA, USA) in the presence of ATP (50μM). Drugs (LP121, gefitinib and crizotinib) were added, followed by 13.3 ng/well of isolated EGFR (0.1μg/μl) or 32ng/well of c-Met (0.75μg/μl). The HRP-conjugated anti-phosphotyrosine antibody (Santa Cruz Biotechnology, CA) was used for phosphorylated substrate detection. The signal was developed using 3,3',5,5'-tetramethylbenzidine peroxidase substrate (Kierkegaard and Perry Laboratories, Gaithersburg, MD) and assessed using a microplate reader ELx808 at 450nm (BioTek Instruments). GraphPad Prism 6.0 (GraphPadSoftware, Inc., San Diego, CA) was used for IC50 determination and each experiment was repeated at least twice, in duplicate.

5.3.6. Western Blot analysis

4T1 cells were plated (~ $1x10^6$ cells/well) and 24h later rinsed twice with PBS and starved overnight using serum-free media. They were next treated with various concentrations of LP121 and 5μM of crizotinib, gefitinib and the equimolar combination of crizotinib + gefitinib (5μM each), for 2h, washed with PBS twice and stimulated with 50ng/ml EGF + HGF, each for 30 min at 37ºC. Western blot analysis was carried out according to methods previously described by Rao *et al.* (12), Phosphotyrosine antibodies against EGFR (Y1068), c-Met (Y1234/1235) and total c-Met antibodies were purchased from Cell Signaling Technology, USA. Total EGFR and actin antibodies were purchased from Santa Cruz Biotechnology, Inc., USA. Immunoblot bands were visualized using Pierce™ ECL Western Blotting Substrate (Life Technologies Inc., ON, Canada).

5.4. RESULTS

5.4.1. Growth inhibitory potency of single versus equimolar combinations of clinical inhibitors on a panel of cancer cell lines

5.4.1.A.EGFR-c-Src targeting

In order to profile the responses, we primarily screened a panel of cancer cell lines using single and equimolar combinations of clinically approved tyrosine kinase inhibitors (TKIs) targeting kinases engaged in synergistic crosstalk, and further extended the screening to kinase-DNA targeting drug combinations. The cell lines used in this study included breast, lung, prostate, ovarian, head and neck and brain cancer cells along with the NIH3T3 panel of wild type, EGFR and Her2 transfected cell lines. Clinical TKIs including gefitinib (EGFR inhibitor), crizotinib (c-Met inhibitor), dasatinib (c-Src inhibitor) and the DNA alkylating agent, temozolomide were used (Fig. 5.1A). In all the

cell lines, the range of IC50 for dasatinib varied from 0.01 ± 0.0003μM to 16.4 ± 5.2μM whereas, those for gefitinib varied from 0.22 ± 0.01μM to as high as 73.7 ± 7.7μM, except in the EGFR TKI sensitive HCC827 cell line with a deletion in exon 19 in the EGFR kinase domain (Del E746-A750), where it showed an IC50 value in the nanomolar range (0.003 ± 0.0005μM). Importantly, when the two drugs were combined (gefitinib + dasatinib) in an equimolar manner in this cell line, the IC50 of the combination fell in the range of that of dasatinib. It is noteworthy that in HCC827 cells that showed an IC50 for dasatinib 30-fold less than that of gefitinib, the IC50 of the combination was in the same range as that of the latter. The IC50 values of the gefitinib + dasatinib equimolar combination fell below that of each individual drug only in MDA-MB-468, 22RV1, UM22A and A2780 cells wherein dasatinib and gefitinib exhibited IC50 values in the 1-4 fold-difference range (Fig. 5.1A). The overall response profiles are depicted in the average graphs as shown in figures 5.1B-G, and calculated as the IC50 of the drug in a given cell line minus the average IC50 of the drug in the entire panel of cell lines. Response profiles were calculated for gefitinib, dasatinib and the equimolar combination of the two for cell lines exhibiting IC50 values of gefitinib and dasatinib in different or similar ranges. As can be seen, the response profile of gefitinib + dasatinib (Fig. 5.1D) resembled more that of dasatinib (the drug that is 6-fold more potent than gefitinib) (Fig. 5.1B-D). By contrast, in the cell panel in which gefitinib and dasatinib showed response profiles of similar magnitude, the combination of gefitinib + dasatinib (Fig. 5.1G) appeared to yield IC50 values in a lower range than that of each individual profile, indicating enhanced potency when compared with each drug alone (Fig. 5.1E-G). This

represents what we define as “balanced targeting”, a sharp contrast with profiles B-D that clearly exemplify a case of “unbalanced targeting”.

A

		Cell line	Gefitinib (μM)	Dasatinib (μM)	Fold Difference (κ)	Gefitinib + Dasatinib (μM)	Potency Index (ε)
Different Range IC50	Breast	MDA-MB-231[1]	19.7 ± 1.2	0.05 ± 0.01	755	0.04 ± 0.02	605.5
		BT549	73.7 ± 7.7	0.15 ± 0.08	491	0.06 ± 0.02	196.8
		4T1[1]	11.4 ± 1.0	0.09 ± 0.01	127	0.09 ± 0.002	128
	Prostate	DU145	9.3 ± 1.1	0.04 ± 0.01	232	0.01 ± 0.007	58.2
		PC3	22.1 ± 5.3	0.05 ± 0.03	442	0.04 ± 0.02	354.4
	Lung	H1975	7.1 ± 0.8	0.17 ± 0.03	42	0.15 ± 0.01	37.9
		HCC827	0.003 ± 0.0005	0.09 ± 0.01	30	0.001 ± 0.0005	10.3
	Ovarian	OVCAR-3	8.4 ± 0.88	0.01 ± 0.0003	840	0.01 ± 0.0002	841
		IGROV-1	0.46 ± 0.15	0.01 ± 0.0003	46	0.01 ± 0.0003	47
		SKOV-3	13.1 ± 4.8	0.01 ± 0.0003	1310	0.01 ± 0.003	1311
		EFO-21	0.22 ± 0.01	0.01 ± 0.001	22	0.01 ± 0.005	23
Similar Range IC50	Prostate	22RV1	47.8 ± 4.8	15.1 ± 1.8	3	8.4 ± 1.3	2.2
	Breast	MDA-MB-468	5.4 ± 0.6	6.2 ± 1.4	1	2.0 ± 0.8	0.7
	Head and Neck	UM22A	1.1 ± 0.2	0.3 ± 0.09	4	0.02 ± 0.018	0.3
	Ovarian	A2780	6.5 ± 1.9	4.8 ± 0.9	1	2.3 ± 0.32	0.8
	Wild type and Transfected	NIH3T3-Wt[1]	12.6 ± 2.1	16.4 ± 5.2	1	5.9 ± 1.1	0.8
		NIH3T3-Her14[1]	0.35 ± 0.04	0.81 ± 0.3	2	0.05 ± 0.006	0.4
		NIH3T3-Neu	0.34 ± 0.03	0.6 ± 0.3	2	0.03 ± 0.009	0.3

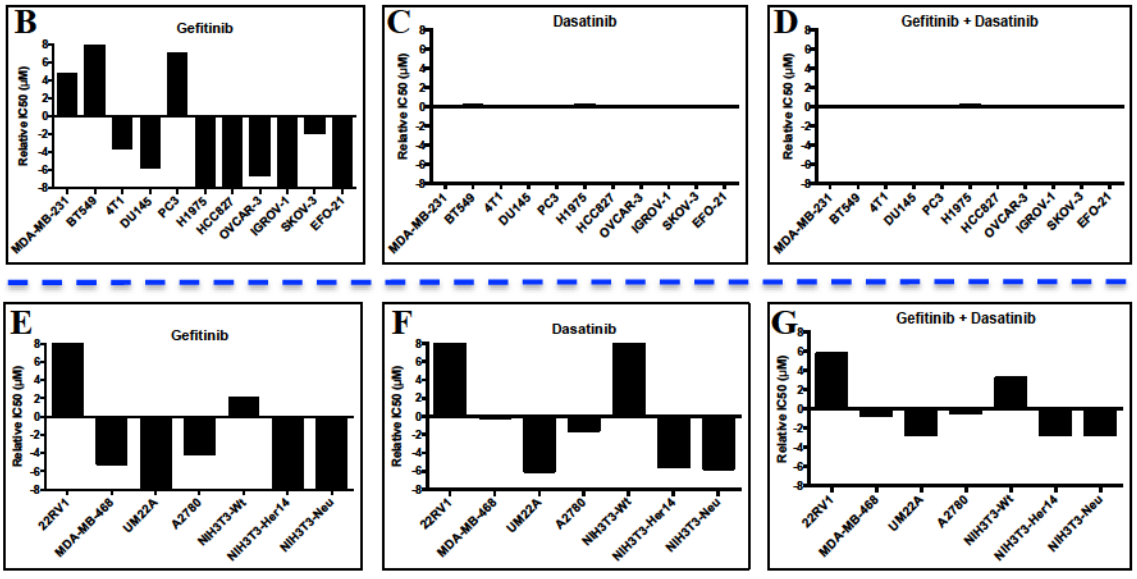

Figure 5.1: (A) IC50 values of tumour cell growth inhibition on a panel of human cancer cell lines using gefitinib (EGFR kinase inhibitor), dasatinib (c-Src kinase inhibitor) and

their equimolar combination [[1]Rao S. *et al.,* 2015 (12)]. The fold-difference between the IC50 values of the two individual drugs is denoted by κ and the potency index as described in equation **1** is defined by ε. **(B-G)** Relative IC50 values (IC50 of individual drug minus the average IC50 of the drug on the entire panel of cell lines) of gefitinib, dasatinib and their equimolar combination for **(B-D)** $\kappa > 6$ and **(E-G)** $\kappa \leq 6$.

5.4.1.B EGFR-c-Met targeting

Further studies targeting c-Met and EGFR with crizotinib and gefitinib, respectively, showed a similar trend as described above, with IC50 values for crizotinib ranging from 0.22 ± 0.01μM to 13.1 ± 4.8μM and generally lower than that for gefitinib (to 0.51 ± 0.24μM to 73.7 ± 7.7μM) (Fig. 5.2A). The IC50 values for the equimolar combination of crizotinib + gefitinib resembled that of crizotinib in cell lines wherein the difference between the IC50 values of gefitinib and crizotinib were 9-fold or higher. However, in MDA-MB-468, PC3, DU145, UM22A, H2170, IGROV-1, SKOV3, EFO-21 and 4T1 cells that exhibited IC50 values for crizotinib and gefitinib in the less than 6-fold difference range, the IC50 of the equimolar combination of crizotinib + gefitinib showed stronger potency than single drug alone (Fig. 5.2A). This is well illustrated by the average graphs shown in figure 5.2B-G, where the response profile of gefitinib (Fig. 5.2B) was marked by significantly higher IC50 values compared with those of crizotinib (Fig. 5.2C). Moreover, the response profile for gefitinib + crizotinib (Fig. 5.2D) resembled that of crizotinib alone. Where differences in IC50 values for gefitinib and crizotinib were less than 5-fold, the response profile of the combination (Fig. 5.2G)

appeared to produce enhanced potency when compared with each drug alone (Fig. 5.2E-G).

A

		Cell line	Gefitinib (μM)	Crizotinib (μM)	Fold Difference (κ)	Crizotinib + Gefitinib (μM)	Potency Index (ε)
Different Range IC50	Prostate	22RV1[2]	47.8 ± 4.8	0.5 ± 0.02	96	0.8 ± 0.08	155.2
	Breast	BT549[2]	73.7 ± 7.7	1.5 ± 0.03	49	1.5 ± 0.2	50.0
		MDA-MB-231[2]	19.7 ± 1.2	1.2 ± 0.07	13	1.0 ± 0.001	11.5
	Lung	A549[2]	17.1 ± 4	2.0 ± 0.3	9	1.8 ± 0.3	9.0
		A427-MGMT	33.3 ± 1.3	1.2 ± 0.4	27	0.5 ± 0.3	11.7
		VC8	14.2 ± 1.8	0.7 ± 0.2	21	1.3 ± 0.2	40.9
		VC8-MGMT	11.4 ± 0.1	0.4 ± 0.1	27	1.4 ± 0.2	97.8
	Ovarian	OVCAR-3	0.92 ± 0.12	8.4 ± 0.88	9	0.77 ± 0.09	8.4
		A2780	0.52 ± 0.14	6.5 ± 1.9	13	0.32 ± 0.01	8.6
Similar Range IC50	Breast	MDA-MB-468[2]	5.4 ± 0.6	1.0 ± 0.08	5	0.3 ± 0.03	1.8
		4T1	11.4 ± 0.1	2.5 ± 0.7	5	1.7 ± 0.04	4.1
	Prostate	PC3[2]	22.1 ± 5.2	4.9 ± 1.6	5	2.0 ± 0.3	0.6
		DU145[2]	9.3 ± 1.1	6.5 ± 1.0	1	2.3 ± 0.4	0.8
	Head and Neck	UM22A	1.1 ± 0.2	2.2 ± 0.1	2	0.3 ± 0.1	1.9
	Lung	H2170[2]	1.8 ± 0.3	3.9 ± 0.6	2	1.2 ± 0.5	0.3
	Ovarian	IGROV-1	0.76 ± 0.22	0.46 ± 0.15	2	0.04 ± 0.01	0.6
		SKOV-3	3.3 ± 0.11	13.1 ± 4.8	4	0.39 ± 0.16	0.1
		EFO-21	0.51 ± 0.24	0.22 ± 0.01	2	0.01 ± 0.0001	4.1

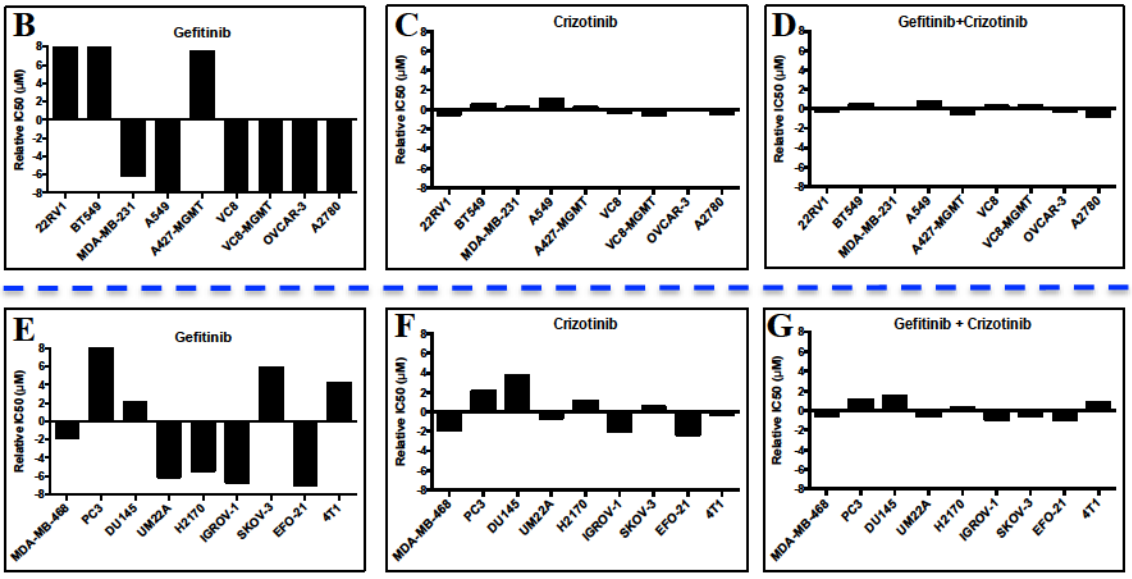

Figure 5.2: (A) IC50 values of tumour cell growth inhibition on a panel of human cancer cell lines using gefitinib, crizotinib (c-Met kinase inhibitor) and their equimolar combination. The fold-difference between the IC50 values of the two individual drugs is

denoted by κ and the potency index as described in equation **1** is defined by ε. **(B-G):** Relative IC50 values (IC50 of individual drug minus the average IC50 of the drug on the entire panel of cell lines) of gefitinib, crizotinib and their equimolar combination for **(B-D)** $\kappa > 6$, and **(E-G)** $\kappa \leq 6$. [2]Rao *et al.* 2015, under review (45).

5.4.1.C c-Met-c-Src targeting

The analysis was extended to c-Met and c-Src targeting using crizotinib and dasatinib (a clinical c-Src/c-Abl inhibitor), respectively. The results showed that the IC50 of dasatinib ranged from 0.01 ± 0.0003μM to 15.1 ± 1.8μM and that of crizotinib ranged from 0.5 ± 0.02μM to 6.5 ± 1.0 μM (Fig. 5.3A). As previously observed, the IC50 of the equimolar combination of crizotinib + dasatinib resembled that of dasatinib in cell lines that demonstrated 9-fold or higher difference between the IC50 of crizotinib and dasatinib. In contrast, in MDA-MB 468 cell line wherein the difference between the IC50 values of crizotinib and dasatinib was 6-fold, the equimolar combination of the two drugs demonstrated 3- and 21-fold superior potency compared with crizotinib and gefitinib, respectively (Fig. 5.3A).

5.4.1.D EGFR- or c-Met-DNA targeting

The analysis was further extended to a more divergent type of targeting involving one kinase inhibitor (e.g. EGFR, c-Met) and a DNA damaging agent. We thus analyzed the growth inhibitory potency of gefitinib (EGFR TKI), temozolomide (DNA alkylating agent) and their equimolar combination (Fig. 5.3B) or crizotinib (c-Met inhibitor) in combination with temozolomide and their equimolar combination on a panel of cell lines

(Fig. 5.3C). The results showed that most of the cell lines were resistant to temozolomide with IC50 values ranging from 259 ± 1.3μM to > 800μM, except in the A427 cell line (12.4 ± 3μM) that does not express the O6-methylguanine DNA methyltransferase (MGMT), a DNA repair enzyme that removes the cytotoxic O6-methyl group of guanine by transferring it to its internal cysteine residues. By contrast, all the cell lines demonstrated sensitivity to gefitinib or crizotinib with IC50 values ranging from 0.3 ± 0.1μM to 1.2 ± 0.4μM for crizotinib and 5.9 ± 0.2μM to 33.3 ± 1.3μM for gefitinib. All cell lines except A427 exhibited more than 18-fold difference in IC50 values between temozolomide and gefitinib or crizotinib. As for the kinase-kinase imbalanced targeting combinations, the trend is that the IC50 values for equimolar combination of gefitinib + temozolomide or crizotinib + temozolomide resembled that of gefitinib alone or crizotinib alone, respectively (Fig. 5.3B, C).

A

		Cell line	Crizotinib (μM)	Dasatinib (μM)	Fold Difference (κ)	Crizotinib + Dasatinib (μM)	Potency Index (ε)
Different Range IC50	Breast	MDA-MB-231	1.2 ± 0.07	0.05 ± 0.01	24	0.03 ± 0.02	15.0
		BT549	1.5 ± 0.03	0.15 ± 0.08	10	0.06 ± 0.04	4.4
	Prostate	DU145	6.5 ± 1.0	0.04 ± 0.01	163	0.01 ± 0.004	41.0
		PC3	4.9 ± 1.6	0.05 ± 0.03	98	0.02 ± 0.006	39.6
		22RV1	0.5 ± 0.02	15.1 ± 1.8	30	0.5 ± 0.05	31.0
	Ovarian	OVCAR-3	0.92 ± 0.12	0.01 ± 0.0003	92	0.01 ± 0.0003	93.0
		IGROV-1	0.76 ± 0.22	0.01 ± 0.0003	76	0.01 ± 0.004	77.0
		A2780	0.52 ± 0.14	4.8 ± 0.9	9	0.25 ± 0.03	4.8
		SKOV-3	3.3 ± 0.11	0.01 ± 0.0003	330	0.01 ± 0.0007	331.0
		EFO-21	0.51 ± 0.24	0.01 ± 0.001	51	0.01 ± 0.0004	52.0
Similar Range IC50	Breast	MDA-MB-468	1.0 ± 0.08	6.2 ± 1.4	6	0.3 ± 0.05	2.1

B

		Cell line	Temozolomide (μM)	Gefitinib (μM)	Fold Difference	Temozolomide + Gefitinib (μM)	Potency Index (ε)
Different Range IC50	Lung	A549	430 ± 49	7.4 ± 0.4	58	10.7 ± 0.7	85.308
		A427-MGMT	>800	33.3 ± 1.3	>24	36.0 ± 1.0	27.026
		VC8	259 ± 1.3	14.2 ± 1.8	18	13.0 ± 0.03	17.382
		VC8-MGMT	>800	11.4 ± 0.1	>35	12.9 ± 1.0	40.170
	Brain	U87	>800	24.6 ± 1.1	>33	21.5 ± 2.9	29.728
		U87-MGMT	>800	22.3 ± 0.8	>36	19.8 ± 0.9	32.855
Similar Range IC50	Lung	A427	12.4 ± 3.0	5.9 ± 0.2	2	7.4 ± 0.4	3.7

C

		Cell line	Temozolomide (μM)	Crizotinib (μM)	Fold Difference (κ)	Temozolomide + Crizotinib (μM)	Potency Index (ε)
Different Range IC50	Lung	A549	430 ± 49	0.3 ± 0.1	1631	1.0 ± 0.1	5440.5
		A427-MGMT	>800	1.2 ± 0.4	>653	1.0 ± 0.4	545.0
		VC8	259 ± 1.3	0.7 ± 0.2	375	1.3 ± 0.2	698.3
		VC8-MGMT	>800	0.4 ± 0.1	>944	1.6 ± 0.1	3777.9

Figure 5.3: (A) IC50 values of growth inhibition assay targeting c-Met and c-Src using crizotinib, dasatinib and their equimolar combination. **(B)** IC50 values of growth inhibition targeting EGFR and DNA using gefitinib, temozolomide (DNA alkylating agent) and their equimolar combination. **(C)** IC50 values of growth inhibition assay targeting c-Met and DNA using crizotinib, temozolomide and their equimolar combination. The fold-difference between the IC50 values of the two individual drugs is denoted by κ and the potency index as described in equation (1) is defined by ε.

5.4.2. Parameterization of the response profiles

Overall, from our results, if we label IC50 values as γ, it appears that when the difference in the IC50 of the less potent drug (γ1) and the more potent drug (γ2) is higher than 6-fold, the IC50 value for the equimolar combination referred to as γ3 is in the same range as γ2 (the more potent drug). However, if γ1 and γ2 are less than or equal to 6-fold different, which we consider to be a similar range of IC50, the equimolar combination exhibits superior potency, when compared with each drug alone. We categorized the data into two groups based on the fold-difference calculated as γ1/γ2 and this term is referred to as **κ**. As depicted in figure 5.4A, the average distribution of all the IC50 values of kinase inhibitor-1 (γ1), kinase inhibitor-2 (γ2) and their equimolar combination (γ3) evaluated on the wide range of cell lines for unbalanced targeting where **κ** > 6 (Fig. 5.4A) showed a significant difference ($p < 0.001$) between the average IC50 values for each drug alone. However the average for γ3 (IC50 of the combination) was in the same range as that γ2 (IC50 of kinase inhibitor-2). By contrast, there was no significant difference between γ1 and γ2 ($p > 0.05$) for data with **κ** ≤ 6 (Fig. 5.4B). In an attempt to develop a mathematical model that will allow to claim effectiveness for a given equimolar combination, we considered the ratio between the IC50 of the two drugs in combination, γ3, and that of drug alone, γ1 or γ2 and given the dependence of the effectiveness on the fold-difference, we used **κ** as a variable, leading to equation (1) and its factorization to equation (2). Plotting the obtained values gave a straight line with R^2=0.95 (Fig. 5.4C), which could be used to establish threshold for effectiveness.

(1) $\varepsilon = \kappa\,(\gamma 3/\gamma 1) + \kappa\,(\gamma 3/\gamma 2)$

(2) $\varepsilon = [(\gamma 3/\gamma 1) + (\gamma 3/\gamma 2)]\ \kappa$

Based on the distribution of the ε values for our kinase-kinase targeting data on different cell lines, we found $\varepsilon = 4.1$ as the maximum within the group of cell lines showing $\kappa \leq 6$ (Fig. 5.4D). Consequently, we set $\varepsilon < 5$ and $\kappa \leq 6$ as the threshold for drugs to be effectively combined in an equimolar combination (Fig. 5.4D lower left quadrant). Based upon on our results, we considered equimolar combinations exhibiting $\varepsilon > 5$ and $\kappa > 6$ (upper right quadrant) to be ineffective equimolar drug combinations and indicate imbalanced targeting in these cells.

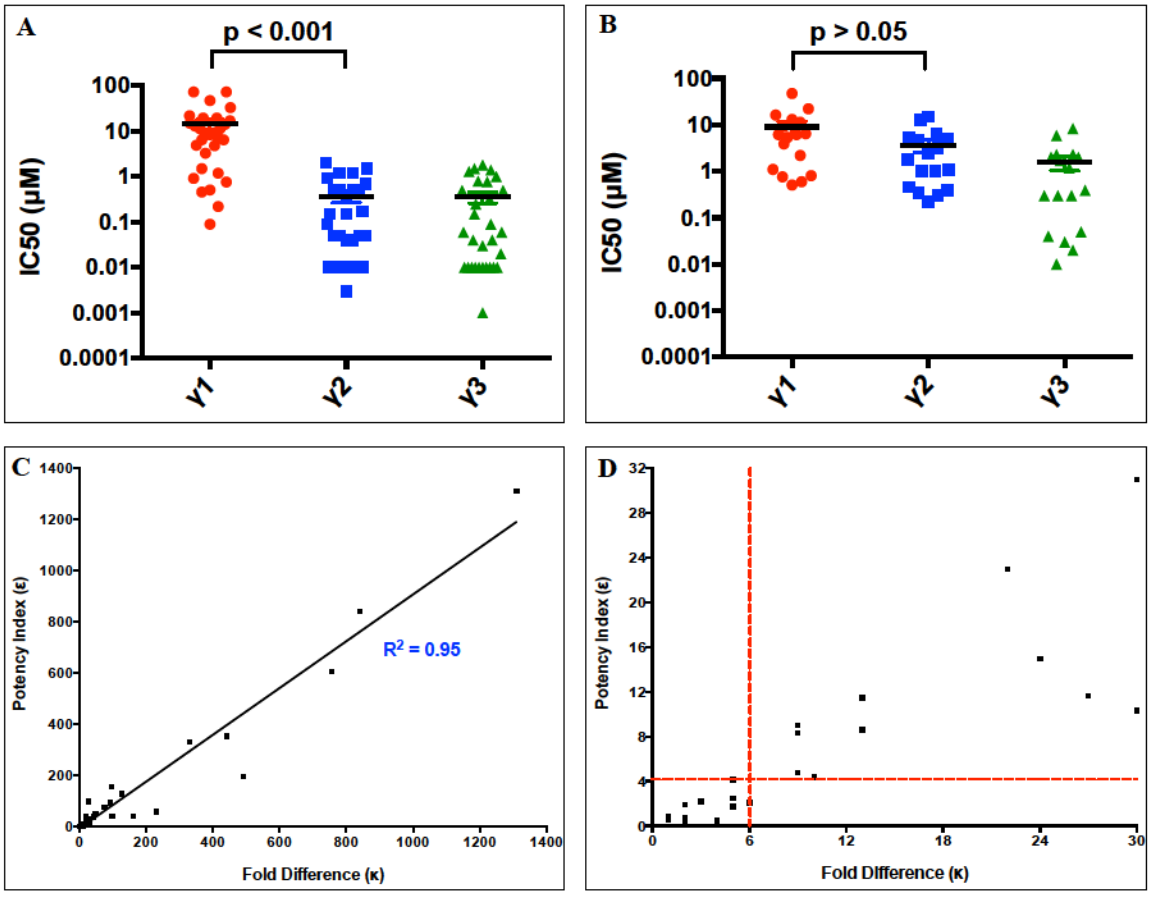

Figure 5.4: Comparing the distribution of IC50 values of kinase inhibitor-1 (γ1), kinase inhibitor-2 (γ2) and their equimolar combination (γ3) represented for cell lines exhibiting fold-difference of **(A)** $\kappa > 6$ and **(B)** $\kappa \leq 6$. Note that $\gamma 1 > \gamma 2$ and κ represents the fold-difference, which is calculated as $\gamma 1/\gamma 2$. Statistical analysis was carried out using unpaired two-tailed student t-test. **(C)** Linear correlation between the potency index, ε [calculated for each cell line using equation (1)] and the fold-difference κ, for the entire panel of cell lines evaluated. $R^2 = 0.95$ and slope = 0.92 was generated using the Graphpad Prism 6.0 software. **(D)** Inset of the graph in **(C)** representing the population of data points showing ε values for $\kappa < 6$, which indicates balanced targeting.

5.4.3. Unimolecular combinations

5.4.3.A EGFR-c-Src targeting combi-molecules

In recent years, as part of our kinase-kinase targeting program, we embarked upon the design and synthesis of EGFR-c-Src targeting combi-molecules, which led to the development of a series of compounds, including AL660, AL690, AL692, AL739 and the optimized combi-molecule AL776 (see Fig. 5.5A) designed to induce tandem blockade of the two kinases, both as an intact structure and upon undergoing hydrolysis (12). AL660, AL690, AL692 and AL739 behave as unbalanced kinase inhibitors due to their inherent ability to inhibit c-Src more potently than EGFR (12). Here we showed that all four combi-molecules were strong inhibitors of c-Src that blocked its phosphorylation at a concentration as low as 1μM in whole cells (Fig. 5.5B). In contrast they were poor inhibitors of EGFR at the same concentration They were unable to induce superior growth inhibitory potency compared with the equimolar combination of gefitinib +

dasatinib in the NIH3T3 panel of cell lines (except for AL692 on NIH3T3-wt cells that showed remarkable potency, which might be due to unspecific kinase binding) (Fig. 5.5C, F). Optimization studies led to the identification of AL776, which not only exhibited potent EGFR and c-Src inhibitory potency in an *in vitro* kinase assay, but also in a whole cell immunoblot assay (12). Consequently, we have a set of non-optimized and optimized EGFR-c-Src targeting compounds that can be used to define criteria for predicting potency in comparison with equimolar combinations of gefitinib and dasatinib.

5.4.3.B Design, synthesis and biological potency of LP121, an EGFR-c-Met targeting combi-molecule

In order to explore situations wherein EGFR and c-Met are co-targeted with a combi-molecule, we developed LP121, containing a carbonate linker bridging an EGFR and c-Met inhibitors. The results showed that LP121 could block both EGFR and c-Met, with an IC50 of 1μM using an *in vitro* kinase assay (Fig. 5.5D). In the 4T1 cell system, a cell line expressing both receptors, LP121 induced a dose-dependent inhibition of EGFR and c-Met phosphorylation following 2h of treatment, indicating that the combi-molecule possessed dual targeting properties (Fig. 5.5E). Thus we have in hand an EGFR-c-Met targeting molecule that can be used to develop potency criteria in comparison with equimolar combinations.

5.4.4. Parameterization of potency of combi-molecules: a new parameter Ω as a potency index.

While equations (1) and (2) were developed with the purpose of parameterizing the potency of equimolar drug combinations, it cannot be applied to combi-targeted molecules since their dual mechanism of action is imprinted in a single chemical entity. The potency index of combi-molecules can only be defined in the context of a comparison with balanced equimolar combinations. Thus, as defined by equation (3), if $\gamma 4$ is the IC50 of the combi-molecule, its potency index $\mathbf{\Omega}$ can be calculated as a ratio of $\gamma 4$ over the IC50 for equimolar combination, $\gamma 3$**.**

(3) $\mathbf{\Omega = \gamma 4/\gamma 3}$

Thus, combi-molecule can be considered effective only when $\mathbf{\Omega} \leq 1$ in cells presenting balanced targeting to the effects of its two arms.

Analysis of the unbalanced combi-molecules AL660-AL739 (except for AL692 in wild type cells) gave $\mathbf{\Omega}$ values far greater than 1 in cells expressing their target oncogenes, indicating that these molecules are not adequately targeted (Fig. 5B). Optimization of their structures gave AL776, which when evaluated in the NIH3T3 panel of cells, demonstrated superior potency compared with single drug alone, but was unable to induce superior potency when compared with the equimolar combination of gefitinib + dasatinib ($\mathbf{\Omega} > 1$) (Fig. 5.5C). However, given the dual inhibitory properties exerted by AL776, we further evaluated it in a panel of cancer cell lines, which like the NIH3T3 cells have previously demonstrated superior potency with the equimolar combination of gefitinib + dasatinib [$\boldsymbol{\varepsilon} < 5$, calculated from equation (1)]. The results showed that in both

22RV1 (prostate cancer) and A2780 (ovarian cancer) cells, AL776 was superior to or equal to the combination of gefitinib + dasatinib with **Ω** = 0.4 in 22RV1 cells (IC50 = 3.7 ± 0.5μM) and **Ω** = 1.0 in A2780 cells (IC50 = 2.2 ± 0.4μM) indicating that this combi-molecule is dual targeted in these cells.

Given the potency of LP121 in blocking both c-Met and EGFR tyrosine kinase activity, we evaluated its growth inhibitory properties in cell lines exhibiting less than 6-fold difference in IC50 values between gefitinib and crizotinib, as previously determined. The cell lines chosen included DU145, PC3 (prostate cancer), 4T1 (mouse mammary tumour cells), IGROV-1, SKOV-3 and EFO-21 (ovarian cancer), which exhibited sensitivity to the equimolar combination of gefitinib + crizotinib, when compared with drug alone (**ε** < 5). The results showed that among all the cell lines analyzed, LP121 showed superior activity compared with the equimolar combination in SKOV-3 cells (IC50 = 0.29 ± 0.04μM and **Ω** = 0.7) and similar potency as the equimolar combination in EFO-21 cells (IC50 = 0.01 ± 0.001μM and **Ω** = 1.0), indicating that LP121 is an effective combi-molecule against these cells.

A

Combi-molecules	Structures
AL660	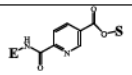
AL690	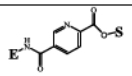
AL692	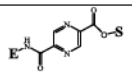
AL739	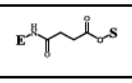
AL776[1]	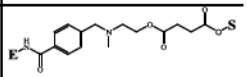
LP121	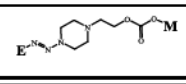

B

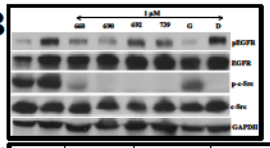

C

	WT (γ4)	Ω = γ4/ γ3	HER14 (γ4)	Ω = γ4/ γ3
AL660[1]	> 10	>1.7	> 10	>200
AL690[1]	> 10	>1.7	0.37 ± 0.01	7.4
AL692[1]	1.4 ± 0.4	0.2	0.36 ± 0.00	7.2
AL739[1]	17.5 ± 2.2	3	0.37 ± 0.06	7.4

D

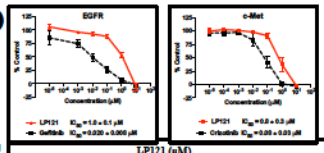

E

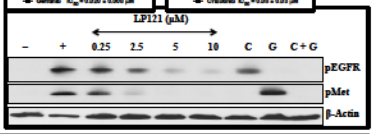

F

	Cell line	Gefitinib (γ1 or γ2)	Dasatinib (γ1 or γ2)	Fold-Difference (κ)	Gefitinib + Dasatinib (γ3)	ε = κ(γ3/γ1) + κ(γ3/γ2	AL776 (γ4)	Ω = γ4/γ3
Wild type and Transfected	NIH3T3-Wt	12.6 ± 2.1	16.4 ± 5.2	1.3	5.9 ± 1.1	1.1	7.6 ± 3.0[1]	1.3
	NIH3T3-Her14	0.35 ± 0.04	0.81 ± 0.3	2	0.05 ± 0.006	0.4	0.18 ± 0.03[1]	3.6
	NIH3T3-Neu	0.34 ± 0.03	0.6 ± 0.3	1.8	0.03 ± 0.009	0.2	0.11 ± 0.04	3.7
Prostate	22RV1	47.8 ± 4.8	15.1 ± 1.8	3	8.4 ± 1.3	2.2	3.7 ± 0.5	0.4
Ovarian	A2780S	6.5 ± 1.9	4.8 ± 0.9	1	2.3 ± 0.32	0.8	2.2 ± 0.44	1.0

G

	Cell line	Gefitinib (γ1)	Dasatinib (γ2)	Fold-Difference (κ)	Gefitinib + Dasatinib (γ3)	ε = κ(γ3/γ1) + κ(γ3/γ2)	AL776 (γ4)
Breast	MDA-MB-231	15.1 ± 1.9	0.02 ± 0.01	755	0.04 ± 0.02	1512.0	0.05 ± 0.004[1]
	4T1	11.4 ± 1.0	0.09 ± 0.01	127	0.09 ± 0.002	128.0	0.07 ± 0.02[1]
Prostate	DU145	9.3 ± 1.1	0.04 ± 0.01	232	0.01 ± 0.007	58.2	0.09 ± 0.008
	PC3	22.1 ± 5.3	0.05 ± 0.03	442	0.04 ± 0.02	354.4	0.05 ± 0.004

H

	Cell line	Gefitinib (γ1 or γ2)	Crizotinib (γ1 or γ2)	Fold-Difference (κ)	Gefitinib + Crizotinib (γ3)	ε = κ(γ3/γ1) + κ(γ3/γ2	LP121 (γ4)	Ω = γ4/γ3
Prostate	DU145	9.3 ± 1.1[2]	6.5 ± 1.0[2]	1	2.3 ± 0.4[2]	0.6	8.5 ± 2.2	3.7
	PC3	22.1 ± 5.2[2]	4.9 ± 1.6[2]	5	2.0 ± 0.3[2]	2.5	3.4 ± 0.3	1.7
Breast	4T1	11.4 ± 0.1	2.5 ± 0.7	5	1.7 ± 0.04	4.1	3.1 ± 0.3	1.8
Ovarian	IGROV-1	0.76 ± 0.22	0.46 ± 0.15	2	0.04 ± 0.01	0.3	0.87 ± 0.09	21.8
	SKOV-3	3.3 ± 0.11	13.1 ± 4.8	4	0.39 ± 0.16	0.6	0.29 ± 0.04	0.7
	EFO-21	0.51 ± 0.24	0.22 ± 0.01	2	0.01 ± 0.0001	0.1	0.01 ± 0.001	1.0

I

	Cell line	Gefitinib (γ1)	Crizotinib (γ2)	Fold-Difference (κ)	Gefitinib + Crizotinib (γ3)	ε = κ(γ3/γ1) + κ(γ3/γ2)	LP121 (γ4)
Prostate	22RV1	47.8 ± 4.8[2]	0.5 ± 0.02[2]	96	0.8 ± 0.08[2]	155.2	3.0 ± 0.6

Figure 5.5: (A) Structures of EGFR-c-Src (AL660-AL776) and EGFR-c-Met (LP121) combi-molecules. E = EGFR targeting head, S = c-Src targeting head and M = c-Met targeting head (structures shown in Fig. 5S2 in the supplementary section). **(B)** Immunoblot analysis of inhibition of EGFR and c-Src phosphorylation by 1 μM dose of

EGFR-c-Src targeting combi-molecules (i.e., AL660, AL690, AL692, AL739) and the clinical inhibitors gefitinib (G) and dasatinib (D) in NIH3T3-Her14 (EGFR transfected) cells stimulated with 50 ng/ml of EGF. **(C)** IC50 values of growth inhibition and the combi-targeting effect, Ω (calculated using equation **2**) for imbalanced targeting combi-molecule on the NIH3T3-wild type and Her14 (EGFR transfected) cells. **(D)** EGFR and c-Met kinase inhibitory potency of LP121 using an *in vitro* kinase assay. **(E)** Target modulation by LP121, crizotinib or C (5 μM), gefitinib or G (5 μM) and an equimolar combination of crizotinib + gefitinib or C + G (5 μM each) in 4T1 cells using western blot analysis under conditions of EGF + HGF (50 ng/ml each) stimulation. **(F, G)** IC50 values of growth inhibition of the balanced targeted combi-molecule, AL776, on cell lines exhibiting $\varepsilon < 5$ and $\varepsilon > 5$, determined using equation (1) and the combi-targeting effect, Ω, was calculated for cell lines with $\varepsilon < 5$ using equation (3). **(H, I)** IC50 values of growth inhibition for the balanced targeted combi-molecule, LP121, on cell lines exhibiting $\varepsilon < 5$ and $\varepsilon > 5$ determined using equation (1)**.** The combi-targeting effect, Ω, was calculated for cell lines showing $\varepsilon < 5$ using equation (3). Note that $\Omega < 1$ indicates strong potency exerted by the combi-molecule. [1]Rao *et al.* 2015 (12). [2]Rao *et al.* 2015, under review (45).

5.5. DISCUSSION

The complexity of signaling networks driving advanced cancers has given rise to several multi-targeted strategies including the use of complex drug cocktails, hybrid or chimeric molecules (e.g. HDAC-tyrosine kinase inhibitors such as HDAC-EGFR/Her2, HDAC-PDGFR inhibitors, microtubule disruptors), which are in preclinical/clinical stages of

evaluation or currently being used in the clinic (32-36). Within the context of developing single drugs with multi-targeted properties, our laboratory has specialized in synthesizing and developing a novel class of compounds termed "combi-molecules" that are designed to inhibit two distinct biological targets, both as an intact structure and/or to generate their potent inhibitory arms directed at the two targets upon hydrolysis. These biological targets (e.g. receptor tyrosine kinases EGFR, c-Met and non-receptor tyrosine kinase c-Src) are known to synergistically potentiate each other's effects in driving tumour growth and provide a strong rationale for developing a multi-targeted approach against their adverse effects. In theory, combi-molecules are designed to generate molar equivalent of their two inhibitory arms upon undergoing hydrolysis in cells, thereby mimicking the effects of an equimolar combination of drugs (9, 11, 37-39). Molar equivalent of activity is also assumed for hybrid molecules. Indeed, Loedige *et al.* (23) recently analyzed the potency of hybrid anti-malarial drugs in comparison with an equimolar combination of drugs representing the two moieties. While methods are available to assess the potency of an equieffective drug combination (i.e., the median-effect principle proposed by Chou-Talalay) that determines synergy, antagonism and additive nature of drug combinations based on their combination index values, the same principles are not applicable to the outcome of equimolar drug combinations or unimolecular entities such as hybrid drugs or combi-molecules (25). We thus sought to develop simple mathematical equations to assess the overall potency of an equimolar combination of two drugs and its comparison with unimolecular analog, using current and past data.

The general trend observed was that when the IC50 value of one drug was 6-fold higher than that of the other, the IC50 of the equimolar combination of the two drugs resembled

that of the more potent inhibitor. However, when the difference in IC50 values of the two drugs was equal to or less than 6-fold, the equimolar combination of the two drugs showed superior potency compared with single drug alone, thereby exhibiting what we designate as "balanced targeting". Simple mathematical equations were thus developed wherein equations (1) and (2) parameterize the effect of an equimolar combination, designated as potency index **ε**, which we defined as a sum of the ratios of the IC50 of the equimolar combination over that of the individual drug, each multiplied by **κ**, the IC50 fold-difference between the two drugs. Based on the linear correlation between **κ** and **ε**, we further showed that under conditions where the IC50 of the less potent drug (γ1) is 6-fold greater than that of the other (γ2), the potency index **ε** was greater than 5. However, under conditions where γ1 is 6-fold or less different from γ2, the potency index **ε** was less than 5. We thus proposed that in a given cell system, if **ε** > 5, it indicates imbalanced targeting and if **ε** < 5, the equimolar combination of the two drugs can be claimed effective (Fig. 5.4C, D).

The biological significance of these observations can be analyzed in light of the dominant pathways that control cell growth and its ability to undergo apoptosis in human tumour cells. c-Src being at the crossroad of multiple signaling pathways, its blockade with the potent inhibitor dasatinib leads to IC50 values in the nanomolar range, which renders the blockade of an upstream receptor such as EGFR (IC50 in the micromolar range) a minor contributor to the overall IC50 in combination. In corroboration, in the HCC827 lung cancer cell line, which expresses activating EGFR mutations (e.g. del E746-A750 and L859R), with IC50 for gefitinib in the nanomolar range, the IC50 in combination with dasatinib resembled that of gefitinib (Fig 5.1A). Clearly in the case of unbalanced

response, equimolecular combinations are ineffective and seem to indicate that the cells are addicted to a particular pathway.

In cells where balanced targeting is observed, perhaps the two targets synergize to promote growth and anti-apoptotic effects. Therefore, their tandem modulation leads to growth inhibitory potency superior compared with that of agents alone. Indeed we recently observed that in some prostate cancer cell lines, due to signaling redundancy between c-Met and EGFR, an equimolar combination of crizotinib and gefitinib is required to suppress the phosphorylation of the two receptors and block downstream signaling pathways [Rao *et al.* 2015, under review (45)].

Importantly, because of their balanced response to equimolar combinations, some cells are more suitable for evaluating the potency of dual targeted hybrid molecules than others. If a combi-molecule achieved $\boldsymbol{\Omega} < 1$ [the potency index for unimolecular drugs calculated according to equation (3)] in these cells, it can be considered worthy of further *in vitro* analysis and *in vivo* studies in xenograft models carrying the latter cell lines.

Steps toward defining potency criteria for combi-molecules are schematized in figure 5.6.

In summary, our studies allowed to conclude the following:

1. If two drugs are combined at equimolar ratio, and one drug shows 6-fold greater IC50 than the other (i.e., $\boldsymbol{\kappa} > 6$), the overall effect will resemble the IC50 of the combination. This principle showed that the potency index $\boldsymbol{\varepsilon}$ linearly correlates with $\boldsymbol{\kappa}$.
2. If two drugs are combined at equimolar ratio, and the IC50 of one drug is 6-fold or less than that of the other (i.e., $\boldsymbol{\kappa \leq 6}$), then the overall effect is superior to that of each individual drug. The threshold is set as $\boldsymbol{\varepsilon} < 5$, with a value below that

considered potent for effective and balanced targeting of an equimolar drug combination.

3. Under conditions of balanced targeting, a unimolecular combination (e.g. combi-molecule) is said to be effective if the IC50 of the combi-molecule is equal to or a fraction of the IC50 of the equimolar 2-drug combination (i.e., $\boldsymbol{\Omega \leq 1}$).

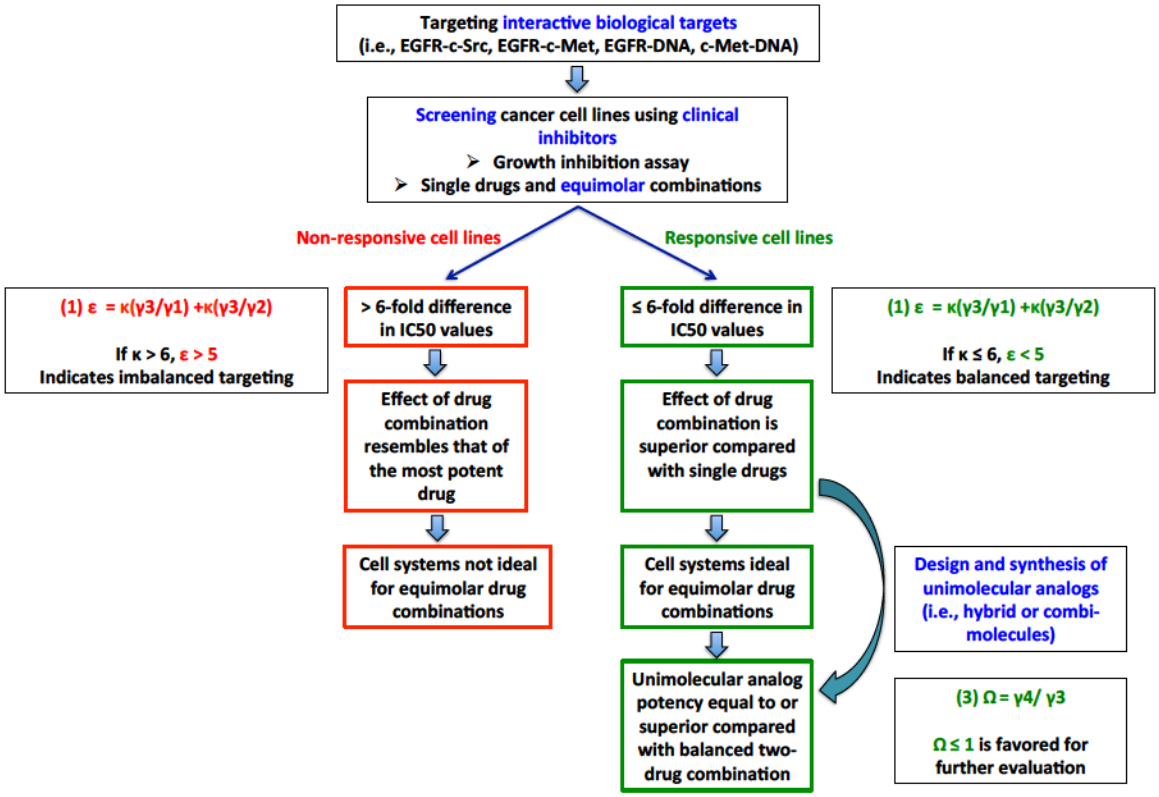

Figure 5.6: Flow chart summarizing the sequence of events leading to the design and synthesis of unimolecular analogs (i.e., hybrid drugs, chimeric molecules, combi-molecules) as predicted on the basis of the fold-difference between individual drugs (κ) and potency index of equimolar combination of drugs (ε) calculated using equation (1).

$\gamma 1$ = IC50 of drug 1, $\gamma 2$ = IC50 of drug 2, $\gamma 3$ = IC50 of equimolar combination of drug 1 + drug 2, $\gamma 4$ = IC50 of unimolecular analog (e.g. combi-molecule), $\kappa = \gamma 1/ \gamma 2$ where $\gamma 1 > \gamma 2$, and Ω = combi-targeting effect of unimolecular analog calculated using equation (3).

5.6. REFERENCES

1. Krause DS, Van Etten RA. Tyrosine kinases as targets for cancer therapy. New England Journal of Medicine. 2005;353(2):172-87.
2. Martin GS. Cell signaling and cancer. Cancer cell. 2003;4(3):167-74.
3. Paul MK, Mukhopadhyay AK. Tyrosine kinase–Role and significance in Cancer. International journal of medical sciences. 2004;1(2):101.
4. Giordano S, Petrelli A. From single-to multi-target drugs in cancer therapy: when aspecificity becomes an advantage. Current medicinal chemistry. 2008;15(5):422-32.
5. Kerr D, La Thangue N. Signal transduction blockade and cancer: combination therapy or multi-targeted inhibitors? Annals of oncology. 2004;15(12):1727-9.
6. Banerjee R, Rachid Z, McNamee J, Jean-Claude BJ. Synthesis of a prodrug designed to release multiple inhibitors of the epidermal growth factor receptor tyrosine kinase and an alkylating agent: a novel tumor targeting concept. Journal of medicinal chemistry. 2003;46(25):5546-51.
7. Huang Y, Rachid Z, Jean-Claude BJ. MGMT Is a Molecular Determinant for Potency of the DNA-EGFR–Combi-Molecule ZRS1. Molecular Cancer Research. 2011;9(3):320-31.
8. Banerjee R, Huang Y, Qiu Q, Mcnamee JP, Belinsky G, Jean-Claude BJ. The combi-targeting concept: mechanism of action of the pleiotropic combi-molecule RB24 and discovery of a novel cell signaling-based combination principle. Cellular signalling. 2011;23(4):630-40.
9. MacPhee M, Rachid Z, Todorova M, Qiu Q, Belinsky G, Jean-Claude BJ. Characterization of the potency of epidermal growth factor (EGFR)-DNA targeting combi-molecules containing a hydrolabile carbamate at the 3-position of the triazene chain. Investigational new drugs. 2011;29(5):833-45.
10. Barchéchath S, Williams C, Saade K, Lauwagie S, Jean-Claude B. Rational design of multitargeted tyrosine kinase inhibitors: A novel approach. Chemical biology & drug design. 2009;73(4):380-7.
11. Larroque-Lombard AL, Ning N, Rao S, Lauwagie S, Halaoui R, Coudray L, et al. Biological Effects of AL622, a Molecule Rationally Designed to Release an EGFR and ac-Src Kinase Inhibitor. Chemical biology & drug design. 2012;80(6):981-91.
12. Rao S, Larroque-Lombard A-L, Peyrard L, Thauvin C, Rachid Z, Williams C, et al. Target Modulation by a Kinase Inhibitor Engineered to Induce a Tandem Blockade of the Epidermal Growth Factor Receptor (EGFR) and c-Src: The Concept of Type III Combi-Targeting. PloS one. 2015;10(2).
13. Matheson SL, McNamee J, Jean-Claude BJ. Design of a chimeric 3-methyl-1, 2, 3-triazene with mixed receptor tyrosine kinase and DNA damaging properties: a novel

tumor targeting strategy. Journal of Pharmacology and Experimental Therapeutics. 2001;296(3):832-40.
14. Banerjee R, Rachid Z, Qiu Q, McNamee J, Tari A, Jean-Claude B. Sustained antiproliferative mechanisms by RB24, a targeted precursor of multiple inhibitors of epidermal growth factor receptor and a DNA alkylating agent in the A431 epidermal carcinoma of the vulva cell line. British journal of cancer. 2004;91(6):1066-73.
15. Ait-Tihyaty M, Rachid Z, Larroque-Lombard A-L, Jean-Claude BJ. ZRX1, the first EGFR inhibitor-capecitabine based combi-molecule, requires carboxylesterase-mediated hydrolysis for optimal activity. Investigational new drugs. 2013;31(6):1409-23.
16. Qiu Q, Domarkas J, Banerjee R, Katsoulas A, McNamee JP, Jean-Claude BJ. Type II combi-molecules: design and binary targeting properties of the novel triazolinium-containing molecules JDD36 and JDE05. Anti-cancer drugs. 2007;18(2):171-7.
17. Huang Y, Rachid Z, Peyrard L, Senhaji Mouhri Z, Williams C, Jean-Claude BJ. Positional Isomerization of A Non-Cleavable Combi-Molecule Dramatically Altered Tumor Cell Response Profile. Chemical biology & drug design. 2015;85(2):153-62.
18. Fortin S, Bérubé G. Advances in the development of hybrid anticancer drugs. Expert opinion on drug discovery. 2013;8(8):1029-47.
19. Gediya LK, Njar VC. Promise and challenges in drug discovery and development of hybrid anticancer drugs. Expert opinion on drug discovery. 2009;4(11):1099-111.
20. El Meskini R, Iacovelli AJ, Kulaga A, Gumprecht M, Martin PL, Baran M, et al. A preclinical orthotopic model for glioblastoma recapitulates key features of human tumors and demonstrates sensitivity to a combination of MEK and PI3K pathway inhibitors. Disease models & mechanisms. 2015;8(1):45-56.
21. Effenberger-Neidnicht K, Schobert R. Combinatorial effects of thymoquinone on the anti-cancer activity of doxorubicin. Cancer chemotherapy and pharmacology. 2011;67(4):867-74.
22. Garcia AG, Nedev H, Bijian K, Su J, Alaoui-Jamali M, Saragovi H. Reduced in vivo lung metastasis of a breast cancer cell line after treatment with Herceptin mAb conjugated to chemotherapeutic drugs. Oncogene. 2013;32(20):2527-33.
23. Lödige M, Hiersch L. Design and Synthesis of Novel Hybrid Molecules against Malaria. International journal of medicinal chemistry. 2015;2015.
24. Lödige M, Lewis MD, Paulsen ES, Esch HL, Pradel G, Lehmann L, et al. A primaquine–chloroquine hybrid with dual activity against Plasmodium liver and blood stages. International Journal of Medical Microbiology. 2013;303(8):539-47.
25. Chou T-C, Talalay P. Quantitative analysis of dose-effect relationships: the combined effects of multiple drugs or enzyme inhibitors. Advances in enzyme regulation. 1984;22:27-55.
26. Chou T-C. Theoretical basis, experimental design, and computerized simulation of synergism and antagonism in drug combination studies. Pharmacological reviews. 2006;58(3):621-81.
27. Chou T-C. Drug combination studies and their synergy quantification using the Chou-Talalay method. Cancer research. 2010;70(2):440-6.
28. Capela R, Cabal GG, Rosenthal PJ, Gut J, Mota MM, Moreira R, et al. Design and evaluation of primaquine-artemisinin hybrids as a multistage antimalarial strategy. Antimicrobial agents and chemotherapy. 2011;55(10):4698-706.

29. Amrein L, Rachid Z, Jean-Claude B, Soulieres D, Aloyz R, Panasci L. ZRF4, a combi-molecule with increased efficacy as compared with the individual components in chronic lymphocytic leukemia lymphocytes in vitro. Leukemia. 2011;25(9).
30. Heppner GH, Miller FR, Shekhar PM. Nontransgenic models of breast cancer. Breast Cancer Research. 2000;2(5):331.
31. Skehan P, Storeng R, Scudiero D, Monks A, McMahon J, Vistica D, et al. New colorimetric cytotoxicity assay for anticancer-drug screening. J Natl Cancer Inst. 1990;82(13):1107-12.
32. RaviáAcharya K, Barry V. Chimeric microtubule disruptors. Chemical Communications. 2010;46(17):2907-9.
33. Seo S-Y. Multi-targeted hybrids based on HDAC inhibitors for anti-cancer drug discovery. Archives of pharmacal research. 2012;35(2):197-200.
34. Uecker A, Sicker M, Beckers T, Mahboobi S, Hägerstrand D, Östman A, et al. Chimeric tyrosine kinase-HDAC inhibitors as antiproliferative agents. Anti-cancer drugs. 2010;21(8):759-65.
35. Canellos GP, Anderson JR, Propert KJ, Nissen N, Cooper MR, Henderson ES, et al. Chemotherapy of advanced Hodgkin's disease with MOPP, ABVD, or MOPP alternating with ABVD. New England Journal of Medicine. 1992;327(21):1478-84.
36. Fisher RI, Gaynor ER, Dahlberg S, Oken MM, Grogan TM, Mize EM, et al. Comparison of a standard regimen (CHOP) with three intensive chemotherapy regimens for advanced non-Hodgkin's lymphoma. New England Journal of Medicine. 1993;328(14):1002-6.
37. Katsoulas A, Rachid Z, McNamee JP, Williams C, Jean-Claude BJ. Combi-targeting concept: an optimized single-molecule dual-targeting model for the treatment of chronic myelogenous leukemia. Molecular cancer therapeutics. 2008;7(5):1033-43.
38. Ait-Tihyaty M, Rachid Z, Mihalcioiu C, Jean-Claude BJ. Inhibition of EGFR phosphorylation in a panel of human breast cancer cells correlates with synergistic interactions between gefitinib and 5′-DFUR, the bioactive metabolite of Xeloda®. Breast cancer research and treatment. 2012;133(1):217-26.
39. Todorova MI, Larroque A-L, Dauphin-Pierre S, Fang Y-Q, Jean-Claude BJ. Subcellular distribution of a fluorescence-labeled combi-molecule designed to block epidermal growth factor receptor tyrosine kinase and damage DNA with a green fluorescent species. Molecular cancer therapeutics. 2010;9(4):869-82.
45. Rao S, Allal B, Larroque-Lombard AL, Chatelut E, Delord JP, Jean-Claude BJ. Pharmacological probing of signaling redundancy mediated by receptor and non-receptor tyrosine kinases revealed Achilles' heels in castrate resistant prostate cancer. Molecular cancer therapeutics, July 2015, under review.

5.7. SUPPLEMENTARY DATA

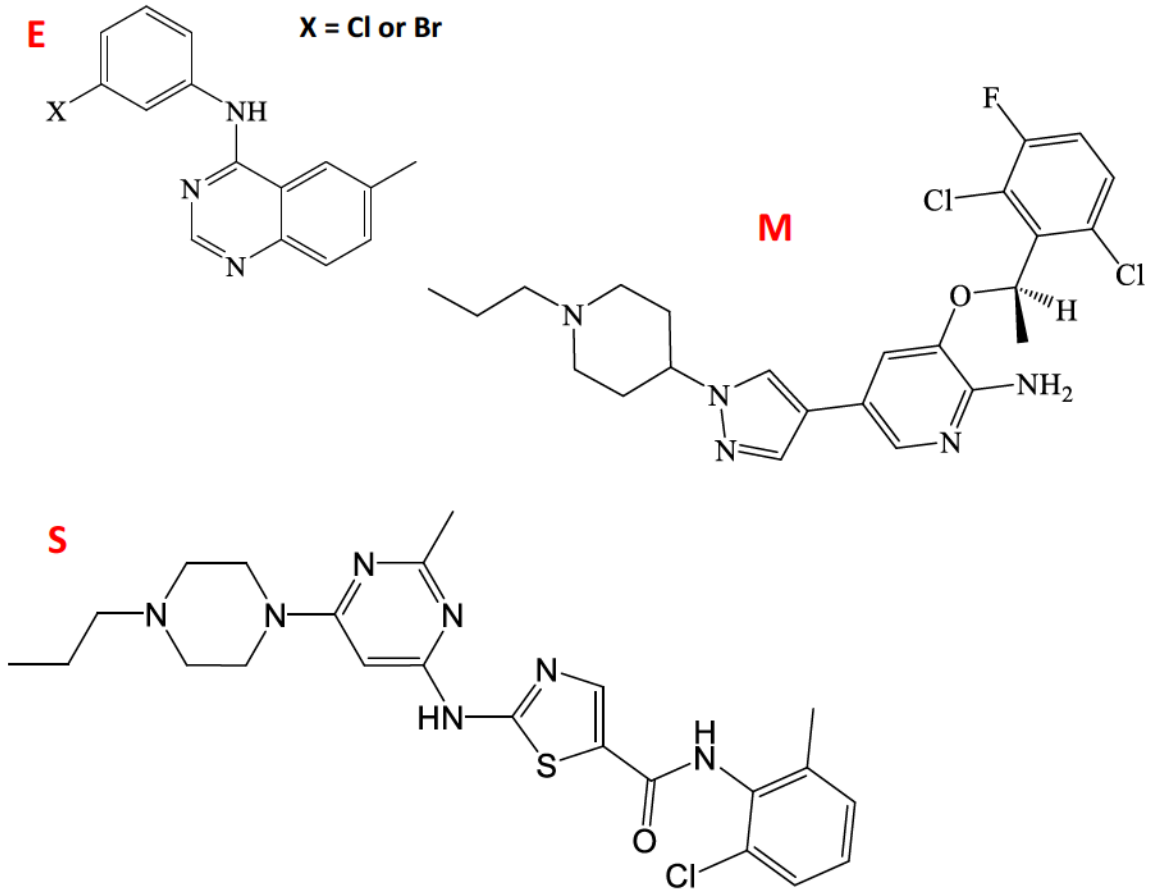

Figure 5.S1: EGFR (E), c-Src (S) and c-Met (M) targeting moieties used in the synthesis of EGFR-c-Src and EGFR-c-Met targeting combi-molecules.

Materials and methods

Chemistry

^{1}H NMR spectra were recorded on a Varian 300 or 400 MHz spectrometer. Chemical shifts are given as δ values in parts per million (ppm) and are referenced to the residual solvent proton. Mass spectrometry was performed by the McGill University Mass spectroscopy Center and electrospray ionization (ESI) spectra were performed on a Finnigan LC QDUO spectrometer. Data are reported as m/z (intensity relative to base

peak = 100). All chemicals were purchased from Sigma-Aldrich, methyl 6-(chlorocarbonyl)nicotinate from Ellanova Laboratories (Hamden, CT, USA), pyrazine-2,5-dicarboxylic acid from Tyger Scientific Inc. (Ewing, NJ, USA), 5-methoxycarbonylpyridine-2-carboxylic acid from Oakwood Products, Inc. (West Columbia, SC, USA), methyl 5-(chlorocarbonyl)picolinate from AB Chem. Inc. (Dorval, QC, Canada), dasatinib (Sprycel) from Ark Pharmaceutical.

Compound 2a.

To a solution of **1** (0.5 g, 1.86 mmol) with triethylamine (260 μL, 1 eq.) in dry THF (10 mL) at 0 ºC, a solution of freshly chlorinated of 5-methoxycarbonylpyridine-2-carboxylic acid (0.44 g, 1.2 eq.), in dry THF (10 mL) was added dropwise at 0 ºC. The mixture was stirred under argon for 3 h, after which it was evaporated to give a crude powder, which was triturated water. The precipitate obtained was filtered, washed with ethyl acetate and ethyl ether. The brown solid was dried under vaccum to give the intermediate compound (0.76 g) which was used without further purification for the deprotect step. The intermediate compound (0.76 g, 1.75 mmol) was dissolved in dry THF (20 mL), heated slowly to help the dissolution, and potassium trimethylsilanoate (2.24 g, 10 eq.) was added. The mixture was stirred at room temperature under argon for 2h after which it was evaporated to dryness. The resulting solid was triturated in ethyl ether, collected by filtration and redissolved in water. The pH of the solution was adjusted to 2 with HCl 1N and the precipitate obtained was filtered to give a pure brown orange solid **2a** (0.76 mg, 98%). ^{1}H NMR (400 MHz, *DMSO-d_6*) d ppm 7.39 (d, J=7.83 Hz, 1 H), 7.52 (t, J=7.83 Hz, 1 H), 7.69 (d, J=8.22 Hz, 1 H), 7.89 (br. s., 1 H), 8.01 (d, J=9.00 Hz, 1 H), 8.33 (d, J=8.22 Hz, 1 H), 8.47 (d, J=8.22 Hz, 1 H), 8.56 (d, J=7.83 Hz, 1 H), 8.95 (s, 1 H), 9.21

(br. s., 1 H), 9.24 (br. s., 1 H), 11.35 (s, 1 H), 11.56 (br. s., 1 H), ESI *m/z* 420.1 (MH^+ with ^{35}Cl).

Compound 3a.

To a solution of **2a** (50 mg, 0.12 mmol) and dasatinib (58 mg, 1 eq) in dry DMF (1 mL) were added 1-ethyl-3-(3-dimethylaminopropyl) carbodiimide (EDCI) (25 μL, 1.2 eq.), hydroxybenzotriazole (HOBt) (19 mg, 1.2 eq.) and DMAP (1.5 mg, 0.1 eq.). The mixture was than stirred at room temperature for 24h under argon. The DMF was azeotroped with heptanes to give a crude solid, which was triturated in water. The precipitate was filtered, washed with ethyl ether and dried under vacuum. The resulting brown solid (92 mg) was purified by silica gel chromatography column (THF 100%) to give **3a** (AL660) as a pure powder (40 mg, 38%). ^1H NMR (400 MHz, *DMSO-d_6*) d ppm 2.21 (s, 3 H), 2.39 (s, 3 H), 2.55 – 2.63 (m, 4 H), 2.80 (m, 2 H), 3.46 – 3.56 (m, 4 H), 4.50 (m, 2 H), 6.03 (s, 1 H), 7.11 - 7.19 (m, 1 H), 7.21 – 7.31 (m, 2 H), 7.36 – 7.46 (m, 2 H), 7.79 – 7.89 (m, 2 H), 8.03 - 8.13 (m, 1 H), 8.20 (s, 1 H), 8.26 - 8.33 (m, 1 H), 8.36 (d, J=8.21 Hz, 1 H), 8.55 - 8.60 (m, 1 H), 8.61 (s, 1 H), 8.93 (d, J=1.95 Hz, 1 H), 9.22 (d, J=1.56 Hz, 1 H), 9.87 (s, 1 H), 9.94 (s, 1 H), 11.09 (s, 1 H), 11.49 (s, 1 H), ESI *m/z* 889.23 (MH^+ with ^{35}Cl, ^{35}Cl).

Compound 3b.

Compound **3b** (18 mg, 28%) light yellow solid, was synthesized using the same method as compound **3a** using compound **2b** starting with the commercial methyl 5-(chlorocarbonyl)picolinate reagent. ^1H NMR (400 MHz, *DMSO-d_6*) d ppm 2.22 (s, 3 H), 2.39 (s, 3 H), 2.54 - 2.63 (m, 4 H), 2.73 - 2.84 (m, 2 H), 3.42 -3.62 (m, 4 H), 4.38 - 4.63 (m, 2 H), 6.04 (s, 1 H), 7.11 - 7.18 (m, 1 H), 7.20 – 7.33 (m, 2 H), 7.33 - 7.46 (m, 2 H), 7.77 - 7.84 (m, 1 H), 7.86 (d, J=8.60 Hz, 1 H), 7.98 - 8.04 (m, 1 H), 8.04 - 8.10 (m, 1 H),

8.20 (s, 1 H), 8.23 - 8.30 (m, 1 H), 8.50 - 8.59 (m, 1 H), 8.62 (s, 1 H), 8.91 (d, J=1.95 Hz, 1 H), 9.29 (d, J=1.56 Hz, 1 H), 9.87 (s, 1 H), 9.99 (s, 1 H), 10.99 (s, 1 H), 11.47 (br. s, 1 H), ESI *m/z* 911.21 (MNa^+ with ^{35}Cl, ^{35}Cl).

Compound 4.

The commercial compound pyrazine-2,5-dicarboxylic acid was firstly chlorinated with an excess of thionyl chloride and a quantitative amount of DMSO. After 24h of reflux under argon, the clear orange mixture was evaporated, well dried under high vacuum and kept under argon at -20°C. Before using it, the solid was dissolved in methylene chloride to remove the unreacted diacid compound, filtered, and dried.

A solution of **1** (50 mg, 0.18 mmol) with triethylamine (180 µL, 7 eq.) in dry CH_2Cl_2/THF (10/2 mL) was added dropwise very slowly via a canula (addition during around 1 hour) to a solution of bischlorocarbonyl linker (76 mg, 2 eq.) dissolved in dry CH_2Cl_2/THF (4/2 mL) at 0 ºC. A precipitate appeared within a few minutes and the mixture was further stirred at room temperature for 1h after the end of the addition, under argon. The orange precipitate was filtered, washed with THF and with water to hydrolyze the acyl chloride (small bubbles can be observed), the brown-orange solid obtained was washed with ethyl ether and dried under vacuum (27 mg). By ^1H NMR, mixture of different compounds was observed: 70% of expected compound **4** with 30% of the dimer and around 30% for starting material pyrazine-2,5-dicarboxylic acid. Without further purification, the mixture was used directly for the last coupling step.

Compound 3c

Compound **3c** was synthesized using the same method as compound **3a,** taking into account the percentage of compound **4** in the mixture estimated by NMR. Compound **3c**

was purified by preparative TLC (silica plate, CH2Cl2/MeOH 9/1) to give a pure yellow solid (13 mg, 8%). ^{1}H NMR (400 MHz, *DMSO-d_6*) d ppm 2.22 (s, 3 H), 2.39 (s, 3 H), 2.55 - 2.63 (m, 4 H), 2.75 - 2.85 (m, 2 H), 3.45 - 3.60 (m, 4 H), 4.50 - 4.60 (m, 2 H), 6.04 (s, 1 H), 7.11 - 7.19 (m, 1 H), 7.19 - 7.31 (m, 2 H), 7.35 - 7.45 (m, 2 H), 7.80 - 7.90 (m, 2 H), 8.08 (t, J=1.95 Hz, 1 H), 8.20 (s, 1 H), 8.22 - 8.29 (m, 1 H), 8.62 (s, 1 H), 8.95 (d, J=1.95 Hz, 1 H), 9.32 (d, J=1.17 Hz, 1 H), 9.48 (d, J=1.17 Hz, 1 H), 9.87 (s, 1 H), 9.97 (s, 1 H), 11.19 (s, 1 H), 11.47 (m, 1 H), ESI *m/z* 888.13 (MH^+ with ^{35}Cl, ^{35}Cl).

Compound 6.

To a solution of **7**(40) (22 mg, 0.037 mmol) and **1** (10 mg, 1 eq) in dry DMF (1 mL) were added 1-ethyl-3-(3-dimethylaminopropyl) carbodiimide (EDCI) (7.9 µL, 1.2 eq.), hydroxybenzotriazole (HOBt) (6 mg, 1.2 eq.). The mixture was further stirred at room temperature for 18 h under argon. The DMF was azeotroped with heptanes to give a crude solid which was purified by preparative TLC (silica plate, CH_2Cl_2/MeOH 93/7) gave **8** (AL739) as a pure white powder (11 mg, 35%). ^{1}H NMR (400 MHz, *DMSO-d_6*) d ppm 2.22 (s, 3 H), 2.36 (s, 3 H), 2.55 - 2.60 (m, 2 H), 2.62 - 2.74 (m, 4 H), 3.39 - 4.55 (m, 4 H), 4.08 - 4.20 (m, 4 H), 4.37 - 4.50 (m, 2 H), 5.98 (s, 1 H), 7.12 (dd, J=8.01, 1.37 Hz, 1 H), 7.18 - 7.31 (m, 2 H), 7.32 - 7.43 (m, 2 H), 7.71 - 7.81 (m, 2 H), 7.84 (dd, J=8.99, 1.95 Hz, 1 H), 8.02 (t, J=1.95 Hz, 1 H), 8.20 (s, 1 H), 8.53 (s, 1 H), 8.71 (d, J=1.56 Hz, 1 H), 9.86 (s, 1 H), 9.90 (s, 1H), 10.38 (s, 1 H), 11.43 (br s, 1 H), ESI *m/z* 840.23 (MH^+ with ^{35}Cl, ^{35}Cl).

Compound 10.

The amino compound **9** (aminoquinazoline synthesized as described (41) RB10) (1 g) was dissolved in dry acetonitrile (40 mL) under argon and, cooled to -5°C. Nitrosonium

tetrafluoroborate (2 eq.) in acetonitrile was added directly. After 30 min at -5°C, the resulting solution was added dropwise to another solution of 1-piperazineethanol (4 eq.) in acetonitrile with triethylamine (4 eq.) at 0°C, after which the mixture was extracted with dichloromethane and brine. The organic layer was dried with magnesium sulfate and evaporated to provide a brown residue, which was purified by silica gel chromatography (CH_2Cl_2/MeOH 9/1) to give the compound **12** as a pure product (354 mg, 24.5%). ^{1}H NMR (300 MHz, *DMSO-d_6*) d ppm 2.51 (m, 2H), 2.63 (br s, 4 H), 3.55 (q, *J = 6.1 Hz*, 2 H), 3.81 (t, *J = 5 Hz*, 4 H), 4.50 (t, *J = 5 Hz*, 1 H), 7.30 (m, 2 H), 7.77 (d, *J = 9 Hz*, 1 H), 7.95 (m, 2 H), 8.26 (t, *J = 1.9 Hz*, 1 H), 8.47 (d, *J = 1.8 Hz*, 1 H), 8.59 (s, 1 H), 9.89 (s, 1 H).

Compound 11.

To a solution of compound **10** (353 mg) with pyridine (2 eq.) and trimethylamine (3 eq.) in dry dichloromethane (10 mL) was added dropwise 2-bromorthylchloroformate (2 eq.) at 0°C. The mixture was further stirred at room temperature for 1h and evaporated. The crude product obtained was purified by silica gel chromatography (CH_2Cl_2/MeOH 9/1) to give the compound **11** as a pure product (161 mg, 34.3%). ^{1}H NMR (300 MHz, *DMSO-d_6*) d ppm 2.68 (m, 6 H), 3.70 (t, *J = 6 Hz*, 2 H), 3.82 (t, *J = 4.8 Hz*, 4 H), 4.25 (t, *J = 5.4 Hz*, 2 H), 4.39 (t, *J = 6 Hz*, 2 H), 7.30 (m, 2 H), 7.77 (d, *J = 8.8 Hz*, 1 H), 7.95 (m, 2 H), 8.26 (t, *J = 1.9 Hz*, 1 H), 8.47 (d, *J = 1.8 Hz*, 1 H), 8.59 (s, 1 H), 9.89 (s, 1 H).

Compound 12 (LP121).

To a solution of **11** (152 mg) in dry DMF (2 mL) was added potassium iodide (1.5 eq.), trimethylamine (3 eq.) and commercial crizotinib (1.1 eq.). The mixture was stirred under argon at 40°C during 4 days. The DMF was azeotroped with heptanes to give a crude

solid, which was purified by silica gel chromatography (CH_2Cl_2/MeOH 9/1) to give the compound **12** as a pure orange powder (93 mg, 38%). ^{1}H NMR (300 MHz, *DMSO-d_6*) d ppm 1.76 (d, *J = 6.7 Hz*, 3 H), 1.90 (m, 4H), 2.14 (m, 2H), 2.65 (m, 8 H), 2.95 (d, *J = 10.8 Hz*, 2 H), 3.81 (t, *J = 5 Hz*, 4 H), 4.*08(m,* 1 H), 4.21 (m, 4 H), 5.63 (m, 2 H), 6.04 (q, *J = 6.9 Hz*, 1 H), 6.86 (d, *J = 1.8 Hz*, 1 H), 7.29 (m, 2 H), 7.40 (m, 1H), 7.56 (s, 1H), 7.53 (m, 1H), 7.75 (m, 2 H), 7.95 (m, 3H), 8.26 (t, *J = 1.8 Hz*, 1 H), 8.46 (d, *J = 2.1 Hz*, 1 H), 8.59 (s, 1 H), 9.88 (s, 1 H), HRMS: m/z calcd for $C_{44}H_{46}BrCl_2FN_{12}O_4.H^+$ 975.23822; found 975.23657 (Δ = -1.69 ppm).

Results

Chemistry

The synthesis of the first series of compounds **3a-b (AL660-690)** and **3c (AL692)** proceeded according to Scheme 1 and 2 respectively. The aminoquinazoline **1 (42)** was treated with an excess of the appropriate chlorocarbonyl linker to give protected intermediates, whose methyl ester was removed in the presence of potassium silanoate base to give acid **2a-b** (Scheme 1). After the acid **2a-b** was coupled with dasatinib in the presence of EDCI, HOBt and DMAP gave **3a-b** (AL660 and AL690).

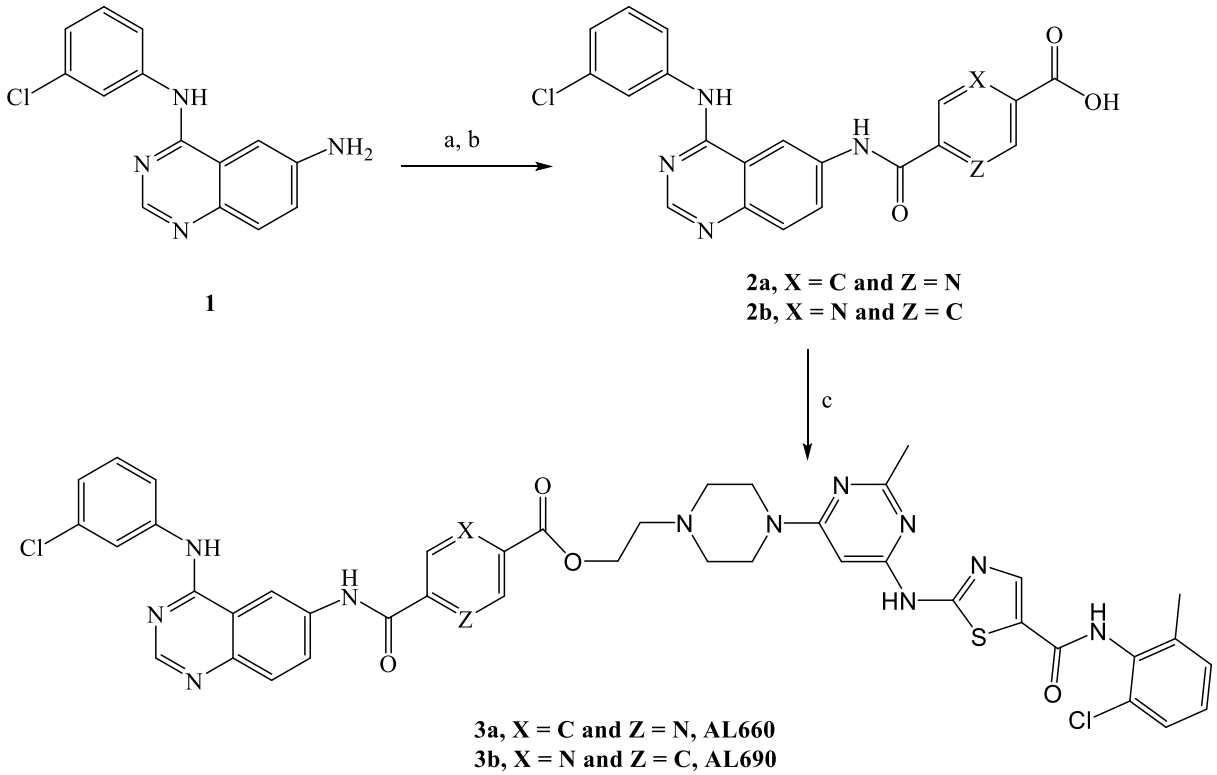

Scheme 1. a) methyl 6-(chlorocarbonyl)nicotinate or methyl 5-(chlorocarbonyl)picolinate, Et_3N, THF, 0°C, 3 h; b) Me_3SiOK, THF, rt, 2 h; c) dasatinib, EDCI, HOBt, DMAP, DMF, rt, 24 h.

Compound **3c** was synthesized following the same method (Scheme 2), only the linker pyrazine-2,5-dicarboxylic acid was commercially available so this diacid reagent was before chlorinated by refluxing in thionyl chloride with catalytic DMSO during 24h. The aminoquinazoline **1** was treated with an excess of the bischlorocarbonyl linker and triethylamine to obtain a not selective coupling reaction, the optimal conditions gave 70% of expected compound **4** with 30% of dimer and also still a presence of starting reagent pyrazine-2,5-dicarboxylic acid. This mixture was directly used to be coupled with

dasatinib in the presence of EDCI, HOBt and DMAP to give the final compound **3c (AL692)** with a very low yield.

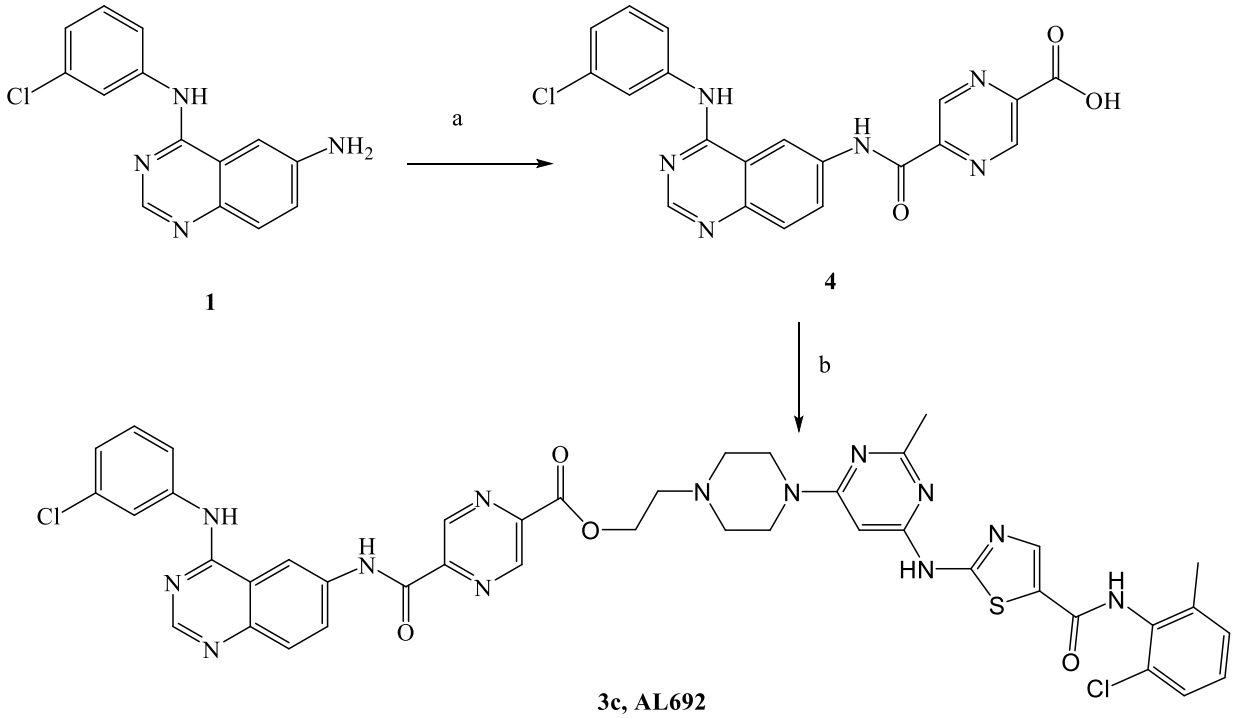

Scheme 2. a) pyrazine-2,5-dicarboxylic acid, $SOCl_2$, DMSO, reflux, 24 h and Et_3N, CH_2Cl_2/THF, 0°C, 1 h; b) dasatinib, EDCI, HOBt, DMAP, DMF, rt, 24 h.

The synthesis of the compounds **6** and **7** proceeded according to Scheme 3 and was already published in Rao *et al.* 2015 (12). Briefly, dasatinib was treated with an excess of succinic anhrydride to give the compound **7**, which was coupled with **1** or 8 (AL621) (43) in the presence of EDCI, HOBt and gave respectively compound **8** (AL739) and **10** (AL776) (40).

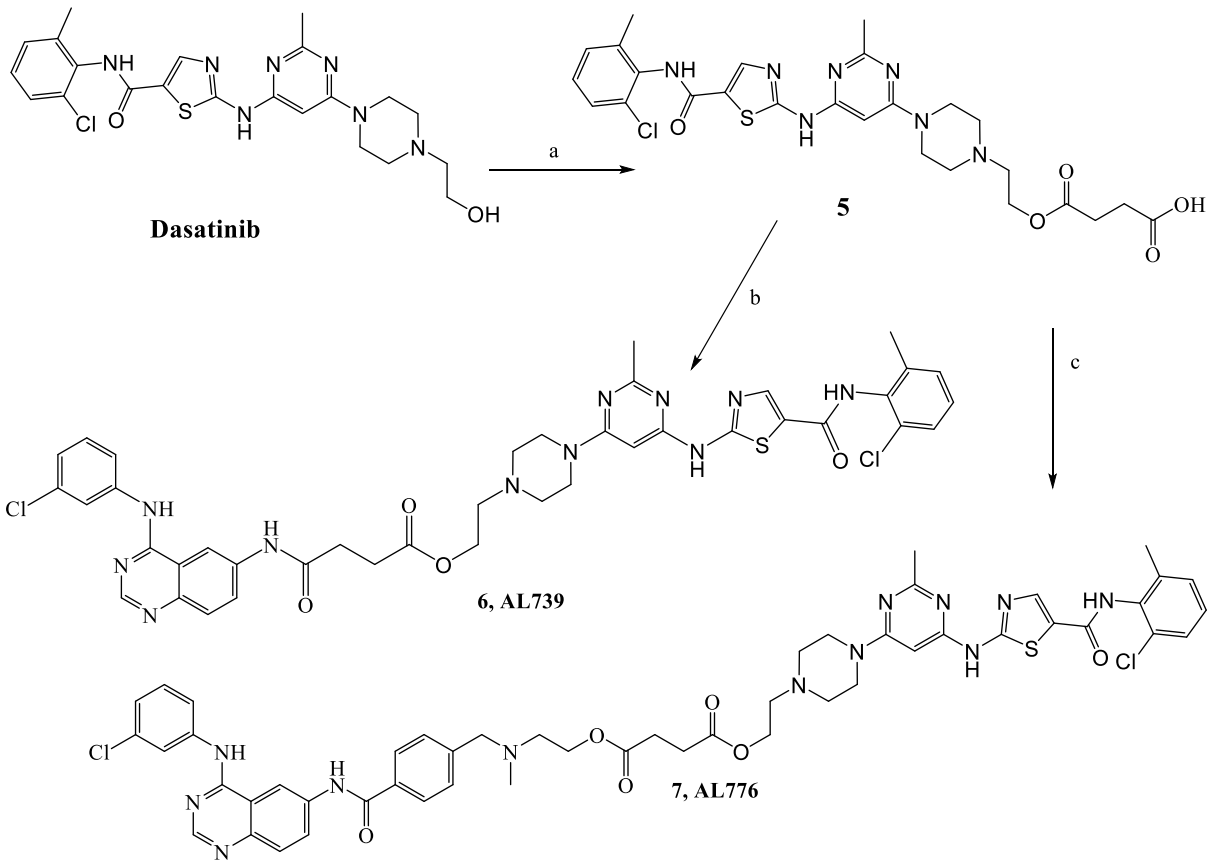

Scheme 3. a) succinic anhydride, DMAP, DMF, 50°C, 18 h; b) compound 1, EDCI, HOBt, DMAP, DMF, rt, 18 h; c) compound **8** (AL621), EDCI, HOBt, DMAP, DMF, rt, 18 h.

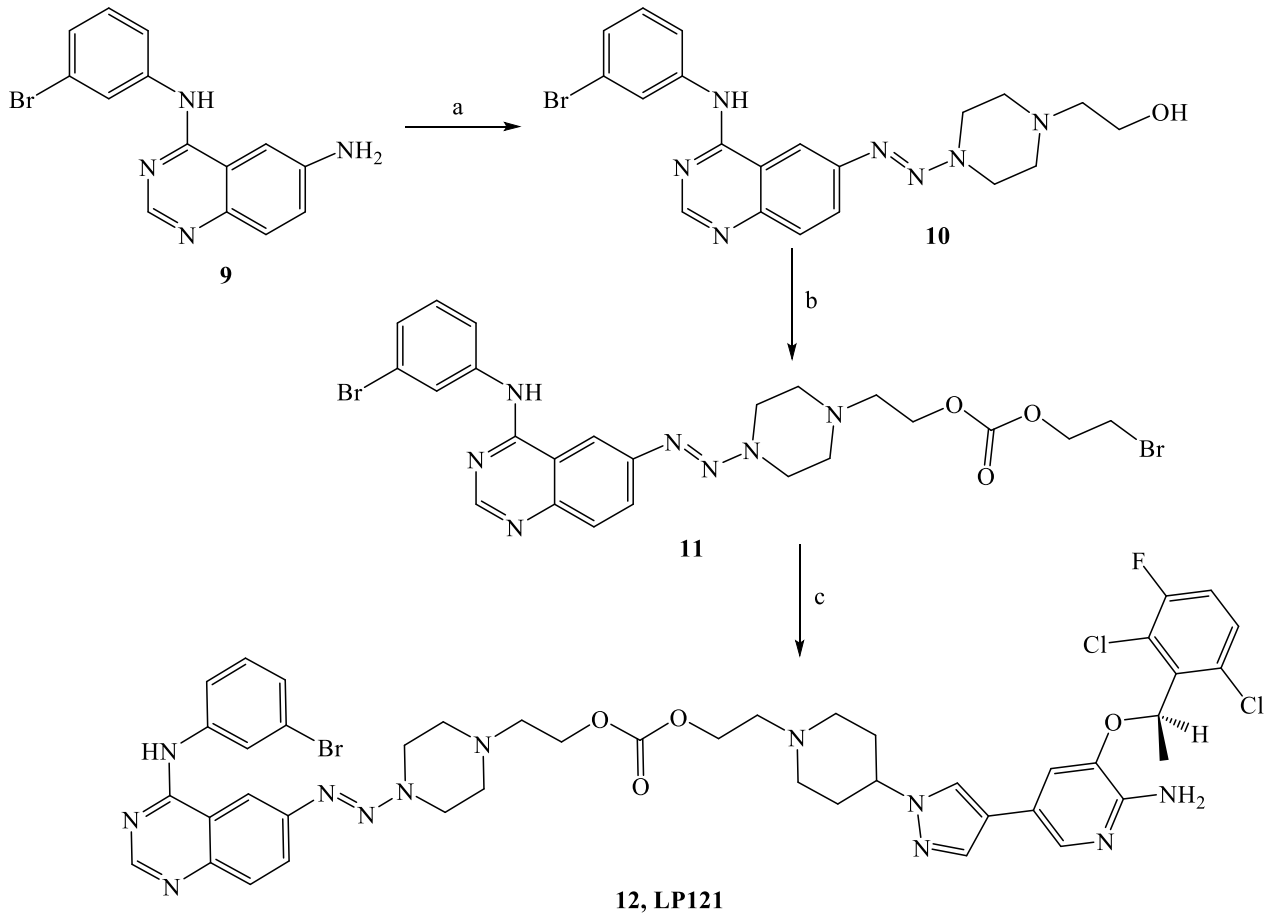

Scheme 4. a) $NOBF_4$,1-piperazineethanol, Et_3N, ACN, -5°C, 1 h; b) 2-bromoethylchloroformate, pyridine, Et_3N, CH_2Cl_2, 0°C to rt, 1 h; c) crizotinib, KI, Et_3N, DMF, 40°C , 4d.

The synthesis of the compounds **12 (LP121)** proceeded according to Scheme 5. The aminoquinazoline **9** (44) was diazotized in dry acetonitrile with nitrosonium tetrafluoroborate to provide the diazonium salt that was coupled with 1-piperazineethanol in the presence of triethylamine *in situ*. The alcohol compound **10** obtained was treated with the commercial 2-bromorthylchloroformate to give intermediate **11**, which was

coupled with crizotinib in the presence of potassium iodide and trimethylamine to give the final compound **12**.

CHAPTER 6

GENERAL DISCUSSION AND CONTRIBUTIONS TO KNOWLEDGE

The past ten years have seen a significant shift towards the design, synthesis and development of drugs with multi-targeted properties. This has led to the emergence of the targeted therapy era, which is primarily sustained by continuous discoveries of new kinase inhibitors and novel biologics. Since 2001, more than 10,000 patents have been filed on kinase inhibitors (1). This historical investment was inspired by the realization of the direct relationship between kinase dysfunctions and tumour progression. Several kinase inhibitors have been targeted with translation into significant antitumour activity in the clinic. However, despite the smashing success of these new targeted therapies, their clinical use is plagued by intrinsic and acquired resistance. In tumour types with high mortality rate (e.g. pancreatic, ovarian, lung, brain), the success of kinase inhibitors is rather mitigated by resistance associated with mutations, amplifications, structural alterations and activation of compensatory signaling pathways. Many attribute the failure of kinase inhibitors to their ability to block pathways that can be bypassed by other oncogenes in the tumour cells. Thus, approaches whereby single kinase inhibitors designed to inhibit several pathways are actively being pursued. The common concept of designing a drug for selectivity in order to avoid toxicity is now being reconsidered. Nearly two decades of work with this approach has led to the more accepted conclusion that the more promiscuous is the drug, the more potent it is in the clinic. As an example, sorafenib, a multi-targeted kinase inhibitor is approved for the treatment of hepatocellular, thyroid and renal cell carcinoma that can hit several targets including B-Raf, VEGFR, PDGFR, c-Kit, etc. (2-5). A recent report showed that the attrition rates for all anti-cancer drugs since 1995 to 2007 was 82%, but dropped to 53% for kinase inhibitors (6). Such a change is being brought by polypharmacology, which is defined as

the science of designing or discovering single molecules that can block multiple targets. Over the past decade, our laboratory has been involved in developing rational polypharmacology directed at kinases inhibitors, in order to improve their potency against advanced cancers.

This work sought to develop a novel mode of targeting signaling nodes controlled by EGFR, c-Src and c-Met. Importantly, two approaches were taken: (1) a unimolecular approach to block two or more signaling pathways, (2) a small-molecule approach for pharmacologically probing signaling nodes and defining multi-drug combinations to abrogate their effects. Ultimately, we sought to develop index of potency that can guide on the efficacy of both unimolecular and individual kinase inhibitor combination approaches.

Contribution 1

To our knowledge, when we started our work on combi-targeting signaling pathways, only one example (SB163) existed that showed imbalanced targeting of EGFR and c-Src (7). This agent was designed as a hybrid molecule to remain intact inside the cells. However, the requirement of the molecule to remain intact led to a bulky c-Src and EGFR inhibitor, a debility that affected both its kinase binding properties. Thus, our contribution in optimizing the potency of EGFR-c-Src targeting combi-molecules began with the complete shift in our approach by redesigning the molecule through a type I strategy. We believed that by designing AL622 to hydrolyze into its two basic sub-constituents (i.e., an EGFR inhibitor, AL621 and a c-Src inhibitor, intact PP2) would be a more efficient approach towards the combi-targeting of EGFR and c-Src (8). However,

despite evidence of release of the two sub-constituents in the cell, AL622 behaved primarily as an EGFR inhibitor. We rationalized that this was due to the fact that the released c-Src inhibitor, PP2 was a much less potent agent than the corresponding EGFR inhibitory moiety. Given the role of EGFR and c-Src in tumour growth, we thought it of importance to resolve the challenging optimization of combi-molecules directed at these two targets. The challenge was to combine via a type I strategy, two moieties that could have strong c-Src inhibitory potency, while retaining submicromolar EGFR inhibitory potency. The ability to optimize the EGFR inhibitory moiety was well established in our laboratory, however the search for a c-Src inhibitory moiety was complicated by the fact that the structure activity relationship for binding to c-Src for many agents was very sensitive to substituent changes (9-11). We ultimately chose the thiazolylaminopyrimidine scaffold associated with dual c-Src/c-Abl activity that was shown to be one of the most tolerant scaffolds towards substituent changes and clinically effective (12, 13). Thus, we synthesized a variety of dasatinib-based combi-molecules that led to the most balanced EGFR-c-Src combi-molecule, AL776 hitherto synthesized.

Contribution 2

Having identified a molecule with optimal EGFR and c-Src targeting potency, we had in hand the first probe to verify our hypothesis on the balanced targeting of EGFR and c-Src *in vitro* and *in vivo* (14). The significant potency of this molecule has led to the first model that we termed "**type III combi-targeting"**. It is to be reminded herein that type I combi-molecules (I-Tz) can bind to one target (e.g. EGFR) as an intact molecule while requiring hydrolysis to target the second target (e.g. DNA) (Fig. 6.1). Type II combi-

molecules were designed to exhibit their dual-targeting potency without a requirement for hydrolytic cleavage. Here we have demonstrated for the first time that a molecule (K1-K2) can be designed to hit its two targets (e.g. EGFR and c-Src) as an intact molecule and to degrade into two species that can further add to the dual targeting of the two targets (Fig. 6.1). Due to the fact that this type of targeting includes type I, for requiring hydrolysis to generate the two species and as type II for being able to hit the two targets without hydrolysis, we termed this mode of targeting **type III targeting.** To our knowledge, this is the first in kind multi-targeted molecule. Importantly, the properties of this type III combi-molecule were proven *in vitro* and further analyzed *in vivo* to bring new data that allowed us to consider other properties of the type III combi-targeting. *In vivo* hydrolysis of the combi-molecule gave rise to novel metabolites that allows us to conclude that these type III combi-molecules can be cleaved to generate novel metabolites, each of them tailed to the cleaved linkers. However, we propose that they are ultimately converted to the intact inhibitory moieties of EGFR and c-Src. Importantly, despite its sensitivity to hydrolysis, pharmacokinetic analysis *in vivo* confirmed that AL776 could be detected as an intact structure in plasma, indicating the accuracy of the hydrolytic profile observed *in vitro,* with only two transient metabolites. Overall, the impact of the study is (a) the discovery and feasibility of type III targeting and (b) the dependence of the efficacy of such molecules on the hydrolysis of the linker. Further work in that direction must focus on programming the linker to resist hydrolysis and deliver the two moieties at reasonable kinetics.

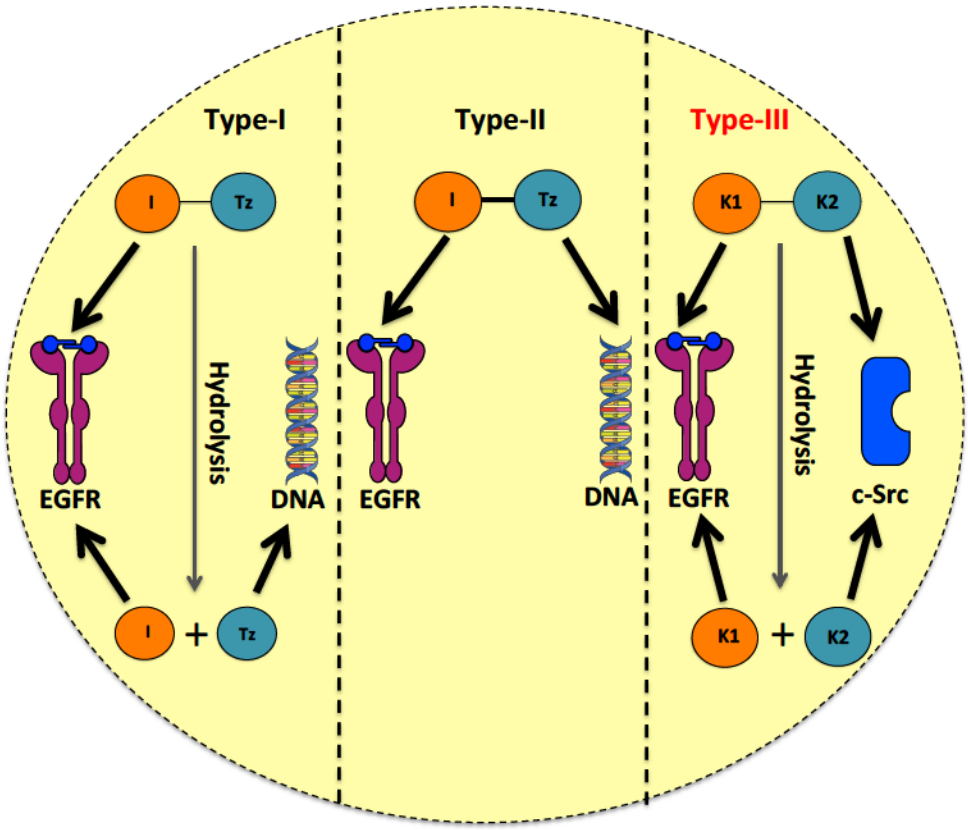

Figure 6.1: The three modes of combi-targeting including type I, type II and the novel type III approach; the latter discovered through kinase-kinase targeting studies.

Contribution 3

Our efforts to target adverse signaling mediated by RTKs and non-RTKs were further directed to the involvement of another RTK, c-Met. Indeed EGFR, c-Met and c-Src have been known to be involved in a complex signaling interplay that is associated with resistance to targeted therapies (15-31). In an effort to identify cells in which the two receptors EGFR and c-Met could be involved in signaling redundancy, we analyzed the potency of an equimolar combination of an EGFR inhibitor (gefitinib) and a c-Met inhibitor (crizotinib) with the prospect of considering redundancy when the IC50 of the combination is lower than that of each drug alone. With this condition, we tested gefitinib

+ crizotinib on a panel of cell lines that included breast, lung and prostate. The set condition of potency of equimolar combination of drugs was met in the subset of prostate cancer cells and a breast cancer cell line. Thus, in order to elucidate the mechanism of action of the putative redundancy detected by the equimolar combination, we chose to study prostate cancer cell lines in which little was known about signaling interplay between EGFR, c-Met and c-Src. This investigation has brought a number of significant observations that led to further understanding of the complex response mediated by c-Src and another player, STAT3 in tumour cells. We found that dual targeting of c-Met and EGFR with crizotinib + gefitinib, abrogated signaling redundancy between the two receptors and led to sustained inhibition of c-Src phosphorylation, cell growth and invasion. By contrast, direct inhibition of c-Src by adding dasatinib to the crizotinib + gefitinib modality (three-drug combination), resulted in strong and delayed re-phosphorylation of c-Src, and did not significantly enhance growth inhibitory and anti-invasive potency. All targeting modalities (2- or 3-drug combinations) induced STAT3 phosphorylation. However, additional blockade of JAK1/2-STAT3 using a JAK1/2 kinase inhibitor ruxolitinib resulted in a four-drug combination that led to sustained blockade of STAT3 phosphorylation. However, this did not significantly enhance growth inhibitory potency ($p > 0.05$). Therefore, we concluded that despite the complexity of the signaling interplay, tandem blockade with complex cocktail with three or four inhibitors did not lead to any further enhancement when compared with targeting just only of the players in the signaling interplay between EGFR, c-Met and c-Src (Rao *et al.* Pharmacological probing of signaling redundancy mediated by receptor and non-receptor tyrosine kinases revealed Achilles' heels in castrate resistant prostate cancer. Molecular

cancer therapeutics, July 2015, under revision). This is an important discovery considering that combinations of multiple drugs often lead to enhanced toxicity.

The identification of dual targeting as a sufficient treatment modality when compared with triple or quadruple targeting lent support to the design and development of dual targeting combi-molecules (e.g. EGFR-c-Src and EGFR-c-Met). However, reference standards to the screening of such type of molecules were lacking since little was known about the criteria of effectiveness of equimolar combinations. Combi-molecules being mimics of equimolar combinations, our next effort was not only directed at creating EGFR-c-Met targeting combi-molecules, but also at setting new quantitative potency parameters that can guide the attrition of combi-molecules (e.g. EGFR-c-Src, EGFR-c-Met).

Contribution 4

Analyses of drug response profiles of the novel EGFR-c-Src, EGFR-c-Met combi-molecules in comparison with their corresponding equimolar combination modalities, shed light on the rules governing their potency (Rao *et al.* Quantitative analysis of the potency of equimolar two-drug combinations and combi-molecules involving kinase inhibitors against human tumour cells: the concept of balanced targeting. Molecular cancer therapeutics, July 2015, under submission), which are summarized below:

1. If two drugs were combined at equimolar ratio, and one drug showed 6-fold greater IC50 than the other, the overall effect was in the same range as that of the more potent drug. This principle led to the discovery of a new potency index

termed **ε**, which linearly linear correlated with the fold-difference between the IC50 values of the two drugs in combination.

2. If two drugs were combined at equimolar ratio, and the IC50 of one drug is 6-fold or less than that of the other, then the overall effect were superior to that of each individual drug. Indeed the highest potency for the combination (low **ε**) was found in the linear portion of the curve, which correlated with the lowest fold-difference in the IC50 values between the two drugs in combination. We thus set **ε** < 5 as the threshold for effective potency or balanced targeting for equimolar combinations.
3. Under conditions of balanced targeting, a unimolecular combination, e.g. combi-molecules, while said to be effective when its IC50 was equal to or a fraction of that of the combination of two individual drugs, leading to a parameter **Ω**, which is equal to or lower than 1.

CONCLUSION

Throughout the study, our efforts towards studying multi-targeting modalities to abrogate signaling interplays in human cancers, have contributed to many novelties: (a) a completely new type III targeting modality using a unimolecular approach, (b) the discovery of the advantage of targeting two key kinases considered to be the Achilles' heels over multiple drug combinations directed at many kinases phosphorylated in the context of complex signaling interplays, and (c) the parameterization of equimolar drug combinations as tools to select combi-targeting molecules. Given the current storming enthusiasm for designing multi-targeted hybrid molecules, we hope that our efforts will

serve in the future as a guiding light for polypharmacology-based drug discovery for the treatment of cancers.

REFERENCES

1. Akritopoulou-Zanze I, Hajduk PJ. Kinase-targeted libraries: the design and synthesis of novel, potent, and selective kinase inhibitors. Drug Discovery Today. 2009;14(5):291-7.
2. Wilhelm SM, Carter C, Tang L, Wilkie D, McNabola A, Rong H, et al. BAY 43-9006 exhibits broad spectrum oral antitumor activity and targets the RAF/MEK/ERK pathway and receptor tyrosine kinases involved in tumor progression and angiogenesis. Cancer research. 2004;64(19):7099-109.
3. Llovet JM, Ricci S, Mazzaferro V, Hilgard P, Gane E, Blanc J-F, et al. Sorafenib in advanced hepatocellular carcinoma. New England Journal of Medicine. 2008;359(4):378-90.
4. Thomas L, Lai SY, Dong W, Feng L, Dadu R, Regone RM, et al. Sorafenib in metastatic thyroid cancer: a systematic review. The oncologist. 2014;19(3):251-8.
5. Escudier B, Eisen T, Stadler WM, Szczylik C, Oudard S, Staehler M, et al. Sorafenib for treatment of renal cell carcinoma: final efficacy and safety results of the phase III treatment approaches in renal cancer global evaluation trial. Journal of Clinical Oncology. 2009;27(20):3312-8.
6. Walker I, Newell H. Do molecularly targeted agents in oncology have reduced attrition rates? Nature reviews Drug discovery. 2009;8(1):15-6.
7. Barchéchath S, Williams C, Saade K, Lauwagie S, Jean‐Claude B. Rational design of multitargeted tyrosine kinase inhibitors: a novel approach. Chemical biology & drug design. 2009;73(4):380-7.
8. Larroque‐Lombard AL, Ning N, Rao S, Lauwagie S, Halaoui R, Coudray L, et al. Biological Effects of AL622, a Molecule Rationally Designed to Release an EGFR and ac‐Src Kinase Inhibitor. Chemical biology & drug design. 2012;80(6):981-91.
9. Das J, Chen P, Norris D, Padmanabha R, Lin J, Moquin RV, et al. 2-aminothiazole as a novel kinase inhibitor template. Structure-activity relationship studies toward the discovery of N-(2-chloro-6-methylphenyl)-2-[[6-[4-(2-hydroxyethyl)-1-piperazinyl)]-2-methyl-4-pyrimidinyl] amino)]-1, 3-thiazole-5-carboxamide (dasatinib, BMS-354825) as a potent pan-Src kinase inhibitor. Journal of medicinal chemistry. 2006;49(23):6819-32.
10. Tandon M, Johnson J, Li Z, Xu S, Wipf P, Wang QJ. New pyrazolopyrimidine inhibitors of protein kinase d as potent anticancer agents for prostate cancer cells. PloS one. 2013;8(9):e75601.
11. Bishop AC, Kung C-y, Shah K, Witucki L, Shokat KM, Liu Y. Generation of monospecific nanomolar tyrosine kinase inhibitors via a chemical genetic approach. Journal of the American Chemical Society. 1999;121(4):627-31.

12. Conchon M, Freitas CMBdM, Rego MAdC, Junior B, Ramos JW. Dasatinib: clinical trials and management of adverse events in imatinib resistant/intolerant chronic myeloid leukemia. Revista brasileira de hematologia e hemoterapia. 2011;33(2):131-9.
13. Lombardo LJ, Lee FY, Chen P, Norris D, Barrish JC, Behnia K, et al. Discovery of N-(2-chloro-6-methyl-phenyl)-2-(6-(4-(2-hydroxyethyl)-piperazin-1-yl)-2-methylpyrimidin-4-ylamino) thiazole-5-carboxamide (BMS-354825), a dual Src/Abl kinase inhibitor with potent antitumor activity in preclinical assays. Journal of medicinal chemistry. 2004;47(27):6658-61.
14. Rao S, Larroque-Lombard A-L, Peyrard L, Thauvin C, Rachid Z, Williams C, et al. Target Modulation by a Kinase Inhibitor Engineered to Induce a Tandem Blockade of the Epidermal Growth Factor Receptor (EGFR) and c-Src: The Concept of Type III Combi-Targeting. PloS one. 2015;10(2).
15. Kim YJ, Choi JS, Seo J, Song JY, Eun Lee S, Kwon MJ, et al. MET is a potential target for use in combination therapy with EGFR inhibition in triple-negative/basal-like breast cancer. International Journal of Cancer. 2014;134(10):2424-36.
16. Puri N, Salgia R. Synergism of EGFR and c-Met pathways, cross-talk and inhibition, in non-small cell lung cancer. Journal of carcinogenesis. 2008;7(1):9.
17. Dulak AM, Gubish CT, Stabile LP, Henry C, Siegfried JM. HGF-independent potentiation of EGFR action by c-Met. Oncogene. 2011;30(33):3625-35.
18. Benedettini E, Sholl LM, Peyton M, Reilly J, Ware C, Davis L, et al. Met activation in non-small cell lung cancer is associated with de novo resistance to EGFR inhibitors and the development of brain metastasis. The American journal of pathology. 2010;177(1):415-23.
19. Mueller KL, Hunter LA, Ethier SP, Boerner JL. Met and c-Src cooperate to compensate for loss of epidermal growth factor receptor kinase activity in breast cancer cells. Cancer research. 2008;68(9):3314-22.
20. Tice DA, Biscardi JS, Nickles AL, Parsons SJ. Mechanism of biological synergy between cellular Src and epidermal growth factor receptor. Proceedings of the National Academy of Sciences. 1999;96(4):1415-20.
21. Yoshida T, Okamoto I, Okamoto W, Hatashita E, Yamada Y, Kuwata K, et al. Effects of Src inhibitors on cell growth and epidermal growth factor receptor and MET signaling in gefitinib-resistant non-small cell lung cancer cells with acquired MET amplification. Cancer science. 2010;101(1):167-72.
22. Zhang J, Kalyankrishna S, Wislez M, Thilaganathan N, Saigal B, Wei W, et al. SRC-family kinases are activated in non-small cell lung cancer and promote the survival of epidermal growth factor receptor-dependent cell lines. The American journal of pathology. 2007;170(1):366-76.
23. Nagaraj NS, Washington MK, Merchant NB. Combined blockade of Src kinase and epidermal growth factor receptor with gemcitabine overcomes STAT3-mediated resistance of inhibition of pancreatic tumor growth. Clinical Cancer Research. 2011;17(3):483-93.
24. Engelman JA, Zejnullahu K, Mitsudomi T, Song Y, Hyland C, Park JO, et al. MET amplification leads to gefitinib resistance in lung cancer by activating ERBB3 signaling. science. 2007;316(5827):1039-43.

25. Herynk MH, Zhang J, Parikh NU, Gallick GE. Activation of Src by c-Met overexpression mediates metastatic properties of colorectal carcinoma cells. Journal of experimental therapeutics & oncology. 2006;6(3):205-17.
26. Jo M, Stolz DB, Esplen JE, Dorko K, Michalopoulos GK, Strom SC. Cross-talk between epidermal growth factor receptor and c-Met signal pathways in transformed cells. Journal of Biological Chemistry. 2000;275(12):8806-11.
27. Sen B, Peng S, Saigal B, Williams MD, Johnson FM. Distinct interactions between c-Src and c-Met in mediating resistance to c-Src inhibition in head and neck cancer. Clinical Cancer Research. 2011;17(3):514-24.
28. Stabile LP, He G, Lui VWY, Thomas SM, Henry C, Gubish CT, et al. c-Src activation mediates erlotinib resistance in head and neck cancer by stimulating c-Met. Clinical Cancer Research. 2013;19(2):380-92.
29. Xu H, Stabile LP, Gubish CT, Gooding WE, Grandis JR, Siegfried JM. Dual blockade of EGFR and c-Met abrogates redundant signaling and proliferation in head and neck carcinoma cells. Clinical Cancer Research. 2011;17(13):4425-38.
30. Yamamoto N, Mammadova G, Song RX-D, Fukami Y, Sato K-i. Tyrosine phosphorylation of p145met mediated by EGFR and Src is required for serum-independent survival of human bladder carcinoma cells. Journal of cell science. 2006;119(22):4623-33.
31. Zucali P, Ruiz MG, Giovannetti E, Destro A, Varella-Garcia M, Floor K, et al. Role of cMET expression in non-small-cell lung cancer patients treated with EGFR tyrosine kinase inhibitors. Annals of oncology. 2008;19(9):1605-12.